Title
Economic Model Predictive Control and Nonlinear Control Actuator Dynamics

Author
Durand, Helen Elaine

Publication Date
2017

Peer reviewed|Thesis/dissertation

UNIVERSITY OF CALIFORNIA

Los Angeles

Economic Model Predictive Control and Nonlinear Control Actuator Dynamics

A dissertation submitted in partial satisfaction of the
requirements for the degree Doctor of Philosophy
in Chemical Engineering

by

Helen E. Durand

2017

ABSTRACT OF THE DISSERTATION

Economic Model Predictive Control and Nonlinear Control Actuator Dynamics

by

Helen E. Durand

Doctor of Philosophy in Chemical Engineering

University of California, Los Angeles, 2017

Professor Panagiotis D. Christofides, Chair

Control valves are the most prevalent final control element in the chemical process industries. However, the behavior of valves (i.e., the manner in which the valve output flow rate changes in response to changes in the control signal to the valve) can contribute to a number of negative effects in a control loop, such as set-point tracking issues and sustained closed-loop oscillations. Valve stiction, for example, is a dynamic valve nonlinearity (i.e., the relationship between the valve output flow rate and the control signal to the valve is described by nonlinear differential equations) resulting from friction that is known to be problematic in the process industries. This dissertation describes the impact of valve behavior on process control loops and methods for compensating for the valve behavior through appropriate control designs. It begins by describing how the addition of input rate of change constraints to an optimization-based control design with a general objective function (economic model predictive control (EMPC)) can be performed in a manner that may reduce actuator wear while simultaneously guaranteeing feasibility of the controller and closed-loop stability of a nonlinear process operated under the control design. It then focuses on a specific type of actuator (a valve) and elucidates that coupled, nonlinear interactions between the process and valve model states and any internal states of the controller model create the negative effects that may be observed in control loops containing valves for which the dynamics cannot be

neglected (e.g., valves subject to significant stiction). These multivariable interactions illustrate the closed-loop nature of the negative effects observed, and this closed-loop perspective is then used to analyze stiction compensation methods from the literature, to develop a novel stiction compensation scheme for control loops under proportional-integral control, and to demonstrate that incorporating models, both first-principles and empirical, of valve behavior within the model used for making state predictions in a model predictive controller is an effective means for compensating for valve behavior in general. The benefits of adding actuation magnitude and input rate of change constraints within EMPC including a model of stiction dynamics are discussed. Throughout the work, process examples are utilized to illustrate the advanced control-based frameworks for understanding and compensating for valve limitations.

The dissertation of Helen E. Durand is approved.

James Davis

Dante Simonetti

Lieven Vandenberghe

Panagiotis D. Christofides, Committee Chair

University of California, Los Angeles

2017

Contents

List of Figures

ACKNOWLEDGEMENTS

I would like to express my extreme gratitude to my advisor, Professor Panagiotis D. Christofides. He has been the greatest advisor that I could have had. He is a great role model to his students of attention to detail and excellence in his work, and also a great role model in terms of character qualities like patience, work ethic, and determination. His method of motivating us is encouragement, and this truly inspires all of us to success not just for the work that we are doing in graduate school, but also for our future because Professor Christofides gives us the confidence that we can do the tasks that we put our minds to. He has made a profound impact on my character and my career goals. I would also like to thank Professor James Davis, Professor Dante Simonetti, and Professor Lieven Vandenberghe for serving on my doctoral committee. They have been great role models as well and have helped me to move to the next stage of my career by helping me in my faculty position search process, and I am very grateful to them.

I would like to thank all of my colleagues with whom I have worked over the years in the Christofides research group, including Dr. Larry Gao, Dr. Joseph S-I Kwon, Dr. Liangfeng Lao, Dr. Mirko Messori, Dr. Michael Nayhouse, Timothy Anderson, Andres Aguirre, Grant Crose, Carlos Garcia, Caio Marcellos, Zhe Wu, Junfeng Zhang, Zhihao Zhang, Robert Parker, and Yangyao Ding. I would particularly like to thank Dr. Anas Alanqar, Dr. Fahad Albalawi, Anh Tran, and Dr. Matthew Ellis, with whom I have collaborated extensively and spent long hours working on papers together. All of my colleagues in the research group have been wonderful to work with on teams and most of all, have been great friends. My graduate school experience would not have been the same without them and I am grateful to have had the opportunity to build life-long friendships with these great engineers.

I gratefully acknowledge financial support from the US Department of Energy (DOE) and the US National Science Foundation (NSF). I also gratefully acknowledge financial support from the UCLA Graduate Division through the UCLA Doctoral Dissertation Year Fellowship and the UCLA Graduate Division Fellowship, from Mohini and Balu Balakrishnan for their generosity in supporting me through the Mohini and Balu Balakrishnan Fellowship, and from Pratt & Whitney

Rocketdyne/Aerojet Rocketdyne for the majority of my Master's Degree funding through the Employee Scholar Program.

I would like to thank my parents Tim and Laura and my siblings Michelle, Kevin, Lisa, and Scott for their encouragement of me throughout my PhD and for always doing so much to help me. I would not be where I am today without them. Back when I first considered being a chemical engineer as an undergraduate, my father would help me with physics over the phone and he has always been knowledgeable on science, mathematics, and computing, which has played a large role in my interests and also has meant so much to me all of the times that I have had questions and needed help. My mother spent countless hours with me as I grew up helping me to learn to write and edit papers, and this has been foundational to allowing me to communicate my ideas as a researcher. I would also like to thank my grandparents, Tom and Lois Ross and Richard and Barbara Durand, for their support and encouragement of me throughout my life that has made me always feel like I can do anything. Most importantly, I would like to thank the Lord for giving me the strength and ability to achieve a PhD and for giving me joy through the salvation that comes through Jesus, which motivates me to continue striving to do my best each day for Him.

Chapter 2 is a version of: H. Durand, M. Ellis, and P. D. Christofides. Economic Model Predictive Control Designs for Input Rate-of-Change Constraint Handling and Guaranteed Economic Performance. *Comput. Chem. Eng.*, 92:18-36, 2016. It is also a version of: H. Durand and P. D. Christofides. Economic Model Predictive Control for Nonlinear Processes Incorporating Actuator Magnitude and Rate of Change Constraints. In *Proceedings of the American Control Conference*, pages 5068-5074, Boston, Massachusetts, 2016; integrated with M. Ellis and P. D. Christofides. On Closed-Loop Economic Performance Under Lyapunov-Based Economic Model Predictive Control. In *Proceedings of the American Control Conference*, pages 1778-1783, Boston, Massachusetts, 2016.

Chapters 3 and 4 are versions of: H. Durand, R. Parker, A. Alanqar, and P. D. Christofides. Elucidating and Handling Effects of Valve-Induced Nonlinearities in Industrial Feedback Control Loops. *Comput. Chem. Eng.*, submitted. They are also versions of: H. Durand and

P. D. Christofides. Empirical Modeling of Control Valve Layer with Application to Model Predictive Control-Based Stiction Compensation. In *Proceedings of the IFAC Symposium on Nonlinear Control Systems,* pages 41-46, Monterey, California, 2016; H. Durand and P. D. Christofides. Elucidation and compensation of valve stiction-induced oscillations in closed-loop systems. In *Proceedings of the American Control Conference,* in press, Seattle, Washington, 2017.

Chapter 5 is a version of: H. Durand and P. D. Christofides. Actuator Stiction Compensation via Model Predictive Control for Nonlinear Processes. *AIChE J.*, 62:2004-2023, 2016. It is also a version of: H. Durand and P. D. Christofides. Stiction Compensation via Model Predictive Control. In *Proceedings of the American Control Conference*, pages 4488-4493, Boston, Massachusetts, 2016.

VITA

2012–2014	Master of Science, Chemical Engineering University of California, Los Angeles
2007–2011	Bachelor of Science, Chemical Engineering University of California, Los Angeles
2014–2017	Graduate Student Researcher / Teaching Assistant Department of Chemical and Biomolecular Engineering University of California, Los Angeles
2011–2014	Engineer, Materials & Processes Engineering Department Aerojet Rocketdyne

SELECTED PUBLICATIONS

1. **Durand, H.**, R. Parker, A. Alanqar and P. D. Christofides, "Elucidating and Handling Effects of Valve-Induced Nonlinearities in Industrial Feedback Control Loops," *Computers & Chemical Engineering*, submitted.
2. **Durand, H.**, M. Ellis and P. D. Christofides, "Economic Model Predictive Control Designs for Input Rate-of-Change Constraint Handling and Guaranteed Economic Performance," *Computers & Chemical Engineering*, 92, 18-36, 2016.
3. **Durand, H.** and P. D. Christofides, "Actuator Stiction Compensation via Model Predictive Control for Nonlinear Processes," *AIChE Journal*, 62, 2004-2023, 2016.
4. **Durand, H.**, M. Ellis and P. D. Christofides, "Integrated Design of Control Actuator Layer and Economic Model Predictive Control for Nonlinear Processes," *Industrial & Engineering Chemistry Research*, 53, 20000-20012, 2014.
5. **Durand, H.** and P. D. Christofides, "Elucidation and Compensation of Valve Stiction-Induced Oscillations in Closed-Loop Systems," *Proceedings of the American Control Conference*, in press, Seattle, Washington, 2017.
6. **Durand, H.** and P. D. Christofides, "Elucidation and Handling of Valve Actuator Nonlinearity in Process Control Loops: An Overview of Recent Results," *Proceedings of Foundations of Computer Aided Process Operations/Chemical Process Control*, 6 pages, Tucson, Arizona, 2017.

7. **Durand, H.** and P. D. Christofides, "Empirical Modeling of Control Valve Layer with Application to Model Predictive Control-Based Stiction Compensation," *Proceedings of the 10th IFAC Symposium on Nonlinear Control Systems*, 41-46, Monterey, California, 2016.

8. **Durand, H.** and P. D. Christofides, "Stiction Compensation via Model Predictive Control," *Proceedings of the American Control Conference*, 4488-4493, Boston, Massachusetts, 2016.

9. **Durand, H.** and P. D. Christofides, "Economic Model Predictive Control for Nonlinear Processes Incorporating Actuator Magnitude and Rate of Change Constraints," *Proceedings of the American Control Conference*, 5068-5074, Boston, Massachusetts, 2016.

10. **Durand, H.**, M. Ellis and P. D. Christofides, "Accounting for the Control Actuator Layer in Economic Model Predictive Control of Nonlinear Processes," *Proceedings of the American Control Conference*, 2968-2973, Chicago, Illinois, 2015.

11. Albalawi, F., **H. Durand** and P. D. Christofides, "Process Operational Safety Using Model Predictive Control Based on a Process Safeness Index," *Computers & Chemical Engineering*, 104, 76-88, 2017.

12. Alanqar, A., **H. Durand** and P. D. Christofides, "Fault-Tolerant Economic Model Predictive Control Using Error-Triggered On-Line Model Identification," *Industrial & Engineering Chemistry Research*, 56, 5652-5667, 2017.

13. Ellis, M., **H. Durand** and P. D. Christofides, "A Tutorial Review of Economic Model Predictive Control Methods," *Journal of Process Control*, 24, 1156-1178, 2014.

14. Tran, A., A. Aguirre, **H. Durand**, M. Crose and P. D. Christofides, "CFD Modeling of an Industrial-Scale Steam Methane Reforming Furnace," *Chemical Engineering Science*, submitted.

15. Tran, A., A. Aguirre, M. Crose, **H. Durand** and P. D. Christofides, "Temperature Balancing in Steam Methane Reforming Furnace via an Integrated CFD/Data-Based Optimization Approach," *Computers & Chemical Engineering*, 104, 185-200, 2017.

Chapter 1

Introduction

1.1 Model Predictive Control

Model predictive control (MPC) has been a critical technology within the chemical process industries for several decades[25, 37, 126, 127] due to its ability to determine optimal inputs to a process by minimizing a quadratic function of the inputs and (predicted) process states. Unlike optimal control problems that optimize a quadratic objective function over an infinite horizon,[28, 74] MPC is implemented with a finite-time horizon known as the prediction horizon. This means that the objective function can be numerically discretized and represented as a sum of a finite number of terms. The prediction horizon is partitioned into N time intervals where each has a length known as a sampling period. Throughout a sampling period, the MPC assigns a constant value to each process input. At every sampling time, the MPC receives feedback of the process state through a state measurement and re-solves the optimization problem consisting of a quadratic objective function and state and input constraints, where every occurrence of the state in both the objective function and state constraints must come from the predictions of a dynamic process model with its initial condition at the state measurement at the beginning of the sampling period. After the solution to the MPC has been obtained (which consists of N values of each manipulated input, each of which will be held constant for a sampling period), it applies only the first of the N values

of each input to the process for one sampling period. At the next sampling period, the remaining $N-1$ values of each input are discarded so that the MPC can re-solve for the N values of each input based on a new state measurement and then apply the first of each of these new values to the process for the next sampling period. This is known as a receding horizon implementation. Many industrial MPC designs employ linear dynamic process models.

Because MPC uses a process model for state predictions given an input trajectory, it can account for multivariable interactions and actuator constraints. The quadratic objective function of an MPC can in general be tuned by adjusting the weighting matrices on the quadratic terms to more significantly penalize set-point deviations (by increasing the weight on the state term) or the use of control inputs (by increasing the weight on the input term). Because the cost function of MPC can be tuned in this manner, MPC has been promoted as a controller that can improve process economics by enforcing either rapid set-point tracking or minimal input use, whichever corresponds to greater profit for a company. In general, however, the tuning of the weighting matrices that achieves economic optimality in this sense is difficult to discern, and in addition a quadratic cost function may not actually represent the process economics (which may be more adequately represented by, for example, a nonlinear Arrhenius rate law expression that quantifies the production rate of a desired product). For these reasons, optimal control actions computed by solving the tracking MPC optimization problem do not typically correspond to economically optimal input trajectories. To increase profits for a process under tracking MPC, MPC has been coupled with an optimizer referred to as a real-time optimizer (RTO)[42,103] that computes economically optimal steady-states for the MPC to track by solving a nonlinear optimization problem with a detailed steady-state plant model and a possibly nonlinear and nonquadratic objective function representing the process economics.

1.2 Economic Model Predictive Control

The RTO-MPC hierarchy described above has a number of disadvantages from an economic point of view, most significantly that steady-state operation may not be the most economically optimal operating strategy. In fact, it has been repeatedly shown in the chemical engineering literature, both experimentally and through a variety of simulated chemical process examples, that a number of industrially relevant processes may achieve higher profits when operated in a time-varying fashion than when operated at steady-state.[20, 122, 131, 139] To achieve dynamic, economically optimal process operation while still incorporating process feedback, the tracking MPC framework was modified by replacing the quadratic objective function with an objective function that specifically represents the process economics (and does not typically have its minimum at a steady-state of the process), forming economic MPC (EMPC).[62, 63] The time-varying operating policies that can be computed by EMPC have been repeatedly shown to be capable of increasing process profits compared to operating a process at steady-state for some systems.[59, 79]

However, this new time-varying operating policy comes with a large number of theoretical and practical challenges, including: 1) evaluating whether the economic performance of a process under EMPC is better than that for steady-state operation, particularly when there are restrictions such as constraints on actuator movement or production schedules that must be met, 2) defining the conditions under which EMPC is guaranteed to be feasible and to maintain closed-loop stability of a nonlinear process for various stability constraints added to the formulation and even when there are disruptions such as preventive maintenance, 3) reducing the computation time of the methodology, which can be prohibitively large since it requires a nonlinear program to be solved due to the non-quadratic objective function and often nonlinear constraints (as opposed to a convex optimization problem like a typical tracking MPC), and 4) guaranteeing operational safety of chemical processes operated under EMPC when the control design is highly focused on process economics. These considerations have been addressed in recent years by a number of works.

One method that has been utilized for addressing the first two considerations is the development of multiple EMPC formulations. Due to differences in these formulations, different guarantees can

be made in terms of economic performance, feasibility, stability, and robustness. Four common designs in the literature are those with a terminal equality constraint requiring the state at the end of the prediction horizon to be at the steady-state,[16,47,128] a terminal region constraint requiring the state at the end of the prediction horizon to be in a region around the steady-state,[11,13] an EMPC formulation without additional constraints (but with technical assumptions such as a sufficiently long prediction horizon or turnpike property of the optimal control problem made for analyzing the closed-loop system under the EMPC),[69,75,76] and a two-mode EMPC formulation with Lyapunov-based stability constraints.[79] Several of these methods have been beneficial for analyzing economic performance guarantees under the EMPC formulations in the absence of disturbances and for showing that steady-state tracking is possible under EMPC if certain conditions are met on the process model and objective function. The Lyapunov-based EMPC formulation has been used to address a number of the major considerations encountered for a process under EMPC listed above, including optimizing economic performance even when schedules must be tracked,[2] maintaining closed-loop stability when sensors are taken off-line for maintenance,[97] and explicitly integrating operational chemical process safety and process control.[7–10] This EMPC formulation has been ideally suited for addressing this wide range of issues because it allows explicit *a priori* characterization of the set of initial conditions from which feasibility of the EMPC optimization problem is guaranteed at every sampling time, and explicit *a priori* characterization of the region in state-space within which the closed-loop state is guaranteed to be maintained for all times in the presence of sufficiently small disturbances and with a sufficiently small sampling period. In general, however, various economic model predictive control formulations have been utilized in the literature to address numerous practical considerations including wastewater treatment,[155] determining zone temperatures for heating, ventilation, and air conditioning systems,[124,144] microgrid dispatch,[154] and fault-tolerant control of systems for which empirical models are available.[5] Infinite horizon results for EMPC have also been developed (e.g.,[84,121]).

A disadvantage of EMPC is that it typically requires the solution of a nonconvex nonlinear

optimization problem and thus may not be able to be solved in a sampling period. Methods that have been looked at for enhancing the ability of EMPC to be applied on-line include using two-tier schemes,[59,65] triggering of the EMPC optimization problem as the error between state predictions and state measurements becomes larger than a threshold,[156] using empirical models in place of first-principles models in EMPC,[6] or simplifying the EMPC formulation through Carleman approximation.[68]

1.3 Stiction

Both MPC and EMPC compute control actions that must be physically implemented on a process. The most common final control elements used to implement control actions at chemical plants and refineries are control valves. Valve dynamics are typically neglected in the chemical process control literature, meaning that the valve output is typically assumed to instantaneously reach the value requested by the controller. However, valves often have dynamics or other behavior that undermines control system performance. Specifically, nonlinearities in control valve dynamics can cause poor set-point tracking and even sustained control loop oscillations.[24] Some nonlinearities can be described by static functions (e.g., an equal percentage valve characteristic, which represents a nonlinear one-to-one relationship between the percent that the valve is open and the percent of flow through the valve),[38] while others are modeled as nonlinear dynamic systems (e.g., stiction).[33] Stiction is a particularly problematic issue for the chemical process industries,[46,117] as it is a friction effect in the valve that causes it to stick until the force on the valve exceeds a certain level, at which point the valve moves and may even jump to a new position. Though there have been efforts to develop compensation techniques for stiction (e.g., methods that add additional signals to the output of a controller such as pulses[77] or optimally-determined signals with respect to a performance metric[135]), they have not yet been able to eradicate this significant industrial concern.

1.4 Dissertation Objectives and Structure

Motivated by next-generation manufacturing objectives,[34,43] including safer and more profitable operating strategies, this dissertation develops formulations of advanced process controllers such as MPC and EMPC, as well as modifications to classical control designs such as proportional-integral (PI) control, that seek to achieve these objectives by improving process economic performance in the presence of actuator nonlinearities.

As noted above, one of the primary concerns within the EMPC literature is determining the conditions that guarantee that a process under EMPC will have an economic performance at least as good as that for the standard industrial operating paradigm (steady-state operation). However, industry is only interested in these performance guarantees if they can be achieved without abuse of the process equipment by the control actions computed by EMPC. This is a concern since EMPC may operate a process in a time-varying fashion, sometimes by calculating bang-bang type control actions which may wear out the control actuators. Therefore, Chapter 2 of this dissertation addresses this issue by adding input rate of change constraints to a specific EMPC formulation that utilizes Lyapunov-based stability constraints for closed-loop stability purposes (termed Lyapunov-based EMPC or LEMPC). The input rate of change constraints are formulated with respect to a Lyapunov-based controller to form an EMPC formulation with both input rate of change constraints and guaranteed feasibility and closed-loop stability properties, even in the presence of disturbances. Furthermore, an additional terminal constraint is developed based on a Lyapunov-based controller and it is shown that when there are no disturbances or plant-model mismatch, the LEMPC with input rate of change constraints and the terminal constraint has guaranteed economic performance properties. Specifically, its economic performance is at least as good as that of a stabilizing Lyapunov-based controller on both the finite-time and infinite-time intervals (when the stabilizing Lyapunov-based controller has certain properties, the infinite-time performance result signifies that the asymptotic average performance of a nonlinear process operated under the LEMPC with input rate of change constraints is at least as good as that for steady-state operation). This result holds regardless of the magnitude of the input rate of change

or whether the input rate of change is penalized in the cost function. These results address a key industrial concern regarding the wear on a physical system under EMPC and also show that EMPC may still provide economic benefits compared to the standard industrial operating paradigm even when the input variability is reduced.

Chapter 3 of this dissertation turns from the focus on controllers designed to improve process economics subject to physical actuator limitations such as wear possibilities to the more general problem of how to enhance process economic performance in the presence of valve behavior, for processes operated under any feedback control design (e.g., proportional-integral (PI) control, MPC) for which the control design objectives such as set-point tracking are not being met due to valve dynamics. Specifically, this chapter develops a unified framework for understanding the negative impacts of valve dynamics on process control, elucidating the manner in which the type of valve nonlinearity, the type of controller, and the control loop architecture impact the consequences of having that nonlinearity within the control loop. It demonstrates that these factors work together to influence set-point tracking, process constraint satisfaction, and the initiation of sustained control loop oscillations. After such issues have been clarified, it is possible to propose novel compensation methods for valve nonlinearities that modify the type of controller already in the control loop containing the valve nonlinearity (rather than adding an additional compensating system). For example, the chapter demonstrates that the manner in which the forces on the valve balance causes stiction-induced oscillations within a control loop containing an integrating linear controller and a sticky valve. From this understanding of the oscillation phenomenon, it then proposes the modification of the integral action with a term reflecting the difference between the valve output set-point and the actual valve output.

Chapter 4 augments the developments of Chapter 3 by proposing that model-based control designs (in particular, model predictive control designs) accounting for valve dynamics provide a systematic method for attempting to remove the negative effects observed in closed-loop systems within which the valve dynamics cannot be neglected. A critical component of the MPC-based valve nonlinearity compensation strategy is the availability of a model describing the valve layer

dynamics. To handle the range of controllers, control loop architectures, and valve nonlinearities for which this dissertation investigates MPC with valve dynamics as a compensation technique, a systematic methodology is utilized to obtain valve layer models. The modeling efforts assume that a higher-level controller (e.g., a PI controller or an MPC controlling a process) communicates a valve output flow rate set-point to a valve. The flow rate set-point is related to the force applied to the valve by the actuation through either a linear relationship (for a valve operated without flow control) or using a dynamic model of a linear controller for the valve that computes the force applied to the valve (for a valve operated under flow control). In accordance with the literature, a force balance is utilized to describe the valve stem position and velocity dynamics. Finally, the valve position and valve output flow rate are related using a static function (e.g., a linear valve characteristic). The flow rate out of the valve is then utilized as the chemical process input.

This first-principles valve layer modeling effort pursued in Chapters 3-4 permits an entire closed-loop process-valve system to be modeled, which allows the dynamics of a nonlinear process influenced by a variety of control loop architectures, nonlinearities, and controllers to be systematically investigated, understood, and improved. It also allows a practical challenge which might otherwise limit the industrial applicability of the MPC-based valve nonlinearity compensation technique (that it can be difficult to determine the parameters of a dynamic first-principles valve model) to be investigated in Chapter 4. Specifically, Chapter 4 uses a first-principles process-valve model as the representation of a plant containing a sticky valve and uses the data from simulations of this plant to address the empirical modeling of the valve layer. It suggests an empirical modeling strategy that can capture all of the valve layer dynamics, including the linear controller for the valve, the stiction dynamics, and the valve characteristic, using only the data on the valve output set-point from the MPC and the valve output flow rate, via a branched model with branches corresponding to sticking and slipping that are identified for standard model structures such as first-order-plus-dead-time and second-order models, and accounting for the effect of the set-point change magnitude on the time that the valve is stuck (delay before it begins moving when the linear controller for the valve is present within the valve layer for a sticky valve)

by fitting a function to the data on the length of the delay versus the set-point change magnitude. Furthermore, because the empirical model may be less stiff than the first-principles valve layer model, the computation time of an EMPC utilizing the empirical valve layer model may be less than that of an EMPC utilizing a first-principles valve layer model.

In Chapter 5 of this dissertation, MPC with stiction dynamics is handled in a rigorous mathematical framework and also is analyzed in terms of additional constraints that may be required in MPC for valve nonlinearity compensation beyond the incorporation of the stiction dynamics within the model used for state predictions. The focus is on a process under EMPC (due to the time-varying operating policies set up under this control design which may cause the valve actuation to be more likely to hit its constraints) where the EMPC computes set-points for a control valve's output, and the valve outputs are regulated to their set-points by flow controllers for consistency with the architectures traditionally utilized within the chemical process industries for MPC. The additional constraints in an MPC focused on stiction compensation, such as input rate of change constraints or actuation magnitude constraints (e.g., the pressure applied by the pneumatic actuation of a pneumatic spring-diaphragm sliding-stem globe valve cannot become negative), may be necessary to include within the MPC for stiction compensation to prevent the MPC from requesting set-points that the valve could reach before stiction worsened but can no longer reach with the available actuation energy.

In the final chapter of this dissertation, the contributions of the various sections are reviewed, establishing a unified framework for compensating for valve limitations and nonlinearities within process control by modifying standard controller designs.

Chapter 2

Economic Model Predictive Control with Input Rate-of-Change Constraints for Actuator Wear Reduction with Economic Performance Guarantees

2.1 Introduction

As environmental requirements tighten and chemical processing companies are increasingly interested in operating processes in the most economically efficient but safe manner, advanced process control is being exploited as a means to achieve these objectives. As noted in Chapter 1, real-time optimization (RTO), coupled with model predictive control (MPC) and a distributed control system (DCS) architecture, has been used in industry to improve production profits.[42, 103] Typical industrial implementations of the RTO-MPC paradigm have structures that are considered to make the advanced control strategy safe to use in the sense that they may include logic steps at the RTO level to evaluate RTO solutions before implementing them,[103] a tracking MPC formulation with a quadratic objective, and penalties on changes in the manipulated inputs between

two sampling periods of the prediction horizon to prevent aggressive movement of the actuation elements.[126]

Chapter 1 reviewed a fairly recent development in the MPC literature that is often viewed as an alternative to the RTO-MPC hierarchy (economic model predictive control) and noted that the objective function of EMPC is not required to have its minimum at a steady-state of the process because it is based on the concept that processes may operate more profitably off steady-state than at steady-state. To attain greater economic profitability than the steady-state operating strategy dictated by the RTO-MPC control architecture, EMPC may calculate widely varying or bang-bang type control actions[20,59,107] (which is consistent with the optimal process operation literature mentioned in Chapter 1, which has demonstrated that the economic results from time-varying operation may be highly favorable). However, the possible extreme movement required by the actuation elements when time-varying operation is dictated brings up safety concerns with respect to whether such movement might cause actuators or other components that regulate the process flow rates, such as pumps, to wear out early and thus fail when they are used for safety-critical processes or are crucial to compliance with environmental regulations. If such an issue were to occur, the economic benefits from time-varying process operation under EMPC would no longer matter or be realized.

The issue of reducing the aggressiveness of input changes has been a consideration in the tracking MPC literature since its inception; however, most theoretical studies in EMPC to date have not focused on this issue, but the majority of the literature has instead focused on other concerns like those mentioned in Chapter 1. To extend the foundational results on EMPC to address the issue of input change aggressiveness, additional constraints may be added to EMPC. One type of constraint that has been used extensively for tracking MPC formulations to prevent rapid changes of the actuator output and consequently to prevent rapid changes of the process states is a rate of change constraint on the values of the inputs calculated by the MPC (see, e.g.,[25,44,125,126] for both industrial and research work incorporating such a constraint). For example, in,[116] feasibility and closed-loop stability of linear, discrete-time systems under MPC with input magnitude and rate of

change constraints are proven for both open-loop stable and unstable systems. In,[109] an MPC formulation for input-affine nonlinear systems accounting for input magnitude constraints and input rate of change constraints using a penalty in the objective and hard constraints when possible is proven to be feasible and to ensure closed-loop stability for bounded process uncertainty. Input rate of change constraints have also been used in several works on EMPC. In particular, an MPC including input magnitude and rate of change constraints was used to improve the economic performance of a heat pump by incorporating electricity price and weather forecasts,[141] and EMPC including magnitude and rate of change constraints on the inputs was applied for power production and use.[83] Though input rate of change constraints have been applied to several EMPC examples in the literature, no proof of general feasibility and closed-loop stability for a nonlinear system under an EMPC strategy incorporating both input magnitude and input rate of change constraints with Lyapunov-based constraints that ensure closed-loop stability in the presence of disturbances has yet been developed. The development of such an EMPC strategy will be one of the topics covered in this chapter.

Despite the benefits from an actuator durability perspective of incorporating constraints that prevent an EMPC from calculating aggressive control actions, it would be expected that limiting the control actions that the EMPC can calculate would reduce the economic profitability of the EMPC compared to the case that no input rate of change constraints are used. However, determining whether there is still an economic benefit of EMPC compared with the traditional steady-state paradigm when input rate of change constraints are used in EMPC requires the development of proofs regarding the economic performance of EMPC with input rate of change constraints. Previous proofs of the economic performance of EMPC have not explicitly addressed the case when input rate of change constraints are included in the EMPC formulation. The proofs for many of the methods use terminal constraints in the EMPC[13,16,63] or an EMPC prediction horizon that is sufficiently long with some additional technical conditions (e.g.,[75,114]). Studies to investigate the economic performance of EMPC have been carried out for EMPC with a stage cost and terminal constraints that change with time,[17] for EMPC with a generalized terminal region constraint and

self-tuning terminal cost,[113] for EMPC without terminal costs or constraints for discrete-time systems meeting certain assumptions including controllability and dissipativity assumptions,[76] and a two-layer EMPC structure including performance constraints.[58]

Motivated by all of the above, in this chapter, we introduce a Lyapunov-based economic model predictive control (LEMPC) architecture that can incorporate input rate of change constraints with provable feasibility, stability, and closed-loop performance properties. First, we introduce input rate of change constraints in the context of LEMPC and show that when the constraints are formulated with reference to a Lyapunov-based controller, the LEMPC can be proven to be feasible and to maintain closed-loop stability for a sufficiently small sampling period. Through a chemical process example, we demonstrate that the incorporation of input magnitude and rate of change constraints in EMPC can prevent significant variations in the process inputs while improving the profit compared to steady-state operation. Subsequently, we develop an LEMPC design incorporating a terminal equality constraint based on an explicit stabilizing Lyapunov-based controller for which closed-loop economic performance improvement guarantees with respect to the Lyapunov-based controller (and with respect to steady-state operation when the Lyapunov-based controller is exponentially stabilizing) may be proven for nominal operation. A chemical process example demonstrates the use of this LEMPC strategy. We then show that LEMPC with the terminal equality constraint based on a Lyapunov-based controller, with input magnitude constraints, and with input rate of change constraints retains these provable performance guarantees for nominal operation. This chapter originally appeared in.[50,55,61]

2.2 Preliminaries

2.2.1 Notation

The symbol $|\cdot|$ signifies the Euclidean norm of a vector. A continuous, strictly increasing function $\alpha : [0,a) \to [0,\infty)$ belongs to class $\mathscr{K}$ if $\alpha(0) = 0$. The notation Ω_ρ signifies a level set of a positive definite scalar-valued function $V : R^n \to R_{\geq 0}$ and is defined by $\Omega_\rho := \{x \in R^n \ : \ V(x) \leq$

$\rho,\ \rho > 0\}$. The notation $t_k = k\Delta$, $k = 0,1,2,\ldots$ signifies the time at the beginning of a sampling period of length Δ for synchronously sampled time intervals. Set subtraction is signified by '/' (e.g., $x \in A/B := \{x \in A \ : \ x \notin B\}$). The symbol $S(\Delta)$ denotes the family of piecewise constant vector-valued functions with period $\Delta > 0$. More specifically, $u(\cdot) \in S(\Delta)$ for $t \in [t_k, t_{k+N})$ where N is a positive integer means that the function u can be described by a sequence $\{u^{(j)}\}_{j=k}^{k+N-1}$ where $u^{(j)} \in R^m$, or

$$u(t) = u^{(j)}$$

for $t \in [t_j, t_{j+1})$, $j = k,\ldots,k+N-1$. The notation x^T denotes the transpose of a vector x.

2.2.2 Class of Systems

The class of systems of nonlinear first-order ordinary differential equations considered in this chapter is that of the general form:

$$\dot{x} = f(x,u,w) \tag{2.1}$$

where $x \in R^n$, $u = [u_1\ u_2\ \cdots\ u_m]^T \in R^m$, and $w \in R^l$ are the state, input, and disturbance vectors, respectively, and are related to the time-derivative of the state vector through the nonlinear vector function f. In addition, we assume that the states $x(t)$ are restricted to the set $\mathbb{X}$ ($x(t) \in \mathbb{X} \subset R^n$), that $u_i(t)$, $i = 1,\ldots,m$, are bounded ($u_i(t) \in \mathbb{U}_i := \{u_{i,\min} \le u_i(t) \le u_{i,\max}\}$), and that the disturbance $w(t)$ is bounded within a set $\mathbb{W} \subset R^l$ ($w(t) \in \mathbb{W} := \{w(t) \ : \ |w(t)| \le \theta,\ \theta > 0\}$). For simplicity of presentation in the following, we will use the notation $u(t) \in \mathbb{U} \subset R^m$ to denote that each component $u_i(t)$ of $u(t)$ is bounded within its respective set $\mathbb{U}_i$. The vector function $f : \mathbb{X} \times \mathbb{U} \times \mathbb{W}$ is assumed to be locally Lipschitz with respect to its arguments.

It is assumed that the process economic cost for the system of Eq. 2.1 can be represented by an economic stage cost function $l_e : \mathbb{X} \times \mathbb{U} \to R$ that is continuous on $\mathbb{X} \times \mathbb{U}$. In addition, it is assumed that there is a steady-state and steady-state input pair (x_s^*, u_s^*) for the nominal ($w(t) \equiv 0$) system (on $\mathbb{X} \times \mathbb{U}$) that minimizes the economic cost in the sense that the minimum of l_e is attained at the pair (x_s^*, u_s^*) when the time derivative of the nominal state in Eq. 2.1 is zero. For simplicity,

the minimizing pair is assumed to be unique. With these assumptions, the minimizing steady-state pair is given by:

$$(x_s^*, u_s^*) = \underset{x\in\mathbb{X},u\in\mathbb{U}}{\arg\min} \{l_e(x,u) : f(x,u,0) = 0\} \ .$$

The minimizing pair will be taken to be the origin of the nominal system of Eq. 2.1.

2.2.3 Lyapunov-Based Controller Stabilizability Assumptions under Continuous Implementation

We initially make two stabilizability assumptions for the system of Eq. 2.1 that a Lyapunov-based controller $h(x) = [h_1(x)\ h_2(x)\ \cdots\ h_m(x)]^T$ exists for the nominal system of Eq. 2.1 that renders the origin either locally asymptotically stable or locally exponentially stable in a sense to be made precise in the following two assumptions,[92,104] while also meeting the input constraints. The first assumption covers the weaker of the two cases, that of asymptotic stability, while the second covers exponential stability. With slight abuse of notation, the same notation is used in both assumptions.

Assumption 2.1. *There exists a locally Lipschitz feedback controller $h : \mathbb{X} \to \mathbb{U}$ with $h(0) = 0$ for the nominal system of Eq. 2.1 that renders the origin of the closed-loop system $\dot{x} = f(x,h(x),0)$ asymptotically stable when applied continuously in the sense that there exists a sufficiently smooth Lyapunov function $V : R^n \to R_{\geq 0}$ such that the following inequalities hold:*

$$\alpha_1(|x|) \leq V(x) \leq \alpha_2(|x|) \tag{2.2a}$$

$$\frac{\partial V(x)}{\partial x} f(x,h(x),0) \leq -\alpha_3(|x|) \tag{2.2b}$$

$$\left|\frac{\partial V(x)}{\partial x}\right| \leq \alpha_4(|x|) \tag{2.2c}$$

for all $x \in D$ where D is an open neighborhood of the origin and $\alpha_i \in \mathscr{K}$, $i = 1,2,3,4$.

Assumption 2.2. *There exists a locally Lipschitz feedback controller $h : \mathbb{X} \to \mathbb{U}$ with $h(0) = 0$ for the nominal system of Eq. 2.1 that renders the origin of the system $\dot{x} = f(x,h(x),0)$ exponentially*

stable when applied continuously in the sense that there exists a sufficiently smooth Lyapunov function $V : R^n \to R_{\geq 0}$ *such that the following inequalities hold:*

$$c_1|x|^2 \leq V(x) \leq c_2|x|^2 \tag{2.3a}$$

$$\frac{\partial V(x)}{\partial x} f(x, h(x), 0) \leq -c_3|x|^2 \tag{2.3b}$$

$$\left|\frac{\partial V(x)}{\partial x}\right| \leq c_4|x| \tag{2.3c}$$

for all $x \in D$ *where* D *is an open neighborhood of the origin and* c_i, $i = 1,2,3,4$ *are positive constants.*

We define the set $\Omega_\rho \subseteq \mathbb{X} \subset D$, which is an estimate of the region of attraction of the nominal closed-loop system under a feedback controller meeting either Assumption 2.1 or Assumption 2.2, as the stability region of the closed-loop system for that controller. Methods for designing Lyapunov-based feedback controllers can be found in works such as.[35, 57, 100, 108]

A consequence of our assumption of the Lipschitz continuity of $h(x)$ meeting either Assumption 2.1 or 2.2 is that its components are Lipschitz continuous in x, and thus $L_{h_L} > 0$ exists such that

$$|h_i(x) - h_i(x')| \leq L_{h_L}|x - x'| \tag{2.4}$$

for all $x, x' \in \Omega_\rho$. Here, L_{h_L} is chosen such that it satisfies the bound in Eq. 2.4 with the same value for each $h_i(x)$ (i.e., $L_{h_L} = \max\{L_{h_{L_1}}, \ldots, L_{h_{L_m}}\}$, where $L_{h_{L_i}}$, $i = 1, \ldots, m$, is the smallest positive constant such that $|h_i(x) - h_i(x')| \leq L_{h_{L_i}}|x - x'|$ for all $x, x' \in \Omega_\rho$). The requirement that $h(x)$ and its components are Lipschitz continuous in x does not pose significant practical restrictions.

We note that from the assumption of Lipschitz continuity of f and the bounds on w and u_i, $i = 1, \ldots, m$, there exist $M > 0$, $L_x > 0$, and $L_w > 0$ such that:

$$|f(x, u, w)| \leq M \tag{2.5}$$

$$|f(x,u,w) - f(x',u,0)| \leq L_x|x-x'| + L_w|w| \tag{2.6}$$

for all $x, x' \in \Omega_\rho$, $u_i \in \mathbb{U}_i$, $i = 1,\ldots,m$, and $|w| \leq \theta$. Furthermore, since V is sufficiently smooth, f is locally Lipschitz and Ω_ρ is compact, there exist $L'_x > 0$ and $L'_w > 0$ such that the following also holds:

$$\left|\frac{\partial V(x)}{\partial x} f(x,u,w) - \frac{\partial V(x')}{\partial x} f(x',u,0)\right| \leq L'_x|x-x'| + L'_w|w| \tag{2.7}$$

for all $x, x' \in \Omega_\rho$, $u_i \in \mathbb{U}_i$, $i = 1,\ldots,m$, and $|w| \leq \theta$.

2.2.4 Lyapunov-Based Controller Stabilizability Results for Sample-and-Hold Implementation

Though the system of Eq. 2.1 is continuous and it is assumed that a controller $h(x)$ can be designed that can stabilize the nominal closed-loop system as described in Assumptions 2.1 and 2.2 when implemented continuously, the Lyapunov-based controller will be used in this dissertation to design stability constraints for an economic model predictive control method that is implemented in sample-and-hold. Thus, we develop in this section the stability properties of the nominal closed-loop system of Eq. 2.1 under $h(x)$ applied in sample-and-hold, where $h(x)$ meets either Assumption 2.1 or Assumption 2.2 and Eq. 2.4 when applied continuously. Specifically, we consider the following nonlinear sampled-data system:

$$\dot{x}(t) = f(x(t), h(x(t_k)), 0) \tag{2.8}$$

for $t \in [t_k, t_{k+1})$, where $k = 0, 1, \ldots$. We present two propositions that follow from standard results in the nonlinear sampled-data systems literature to state the stability results for the process under a sample-and-hold controller. The first proposition states that the origin of the sampled-data system of Eq. 2.8 using $h(x)$ that satisfies Assumption 2.1 is rendered practically stable (i.e., the closed-loop state trajectory will converge to a small neighborhood of the origin where it will be maintained thereafter). This result follows from standard results found in the literature

(e.g.,[112,142]). The second proposition states that the origin of the sampled-data system of Eq. 2.8 using $h(x)$ that satisfies Assumption 2.2 is rendered exponentially stable. This result is stronger than the result that can be obtained when $h(x)$ satisfies Assumption 2.1, and the proof can be found, for example, in Corollary 1 of [64] as well as[93] and the results contained therein.

Proposition 2.1. *Let Assumption 2.1 hold and V and Ω_ρ be the Lyapunov function that satisfies Eq. 2.2 and the resulting stability region, respectively. Given $\rho_{\min} \in (0,\rho)$, there exists $\Delta^* > 0$ such that for any $\Delta \in (0,\Delta^*)$ and $x(t_0) \in \Omega_\rho$, the closed-loop state trajectory of the sampled-data system of Eq. 2.8 is always bounded in Ω_ρ and is (uniformly) ultimately bounded in $\Omega_{\rho_{\min}}$ and*

$$\limsup_{t\to\infty} x(t) \in \Omega_{\rho_{\min}} \,. \tag{2.9}$$

Proposition 2.2. *Let Assumption 2.2 hold and V and Ω_ρ be the Lyapunov function that satisfies Eq. 2.3 and the resulting stability region, respectively. There exists $\Delta_e^* > 0$ such that for any $\Delta \in (0,\Delta_e^*)$ the closed-loop state trajectory of the sampled-data system of Eq. 2.8 is always bounded in Ω_ρ and the origin of the sampled-data system of Eq. 2.8 is exponentially stable for all initial states in Ω_ρ.*

We can also develop stability properties for the closed-loop system of Eq. 2.1 in the presence of disturbances under $h(x)$ applied in sample-and-hold, where $h(x)$ meets either Assumption 2.1 or Assumption 2.2 and Eq. 2.4 when applied continuously. Specifically, these results are derived for the following nonlinear sampled-data system:

$$\dot{x}(t) = f(x(t), h(x(t_k)), w(t)) \tag{2.10}$$

for $t \in [t_k, t_{k+1})$, where $k = 0, 1, \ldots$. The following two properties address this sample-and-hold system with disturbances. In both the case that $h(x)$ in Eq. 2.10 meets Assumption 2.1 and the case that it meets Assumption 2.2, only uniform ultimate boundedness of the closed-loop state can be proven. We note that the sampling times and regions within which uniform ultimate boundedness

of the state are proven are different from those in Propositions 2.1-2.2. The proof of the results of the following two propositions can be found, for example, in.[112]

Proposition 2.3. *Let Assumption 2.1 hold and V and Ω_ρ be the Lyapunov function that satisfies Eq. 2.2 and the resulting stability region, respectively. If $\rho_s > 0$, $\Delta > 0$, $\varepsilon_w > 0$, and $\rho^*_{\min} < \rho$ satisfy*

$$\rho^*_{\min} = \max\{V(\bar{x}(t+\Delta)) \ : \ V(\bar{x}(t)) \leq \rho_s\} \tag{2.11}$$

and

$$-\alpha_3(\alpha_2^{-1}(\rho_s)) + L'_x M\Delta + L'_w\theta \leq -\varepsilon_w/\Delta \tag{2.12}$$

for all $\bar{x}(t) \in \Omega_{\rho_s}$ and $\bar{x}(t+\Delta) \in \Omega_\rho$, where $\bar{x}(t)$ is the solution of Eq. 2.1 under a sequence of sample-and-hold control actions $u \in \mathbb{U}$, then there exists Δ^*_w such that for $\Delta < \Delta^*_w$ and $x(t_0) \in \Omega_\rho$, the closed-loop state trajectory of the sampled-data system of Eq. 2.10 is always bounded in Ω_ρ and is (uniformly) ultimately bounded in $\Omega_{\rho^*_{\min}}$ and

$$\limsup_{t\to\infty} x(t) \in \Omega_{\rho^*_{\min}} \ . \tag{2.13}$$

Proposition 2.4. *Let Assumption 2.2 hold and V and Ω_ρ be the Lyapunov function that satisfies Eq. 2.3 and the resulting stability region, respectively. If $\bar{\rho}_s > 0$, $\Delta > 0$, $\bar{\varepsilon}_w > 0$, and $\rho^*_{\min,e} < \rho$ satisfy*

$$\rho^*_{\min,e} = \max\{V(\bar{x}(t+\Delta)) \ : \ V(\bar{x}(t)) \leq \bar{\rho}_s\} \tag{2.14}$$

and

$$-\frac{c_3}{c_2}\bar{\rho}_s + L'_x M\Delta + L'_w\theta \leq \frac{-\bar{\varepsilon}_w}{\Delta} \tag{2.15}$$

for all $\bar{x}(t) \in \Omega_{\bar{\rho}_s}$ and $\bar{x}(t+\Delta) \in \Omega_\rho$, where $\bar{x}(t)$ is the solution of Eq. 2.1 under a sequence of sample-and-hold control actions $u \in \mathbb{U}$, then there exists $\Delta^*_{w,e}$ such that for $\Delta < \Delta^*_{w,e}$ and $x(t_0) \in \Omega_\rho$, the closed-loop state trajectory of the sampled-data system of Eq. 2.10 is always bounded in Ω_ρ

and is (uniformly) ultimately bounded in $\Omega_{\rho^*_{\min,e}}$ *and*

$$\limsup_{t\to\infty} x(t) \in \Omega_{\rho^*_{\min,e}} . \tag{2.16}$$

The requirement that $\rho^*_{\min}$ and $\rho^*_{\min,e}$ be defined with respect to $\bar{x}(t)$ and $\bar{x}(t+\Delta)$, where $\bar{x}(t)$ refers to the closed-loop state of the system of Eq. 2.1 at time t under any sample-and-hold control actions $u \in \mathbb{U}$ (i.e., u is not necessarily represented as an explicit function of x), is made because the results of Propositions 2.3-2.4 will be used later to prove closed-loop stability of the system of Eq. 2.1 under an optimization-based controller with constraints designed based on $h(x)$ but which may compute a control action to implement for a sampling period that is not necessarily equal to $h(x(t_k))$. Therefore, Eqs. 2.11 and 2.14 are written for general $\bar{x}$ so that the definitions of $\rho^*_{\min}$, Δ^*_w, $\rho^*_{\min,e}$, and $\Delta^*_{w,e}$ can be utilized in these later proofs for analyzing a closed-loop system that is not necessarily under $h(x(t_k))$.

It is noted that Assumption 2.2 is stronger than Assumption 2.1 (i.e., whenever Assumption 2.2 is satisfied, Assumption 2.1 is also satisfied). Therefore, for clarity in the remainder of this chapter regarding which results require the stronger conditions in Assumption 2.2 to hold, we will state that the results require Assumption 2.1 when only the conditions of that assumption are required (though the result is then also satisfied if Assumption 2.2 is met), and we will reserve mention of Assumption 2.2 only for those results that require the stronger conditions in that assumption to hold.

2.2.5 Economic Model Predictive Control

This chapter develops a formulation for EMPC with constraints guaranteeing closed-loop stability, satisfaction of bounds on the input rate of change, and an upper bound on the economic cost for the process under the controller. The general formulation of EMPC (which can be augmented with various constraints, model adjustments, or objective function adjustments to give the various

EMPC formulations in Chapter 1) is given by:

$$\min_{u(\cdot)\in S(\Delta)} \quad \int_{t_k}^{t_{k+N}} l_e(\tilde{x}(\tau), u(\tau))\, d\tau \tag{2.17a}$$

$$\text{s.t.} \quad \dot{\tilde{x}}(t) = f(\tilde{x}(t), u(t), 0) \tag{2.17b}$$

$$\tilde{x}(t_k) = x(t_k) \tag{2.17c}$$

$$u_i(t) \in \mathbb{U}_i,\ i = 1, \ldots, m \tag{2.17d}$$

$$\tilde{x}(t) \in \mathbb{X},\ \forall\, t \in [t_k, t_{k+N}) \tag{2.17e}$$

Eq. 2.17 is a general nonlinear optimization problem that minimizes a stage cost $l_e(x(t), u(t))$ (Eq. 2.17a) subject to a model of the nominal system (Eq. 2.17b) and the initial condition in Eq. 2.17c that comes from a measurement of the process state at time t_k. The calculated inputs u_i, $i = 1, \ldots, m$, and the predicted states $\tilde{x}(t)$, $t \in [t_k, t_{k+N})$, are restricted to their respective sets as shown in Eqs. 2.17d-2.17e. In general, additional equality or inequality constraints may be added to a general EMPC with the form in Eq. 2.17 as desired.

The optimization variable in Eq. 2.17 is the piecewise constant optimal control trajectory $u(t)$ over a prediction horizon with N sampling periods of length Δ. Thus, the input profile that is the solution to the EMPC optimization problem is a set of N vectors denoted by $u^*(t|t_k)$, $t = t_k, \ldots, t_{k+N-1}$, of which only the first, $u^*(t_k|t_k)$, is implemented on the process in a sample-and-hold fashion. At t_{k+1}, the EMPC optimization problem is re-solved.

2.2.6 Lyapunov-Based Economic Model Predictive Control

The specific type of EMPC that will be the focus of this chapter is Lyapunov-based economic model predictive control (LEMPC),[79] which is an EMPC with the form of Eq. 2.17 but with the addition of Lyapunov-based stability constraints that define two modes of operation, as shown

below:

$$\min_{u(\cdot)\in S(\Delta)} \quad \int_{t_k}^{t_{k+N}} l_e(\tilde{x}(\tau), u(\tau))\, d\tau \tag{2.18a}$$

$$\text{s.t.} \quad \dot{\tilde{x}}(t) = f(\tilde{x}(t), u(t), 0) \tag{2.18b}$$

$$\tilde{x}(t_k) = x(t_k) \tag{2.18c}$$

$$u_i(t) \in \mathbb{U}_i,\ i = 1, \ldots, m \tag{2.18d}$$

$$\tilde{x}(t) \in \mathbb{X},\ \forall\, t \in [t_k, t_{k+N}) \tag{2.18e}$$

$$V(\tilde{x}(t)) \leq \rho_e,\ \forall\, t \in [t_k, t_{k+N}) \quad \text{if } t_k < t' \text{ and } V(x(t_k)) \leq \rho_e \tag{2.18f}$$

$$\frac{\partial V(x(t_k))}{\partial x} f(x(t_k), u(t_k), 0) \leq \frac{\partial V(x(t_k))}{\partial x} f(x(t_k), h(x(t_k)), 0) \quad \text{if } t_k \geq t' \text{ or } V(x(t_k)) > \rho_e \tag{2.18g}$$

where the notation follows that in Eq. 2.17, with the added constraints in Eqs. 2.18f-2.18g that define two modes of operation of the LEMPC (Modes 1 and 2), and t' is a pre-determined time at which it is desired to apply only Mode 2 of the LEMPC. Mode 1 is active when $t_k < t'$ and when the measured state is within Ω_{ρ_e}, which is a subset of Ω_ρ defined such that if the state at t_k is within Ω_{ρ_e}, then by t_{k+1}, it is still within Ω_ρ, even in the presence of bounded process disturbances or plant-model mismatch. Mode 2 is activated when the measured state is outside of Ω_{ρ_e} due to process disturbances or plant-model mismatch, or once the time t' has been reached. This dual-mode strategy guarantees that the closed-loop state trajectories of the process under LEMPC are maintained within Ω_ρ at all times.

2.3 LEMPC Formulation with Input Magnitude Constraints, Input Rate of Change Constraints, and an Equality Terminal Constraint Based on a Lyapunov-Based Controller

This chapter introduces input rate of change constraints that can be used in an LEMPC framework while guaranteeing closed-loop stability and feasibility of the controller, and it also addresses the performance guarantees that can be made for this LEMPC incorporating input rate of change constraints for nominal process operation (the performance guarantees are also shown to hold in the absence of the input rate of change constraints). The guarantees will be made for a general cost function, so that they will hold even if the objective function of the LEMPC is designed to reduce the input rate of change (for example, a penalty on the input rate of change may be added to the objective function). This chapter thus addresses the questions of not only how to add input rate of change constraints to LEMPC in a manner that does not affect the feasibility and closed-loop stability of the controller, but also of whether that reduces the economic benefits of using LEMPC for a given process.

To develop the answers to these questions, the contributions of this chapter are divided into three parts. In Part 1, we introduce a Lyapunov-based economic model predictive control (LEMPC) architecture that incorporates input magnitude and rate of change constraints with provable feasibility and stability properties, even in the presence of disturbances. In Part 2, we develop a terminal equality constraint based on a Lyapunov-based controller that, when used in an LEMPC for a process with no disturbances or plant-model mismatch (nominal process) ensures that the economic performance of the resulting LEMPC is at least as good as that of the Lyapunov-based controller implemented in sample-and-hold. In Part 3, the results of the first two sections will be combined to show that the nominal process of Eq. 2.1 under an LEMPC with input magnitude and rate of change constraints and a terminal equality constraint based on a

Lyapunov-based controller performs at least as well as it does under the Lyapunov-based controller implemented in sample-and-hold.

2.3.1 Part 1: LEMPC with Input Magnitude and Rate of Change Constraints

In this section, we develop LEMPC with input magnitude constraints that restrict the calculated control actions between an upper and a lower bound, as well as input rate of change constraints, which prevent the calculated inputs between two sampling periods from differing from each other by more than a pre-specified amount. Specifically, we add input rate of change constraints to the LEMPC of Eq. 2.18 (which has input magnitude constraints in Eq. 2.18d). The input rate of change constraints developed are written with respect to a Lyapunov-based controller, but we demonstrate that for a sufficiently small sampling period and an appropriate value of a parameter of the constraints, the constraints developed ensure that the difference between the control actions calculated for two subsequent sampling periods can be bounded by any desired value. We prove that the LEMPC incorporating input rate of change constraints is feasible and furthermore that it ensures closed-loop stability of a process even in the presence of bounded disturbances. The results presented hold for the case that the Lyapunov-based controller meets Assumption 2.1, except where it is noted that Assumption 2.2 is required. Finally, we present a chemical process example to demonstrate the effect of incorporating input rate of change constraints in addition to input magnitude constraints in EMPC, which shows that the manner in which the input rate of change constraints are enforced in EMPC can significantly affect whether the closed-loop process is able to meet other hard constraints.

2.3.1.1 Part 1: Formulation of LEMPC with Input Magnitude and Input Rate of Change Constraints

As noted in Section 2.1 of this chapter, it may be desirable to add input rate of change constraints to LEMPC, especially since Mode 1 of LEMPC attempts to dynamically optimize process operation

within the stability region and does not drive the process to a steady-state. The result of this is that an LEMPC may request input trajectories with sharp changes in the requested control actions (an example is shown in Section 2.3.1.4 of this chapter) to maximize profit subject to the constraints. Restricting the range of allowable control actions in such a case (e.g., increasing $u_{i,\min}$ and/or decreasing $u_{i,\max}$) may ameliorate this issue, but it may be necessary to drastically decrease this range to reduce the difference between two calculated control actions to a desired level, particularly if the LEMPC calculates bang-bang type control actions. Such a drastic reduction in the allowable range of control actions may significantly reduce the process profit; thus, input rate of change constraints may instead be considered as an alternative constraint that achieves the same goal but with potentially higher profit.

The desired form of the input rate of change constraints, assuming that the actuators bring the actuator outputs to the requested values $u_i^*(t_{k-1}|t_{k-1})$, $i = 1,\ldots,m$, before t_k when the LEMPC is re-solved, is as follows:

$$|u_i^*(t_k|t_k) - u_i^*(t_{k-1}|t_{k-1})| \leq \varepsilon_{desired},\ \forall\ i = 1,\ldots,m \tag{2.19}$$

where $\varepsilon_{desired} > 0$ is a bound on the difference between the control action $u_i^*(t_k|t_k)$ implemented at t_k and the immediate past value of the actuator output that was implemented on the process. To make the predicted state trajectories within the LEMPC more consistent with the actual state trajectory, it may also be desirable that the other control actions in the prediction horizon that are not implemented meet the following constraints:

$$|u_i^*(t_j|t_k) - u_i^*(t_{j-1}|t_k)| \leq \varepsilon_{desired},\ \forall\ i = 1,\ldots,m,\ j = k+1,\ldots,k+N-1 \tag{2.20}$$

The chemical process example in Section 2.3.1.4 will show that the decision to enforce both Eqs. 2.19 and 2.20 (imposing restrictions on both the implemented and not implemented control actions) or only Eq. 2.19 (imposing a constraint on the implemented control actions only) may significantly affect the results obtained for LEMPC with input rate of change constraints, and thus

should be carefully considered.

If the input rate of change constraints are written as in Eqs. 2.19-2.20 and directly added into the LEMPC of Eq. 2.18, it is not possible to prove feasibility of the resulting LEMPC, as will be further discussed in Section 2.3.1.3 of this chapter. For this reason, modified constraints are added to the LEMPC of Eq. 2.18 that constrain the calculated control actions to differ by no more than a constant $\varepsilon_r \geq 0$ from the value of the Lyapunov-based control law at $\tilde{x}(t_j),\ j = k,\ldots,k+N-1$. These modified constraints ensure, as will be demonstrated in Section 2.3.1.3, that the LEMPC is feasible, and they also ensure that the desired constraints of Eqs. 2.19-2.20 are met for any $\varepsilon_{desired}$ when ε_r and Δ are suitably chosen.

Incorporating the above considerations, the proposed LEMPC with both input magnitude and rate of change constraints is as follows:

$$\min_{u(\cdot)\in S(\Delta)} \quad \int_{t_k}^{t_{k+N}} l_e(\tilde{x}(\tau),u(\tau))\,d\tau \tag{2.21a}$$

$$\text{s.t.} \quad \dot{\tilde{x}}(t) = f(\tilde{x}(t),u(t),0) \tag{2.21b}$$

$$\tilde{x}(t_k) = x(t_k) \tag{2.21c}$$

$$u_i(t) \in \mathbb{U}_i,\ i = 1,\ldots,m \tag{2.21d}$$

$$\tilde{x}(t) \in \mathbb{X},\ \forall\, t \in [t_k, t_{k+N}) \tag{2.21e}$$

$$|u_i(t_k) - h_i(x(t_k))| \leq \varepsilon_r,\ i = 1,\ldots,m \tag{2.21f}$$

$$|u_i(t_j) - h_i(\tilde{x}(t_j))| \leq \varepsilon_r,\ i = 1,\ldots,m,\ j = k+1,\ldots,k+N-1 \tag{2.21g}$$

$$V(\tilde{x}(t)) \leq \rho_e,\ \forall\, t \in [t_k, t_{k+N})$$

$$\text{if } t_k < t' \text{ and } V(x(t_k)) \leq \rho_e \tag{2.21h}$$

$$\frac{\partial V(x(t_k))}{\partial x} f(x(t_k),u(t_k),0) \leq \frac{\partial V(x(t_k))}{\partial x} f(x(t_k),h(x(t_k)),0)$$

$$\text{if } t_k \geq t' \text{ or } V(x(t_k)) > \rho_e \tag{2.21i}$$

where the notation follows that in Eqs. 2.17 and 2.18. The rate of change constraints of Eqs. 2.19-2.20 are imposed through Eqs. 2.21f-2.21g, which require that the values of $u_i^*(t_j|t_k), i =$

$1,\ldots,m,\ j=k,\ldots,k+N-1$, be within $\varepsilon_r \geq 0$ of the values of $h_i(\tilde{x}(t_j))$. Note that ε_r in Eqs. 2.21f-2.21g is not the same as $\varepsilon_{desired}$ in Eqs. 2.19-2.20, which will be justified in the next section.

Remark 2.1. *It is noted that in the LEMPC formulation of Eq. 2.21, as well as in the other LEMPC formulations developed throughout this chapter, the number of constraints considered is kept to a minimum, and the form of the objective function and the manner of developing such an objective function are not discussed. This is done so that the theoretical developments in this chapter in the proofs to be presented are kept as general as possible and are not obscured by the additional considerations that may arise when the optimization problem is augmented. The results presented in this chapter could be extended, however, to certain cases with additional constraints and may hold practically even when the formulation/assumptions of this chapter are not met, though such an extended study is outside the scope of the present chapter.*

2.3.1.2 Part 1: Rate of Change Constraints Analysis

In this section, we prove that given $\varepsilon_{desired}$, we can ensure that the desired rate of change constraints of Eqs. 2.19-2.20 are met by enforcing the rate of change constraints with respect to $h_i(\tilde{x}(t_j))$, $i=1,\ldots,m,\ j=k,\ldots,k+N-1$, in Eqs. 2.21f-2.21g for a suitable ε_r value, with $h(x)$ meeting Assumption 2.1.

Theorem 2.1. *Consider the closed-loop input trajectories of the process of Eq. 2.1 operated under the LEMPC of Eq. 2.21, with $h(x)$ meeting Assumption 2.1 and Eq. 2.4. If there exist ε_r and $\Delta < \Delta_w^*$ such that for any chosen $\varepsilon_{desired} > 0$,*

$$2\varepsilon_r + L_{h_L} M\Delta \leq \varepsilon_{desired} \tag{2.22}$$

then Eqs. 2.19-2.20 are satisfied for all t_k with $k > 0$ and $u_i^*(t_0|t_0) = h_i(x(t_0))$, $i=1,\ldots,m$.

Proof. From the bound on f in Eq. 2.5 and continuity of x, the following bound holds for all $x(t)$,

$x(t_{k-1}) \in \Omega_\rho$ and $t \in [t_{k-1}, t_k]$, where $x(t)$ is the solution of Eq. 2.1 at time t:

$$|x(t) - x(t_{k-1})| \leq M\Delta \tag{2.23}$$

for Δ sufficiently small (i.e., $\Delta < \Delta_w^*$). In addition, because the bound in Eq. 2.5 and continuity of x hold when $w(t) \equiv 0$ as well, the following inequality holds for the predicted state of the nominal closed-loop system for the LEMPC of Eq. 2.21 (Eq. 2.21b):

$$|\tilde{x}(t) - \tilde{x}(t_{j-1})| \leq M\Delta \tag{2.24}$$

for $\tilde{x}(t)$, $\tilde{x}(t_{j-1}) \in \Omega_\rho$, $t \in [t_{j-1}, t_j]$, $j = k+1, \ldots, k+N$, and $\Delta < \Delta_w^*$. It is noted that because $\Omega_\rho \subseteq \mathbb{X}$, $x(t) \in \Omega_\rho$ implies that $x(t) \in \mathbb{X}$ as required by Eq. 2.21e; the fact that the LEMPC formulation of Eq. 2.21 maintains the state within Ω_ρ is proven in Section 2.3.1.3.

From Eqs. 2.23-2.24 and the Lipschitz continuity property of $h_i(x)$ in x (Eq. 2.4), the following bounds hold for $x(t_k) \in \Omega_\rho$ and $x(t_{k-1}) \in \Omega_\rho$:

$$|h_i(x(t_k)) - h_i(x(t_{k-1}))| \leq L_{h_L}|x(t_k) - x(t_{k-1})| \leq L_{h_L} M\Delta \tag{2.25}$$

$$|h_i(\tilde{x}(t_j)) - h_i(\tilde{x}(t_{j-1}))| \leq L_{h_L}|\tilde{x}(t_j) - \tilde{x}(t_{j-1})| \leq L_{h_L} M\Delta \tag{2.26}$$

for $\Delta < \Delta_w^*$, $j = k+1, \ldots, k+N-1$.

Under the assumption that a feasible solution to the LEMPC of Eq. 2.21 exists and thus that Eqs. 2.21f-2.21g are satisfied (which will be proven in Section 2.3.1.3), we use the constraints of Eqs. 2.21f-2.21g and Eqs. 2.25 and 2.26, in addition to the triangle inequality, to develop upper bounds on the value of the desired rate of change constraints in Eqs. 2.19-2.20 when the LEMPC

of Eq. 2.21 is used to control the process as follows:

$$\begin{aligned}
&|u_i^*(t_k|t_k) - u_i^*(t_{k-1}|t_{k-1})| = \\
&|u_i^*(t_k|t_k) - u_i^*(t_{k-1}|t_{k-1}) - h_i(x(t_k)) + h_i(x(t_k)) - h_i(x(t_{k-1})) + h_i(x(t_{k-1}))| \\
&\qquad \leq |u_i^*(t_k|t_k) - h_i(x(t_k))| + |u_i^*(t_{k-1}|t_{k-1}) - h_i(x(t_{k-1}))| + |h_i(x(t_k)) - h_i(x(t_{k-1}))| \\
&\qquad \leq 2\varepsilon_r + L_{h_L} M\Delta
\end{aligned} \tag{2.27}$$

$$\begin{aligned}
&|u_i^*(t_j|t_k) - u_i^*(t_{j-1}|t_k)| = \\
&|u_i^*(t_j|t_k) - u_i^*(t_{j-1}|t_k) - h_i(\tilde{x}(t_j)) + h_i(\tilde{x}(t_j)) - h_i(\tilde{x}(t_{j-1})) + h_i(\tilde{x}(t_{j-1}))| \\
&\qquad \leq |u_i^*(t_j|t_k) - h_i(\tilde{x}(t_j))| + |u_i^*(t_{j-1}|t_k) - h_i(\tilde{x}(t_{j-1}))| + |h_i(\tilde{x}(t_j)) - h_i(\tilde{x}(t_{j-1}))| \\
&\qquad \leq 2\varepsilon_r + L_{h_L} M\Delta
\end{aligned} \tag{2.28}$$

for $\Delta < \Delta_w^*$ and $j = k+1, \ldots, k+N-1$. It is noted that by assuming $u_i^*(t_0|t_0) = h_i(x(t_0))$, $i = 1, \ldots, m$, then $|u_i^*(t_{k-1}|t_{k-1}) - h_i(x(t_{k-1}))| = 0 \leq \varepsilon_r$ in Eq. 2.27 when $k = 1$, which allows the result of Eq. 2.27 to hold for all $k > 0$. For any $\varepsilon_{desired} > 0$, there always exist ε_r and Δ that are sufficiently small such that $2\varepsilon_r + L_{h_L} M\Delta \leq \varepsilon_{desired}$ if Δ_w^* exists (i.e., Eqs. 2.11-2.12 are satisfied for some $\rho_{\min}^* < \rho$, $\rho_s > 0$, $\theta > 0$, $\Delta > 0$, and $\varepsilon_w > 0$). When these values of ε_r and Δ are chosen, the desired rate of change constraints in Eqs. 2.19-2.20 are met, which follows from Eqs. 2.27-2.28 with the bound in Eq. 2.22. □

Remark 2.2. *The value of $\varepsilon_{desired}$ would typically be chosen based on practical considerations. Because $\varepsilon_{desired}$ depends on the sampling time in Eq. 2.22, one of these practical considerations may be the minimum sampling time possible with the controller software/hardware.*

2.3.1.3 Part 1: Feasibility and Stability Analysis

In this section, we extend the proofs of feasibility and closed-loop stability from[79] for nonlinear processes under LEMPC without input rate of change constraints to those under LEMPC including input rate of change constraints. The results are developed when $h(x)$ used in the design of LEMPC

meets Assumption 2.1, and stronger closed-loop stability results are presented for that case that it meets Assumption 2.2. We first state several propositions to define functions used to state the theorems giving the conditions under which feasibility and closed-loop stability of nonlinear processes under LEMPC with input magnitude and rate of change constraints are guaranteed.

Proposition 2.5. *(c.f.[79,110]) Consider the systems*

$$\dot{x}_a(t) = f(x_a(t), u(t), w(t))$$

$$\dot{x}_b(t) = f(x_b(t), u(t), 0)$$

with initial states $x_a(t_0) = x_b(t_0) \in \Omega_\rho$. There exists a $\mathscr{K}$ function $f_W(\cdot)$ such that

$$|x_a(t) - x_b(t)| \leq f_W(t - t_0),$$

for all $x_a(t), x_b(t) \in \Omega_\rho$ and all $w(t) \in W$ with

$$f_W(\tau) = \frac{L_w \theta}{L_x}(e^{L_x \tau} - 1).$$

Proposition 2.6. *(c.f.[79,110]) Consider the Lyapunov function $V(\cdot)$ of the system of Eq. 2.1 under $h(x)$ meeting Assumption 2.1. There exists a quadratic function $f_V(\cdot)$ such that*

$$V(x) \leq V(x') + f_V(|x - x'|)$$

for all $x, x' \in \Omega_\rho$ with

$$f_V(s) := \alpha_4(\alpha_1^{-1}(\rho))s + M_V s^2$$

where M_V is a positive constant.

Proposition 2.7. *(c.f.[6,112]) Consider the Lyapunov function $V(\cdot)$ of the system of Eq. 2.1 under*

$h(x)$ meeting Assumption 2.2. There exists a quadratic function $f_V(\cdot)$ such that

$$V(x) \leq V(x') + f_V(|x - x'|)$$

for all $x, x' \in \Omega_\rho$ with

$$f_V(s) := \frac{c_4\sqrt{\rho}}{\sqrt{c_1}}s + \beta s^2$$

where β is a positive constant.

In the following theorems, we use the notation developed in Propositions 2.5-2.7 and prove feasibility and closed-loop stability of a process under LEMPC with input magnitude and rate of change constraints in the presence of bounded process disturbances. The theorems extend the results of[79] by requiring a modified bound on Δ based on the results of Section 2.3.1.2 to ensure that the LEMPC of Eq. 2.21 computes control actions that satisfy the desired constraints in Eqs. 2.19-2.20. We present proofs for LEMPC designed using both the asymptotically stabilizing $h(x)$ (Assumption 2.1) and the exponentially stabilizing $h(x)$ (Assumption 2.2).

Theorem 2.2. *Consider the system of Eq. 2.1 in closed-loop under the LEMPC design of Eq. 2.21 based on a controller $h(x)$ that satisfies the conditions of Eq. 2.4 and Assumption 2.1, and assume that $u_i^*(t_0|t_0) = h_i(x(t_0))$, $i = 1, \ldots, m$. Let $\varepsilon_w > 0$, $0 < \Delta < \Delta_w^*$, $\theta > 0$, $\rho > \rho_e \geq \rho_{\min}^* \geq \rho_s > 0$ satisfy*

$$\rho_e \leq \rho - f_V(f_W(\Delta)), \tag{2.29}$$

$$-\alpha_3(\alpha_2^{-1}(\rho_s)) + L_x' M\Delta + L_w'\theta \leq \frac{-\varepsilon_w}{\Delta}, \tag{2.30}$$

and

$$2\varepsilon_r + L_{h_L} M\Delta \leq \varepsilon_{desired} \tag{2.31}$$

where f_V and f_W are defined in Propositions 2.5-2.6. If $x(t_0) \in \Omega_\rho$ and $N \geq 1$ where

$$\rho_{\min}^* = \max\{V(\bar{x}(t+\Delta)) : V(\bar{x}(t)) \leq \rho_s\} \tag{2.32}$$

then the state $x(t)$ of the closed-loop system is always bounded in Ω_ρ and is (uniformly) ultimately bounded in $\Omega_{\rho^*_{\min}}$.

Proof. The proof of closed-loop stability of nonlinear processes under LEMPC with both input magnitude and rate of change constraints, where $h(x)$ satisfies Eq. 2.4 and Assumption 2.1, follows along the lines of that for the LEMPC without input rate of change constraints in[79] because the stability proof depends only on the Lyapunov-based stability constraints in Eqs. 2.21h-2.21i and is unaffected by the added rate of change constraints. Feasibility follows because $u_i(t_k) = h_i(x(t_k))$, $i = 1,\ldots,m$, and $u_i(t_j) = h_i(\tilde{x}(t_j))$, $i = 1,\ldots,m$, $j = k+1,\ldots,k+N-1$, is a solution that meets the Lyapunov-based constraints of Eqs. 2.21h-2.21i, the input constraints of Eq. 2.21d, and the rate of change constraints of Eqs. 2.21f-2.21g, as well as the assumption that the first value of u_i calculated, $u_i^*(t_0|t_0)$, $i = 1,\ldots,m$, is set to $h_i(x(t_0))$, $i = 1,\ldots,m$ (the assumption that $u_i^*(t_0|t_0) = h_i(x(t_0))$, $i = 1,\ldots,m$, is made so that every input calculated by the EMPC, which is all inputs calculated from time t_1 and above since the components of the input vector at t_0 are fixed to $h_i(x(t_0))$, meets the desired constraints of Eqs. 2.19-2.20). The constraint of Eq. 2.21e is satisfied when $x(t) \in \Omega_\rho$ due to the definition of Ω_ρ, and is thus always satisfied when the LEMPC optimization problem is feasible due to the closed-loop stability proof of the LEMPC which shows that $x(t) \in \Omega_\rho$ for $t \geq t_0$ if the LEMPC is feasible and $x(t_0) \in \Omega_\rho$. □

Theorem 2.3. *Consider the system of Eq. 2.1 in closed-loop under the LEMPC design of Eq. 2.21 based on a controller $h(x)$ that satisfies the conditions of Eq. 2.4 and Assumption 2.2, and assume that $u_i^*(t_0|t_0) = h_i(x(t_0))$, $i = 1,\ldots,m$. Let $\bar{\varepsilon}_w > 0$, $0 < \Delta < \Delta^*_{w,e}$, $\theta > 0$, $\rho > \rho_e \geq \rho^*_{\min,e} \geq \bar{\rho}_s > 0$ satisfy*

$$\rho_e \leq \rho - f_V(f_W(\Delta)), \tag{2.33}$$

$$-\frac{c_3}{c_2}\bar{\rho}_s + L'_x M\Delta + L'_w\theta \leq \frac{-\bar{\varepsilon}_w}{\Delta}, \tag{2.34}$$

and

$$2\varepsilon_r + L_{h_L} M\Delta \leq \varepsilon_{desired} \tag{2.35}$$

where f_V and f_W are defined in Propositions 2.5 and 2.7. If $x(t_0) \in \Omega_\rho$ and $N \geq 1$ where

$$\rho^*_{\min,e} = \max\{V(\bar{x}(t+\Delta)) : V(\bar{x}(t)) \leq \bar{\rho}_s\} \tag{2.36}$$

then the state $x(t)$ of the closed-loop system is always bounded in Ω_ρ, and is (uniformly) ultimately bounded in $\Omega_{\rho^*_{\min,e}}$.

Proof. The proof of feasibility of the LEMPC with both input magnitude and rate of change constraints, where $h(x)$ satisfies Eq. 2.4 and Assumption 2.2, is the same as the proof of feasibility of the LEMPC where $h(x)$ satisfies Assumption 2.1 (the proof for feasibility for Theorem 2.2). The proof of closed-loop stability of a process under this LEMPC is an extension of the results in,[79] and the major steps of this proof will be presented here to outline how this extension proceeds.

We first examine the case when $x(t_k) \in \Omega_{\rho_e}$. In this case, the proof that $x(t_{k+1}) \in \Omega_\rho$ when $x(t_k) \in \Omega_{\rho_e}$ and Eq. 2.33 holds follows that in.[79] When instead $x(t_k) \in \Omega_\rho / \Omega_{\rho_e}$, the Mode 2 constraint of Eq. 2.21i is activated which leads to the following bound:

$$\frac{\partial V(x(t_k))}{\partial x} f(x(t_k), u(t_k), 0) \leq \frac{\partial V(x(t_k))}{\partial x} f(x(t_k), h(x(t_k)), 0) \leq -c_3 |x(t_k)|^2 \tag{2.37}$$

where the upper bound follows from Eq. 2.3b. The bound in Eq. 2.37 is then used to bound the time derivative of the Lyapunov function as follows:

$$\dot{V}(x(t)) \leq -c_3|x(t_k)|^2 + \left| \frac{\partial V(x(t))}{\partial x} f(x(t), u(t_k), w(t)) - \frac{\partial V(x(t_k))}{\partial x} f(x(t_k), u(t_k), 0) \right| \tag{2.38a}$$

$$\overset{\text{Eq. 2.7, } |w| \leq \theta}{\leq} -c_3|x(t_k)|^2 + L'_x |x(t) - x(t_k)| + L'_w \theta \tag{2.38b}$$

$$\overset{\text{Eqs. 2.23, 2.3a}}{\leq} -\frac{c_3}{c_2}\bar{\rho}_s + L'_x M\Delta + L'_w \theta \tag{2.38c}$$

for all $t \in [t_k, t_{k+1})$.

If Eq. 2.34 holds, then the time derivative of the Lyapunov function along the closed-loop state trajectories is negative and can be integrated as in[79] to show that when $x(t_k) \in \Omega_\rho / \Omega_{\rho_e}$, the

Lyapunov function decreases between two sampling times, bringing the state back into Ω_{ρ_e} in finite time. When the state re-enters Ω_{ρ_e}, either the Mode 1 constraint in Eq. 2.21h is re-activated, which maintains the state within Ω_ρ between two sampling times as noted above in this proof, or if $t_k \geq t'$, the Mode 2 constraint continues to be enforced, which continues to decrease the Lyapunov function value for $x(t_k) \in \Omega_\rho / \Omega_{\bar{\rho}_s}$ from Eqs. 2.37-2.38c. This causes the state to enter the region $\Omega_{\rho^*_{\min,e}}$ as stated in Proposition 2.4 and maintains it there thereafter. This completes the proof of Theorem 2.3. □

Remark 2.3. *In prior sections, it was mentioned that* $\varepsilon_r \geq 0$ *and* $\varepsilon_{desired} > 0$*, for practical implementation reasons related to controller feasibility. Specifically, the optimization problem of Eq. 2.21 is feasible if* $\varepsilon_r = 0$*, but the only feasible solution is* $u_i(t_k) = h_i(x(t_k))$*,* $i = 1, \ldots, m$*, and* $u_i(t_j) = h_i(\tilde{x}(t_j))$*,* $i = 1, \ldots, m$*,* $j = k+1, \ldots, k+N-1$*, in which case the application of LEMPC to a process when* $\varepsilon_r = 0$ *will be the same as applying the Lyapunov-based controller in sample-and-hold (Eq. 2.10), for which the more complex LEMPC architecture is not necessary. If* $\varepsilon_{desired} = 0$*, however, no* $\Delta > 0$ *can be chosen to satisfy Eqs. 2.31 and 2.35, so it could not be guaranteed through the proofs of Theorems 2.1-2.3 that Eqs. 2.19-2.20 are satisfied if* $\varepsilon_{desired} = 0$ *in this LEMPC.*

Remark 2.4. *The reason that the constraints of Eqs. 2.21f-2.21g are enforced with respect to* $h(x)$*, rather than being enforced as the desired constraints of Eqs. 2.19-2.20, is because there is no guarantee that the constraints of Eqs. 2.19-2.20 are feasible within the LEMPC since they are unrelated to the controller* $h(x)$ *upon which the two constraints of Eqs. 2.21h-2.21i that also must be satisfied are based.*

2.3.1.4 Part 1: Application to a Chemical Process Example

In this section, we use a chemical process example to demonstrate the effect on the computed control actions and process profit of incorporating input rate of change constraints in EMPC. We perform this demonstration by comparing the closed-loop results for a process under three EMPC's: one which does not incorporate input rate of change constraints, a second which imposes

input rate of change constraints only on the implemented inputs, and a third which imposes input rate of change constraints on all control actions in the prediction horizon. This chemical process example shows that input rate of change constraints can be used to reduce wide variations in the control actions and thus process variables while still providing economic benefit compared to steady-state operation, and furthermore shows that the number of sampling periods of the prediction horizon over which the input rate of change constraints are enforced in an EMPC can have a significant impact on whether the EMPC can satisfy other process constraints.

The chemical process considered is the oxidation of ethylene to ethylene oxide in a nonisothermal continuous stirred tank reactor (CSTR), which is assumed to occur according to the following three complex reactions:

$$C_2H_4 + \frac{1}{2}O_2 \rightarrow C_2H_4O \tag{2.39}$$

$$C_2H_4 + 3O_2 \rightarrow 2CO_2 + 2H_2O \tag{2.40}$$

$$C_2H_4O + \frac{5}{2}O_2 \rightarrow 2CO_2 + 2H_2O \tag{2.41}$$

In,[122] the dimensionless material and energy balances for this reactor are developed, with the rate laws for the reactions in Eqs. 2.39-2.41 taken from.[12] The resulting dimensionless equations defining the relationship $\dot{x} = f(x,u,0)$ where $u = [u_1\ u_2]^T$ are as follows:

$$\dot{x}_1 = u_1(1 - x_1x_4) \tag{2.42a}$$

$$\dot{x}_2 = u_1(u_2 - x_2x_4) - A_1e^{\frac{\gamma_1}{x_4}}(x_2x_4)^{0.5} - A_2e^{\frac{\gamma_2}{x_4}}(x_2x_4)^{0.25} \tag{2.42b}$$

$$\dot{x}_3 = -u_1x_3x_4 + A_1e^{\frac{\gamma_1}{x_4}}(x_2x_4)^{0.5} - A_3e^{\frac{\gamma_3}{x_4}}(x_3x_4)^{0.5} \tag{2.42c}$$

$$\dot{x}_4 = \frac{u_1}{x_1}(1 - x_4) + \frac{B_1}{x_1}e^{\frac{\gamma_1}{x_4}}(x_2x_4)^{0.5} + \frac{B_2}{x_1}e^{\frac{\gamma_2}{x_4}}(x_2x_4)^{0.25} + \frac{B_3}{x_1}e^{\frac{\gamma_3}{x_4}}(x_3x_4)^{0.5} - \frac{B_4}{x_1}(x_4 - T_c) \tag{2.42d}$$

where the dimensionless state variables x_1, x_2, x_3, and x_4 represent the dimensionless gas density, ethylene concentration, ethylene oxide concentration, and temperature in the reactor, respectively, and u_1 and u_2 are inputs to the process, with u_1 being the feed volumetric flow rate and u_2 the

Table 2.1: Ethylene Oxide Process Parameters[122]

Parameter	Value	Parameter	Value
γ_1	-8.13	B_1	7.32
γ_2	-7.12	B_2	10.39
γ_3	-11.07	B_3	2170.57
A_1	92.80	B_4	7.02
A_2	12.66	T_c	1.0
A_3	2412.71		

concentration of ethylene in the feed. The parameters in Eqs. 2.42a-2.42d are constants and have the values defined in Table 2.1, which are taken from.[122]

The goal of the process operating strategy is to maximize the yield of ethylene oxide for a limited reactant feedstock, where the yield is defined by the following equation:

$$Y(t_f) = \frac{\int_0^{t_f} u_1(\tau)x_3(\tau)x_4(\tau)d\tau}{\int_0^{t_f} u_1(\tau)u_2(\tau)d\tau} \tag{2.43}$$

where t_f is the time at the end of operation. We assume that the available reactant material is fixed by the following integral material constraint:

$$\int_0^{t_f} u_1(\tau)u_2(\tau)d\tau = 0.175t_f \tag{2.44}$$

Thus, the EMPC's considered in this example will maximize the following stage cost:

$$l_e(x,u) = u_1(t)x_3(t)x_4(t) \tag{2.45}$$

In addition, due to actuator limitations, u_1 and u_2 are restricted to the following sets:

$$0.0704 \leq u_1 \leq 0.7042, \qquad 0.2465 \leq u_2 \leq 2.4648 \tag{2.46}$$

The reactor is initialized at $x_I = [x_{1I}\ x_{2I}\ x_{3I}\ x_{4I}]^T = [0.997\ 1.264\ 0.209\ 1.004]^T$, and a sampling period of $\Delta = 9.36$ is used. The Explicit Euler numerical integration method is used to integrate the ordinary differential equations in Eqs. 2.42a-2.42d using an integration step size of $h_I = 10^{-4}$

within the EMPC and $h_p = 10^{-5}$ for the model used to simulate the process behavior (which is again Eqs. 2.42a-2.42d since it is assumed that there are no disturbances/plant-model mismatch). The open-source interior point optimization software Ipopt[148] was used for all optimizations.

To accomplish the above control objectives, we develop an EMPC, referred to as $EMPC-1$, as follows:

$$\min_{u(\cdot)\in S(\Delta)} \quad \int_{t_k}^{t_{k+N_k}} -u_1(\tau)\tilde{x}_3(\tau)\tilde{x}_4(\tau)d\tau \tag{2.47a}$$

$$\text{s.t.} \quad \dot{\tilde{x}}(t) = f(\tilde{x}(t), u(t), 0) \tag{2.47b}$$

$$\tilde{x}(t_k) = x(t_k) \tag{2.47c}$$

$$0.0704 \leq u_1(t) \leq 0.7042, \; \forall \, t \in [t_k, t_{k+N_k}) \tag{2.47d}$$

$$0.2465 \leq u_2(t) \leq 2.4648, \; \forall \, t \in [t_k, t_{k+N_k}) \tag{2.47e}$$

$$\frac{1}{t_p}\int_{jt_p}^{t_k} u_1^*(\tau)u_2^*(\tau)d\tau + \frac{1}{t_p}\int_{t_k}^{t_{k+N_k}} u_1(\tau)u_2(\tau)d\tau = 0.175 \tag{2.47f}$$

where the notation is as in Eq. 2.21 except that the problem is implemented with a shrinking horizon of length N_k and the material constraint is implemented over operating periods of length t_p to reduce the computation time. Ten operating periods, each of length $t_p = 46.8$, under this EMPC were simulated. The index j signifies the number of operating periods that have passed prior to the current one ($j = 0, \ldots, 9$), and $u_1^*(t)$ and $u_2^*(t)$ represent the previously computed and applied input trajectories ($u_1^*(t) = u_1^*(t_q|t_q)$ for $t \in [t_q, t_{q+1})$, and $u_2^*(t) = u_2^*(t_q|t_q)$ for $t \in [t_q, t_{q+1})$, where t_q varies between jt_p and t_{k-1} in Eq. 2.47f). N_k is initialized to $\frac{t_p}{\Delta} = 5$ at the beginning of each operating period and is decremented by one at the beginning of each sampling period. The results of the simulations under $EMPC-1$ are shown as the solid lines in Figs. 2.1-2.2. As seen in Fig. 2.2, the EMPC determines that the optimal input trajectories are those for which the inputs make extreme jumps throughout each operating period, which in turn causes significant variation in the state variables, as shown in Fig. 2.1, especially in x_2 and x_3.

We now suppose that we do not want to have such rapid changes in the requested control actions. As a result, we impose input rate of change constraints in the EMPC to allow it to continue

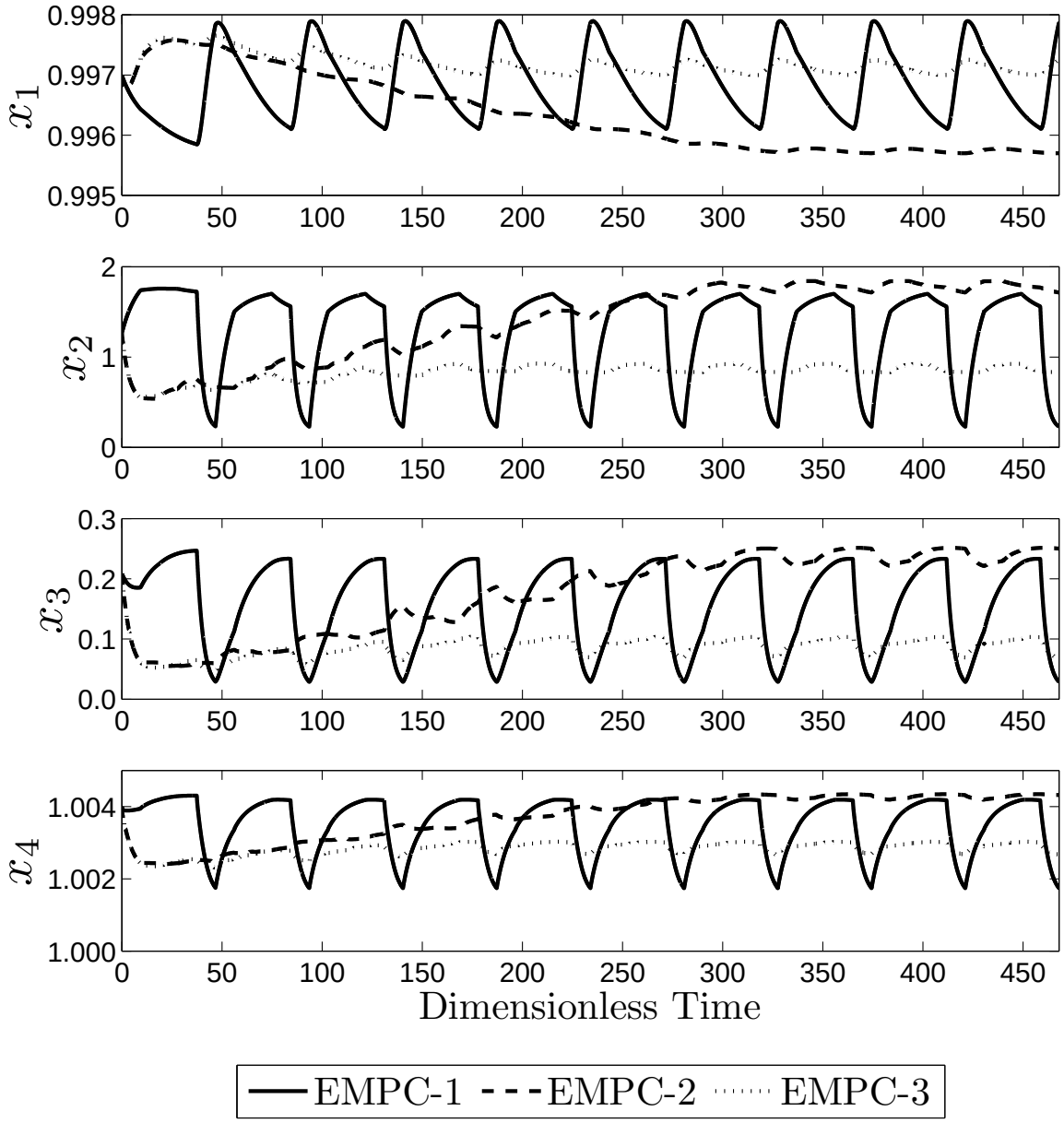

Figure 2.1: State trajectories for the process of Eqs. 2.42a-2.42d under $EMPC-1$, $EMPC-2$, and $EMPC-3$.

to optimize the process economics throughout the whole range of u_1 and u_2, but without taking extreme, sudden action to do so. We enforce that the difference between two control actions can be no more than 0.1. We formulate two EMPC's with input rate of change constraints, the first of which ($EMPC-2$) enforces the rate of change constraint only on the first control action that will be implemented, and the second of which ($EMPC-3$) enforces the rate of change constraint at each sampling period in the shrinking prediction horizon N_k. Thus, $EMPC-2$ solves the optimization problem of Eq. 2.47 with the added constraints:

$$|u_1(t_k) - u_1^*(t_{k-1}|t_{k-1})| \leq 0.1 \tag{2.48a}$$

$$|u_2(t_k) - u_2^*(t_{k-1}|t_{k-1})| \leq 0.1 \tag{2.48b}$$

and $EMPC-3$ solves the optimization problem of Eq. 2.47 with the added constraints in Eqs. 2.48a-2.48b plus the additional constraints:

$$|u_1(t_j) - u_1(t_{j-1})| \leq 0.1,\ j = k+1,\ldots,k+N_k-1 \tag{2.49a}$$

$$|u_2(t_j) - u_2(t_{j-1})| \leq 0.1,\ j = k+1,\ldots,k+N_k-1 \tag{2.49b}$$

The Lyapunov-based constraints in Eqs. 2.21h-2.21i were not considered for this example because the process is operated within a region around an open-loop asymptotically stable steady-state and showed no closed-loop stability issues during the simulations of the three EMPC's. Because no Lyapunov-based constraints were employed, the input rate of change constraints used were those in Eqs. 2.48a-2.49b, which are written in terms of the desired rate of change as in Eqs. 2.19-2.20, rather than based off of the controller $h(x)$ as was done in the LEMPC of Eq. 2.21. The state and input trajectories for the simulations of the closed-loop system of Eqs. 2.42a-2.42d under $EMPC-2$ and $EMPC-3$ are plotted against the state and input trajectories for the closed-loop system under $EMPC-1$ in Figs. 2.1-2.2.

The yields (according to Eq. 2.43) for the process under the three different EMPC's are shown

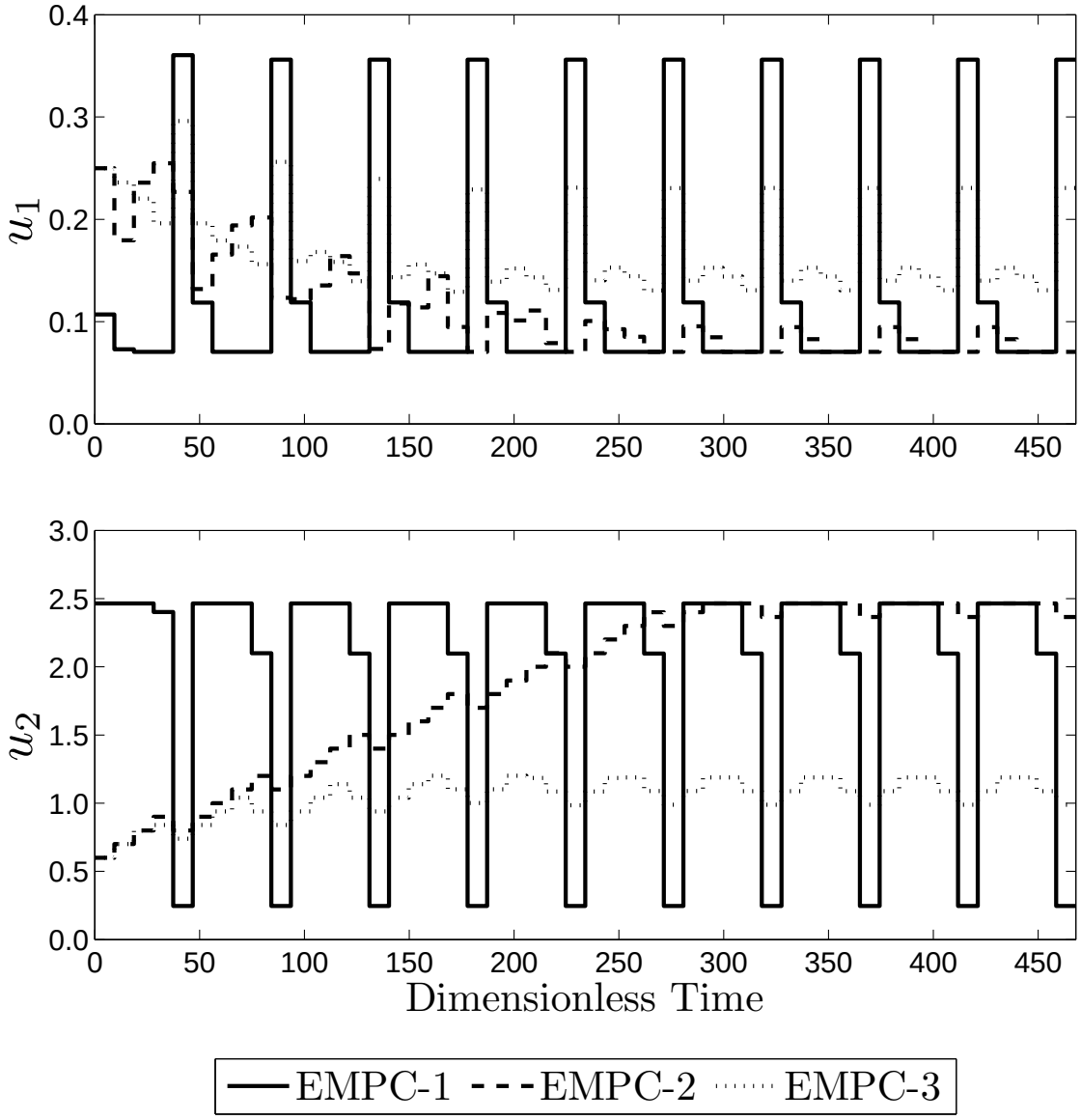

Figure 2.2: Input trajectories for the process of Eqs. 2.42a-2.42d under $EMPC-1$, $EMPC-2$, and $EMPC-3$.

Table 2.2: Process Yield

Process	Yield
$EMPC-1$	9.61%
$EMPC-2$	9.56%
$EMPC-3$	8.23%
SS	6.63%

in Table 2.2 and compared to the yield for the steady-state case (SS in the table) obtained by starting at x_I and using the constant input vector $u_s = [u_{1s}\ u_{2s}]^T = [0.35\ 0.5]^T$ to bring the process states to the open-loop asymptotically stable steady-state $[x_{1s}\ x_{2s}\ x_{3s}\ x_{4s}] = [0.998\ 0.424\ 0.032\ 1.002]$.

As shown in Figs. 2.1-2.2, the input rate of change constraints significantly reduce the variability in the state and input trajectories as desired, while still allowing optimization of the process economics, as shown by the periodic trajectories that still exist in the state and input trajectories for $EMPC-3$, though with reduced amplitude compared to those under $EMPC-1$. As expected, the addition of input rate of change constraints reduces the ability of the EMPC to maximize the yield of the process to its fullest extent (the yield under $EMPC-1$ is 16.8% greater than that under $EMPC-3$). However, even with the input rate of change constraints, $EMPC-3$ outperforms steady-state operation (the yield under $EMPC-3$ is 24.1% greater than that for steady-state operation).

Because the input rate of change constraints in $EMPC-2$ are not enforced at every sampling period, $EMPC-2$ becomes infeasible in the last sampling period of all operating periods after the third (when Ipopt determines a problem is locally infeasible, it returns a solution that locally minimizes the constraint violation using a separate optimization problem[147]). In each of the operating periods in which $EMPC-2$ is infeasible, the process' use of reactant material exceeded the value of the integral constraint, in some operating periods by as much as 8.7%. Thus, the value of the yield reported in Table 2.2 for $EMPC-2$ cannot be compared with the yields of $EMPC-1$ and $EMPC-3$ because $EMPC-1$ and $EMPC-3$ met the process constraints, while $EMPC-2$ did not. The violation of the integral constraint by $EMPC-2$ occurs because $EMPC-2$ predicts that there can be sharp changes in all inputs in the prediction horizon except those for the first

sampling period, which are forced to stay within 0.1 of the previous input value. Thus, because of the lack of foresight of $EMPC-2$, the implemented control actions for the first four sampling periods in most of the operating periods use too much of the reactant material, with the result that there is no way that the integral constraint can be met in the last sampling period of the operating periods if the rate of change constraints and hard bounds on the inputs are also to be met.

We note that though we did not formulate the constraints of $EMPC-3$ with respect to a Lyapunov-based controller which, as was proven above in this chapter, ensures feasibility of the optimization problem, no issues with feasibility of the solution of $EMPC-3$ were encountered. This can occur in practice, and emphasizes that the requirements for feasibility of an EMPC with input rate of change constraints as developed in this chapter, such as formulating the constraints as in Eqs. 2.21f-2.21g rather than as in Eqs. 2.19-2.20, are conservative. For example, in this problem, we set $u^*(t_{-1}|t_{-1}) = u_s$. The input vector u_s satisfies all constraints in Eqs. 2.47-2.49b, and thus is itself a feasible input trajectory. Because $EMPC-3$ recognizes that all future inputs in the prediction horizon must meet the input rate of change constraint, when it finds a solution that outperforms steady-state operation but is able to satisfy the constraints, this solution is feasible both in the current operating period and also, in reverse, in the next (because for this problem, we assume that the plant follows the nominal process model and that all constraints depend only on u_1 and u_2, not on process states, so the input trajectory just implemented, in reverse, will be feasible for the next operating period). By progressing in this manner, the full input trajectory that $EMPC-3$ takes is feasible in reverse, and it is able to settle to an off steady-state input trajectory without feasibility issues.

To evaluate the robustness of $EMPC-3$ when there are process disturbances ($w(t) \not\equiv 0$), the process of Eqs. 2.42a-2.42d was simulated under $EMPC-3$, but with bounded Gaussian white noise added to the right-hand side of Eqs. 2.42a-2.42d for the simulation of the process outside of the EMPC, with zero mean, standard deviation vector $[\sigma_{x_1}\ \sigma_{x_2}\ \sigma_{x_3}\ \sigma_{x_4}]^T = [0.6\ 10\ 1.8\ 0.6]^T$, and bound vector $[\theta_{x_1}\ \theta_{x_2}\ \theta_{x_3}\ \theta_{x_4}]^T = [1.8\ 30\ 5.4\ 1.8]^T$. The standard deviations and bounds were chosen such that the noise had a significant effect on the process states. The simulation

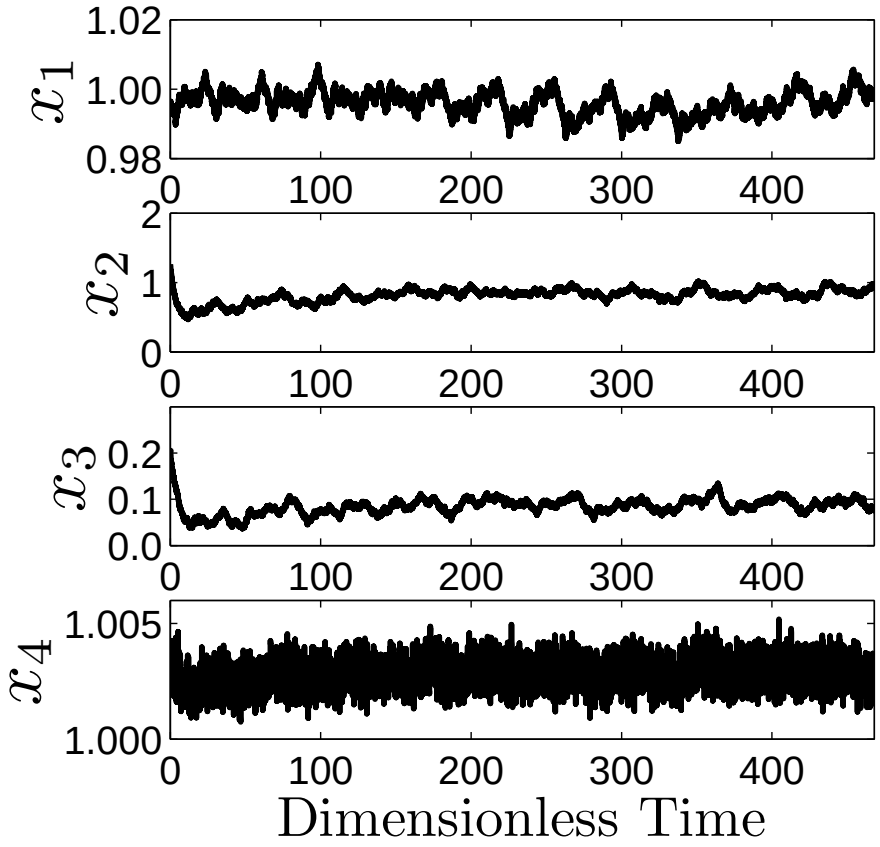

Figure 2.3: State trajectories for the process of Eqs. 2.42a-2.42d under $EMPC-3$ in the presence of bounded disturbances.

results are shown in Figs. 2.3-2.4, and demonstrate that $EMPC-3$ incorporating input rate of change constraints maintained closed-loop stability of the process in the presence of bounded disturbances. In addition, it met the integral material constraint and was feasible in all sampling periods, demonstrating the robustness of the controller.

Remark 2.5. *It is noted that the periodic state trajectories for* $EMPC-1$ *and* $EMPC-3$ *in Fig. 2.1 are the result of the periodic input policies in Fig. 2.2. The periodic input policies are chosen by the EMPC because the EMPC found that that was the most economically optimal input policy; this is consistent with prior work on the ethylene oxide production process example (e.g.,*[59,122]*), which showed that a periodic operating policy is more economically optimal than steady-state operation for this example. The integral constraint of Eq. 2.44 plays a role in the periodic trajectories observed because it requires that within each operating period, only a certain*

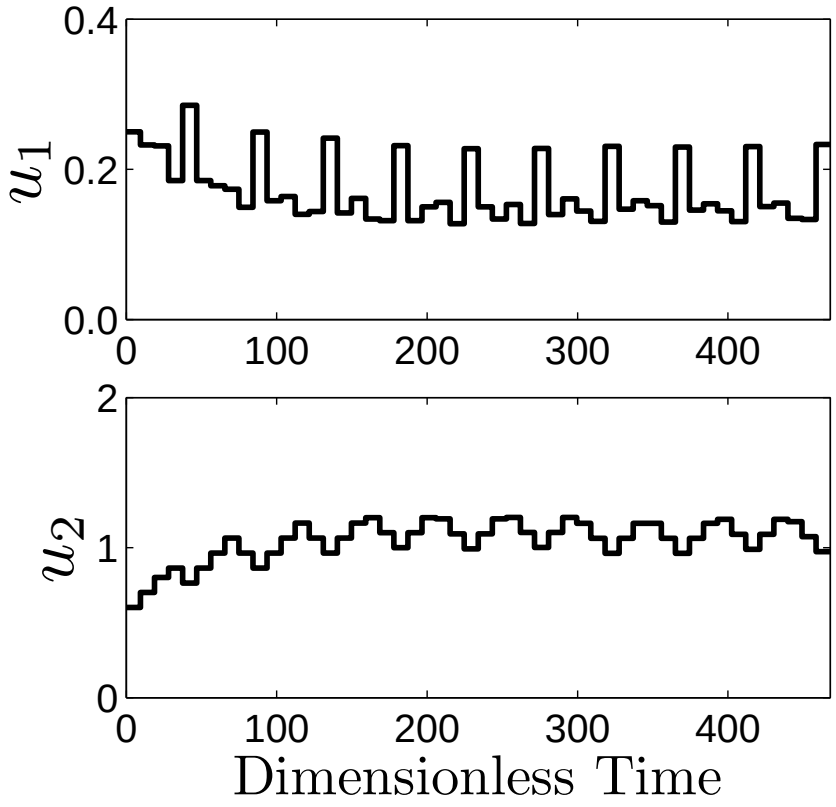

Figure 2.4: Input trajectories for the process of Eqs. 2.42a-2.42d under *EMPC* – 3 in the presence of bounded disturbances.

amount of material can be used. Despite the periodic nature of the trajectories, the closed-loop states remain in a bounded region in state-space around the asymptotically stable steady-state such that the closed-loop process is stable in the sense that the states remain within a bounded region.

2.3.2 Part 2: LEMPC with a Terminal Constraint Design Based on a Lyapunov-Based Controller

In this section, we further build toward the development of provable performance guarantees for LEMPC with input rate of change constraints by developing an LEMPC formulation (without input rate of change constraints) for which provable performance guarantees can be made for nominal operation. Specifically, an LEMPC incorporating a terminal equality constraint based on a Lyapunov-based controller will be developed, and performance guarantees will be made for this LEMPC for both finite-time and infinite-time. While a number of performance results have been developed for other EMPC formulations (such as EMPC with a terminal steady-state equality constraint[16,47] or a terminal region constraint[13]), few performance results have appeared for LEMPC. Previous performance results for LEMPC have been developed utilizing solutions from an auxiliary tracking MPC;[58,80] the performance guarantees for LEMPC developed in this section compare the closed-loop performance under LEMPC not with that under MPC but with that under a Lyapunov-based controller implemented in sample-and-hold. Like many other EMPC performance guarantees, those made in this chapter rely on the use of a terminal constraint and thus hold only for nominal process operation; however, they have several advantages over performance guarantees developed for some other formulations of EMPC in that an *a priori* characterization of the feasible region is possible and because the terminal constraint is not necessarily the economically optimal steady-state (in the design the terminal constraint asymptotically converges to the economically optimal steady-state or a neighborhood of it, depending on the properties of $h(x)$), the resulting LEMPC may give a larger feasible region relative to an EMPC with a terminal equality constraint equal to the economically optimal steady-state.

To develop the LEMPC with a terminal equality constraint based on a Lyapunov-based

controller and its provable performance guarantees, this section begins with a description of the LEMPC formulation for which provable performance guarantees can be made, which is an LEMPC of the form of Eq. 2.18 but without Eq. 2.18g (since only nominal operation is considered) and with the addition of a terminal equality constraint based on the same Lyapunov-based controller as is used to develop the Lyapunov-based stability constraint of Eq. 2.18f (we note that the LEMPC, like that with input magnitude and rate of change constraints developed in Part 1, has input magnitude constraints with the form in Eq. 2.18d, but since the input trajectories themselves are not the focus of Part 2, this will not be further highlighted in Part 2). Subsequently, it is shown that when there are no disturbances and when there is no plant-model mismatch, the LEMPC with a terminal equality constraint based on $h(x)$ is feasible and maintains closed-loop stability of the nominal process in the sense of boundedness of the closed-loop state. Following this development, the performance properties of the controller are proven on both the finite-time and infinite-time intervals for a Lyapunov-based controller satisfying Assumption 2.1 and for a Lyapunov-based controller satisfying Assumption 2.2 (for $h(x)$ meeting Assumption 2.2, the infinite-time performance result is equivalent to the statement that the nominal process under LEMPC with a terminal constraint based on a Lyapunov-based controller performs at least as well in infinite-time as it does under steady-state operation). Finally, a chemical process example is presented that demonstrates the use of the LEMPC incorporating a terminal equality constraint based on a Lyapunov-based controller and shows that for a short prediction horizon used in an EMPC, the use of terminal equality constraints in the EMPC may be crucial to improving process economic performance over steady-state operation.

2.3.2.1 Part 2: Formulation of LEMPC with a Terminal Equality Constraint Based on a Lyapunov-Based Controller

In the standard LEMPC design,[79] an EMPC scheme is designed by taking advantage of a Lyapunov-based controller (meeting Assumption 2.1 or Assumption 2.2), a corresponding Lyapunov function, and the stability region. Though feasibility, closed-loop stability, and

robustness to sufficiently small disturbances may be proven for this standard LEMPC design, guaranteed closed-loop performance under the resulting LEMPC cannot be proven in general without additional conditions or constraints (the standard LEMPC design does not incorporate terminal constraints[75,114]). Nevertheless, owing to the availability of the Lyapunov-based controller of Assumption 2.1 or Assumption 2.2, the corresponding Lyapunov function, and the stability region used to design LEMPC, a terminal equality constraint may be readily designed for the LEMPC problem that allows performance guarantees to be made for nominal process operation while maintaining the unique recursive feasibility property of LEMPC for all initial states in Ω_ρ. In this chapter, the terminal constraint is computed from the solution of the sampled-data system of Eq. 2.8 (where h meets either Assumption 2.1 or Assumption 2.2).

Because the terminal constraint is derived from the solution of Eq. 2.8, it is necessary to define notation that distinguishes the solution of Eq. 2.8 from the solution of the LEMPC. To distinguish the state and input trajectories of the system under the Lyapunov-based controller implemented in sample-and-hold (Eq. 2.8) from the state and input trajectories of the closed-loop system under LEMPC incorporating a terminal equality constraint derived from Eq. 2.8, z and v will be used for the former, and x and u^* will be used for the latter. Thus, for simplicity of notation, the sampled-data system consisting of the nominal system of Eq. 2.1 under the sample-and-hold implementation of the Lyapunov-based controller is given by:

$$\begin{aligned} \dot{z}(t) &= f(z(t), v(t), 0) \\ v(t) &= h(z(t_k)) \end{aligned} \tag{2.50}$$

for $t \in [t_k, t_{k+1})$, $k = 0, 1, \ldots$ with initial condition $z(0) = z_0 \in \Omega_\rho$. The sampled-data system consisting of the nominal system of Eq. 2.1 under the sample-and-hold inputs computed by the LEMPC with a terminal equality constraint based on the Lyapunov-based controller is given by:

$$\begin{aligned} \dot{x}(t) &= f(x(t), u^*(t), 0) \\ u^*(t) &= u^*(t_k|t_k) \end{aligned} \tag{2.51}$$

for $t \in [t_k, t_{k+1})$, $k = 0, 1, \ldots$ with initial condition $x(0) = x_0 \in \Omega_\rho$, where $x_0 = z_0$. It is noted that the two sampled-data systems in Eqs. 2.50 and 2.51 are initiated from the same initial condition, but the system of Eq. 2.50 only incorporates feedback of $z(t_k)$ without any reference to the measured state of the sampled-data system of Eq. 2.51, and the sampled-data system of Eq. 2.51 only incorporates feedback of $x(t_k)$ (though it does require $z(t_{k+N})$ for the determination of the input $u^*(t)$ that is applied to the system, as will be shown subsequently).

The solution of the sampled-data system of Eq. 2.50 is used to design a terminal equality constraint for LEMPC that requires that the predicted state at the end of the prediction horizon ($\tilde{x}(t_{k+N})$) be equal to the solution of Eq. 2.50 at time t_{k+N} ($z(t_{k+N})$), where the function h in Eq. 2.50 is the same h used to design V and Ω_ρ in the LEMPC. The terminal condition $z(t_{k+N})$ is determined at each sampling time as follows:

Step 1. At the initial time $t_0 = 0$, $z(t_N)$ is computed by first initializing the system of Eq. 2.50 at $z_0 = x_0$ (a measurement of the state of Eq. 2.51 at the initial time) and recursively solving the system from the initial time to $t_N = N\Delta$. Then, the state $z(t_N)$ is used as a terminal equality constraint in an LEMPC problem solved at $t = 0$.

Step 2. For all sampling times after t_0, the terminal constraint that is imposed in the LEMPC problem at t_k is computed by recursively solving the system of Eq. 2.50 from $z(t_k)$ to $z(t_{k+N})$ (because only nominal operation is considered and $z(t_{k+N-1})$ was computed at the previous sampling time, it is only necessary to recursively solve the system of Eq. 2.50 from t_{k+N-1} to t_{k+N} to obtain the solution from $z(t_k)$ to $z(t_{k+N})$ if the solution from the previous sampling time was stored; for added robustness, especially to numerical and discretization errors, one may reinitialize the system of Eq. 2.50 with a state measurement $z(t_k)$ at each sampling time and numerically integrate forward from this measurement to compute $z(t_{k+N})$, but in the nominal operating setting considered here, numerical and discretization errors are not considered).

Using the terminal equality constraint described above, the formulation of the LEMPC with the terminal equality constraint formulated based on the state z obtained under the Lyapunov-based

controller is given by the problem:

$$\min_{u(\cdot)\in S(\Delta)} \int_{t_k}^{t_{k+N}} l_e(\tilde{x}(\tau), u(\tau))\, d\tau \tag{2.52a}$$

$$\text{s.t.} \quad \dot{\tilde{x}}(t) = f(\tilde{x}(t), u(t), 0) \tag{2.52b}$$

$$\tilde{x}(t_k) = x(t_k) \tag{2.52c}$$

$$\tilde{x}(t_{k+N}) = z(t_{k+N}) \tag{2.52d}$$

$$u(t) \in \mathbb{U},\ \forall\, t \in [t_k, t_{k+N}) \tag{2.52e}$$

$$\tilde{x}(t) \in \mathbb{X},\ \forall\, t \in [t_k, t_{k+N}) \tag{2.52f}$$

$$V(\tilde{x}(t)) \leq \rho,\ \forall\, t \in [t_k, t_{k+N}) \tag{2.52g}$$

where the notation follows that in Eqs. 2.17 and 2.18 and, as noted in Section 2.2.2, $u(t) \in \mathbb{U}$ is equivalent to $u_i \in \mathbb{U}_i$, $i = 1, \ldots, m$. Because $\rho_e = \rho$ for nominal process operation, the Mode 1 constraint of Eq. 2.52g enforces that the predicted state remain in Ω_ρ throughout the prediction horizon. The terminal constraint of Eq. 2.52d forces the computed input trajectory to steer the predicted state trajectory to the state $z(t_{k+N})$ at the end of the prediction horizon. This terminal constraint differs from traditional terminal equality constraints in the sense that it is not necessarily a steady-state. However, the terminal constraint in the LEMPC of Eq. 2.52 converges to a neighborhood of the steady-state owing to the stability properties of the Lyapunov-based controller (if h used in the design of Eq. 2.52 meets Assumption 2.1 and $\Delta < \Delta^*$, then $z(t)$ eventually enters $\Omega_{\rho_{\min}}$ from Proposition 2.1, and if h used in the design of Eq. 2.52 meets Assumption 2.2 and $\Delta < \Delta_e^*$, then $z(t)$ reaches the steady-state in infinite-time from Proposition 2.2). A difference between the standard LEMPC design of Eq. 2.18 and the LEMPC incorporating a terminal equality constraint in Eq. 2.52 is that there is no contractive constraint in the LEMPC with a terminal equality constraint. The reason for this difference is that only nominal operation is considered for the LEMPC with a terminal equality constraint, so only the constraint in Eq. 2.52g is required to ensure closed-loop stability in the sense that the state trajectory will be maintained within the

stability region Ω_ρ for all times. The effect of including the contractive constraint will be discussed in Section 2.3.2.2, along with the stability and feasibility properties of the LEMPC incorporating a terminal equality constraint based on the Lyapunov-based controller.

The LEMPC of Eq. 2.52 is implemented according to a standard receding horizon implementation. At each sampling time t_k, a state measurement $x(t_k)$ is received and the terminal constraint $z(t_{k+N})$ is computed. The optimization problem of Eq. 2.52 is solved with the computed $z(t_{k+N})$ to obtain the input trajectory over the prediction horizon. However, only the control action computed for the first sampling period of the prediction horizon is implemented on the system. At the next sampling time, a new state measurement is obtained, a new terminal constraint is computed, and the optimization problem is re-solved with the updated parameters to obtain the control action for the next sampling period.

2.3.2.2 Part 2: Feasibility and Stability Analysis

In this section, we develop a theorem stating that the LEMPC of Eq. 2.52 is feasible and maintains closed-loop stability of the nominal system of Eq. 2.1 when the Lyapunov-based controller used in the design of the LEMPC meets Assumption 2.1 and a sufficiently small sampling period is utilized.

Theorem 2.4. *Consider the system of Eq. 2.1 with $w(t) \equiv 0$ in closed-loop under the LEMPC design of Eq. 2.52 based on a controller h that satisfies the conditions of Eq. 2.4 and Assumption 2.1. Let $\rho > 0$, and $0 < \Delta < \Delta^*$. If $x(t_0) \in \Omega_\rho$ and $N \geq 1$, then the state $x(t)$ of the closed-loop system is always bounded in Ω_ρ.*

Proof. Recursive feasibility of the optimization problem of Eq. 2.52 is guaranteed when the conditions of Theorem 2.4 are met because the sample-and-hold input trajectory obtained from the Lyapunov-based controller is a feasible solution to the optimization problem at t_0 (i.e., the input trajectory $u(t) = v(t)$, $t \in [t_0, t_N)$ satisfies the input constraint of Eq. 2.52e and the terminal constraint of Eq. 2.52d by design, it satisfies Eq. 2.52g because the Lyapunov-based controller implemented in sample-and-hold maintains the state within Ω_ρ from Proposition 2.1 when $\Delta < \Delta^*$,

and it satisfies Eq. 2.52f since Eq. 2.52g is satisfied and $\Omega_\rho \subseteq \mathbb{X}$). At the next sampling time (t_1), $u(t) = u^*(t_j|t_0)$ for $t \in [t_j, t_{j+1})$, $j = 1, \ldots, N-1$ (which drives $\tilde{x}(t_N)$ to $z(t_N)$ since $u^*(t_j|t_0)$, $j = 0, \ldots, N-1$, was feasible at the previous sampling time and thus Eq. 2.52d is satisfied for this input trajectory), and $u(t) = h(z(t_N))$ for $t \in [t_N, t_{N+1})$ is a feasible solution to the optimization problem because nominal operation is considered. At subsequent sampling times (i.e., at t_k), a feasible solution to the LEMPC of Eq. 2.52 is, similarly, the part of the solution from the previous sampling time that was not implemented followed by $h(z(t_{k+N-1}))$ utilized for the last sampling period in the prediction horizon. This shows that for nominal operation, the LEMPC of Eq. 2.52 is always feasible. Closed-loop stability of the LEMPC of Eq. 2.52 in the sense that the closed-loop state trajectory is maintained within Ω_ρ at all times is guaranteed when the optimization problem is feasible owing to the fact that the Lyapunov-based constraint of Eq. 2.52g is imposed in the optimization problem and nominal operation is considered. □

Though the terminal condition itself converges to the origin or a neighborhood of it, the input trajectory generated by applying the input calculated for the first sampling period of each prediction horizon may not drive the process state to the origin or a small neighborhood of it. The LEMPC of Eq. 2.52 may be extended to include the two-mode control strategy of Eq. 2.18, or the contractive constraint in Eq. 2.18g may be added to the LEMPC of Eq. 2.52 to drive the process state to a neighborhood of the origin, even in the presence of disturbances, if the resulting LEMPC remains feasible. However, the performance results to be developed in Section 2.3.2.3 hold for the nominal case.

Remark 2.6. *It has been previously noted in this chapter that the feasible region of LEMPC with a terminal equality constraint based on a Lyapunov-based controller can be explicitly characterized a priori. Theorem 2.4 and its proof show that the feasible region is the stability region of the LEMPC.*

2.3.2.3 Part 2: Closed-Loop Performance Analysis

In this section, we prove that the economic performance of the LEMPC of Eq. 2.52 is at least as good as that of the Lyapunov-based controller used in its design in both finite-time and infinite-time. The analysis techniques used follow those of,[16] which analyzes the closed-loop performance of EMPC formulated with an equality terminal constraint equal to x_s^*. In the following, $J_e^*(x(t_k))$ denotes the optimal value of the objective function of the optimization problem of Eq. 2.52 at time t_k given the state measurement $x(t_k)$.

The first performance result, presented in the following theorem, gives the finite-time performance of the process under the LEMPC of Eq. 2.52 designed with a Lyapunov-based controller that satisfies Assumption 2.1.

Theorem 2.5. *Consider the closed-loop system of Eq. 2.1 with $w(t) \equiv 0$ under the LEMPC of Eq. 2.52 based on a Lyapunov-based controller that satisfies Assumption 2.1. Let $\Delta \in (0, \Delta^*)$ where $\Delta^* > 0$ is the conclusion of Proposition 2.1. For any strictly positive finite integer T, the closed-loop economic performance under the LEMPC of Eq. 2.52 is bounded by:*

$$\int_0^{T\Delta} l_e(x(t), u^*(t))\, dt \leq \int_0^{(T+N)\Delta} l_e(z(t), v(t))\, dt \tag{2.53}$$

where x and u^* denote the closed-loop state and input trajectories of the system of Eq. 2.51 and z and v denote the state and input trajectories of the system of Eq. 2.50 where $z(0) = x(0) \in \Omega_\rho$.

Proof. Let $u^*(t|t_k)$ for $t \in [t_k, t_{k+N})$ be the optimal input trajectory of Eq. 2.52 at t_k. The piecewise defined input trajectory consisting of $u(t) = u^*(t|t_k)$ for $t \in [t_{k+1}, t_{k+N})$ and $u(t) = h(z(t_{k+N}))$ for $t \in [t_{k+N}, t_{k+N+1})$ is a feasible solution to the optimization problem at t_{k+1}. Utilizing this feasible solution to the problem of Eq. 2.52 at t_{k+1}, the difference between the optimal values of Eq. 2.52 at any two successive sampling times t_k and t_{k+1} may be bounded as follows:

$$J_e^*(x(t_{k+1})) - J_e^*(x(t_k)) \leq \int_{t_{k+N}}^{t_{k+N+1}} l_e(z(t), h(z(t_{k+N})))\, dt - \int_{t_k}^{t_{k+1}} l_e(x(t), u^*(t_k|t_k))\, dt\ . \tag{2.54}$$

Let T be any positive finite integer. Summing the differences between the optimal values of Eq. 2.52 at two subsequent sampling times, the following upper bound is derived:

$$\sum_{k=0}^{T-1} [J_e^*(x(t_{k+1})) - J_e^*(x(t_k))] \leq \int_{t_N}^{(T+N)\Delta} l_e(z(t), v(t))\, dt - \int_0^{T\Delta} l_e(x(t), u^*(t))\, dt \tag{2.55}$$

We take $l_e(x,u) \geq 0$ for all $x \in \Omega_\rho$ and $u \in \mathbb{U}$. Then the left-hand side of Eq. 2.55 is bounded below by:

$$\begin{aligned} \sum_{k=0}^{T-1} [J_e^*(x(t_{k+1})) - J_e^*(x(t_k))] &= J_e^*(x(T\Delta)) - J_e^*(x(0)) \\ &\geq -J_e^*(x(0)) \end{aligned} \tag{2.56}$$

where the inequality follows from the fact that $l_e(x,u) \geq 0$ for all $x \in \Omega_\rho$ and $u \in \mathbb{U}$. Owing to optimality, the optimal value of Eq. 2.52 at the initial time may be bounded by the cost under a feasible solution; thus, it may be bounded by the cost under the Lyapunov-based controller implemented in sample-and-hold over the prediction horizon:

$$J_e^*(x(0)) \leq \int_0^{t_N} l_e(z(t), v(t))\, dt\ . \tag{2.57}$$

Combining Eqs. 2.55-2.57, the closed-loop economic performance from the initial time to $T\Delta$ is no worse than the closed-loop performance under the Lyapunov-based controller from the initial time to $(T+N)\Delta$, which proves the bound of Eq. 2.53. □

It is noted that due to continuity of $l_e(x,u)$ on $\mathbb{X} \times \mathbb{U}$ and the fact that x and u are bounded within Ω_ρ and $\mathbb{U}$ respectively, l_e achieves a minimum on $\Omega_\rho \times \mathbb{U}$. Therefore, the assumption that $l_e(x,u) \geq 0$ can be made in the proof of Theorem 2.5 without loss of generality because the minimum value of $l_e(x,u)$ on $\Omega_\rho \times \mathbb{U}$ exists and can always be subtracted from $l_e(x,u)$ to make the resulting objective function defined as $\overline{l_e}(x,u)$ take it minimum at zero. This objective function can then be used in Eq. 2.52 without changing the optimal solution to the optimization problem, and

therefore we assume that $l_e(x,u) \geq 0$ in the proofs of this section.

The upper limit of integration of the right-hand side of Eq. 2.53 ($(T+N)\Delta$) arises from the fact that a fixed prediction horizon is used in the LEMPC of Eq. 2.52. If, instead, $T\Delta$ represents the final operating time of a given system, one could employ a shrinking horizon from time $(T-N)\Delta$ to $T\Delta$ in the LEMPC and the upper limit of integration of the right-hand side of Eq. 2.53 would be $T\Delta$. Specifically, for $t_k \in [t_0, t_{T-N})$, we have from Eq. 2.55:

$$\sum_{k=0}^{T-N-1} [J_e^*(x(t_{k+1})) - J_e^*(x(t_k))] \leq \int_{N\Delta}^{T\Delta} l_e(z(t), v(t))\, dt - \int_0^{(T-N)\Delta} l_e(x(t), u^*(t))\, dt \tag{2.58}$$

and from Eq. 2.53 we have:

$$\int_0^{(T-N)\Delta} l_e(x(t), u^*(t))\, dt \leq \int_0^{T\Delta} l_e(z(t), v(t))\, dt\ . \tag{2.59}$$

For sampling times between t_{T-N} and t_T, we employ a shrinking horizon in the EMPC. That is, let $\bar{N}_k = N - j$ be the horizon used at sampling time t_k for $k \in \{T-N, \ldots, T-1\}$ where $j = k - T + N$. With slight abuse of notation, let

$$J_e^*(x(t_k)) = \int_{t_k}^{t_{k+\bar{N}_k}} l_e(x(t), u^*(t|t_k))\, dt \tag{2.60}$$

be the optimal value of the EMPC problem at sampling times t_k, $k \in \{T-N, \ldots, T-1\}$ where the EMPC is formulated with a prediction horizon of $\bar{N}_k$. By the principle of optimality, the difference between the optimal value of the EMPC problem at two subsequent sampling times is

$$J_e^*(x(t_{k+1})) - J_e^*(x(t_k)) = -\int_{t_k}^{t_{k+1}} l_e(x(t), u^*(t_k|t_k))\, dt \tag{2.61}$$

for $k \in \{T-N, \ldots, T-2\}$. Because $T\Delta$ for this shrinking horizon case represents the final time of operation, the EMPC is not solved at that time and thus there is no value of $J_e^*(x(t_T))$. For this

reason, we consider the following summation of the terms in Eq. 2.61:

$$\sum_{k=T-N}^{T-2}[J_e^*(x(t_{k+1}))-J_e^*(x(t_k))]-J_e^*(x(t_{T-1}))=-J_e^*(x(t_{T-N}))=-\int_{(T-N)\Delta}^{T\Delta}l_e(x(t),u^*(t))\,dt\,. \tag{2.62}$$

where the left-hand side is equivalent to the summation of the terms in Eq. 2.61 from $k=T-N$ to $k=T-1$ with $J_e^*(x(t_T)):=0$. The sum of the differences between the optimal values of Eq. 2.52 at two subsequent sampling times between 0 and $T-2$ with $J_e^*(x(t_{T-1}))$ subtracted from this sum gives:

$$\begin{aligned}
&\sum_{k=0}^{T-2}[J_e^*(x(t_{k+1}))-J_e^*(x(t_k))]-J_e^*(x(t_{T-1}))\\
&=\sum_{k=0}^{T-N-1}[J_e^*(x(t_{k+1}))-J_e^*(x(t_k))]+\sum_{k=T-N}^{T-2}[J_e^*(x(t_{k+1}))-J_e^*(x(t_k))]-J_e^*(x(t_{T-1}))\\
&\overset{(2.58),(2.62)}{\leq}\int_{N\Delta}^{T\Delta}l_e(z(t),v(t))\,dt-\int_0^{(T-N)\Delta}l_e(x(t),u^*(t))\,dt-\int_{(T-N)\Delta}^{T\Delta}l_e(x(t),u^*(t))\,dt
\end{aligned} \tag{2.63}$$

Also,

$$\begin{aligned}
\sum_{k=0}^{T-2}[J_e^*(x(t_{k+1}))-J_e^*(x(t_k))]-J_e^*(x(t_{T-1}))&=J_e^*(x(t_{T-1}))-J_e^*(x(0))-J_e^*(x(t_{T-1}))=-J_e^*(x(0))\\
&\geq-\int_0^{N\Delta}l_e(z(t),v(t))\,dt
\end{aligned} \tag{2.64}$$

where the last inequality follows from the same arguments used to write Eq. 2.57 above. Combining Eqs. 2.63-2.64, the required performance bound is obtained for the shrinking horizon case as follows:

$$\int_0^{T\Delta}l_e(x(t),u^*(t))\,dt\leq\int_0^{T\Delta}l_e(z(t),v(t))\,dt \tag{2.65}$$

This completes the proof of the finite-time performance bound for the shrinking horizon case.

Again considering the case that no shrinking horizon is used, we note that as a consequence of the performance bound of Eq. 2.53, the average finite-time economic performance may be bounded

as follows:

$$\frac{1}{T\Delta}\int_0^{T\Delta} l_e(x,u^*)\,dt \quad \leq \frac{1}{T\Delta}\int_0^{T\Delta} l_e(z,v)\,dt + \frac{1}{T\Delta}\int_{T\Delta}^{(T+N)\Delta} l_e(z,v)\,dt \tag{2.66}$$

for any integer $T > 0$. From the right-hand side of Eq. 2.66, the significance of the second term on the right-hand side dissipates as T gets large. Thus, the results of Theorem 2.5 show that the average closed-loop economic performance over a finite-time operating interval under LEMPC with a terminal equality constraint based on h that meets Assumption 2.1 is at least as good as the average closed-loop economic performance under h implemented in sample-and-hold plus a term that dissipates as the length of operation increases.

In the above discussion, we developed economic performance guarantees for LEMPC with a terminal equality constraint based on a Lyapunov-based controller satisfying Assumption 2.1 on the finite-time interval. We now consider the infinite-time (asymptotic average) performance. The provable result on asymptotic average economic performance varies depending on whether the Lyapunov-based controller satisfies Assumption 2.1 or Assumption 2.2. We first present a theorem for the infinite-time performance for a controller satisfying Assumption 2.1 (the performance result when the Lyapunov-based controller satisfies Assumption 2.2 is stronger and will be presented subsequently).

Theorem 2.6. *Consider the closed-loop system of Eq. 2.1 with $w(t) \equiv 0$ under the LEMPC of Eq. 2.52 where the Lyapunov-based controller satisfies Assumption 2.1 and $z(0) = x(0) \in \Omega_\rho$. Let $\Delta \in (0, \Delta^*)$ where Δ^* is the conclusion of Proposition 2.1. The asymptotic average performance is bounded by:*

$$\limsup_{T\to\infty} \frac{1}{T\Delta}\int_0^{T\Delta} l_e(x(t),u^*(t))\,dt \leq \max_{x,y\in\Omega_{\rho_{\min}}} l_e(x,h(y)). \tag{2.67}$$

Proof. To develop the proof of Theorem 2.6, we first consider the asymptotic average economic performance of the nominal system of Eq. 2.1 under the Lyapunov-based controller that satisfies Assumption 2.1 implemented in sample-and-hold (i.e., the sampled-data system of Eq. 2.50) for $\Delta \in (0, \Delta^*)$ where $\Delta^* > 0$ is the conclusion of Proposition 2.1. Owing to the fact that z and

v are bounded in compact sets and l_e and h are continuous on $\Omega_\rho \times \mathbb{U}$ and Ω_ρ, respectively, the asymptotic average economic performance, which is given by the left-hand side of Eq. 2.68 below, is bounded. Moreover, z converges to $\Omega_{\rho_{\min}}$ from Proposition 2.1. Therefore, the following inequality, which represents the worst-case asymptotic average performance under the sample-and-hold Lyapunov-based controller, follows:

$$\limsup_{T\to\infty} \frac{1}{T\Delta} \int_0^{T\Delta} l_e(z(t), v(t))\, dt \leq \max_{x,y\in\Omega_{\rho_{\min}}} l_e(x, h(y)) \,. \tag{2.68}$$

where the Lyapunov-based controller is evaluated at y instead of x since y does not necessarily equal x due to the sample-and-hold implementation of the controller. Given that for any finite-time interval, the bound of Eq. 2.53 holds, the inequality of Eq. 2.67 follows from the fact that x and u^* are bounded in compact sets, the fact that l_e is continuous on $\Omega_\rho \times \mathbb{U}$, and the bound of Eq. 2.68.

□

As noted, Theorem 2.6 characterizes the worst-case infinite-time (asymptotic average) performance for the process under the LEMPC based on a Lyapunov-based controller that satisfies Assumption 2.1, and states that it is no worse than the worst-case asymptotic average performance under the Lyapunov-based controller. Though this is a weaker result than showing that the asymptotic average performance is at least as good as that for steady-state operation, the level set $\Omega_{\rho_{\min}}$ may be selected arbitrarily small, at the expense of requiring a faster sampling rate.

We now focus on the performance guarantees that can be made in infinite-time when h meets Assumption 2.2. We first present a lemma on the infinite-time performance of the nominal process of Eq. 2.1 under the Lyapunov-based controller meeting Assumption 2.2 implemented in sample-and-hold (Eq. 2.50). We will then present a theorem relating this result to the infinite-time performance of the process under the LEMPC with a terminal constraint based on h. The lemma that will now be presented states that the asymptotic average economic performance under a Lyapunov-based controller that satisfies Assumption 2.2 is no worse than the economic cost at the optimal steady-state pair (x_s^*, u_s^*).

Lemma 2.1. *The asymptotic average economic cost of the closed-loop system of Eq. 2.50 under a feedback controller that satisfies Assumption 2.2 for any initial condition $z(0) \in \Omega_\rho$ is*

$$\lim_{T\to\infty} \frac{1}{T\Delta} \int_0^{T\Delta} l_e(z(t), v(t))\, dt = l_e(x_s^*, u_s^*) \tag{2.69}$$

where $\Delta \in (0, \Delta_e^*)$ ($\Delta_e^* > 0$ is the conclusion of Proposition 2.2) and z and v denote the state and input trajectories of the system of Eq. 2.50.

Proof. Recall, the economic stage cost function l_e is continuous on the compact set $\Omega_\rho \times \mathbb{U}$ and $z(t) \in \Omega_\rho$ and $v(t) \in \mathbb{U}$ for all $t \geq 0$. Thus, the integral:

$$\frac{1}{T\Delta} \int_0^{T\Delta} l_e(z(t), v(t))\, dt < \infty \tag{2.70}$$

for any integer $T > 0$. Since $z(t)$ and $v(t)$ exponentially converge to the optimal steady-state pair (x_s^*, u_s^*) as $t \to \infty$, the limit of the integral of Eq. 2.70 as T tends to infinity exists and is equal to $l_e(x_s^*, u_s^*)$. To prove the limit, it is sufficient to show that for any $\varepsilon > 0$, there exists a T^* such that for $T > T^*$, the following holds:

$$\left| \frac{1}{T\Delta} \int_0^{T\Delta} l_e(z(t), v(t))\, dt - l_e(x_s^*, u_s^*) \right| < \varepsilon \tag{2.71}$$

To simplify the presentation, define $I(T_1, T_2)$ as the following integral:

$$I(T_1, T_2) := \int_{T_1\Delta}^{T_2\Delta} l_e(z(t), v(t))\, dt \tag{2.72}$$

where the arguments of I are integers representing the integers of the lower and upper limits of integration, respectively. Since $z(t)$ and $v(t)$ converge to x_s^* and u_s^* as t tends to infinity, respectively, $l_e(x(t), v(t)) \to l_e(x_s^*, u_s^*)$ as t tends to infinity. Furthermore, $z(t) \in \Omega_\rho$ and $v(t) \in \mathbb{U}$ for all $t \geq 0$,

so for every $\varepsilon > 0$, there exists an integer $\tilde{T} > 0$ such that

$$|l_e(z(t), v(t)) - l_e(x_s^*, u_s^*)| < \varepsilon/2 \tag{2.73}$$

for $t \geq \tilde{T}\Delta$. For any $T > \tilde{T}$,

$$\begin{aligned} |I(0,T) - T\Delta l_e(x_s^*, u_s^*)| &= |I(0,\tilde{T}) + I(\tilde{T},T) - T\Delta l_e(x_s^*, u_s^*)| \\ &\leq \int_0^{\tilde{T}\Delta} |l_e(z(t), v(t)) - l_e(x_s^*, u_s^*)| \, dt + \int_{\tilde{T}\Delta}^{T\Delta} |l_e(z(t), v(t)) - l_e(x_s^*, u_s^*)| \, dt \\ &< \tilde{T}\tilde{M}\Delta + (T - \tilde{T})\Delta\varepsilon/2 \end{aligned} \tag{2.74}$$

where

$$\tilde{M} := \sup_{t \in [0, \tilde{T}\Delta]} \{|l_e(z(t), v(t)) - l_e(x_s^*, u_s^*)|\} \ .$$

For any $T > T^* = 2\tilde{T}(\tilde{M} - \varepsilon/2)/\varepsilon$ (which implies $(\tilde{M} - \varepsilon/2)\tilde{T}/T < \varepsilon/2$), the following inequality is satisfied:

$$\begin{aligned} |I(0,T)/(T\Delta) - l_e(x_s^*, u_s^*)| &< \tilde{T}\tilde{M}/T + (1 - \tilde{T}/T)\varepsilon/2 \\ &= (\tilde{M} - \varepsilon/2)\tilde{T}/T + \varepsilon/2 < \varepsilon \end{aligned} \tag{2.75}$$

which proves the limit of Eq. 2.69. □

Utilizing Lemma 2.1, one may prove that the asymptotic average closed-loop economic performance under the LEMPC of Eq. 2.52 designed with a Lyapunov-based controller that satisfies Assumption 2.2 is no worse than the closed-loop performance at the economically optimal steady-state (from Lemma 2.1, this is the same as stating that the asymptotic average performance of the nominal process under the LEMPC of Eq. 2.52 designed with h that meets Assumption 2.2 is no worse than the asymptotic average performance under h implemented in sample-and-hold). This result is stated in the following theorem.

Theorem 2.7. *Consider the system of Eq. 2.1 with $w(t) \equiv 0$ under the LEMPC of Eq. 2.52 based on a Lyapunov-based controller that satisfies Assumption 2.2. Let $\Delta \in (0, \Delta_e^*)$ where $\Delta_e^* > 0$ is the conclusion of Proposition 2.2. The closed-loop asymptotic average economic performance is no worse than the economic cost at steady-state; that is, the following bound holds:*

$$\limsup_{T\to\infty} \frac{1}{T\Delta} \int_0^{T\Delta} l_e(x(t), u^*(t))\, dt \leq l_e(x_s^*, u_s^*)\ . \tag{2.76}$$

Proof. From Theorem 2.5, for any $T > 0$:

$$\frac{1}{T\Delta} \int_0^{T\Delta} l_e(x(t), u^*(t))\, dt \leq \frac{1}{T\Delta} \int_0^{(T+N)\Delta} l_e(z(t), v(t))\, dt\ . \tag{2.77}$$

As T increases, both sides of the inequality of Eq. 2.77 remain finite owing to the fact that l_e is continuous and the state and input trajectories are bounded in compact sets. The limit of the right-hand side as $T \to \infty$ is equal to $l_e(x_s^*, u_s^*)$ (Lemma 2.1). Therefore, the result in Eq. 2.76 is obtained. □

Remark 2.7. *The performance results of this section hold for any prediction horizon size even when $N = 1$. The use of a short horizon may be computationally advantageous for real-time application. Also, owing to the fact that the terminal equality constraint of Eq. 2.52d may be a point in the state-space away from the steady-state, the feasible region of the LEMPC of Eq. 2.52 may be larger than the feasible region of EMPC with a terminal equality constraint equal to the steady-state especially when a short prediction horizon is used.*

2.3.2.4 Part 2: Application to a Chemical Process Example

In this section, we use a chemical process example to demonstrate that the nominal process under LEMPC with a terminal equality constraint based on a Lyapunov-based controller can show improved economic performance compared to the process under the sample-and-hold Lyapunov-based controller. The LEMPC of Eq. 2.52 is applied to a chemical process example

consisting of a continuous stirred-tank reactor (CSTR) within which two parallel reactions occur:[20]

$$R \rightarrow P_1 \tag{2.78a}$$

$$R \rightarrow P_2 \tag{2.78b}$$

where P_1 is the desired product and P_2 is a by-product. The rates of the reactions are second-order and first-order in R, respectively.

To model the reactor, it is assumed that there is no significant heat of reaction or heat of mixing, that the temperature dependence of the reaction rates can be modeled through the Arrhenius equation, and that the reactor mixture density, heat capacity, and inlet and outlet volumetric flow rates are constant. Applying these assumptions, the dimensionless dynamic model of the reactor, obtained from the conservation equations, is

$$\dot{x}_1 = -a_1 e^{-1/x_3} x_1^2 - a_2 e^{-\delta/x_3} x_1 - x_1 + 1 \tag{2.79a}$$

$$\dot{x}_2 = a_1 e^{-1/x_3} x_1^2 - x_2 \tag{2.79b}$$

$$\dot{x}_3 = -x_3 + u \tag{2.79c}$$

where x_1 is the dimensionless R concentration, x_2 is the dimensionless P_1 concentration, x_3 is the dimensionless temperature, and the manipulated input, denoted by u, is a dimensionless quantity related to the heat flux provided to the reactor. The process parameters are $a_1 = 1.0 \times 10^4$, $a_2 = 400$, and $\delta = 0.55$, and the input is restricted to take values in the interval $[0.049, 0.449]$.

The operating profit of the CSTR is assumed to scale with the flow of the desired product out of the reactor. Owing to the fact that the volumetric inlet and outlet flow rates are constant, the stage cost minimized in LEMPC to maximize the operating profit of the reactor is given by:

$$l_e(x,u) = -x_2 \ . \tag{2.80}$$

The economically optimal steady-state that minimizes Eq. 2.80 is $x_s^* = [0.0832\ 0.0846\ 0.149]^T$

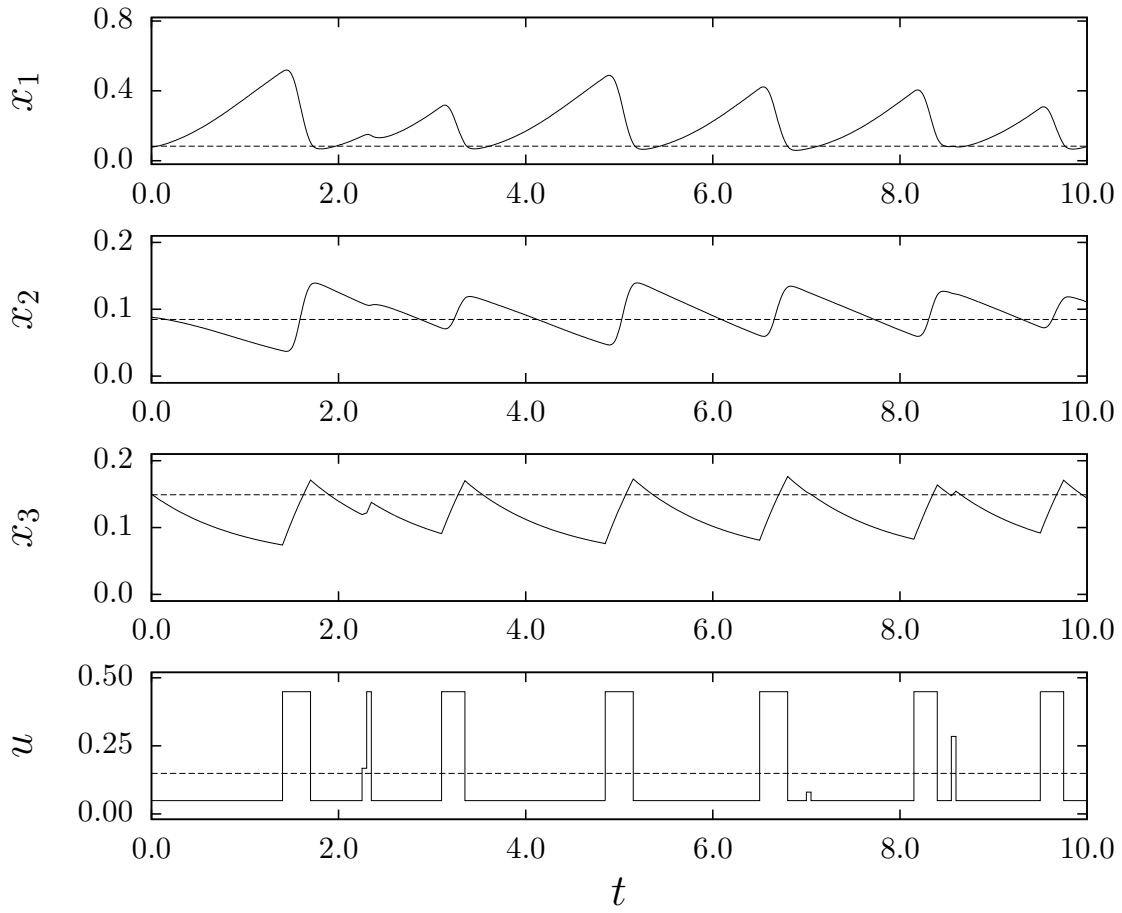

Figure 2.5: Closed-loop trajectories for the system of Eq. 2.79 under the LEMPC of Eq. 2.52 (solid trajectories). The horizontal (dashed) trajectories indicate the steady-state value of each state and input.

corresponding to the steady-state input $u_s^* = 0.149$. Regarding the implementation details of the LEMPC, the sampling period is $\Delta = 0.05$, the prediction horizon consists of sixty sampling periods ($N = 60$), and the Lyapunov-based controller is chosen to be a proportional controller with saturation to account for the bound on the input (i.e., $\bar{h}(x) = -K(x_2 - x_{2s}^*) + u_s^*$ where $K = 3.3$ and $h(x) = \bar{h}(x)$ if $\bar{h}(x) \in [0.049, 0.449]$; else if $\bar{h}(x) < 0.049$ then $h(x) = 0.049$; else $h(x) = 0.449$). The closed-loop simulations were written in Python. To integrate the ODEs and solve the corresponding sensitivity information required to solve the nonlinear optimization problem, CVODE[81] and automatic differentiation via CasADi[15] were used, respectively. The resulting nonlinear program was solved using Ipopt.[148]

To demonstrate that using the LEMPC with a terminal equality constraint based on h can

indeed lead to better economic performance than using the Lyapunov-based controller (in this case, the proportional controller with saturation) in sample-and-hold, two closed-loop simulations were completed: the closed-loop system under the LEMPC and the closed-loop system under the Lyapunov-based feedback controller. Fig. 2.5 gives the closed-loop trajectories under LEMPC for a closed-loop simulation over a length of 10.0 dimensionless time units. From Fig. 2.5, the LEMPC of Eq. 2.52 dictates a periodic-like operating policy. On the other hand, the Lyapunov-based controller dictates a steady-state operating policy. The average closed-loop economic performance is given by the index:

$$\bar{J_e} = \frac{1}{10.0}\int_0^{10.0} x_2(t)\, dt\ . \tag{2.81}$$

The average performance under the LEMPC is 0.0919, while the average performance under the feedback controller is 0.0849; the performance under LEMPC is 8.3% better than that under the feedback controller. It is important to note that it has been demonstrated that time-varying operation of this example improves closed-loop performance relative to steady-state operation.[20]

Two potentially interesting issues to address are the closed-loop performance under EMPC with and without a terminal constraint and the closed-loop performance under EMPC with different terminal constraint formulations. While these issues may be difficult to address in general, we may explore these issues with simulation for this particular example. Fig. 2.6 displays the average closed-loop performance for several closed-loop simulations over 10.0 dimensionless time units for three different EMPC schemes and different horizon lengths. In particular, the three EMPC's considered are the LEMPC of Eq. 2.52, EMPC with a terminal constraint equal to the economically optimal steady-state, and EMPC without terminal constraints. Overall, the closed-loop performance for the two EMPC schemes with terminal constraints is relatively similar and for each horizon length the closed-loop performance realized was better than the profit at the economically optimal steady-state and also better than the closed-loop performance under the Lyapunov-based controller. On the other hand, there is a noticeable dependence of the average closed-loop performance on the prediction horizon length. For $N = 10$, the closed-loop performance under the EMPC without terminal constraints was worse than that under

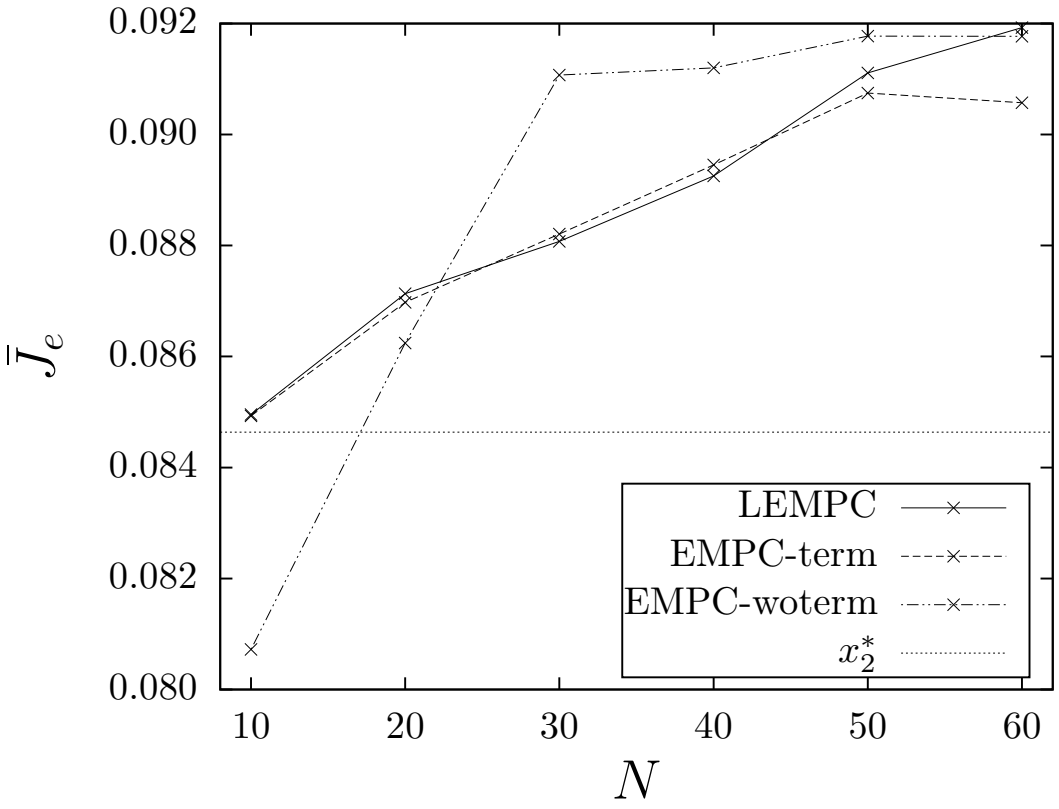

Figure 2.6: Closed-loop economic performance with prediction horizon length for the process of Eq. 2.79 under the LEMPC of Eq. 2.52 (solid line, denoted as LEMPC), under an EMPC with a terminal equality constraint equal to the economically optimal steady-state (dashed line, denoted as EMPC-term), and under EMPC without a terminal constraint (dashed-dotted line, denoted as EMPC-woterm). For comparison, the closed-loop economic performance for operation at the economically optimal steady-state is also plotted (dotted line, denoted as x_2^*).

the Lyapunov-based controller, illustrating that performance-based constraints imposed in EMPC may be needed to ensure acceptable closed-loop economic performance for shorter prediction horizons.

2.3.3 Part 3: LEMPC with Input Magnitude Constraints, Input Rate of Change Constraints, and an Equality Terminal Constraint Based on a Lypaunov-Based Controller

In this section, we combine the results of Parts 1 and 2 on LEMPC with input magnitude and rate of change constraints and on LEMPC with a terminal state constraint based on a Lyapunov-based controller to show that the performance of LEMPC with input magnitude and rate of change constraints can be proven to be at least as good as it would be under a Lyapunov-based controller implemented in sample-and-hold for nominal process operation.

The formulation of LEMPC incorporating a terminal state constraint based on the Lyapunov-based controller, input magnitude constraints, and input rate of change constraints, assuming nominal process operation, is as follows:

$$\min_{u(\cdot)\in S(\Delta)} \int_{t_k}^{t_{k+N}} l_e(\tilde{x}(\tau),u(\tau))\, d\tau \tag{2.82a}$$

$$\text{s.t.} \quad \dot{\tilde{x}}(t) = f(\tilde{x}(t),u(t),0) \tag{2.82b}$$

$$\tilde{x}(t_k) = x(t_k) \tag{2.82c}$$

$$\tilde{x}(t_{k+N}) = z(t_{k+N}) \tag{2.82d}$$

$$u(t) \in \mathbb{U},\ \forall\, t \in [t_k, t_{k+N}) \tag{2.82e}$$

$$\tilde{x}(t) \in \mathbb{X},\ \forall\, t \in [t_k, t_{k+N}) \tag{2.82f}$$

$$|u_i(t_j) - h_i(z(t_j))| \leq \varepsilon_r,\ i = 1,\ldots,m,\ j = k,\ldots,k+N-1 \tag{2.82g}$$

$$V(\tilde{x}(t)) \leq \rho,\ \forall\, t \in [t_k, t_{k+N}) \tag{2.82h}$$

where the notation follows that of Eqs. 2.21 and 2.52, and the implementation strategy is like that of

Eq. 2.52 (at each t_k, a state measurement $x(t_k)$ is received and $z(t_{k+N})$ is updated before the LEMPC optimization problem is solved), except that each $h_i(z(t_j))$, $i = 1,\ldots,m$, $j = k,\ldots,k+N-1$, is also determined and incorporated into the LEMPC of Eq. 2.82 at each sampling time.

We will now briefly address how the properties of the LEMPC in Eq. 2.82 compare with those of the LEMPC of Eq. 2.21 and of the LEMPC of Eq. 2.52. Specifically, we will address the bounds on ε_r and Δ required for the LEMPC of Eq. 2.82 to satisfy the desired input rate of change constraints in Eqs. 2.19-2.20 when $h(x)$ meets Assumption 2.1, the feasibility of the LEMPC optimization problem, the closed-loop stability properties of a process under the LEMPC, and the performance guarantees that can be made for the nominal process under LEMPC. We note that we will not address the robustness of the method, because only nominal operation is considered for the LEMPC of Eq. 2.82 due to the use of the terminal equality constraint.

Using arguments similar to those in Eqs. 2.23-2.28, it can be shown that the desired input rate of change constraints of Eqs. 2.19-2.20 are met when the sampling period is sufficiently small, the LEMPC of Eq. 2.82 is feasible (Eq. 2.82g is met by the calculated control actions), and $2\varepsilon_r + L_{h_L} M\Delta \leq \varepsilon_{desired}$. The proof of feasibility of the LEMPC is similar to that noted in the proof of Theorem 2.4 in that, because nominal operation is considered, $u(t) = h(z(t_j))$ for $j = k,\ldots,k+N-1$, is a feasible solution to the LEMPC of Eq. 2.82 at t_0, with $u(t) = u^*(t|t_k)$ for $t \in [t_{k+1}, t_{k+N})$ and $u(t) = h(z(t_{k+N}))$ for $t \in [t_{k+N}, t_{k+N+1})$ being a feasible solution at time t_{k+1} when $u(t) = u^*(t|t_k)$ for $t \in [t_k, t_{k+N})$ is the solution at time t_k. Closed-loop stability of a process under the LEMPC in Eq. 2.82 is ensured for nominal operation in the sense that the state is always maintained within the compact set Ω_ρ due to the constraint in Eq. 2.82h.

Finally, we compare the performance of the nominal process of Eq. 2.1 under the LEMPC of Eq. 2.82 with the performance of the process under the Lyapunov-based controller implemented in sample-and-hold. Because this comparison can only be made if the constraints are met under both controllers, we note that the Lyapunov-based controller implemented in sample-and-hold meets all input constraints in Eq. 2.82 and causes the states to meet all constraints for the reasons mentioned in the proof that this control law is a feasible solution to the LEMPC at t_0; it also

satisfies the desired rate of change constraints of Eqs. 2.19-2.20 if the terms $u^*(t_k|t_k)$ are replaced by $h_i(z(t_k))$, $i = 1,\ldots,m$, since these are the implemented control actions under the sample-and-hold Lyapunov-based controller. With that replacement, Eqs. 2.19-2.20 become a requirement that $|h_i(z(t_k)) - h_i(z(t_{k-1}))| \leq \varepsilon_{desired}$, $i = 1,\ldots,m$, which holds for all $\varepsilon_{desired} > 0$ for $L_{h_L} M\Delta \leq \varepsilon_{desired}$ from Eq. 2.25. Thus, when the control actions calculated by the LEMPC meet Eqs. 2.19-2.20 (i.e., $2\varepsilon_r + L_{h_L} M\Delta \leq \varepsilon_{desired}$), it is also true that $L_{h_L} M\Delta \leq \varepsilon_{desired}$ so that the control actions implemented by the sample-and-hold Lyapunov-based controller also satisfy the desired input rate of change constraints. This establishes that a comparison can be made between the performance of the process under the LEMPC of Eq. 2.82 and the sample-and-hold Lyapunov-based controller. The performance results of Theorem 2.5 hold for h meeting Assumption 2.1 on the finite-time interval, the performance results of Theorem 2.6 hold for h meeting Assumption 2.1 on the infinite-time interval, and the performance results of Theorem 2.7 hold for h meeting Assumption 2.2 on the infinite-time interval. It is noted that these performance results hold for the LEMPC of Eq. 2.82 regardless of the form of the cost function; this proves that for nominal operation, the performance of LEMPC with a terminal equality constraint and input rate of change constraints is no worse on both the finite-time and infinite-time intervals than that of an alternative controller that enforces steady-state operation, regardless of whether the cost function includes additional penalties on the input rate of change to reduce actuator wear. Like the LEMPC with a terminal equality constraint but without input rate of change constraints (Eq. 2.52), the LEMPC of Eq. 2.82 has a number of advantages over other EMPC formulations for which performance guarantees have been made, particularly that the feasible region can be characterized *a priori*.

Remark 2.8. *The motivation for adding input rate of change constraints to LEMPC (that the LEMPC may dictate a dynamic operating policy) is also motivation for the addition of input rate of change constraints to EMPC in general. Thus, it is noted that input rate of change constraints can be added to other EMPC formulations for which performance guarantees have been previously developed (such as the steady-state terminal equality constraint formulation) as well. However, as noted above, LEMPC has a number of advantages over some of the other EMPC formulations that*

make it more attractive for incorporating input rate of change constraints and making performance guarantees for the resulting formulation.

2.4 Conclusions

In this chapter, we developed a formulation of LEMPC incorporating input magnitude and rate of change constraints and a terminal equality constraint based on a Lyapunov-based controller that allows provable performance guarantees to be made for the LEMPC. The LEMPC formulation was developed in three parts. In Part 1 of this chapter, we demonstrated that input rate of change constraints written with respect to a Lyapunov-based controller can be added to LEMPC, and that the implemented inputs can then be ensured to differ by no more than a desired bound between two subsequent sampling periods. The formulation of LEMPC with input rate of change constraints developed was shown to be feasible and to maintain closed-loop stability of a process even in the presence of bounded disturbances. A chemical process example demonstrated that the number of sampling periods of the prediction horizon over which the input rate of change constraints are enforced may have a significant impact on whether other process constraints such as integral material constraints can be met.

In Part 2, we developed an LEMPC formulation with a terminal equality constraint based on the Lyapunov-based controller utilized in the formulation of the LEMPC. With this terminal equality constraint, the LEMPC formulation was proven to be not only feasible and stable in the sense of boundedness of the closed-loop state for nominal operation, but was also proven to have finite-time and infinite-time economic performance properties such that the process under LEMPC performs no worse than it does under an asymptotically stabilizing or exponentially stabilizing Lyapunov-based controller implemented in sample-and-hold. When the exponentially stabilizing controller is utilized to design the LEMPC, the asymptotic average performance of the process under the LEMPC was proven to be no worse than that under steady-state operation. The LEMPC formulation presented has advantages over other EMPC's for which performance guarantees

have been made, such as that the feasible region can be explicitly characterized *a priori*. A chemical process example demonstrated the economic benefits of incorporating a terminal equality constraint in EMPC when a short prediction horizon is used.

In Part 3, the results of Parts 1 and 2 were combined to develop an LEMPC formulation incorporating a terminal equality constraint based on a Lyapunov-based controller that also had input magnitude and rate of change constraints. It was proven that the closed-loop performance under this LEMPC with input magnitude and rate of change constraints is no worse than that under an asymptotically or exponentially stabilizing Lyapunov-based controller for nominal operation on the finite-time and infinite-time operating intervals (this means that the infinite-time performance under the LEMPC based on an exponentially stabilizing controller is no worse than that under steady-state operation), regardless of the form of the cost function or any penalties on the input rate of change in the cost function. This is significant because it may be desirable from a safety perspective to reduce input variations under EMPC but without reducing the economic performance of the process below that obtainable with the traditional steady-state operating strategies.

Chapter 3

Elucidation of the Cause of Stiction-Induced Oscillations and Valve Nonlinearity Compensation within the Classical Control Framework

3.1 Introduction

The results of the prior chapter indicate that control actuator limitations, such as the ability of actuators to wear, should influence control design since proper functioning of the actuators that implement control actions is critical to effective process control loops. In the remainder of this dissertation, we examine other limitations of control actuators (specifically, valve dynamics), their impacts on control loop performance, and how these impacts can be mitigated.

In undergraduate process control courses, valve dynamics are often modeled with linear transfer function models; such dynamics can be related to, for example, resistance of the gas used to apply pressure in a pneumatic actuator to flow at the top of a valve.[38] Valve characteristics (e.g., linear, equal percentage, and square root) may be reviewed in undergraduate coursework to provide

undergraduates with fundamentals regarding valve sizing and the effects of installing a valve on the valve's flow characteristics (the manner in which the flow through the valve is related to the valve opening).[38,118,129] Though there may be some discussion of other types of valve behavior described by nonlinear models (e.g., saturation of the valve output at its maximum value, failure of a valve to respond to changes in the control signal to the valve for some time after a valve movement direction change due to mechanical parts in a valve (deadband due to backlash),[33] or stiction,[18,24] which refers to valve behavior due to friction that can be described by nonlinear dynamic equations), time constraints in a semester/quarter and also a general focus in undergraduate process control on linear dynamic systems do not typically permit an in-depth treatment of nonlinear valve behavior and its impact on process control from a first-principles perspective. The chemical process control literature also typically neglects valve dynamics. However, at chemical plants throughout the world, valve issues such as stiction, deadband, saturation, hysteresis, and deadzone prevent adequate set-point tracking.[31,89]

A variety of methods for analyzing and/or compensating for valve dynamics of various types have been proposed. For example,[54] demonstrates that even linear valve dynamics can be problematic for a process operated under EMPC when the valve dynamics are neglected in the model utilized by the EMPC for making state predictions; therefore, that work suggests incorporating the valve dynamics in the dynamic process model for the controller. Reference[31] analyzes the range of valve travel over which linear control design theory would be expected to be adequate when a process that can be effectively modeled with a linear model receives a flow rate from a valve with a square root or an equal percentage inherent valve characteristic. Reference[152] develops an MPC-based method for linear processes where the valve is subject to backlash. The literature analyzing and compensating for the stiction nonlinearity is particularly extensive, with reviews such as[24] categorizing the methods, though stiction compensation remains an important research topic with newer works such as those in[19,115] expanding the compensation literature.

It has been noted[33,89,143] that the controller, process, and valve dynamics all play a role in determining the trajectories of the measured outputs of a closed-loop system. For example,[143]

presents a table showing whether various combinations of linear processes (integrating and non-integrating) and linear controllers (proportional (P) and proportional-integral (PI)) with different stiction characteristics for a valve in the control loop are expected to result in limit cycling of the valve output or not. In the present chapter, we analyze the difficulty of determining, *a priori*, the process output trajectories for nonlinear processes with various types of feedback control designs, loop architectures, and types of valve behavior exhibited by the valves in the loop. We begin by examining the coupled and nonlinear dynamics of such process-valve systems in a general sense using systems of differential equations. This treatment provides a uniform mathematical platform from which both the valve behavior commonly taught in undergraduate coursework and also nonlinear valve dynamics known to cause problems in industry can be understood and related. We then use the insights gained from this study to describe the relationship between our analysis and a number of valve behavior compensation methods in the literature, ending with a new integral term modification stiction compensation technique for processes under PI control. The next chapter continues the discussion of valve nonlinearity compensation methods with a focus on those for processes under MPC. A level control example and ethylene oxidation continuous stirred tank reactor example demonstrate the various points throughout the next two chapters. This chapter and the next originally appeared in.[51,53,56]

3.2 Preliminaries

3.2.1 Notation

The transpose of a vector x is denoted by x^T. The notation $u \in S(\Delta)$ signifies that the vector u is a member of the set of piecewise-continuous (from the right) functions with period Δ. The notation $t_k = k\Delta$, $k = 0, 1, 2, \ldots$, and the notation $\tilde{t}_j = j\Delta_e$, $j = 0, 1, 2, \ldots$, refer to elements of a time sequence separated by sampling time periods of lengths Δ and Δ_e, respectively. The notation $|\cdot|$ signifies the Euclidean norm of a vector.

3.2.2 Class of Systems

We consider a nonlinear chemical process system with the following form:

$$\dot{x} = f(x, u_a, w) \tag{3.1}$$

where $x \in X \subseteq R^n$ is the process state vector (bounded in the set X), $u_a \in R^m$ is the vector of process inputs, $w \in R^l$ is a vector of bounded process disturbances (i.e., $w \in W := \{w \ : \ |w| \leq \theta\}$), and $f : R^n \times R^m \times R^l$ is a locally Lipschitz vector function of its arguments with $f(0,0,0) = 0$. Each component $u_{a,i}$, $i = 1, \ldots, m$, of the process input vector is an output of a valve that is adjusted utilizing a feedback controller for the nonlinear process that outputs a set-point $u_{m,i}$, $i = 1, \ldots, m$, for each valve output. Because the valve output flow rates are bounded by physical valve constraints, each input $u_{a,i}$ is bounded between a minimum ($u_{a,i,\min}$) and a maximum ($u_{a,i,\max}$) flow rate, with the resulting input constraint on u_a denoted by U (i.e., $u_a \in U$, where $U := \{u_a \in R^m \mid u_{a,i,\min} \leq u_{a,i} \leq u_{a,i,\max}, \ i = 1, \ldots, m\}$). Since the flow rates out of the valve are bounded, the set-points are bounded also (i.e., $u_m \in U_m$, where $U_m := \{u_m \in R^m \ : \ u_{m,i,\min} \leq u_{m,i} \leq u_{m,i,\max}, \ i = 1, \ldots, m\}$). The relationship between each $u_{m,i}$ and each $u_{a,i}$ depends on the valve behavior. We will consider valve behavior for which the $u_{a,i} - u_{m,i}$ relationship is either static or dynamic. In the case that the $u_{a,i} - u_{m,i}$ relationships are static, the following equation holds:

$$u_{a,i} = f_{static,i}(u_{m,i}) \tag{3.2}$$

where $f_{static,i}$ is a nonlinear vector function ($f_{static}(u_m) = [f_{static,1}(u_{m,1}) \cdots f_{static,m}(u_{m,m})]^T$). Alternatively, a dynamic model may characterize the $u_{a,i} - u_{m,i}$ relationship, where $u_{a,i}$ is related to both $u_{m,i}$ and the dynamic state vector $x_{dyn,i} \in R^{p_i}$, for which the components $x_{dyn,i,j}$, $j = 1, \ldots, p_i$, are states of the valve model. In this case, the following equations describe the dynamics of the valve model for the $i-th$ valve:

$$\dot{x}_{dyn,i} = \hat{x}_{dyn,i}(x_{dyn,i}, u_{m,i}) \tag{3.3}$$

$$u_{a,i} = f_{dynamic,i}(x_{dyn,i}) \tag{3.4}$$

where $\hat{x}_{dyn,i}$ is a nonlinear vector function characterizing the dynamics of the internal states of the model for the $i-th$ valve, and $f_{dynamic,i}$ is a nonlinear vector function relating $u_{a,i}$ and the internal dynamic states of the valve model. We define $x_{dyn} = [x_{dyn,1} \cdots x_{dyn,m}]^T$, $\hat{x}_{dyn}(x_{dyn}, u_m) = [\hat{x}_{dyn,1}(x_{dyn,1}, u_{m,1}) \cdots \hat{x}_{dyn,m}(x_{dyn,m}, u_{m,m})]^T$, and $f_{dynamic}(x_{dyn}) = [f_{dynamic,1}(x_{dyn,1}) \cdots f_{dynamic,m}(x_{dyn,m})]^T$.

We assume in this chapter that the value of each $u_{m,i}$ is determined utilizing a feedback controller that utilizes knowledge of at least one process state to compute control actions. This means that the value of each $u_{m,i}$ is affected by some subset of the state vector as follows:

$$u_{m,i} = f_{controller,i}(x, \hat{\zeta}_i) \tag{3.5}$$

where $\hat{\zeta}_i \in R^{r_i}$, $i = 1, \ldots, m$, is a vector of internal states of the controller calculating $u_{m,i}$. These internal states may be dynamic as follows:

$$\dot{\hat{\zeta}}_i = f_{internal,i}(x, x_{dyn}, \hat{\zeta}_i) \tag{3.6}$$

Defining $f_{controller}(x, \hat{\zeta}) = [f_{controller,1}(x, \hat{\zeta}_1) \cdots f_{controller,m}(x, \hat{\zeta}_m)]^T$, $\hat{\zeta} = [\hat{\zeta}_1 \cdots \hat{\zeta}_m]^T$, and $f_{internal}(x, x_{dyn}, \hat{\zeta}) = [f_{internal,1}(x, x_{dyn}, \hat{\zeta}_1) \cdots f_{internal,m}(x, x_{dyn}, \hat{\zeta}_m)]^T$, we can write the process-valve system as follows for the case of a static relationship between u_a and u_m (i.e., Eq. 3.2 holds):

$$\begin{bmatrix} \dot{x} \\ \dot{\hat{\zeta}} \end{bmatrix} = \begin{bmatrix} f(x(t), f_{static}(f_{controller}(x, \hat{\zeta})), w(t)) \\ f_{internal}(x, x_{dyn}, \hat{\zeta}) \end{bmatrix} \tag{3.7}$$

For the case of a dynamic relationship between u_a and u_m (i.e., Eqs. 3.3-3.4 hold), the following

process-valve system results:

$$\begin{bmatrix} \dot{x} \\ \dot{x}_{dyn} \\ \dot{\hat{\zeta}} \end{bmatrix} = \begin{bmatrix} f(x(t), f_{dynamic}(x_{dyn}), w(t)) \\ \hat{x}_{dyn}(x_{dyn}, f_{controller}(x, \hat{\zeta})) \\ f_{internal}(x, x_{dyn}, \hat{\zeta}) \end{bmatrix} \tag{3.8}$$

With slight abuse of notation, the right-hand sides of both Eqs. 3.7 and 3.8 will be denoted by $f_q(q(t), u_m(t), w(t))$ (f_q signifies the right-hand side of Eq. 3.7 when Eq. 3.2 characterizes the $u_{a,i} - u_{m,i}$ relationship, and it signifies the right-hand side of Eq. 3.8 when Eqs. 3.3-3.4 characterize the $u_{a,i} - u_{m,i}$ relationship), where $q(t)$ represents the vector of process-valve states (i.e., $q = [x\ \hat{\zeta}]^T$ when Eq. 3.7 describes the process-valve dynamics, and $q = [x\ x_{dyn}\ \hat{\zeta}]^T$ when Eq. 3.8 describes the process-valve dynamics). We assume that f_q is a locally Lipschitz vector function of its arguments with $f_q(0,0,0) = 0$.

Remark 3.1. *Disturbances could also be considered in other dynamic states of the process-valve model besides x, such as in x_{dyn}, and the analysis presented throughout this chapter would continue to hold.*

3.2.3 Feedback Control Designs for Obtaining Valve Output Set-Points

Though in general any state feedback controller can be used to compute the values of $u_{m,i}$, $i = 1, \ldots, m$, the examples in this chapter will obtain u_m utilizing a standard linear control design with an integral term (PI control) and model predictive control (MPC).

3.2.3.1 Classical Linear Control with Integral Action

Linear control designs with an integral term are designed to drive a selected process output (here taken to be a process state, which is consistent with standard industrial practice in the chemical process industries) to its set-point. Thus, we assume that the process state vector or a subset of it comprises the vector $\hat{x} \in R^{\hat{n}}$, $\hat{n} \leq n$, of measured outputs being driven to the set-point vector

$\hat{x}_{sp} \in R^{\hat{n}}$. When a PI controller is used, each component of $\hat{x}$ is regulated to its set-point by an individual linear controller that outputs a valve output flow rate set-point for an individual valve, and thus $\hat{n} = m$. The dynamics of the $i-th$ PI controller are represented by:

$$u_{m,i} = g_{A,i}(\hat{x}_i, \zeta_i) \tag{3.9}$$

$$\dot{\zeta}_i = A_{con,i} \begin{bmatrix} \hat{x}_i \\ \zeta_i \end{bmatrix} + B_{con,i}\hat{x}_{i,sp} \tag{3.10}$$

The form of these equations follows that in Eqs. 3.5-3.6, with $\hat{\zeta}_i = \zeta_i$, $f_{controller,i}$ given by $g_{A,i}$, and $f_{internal,i}$ given by the right-hand side of Eq. 3.10. $A_{con,i}$ and $B_{con,i}$ are a matrix and scalar.

3.2.3.2 Model Predictive Control

Model predictive control[126] is an optimization-based control strategy that computes piecewise-constant set-points u_m for the control actuators with period Δ (i.e., $u_m \in S(\Delta)$) based on the following optimization problem:

$$\min_{u_m(t) \in S(\Delta)} \quad \int_{t_k}^{t_{k+N}} L_e(\tilde{x}(\tau), u_m(\tau))\, d\tau \tag{3.11a}$$

$$\text{s.t.} \quad \dot{\tilde{x}}(t) = f(\tilde{x}(t), u_m(t), 0) \tag{3.11b}$$

$$\tilde{x}(t_k) = x(t_k) \tag{3.11c}$$

$$\tilde{x}(t) \in X, \forall t \in [t_k, t_{k+N}) \tag{3.11d}$$

$$u_m(t) \in U_m, \ \forall t \in [t_k, t_{k+N}) \tag{3.11e}$$

$$g_{MPC,1}(\tilde{x}(t), u_m(t)) = 0 \tag{3.11f}$$

$$g_{MPC,2}(\tilde{x}(t), u_m(t)) \leq 0 \tag{3.11g}$$

The stage cost $L_e(x, u_m)$ is minimized subject to bounds on the states (Eq. 3.11d), bounds on the inputs (Eq. 3.11e), equality and inequality constraints (Eqs. 3.11f-3.11g), and the restriction

that the states must evolve according to the nominal ($w(t) \equiv 0$) dynamic model in Eq. 3.11b when initialized from a measurement of the state (Eq. 3.11c). In Eq. 3.11b, $u_m(t)$ is used in place of $u_a(t)$ because the standard formulation of MPC in industry and the literature neglects valve behavior in general (i.e., it assumes that $u_a = u_m$; therefore, no reference is made to u_a in Eq. 3.11). MPC can, however, handle valve saturation through the constraint of Eq. 3.11e, assuming $u_a = u_m$. A vector of control actions u_m is computed for each of the N sampling periods of length Δ (N is the prediction horizon), and only the first of these vectors is applied to the process in a sample-and-hold fashion according to a receding horizon strategy. The notation $u_m^*(t|t_k)$, $t \in [t_k, t_{k+N})$, signifies the optimal value of u_m for time t for the optimization problem initiated at time t_k.

A form of MPC that is commonly used in the chemical process industries is tracking MPC, which drives $\hat{x}$ to $\hat{x}_{sp}$ (though it is not necessary in this case that $\hat{n} = m$) by utilizing a quadratic stage cost with its minimum at the set-point vector $\hat{x}_{sp}$ with corresponding steady-state input vector $u_{m,sp}$ as follows:

$$L_e(\tilde{x}(\tau), u_m(\tau)) = (\hat{x}_{sp} - \tilde{\hat{x}})^T Q(x_{sp} - \tilde{\hat{x}}) + (u_{m,sp} - u_m)^T R(u_{m,sp} - u_m) \tag{3.12}$$

where $Q > 0$ and $R > 0$ are tuning matrices, and $\tilde{\hat{x}}$ denotes the predicted value of the vector $\hat{x}$.

The value of each $u_{m,i}$ calculated by the MPC has the form of Eq. 3.5 with $\hat{\zeta}_i = 0$ (which leaves $u_{m,i}$ as a function of the process state), though the function $f_{controller,i}$ is not explicitly defined in this case but is defined implicitly by the optimization problem in Eq. 3.11.

Remark 3.2. *We assume that full state feedback is available for all MPC designs presented in this chapter. When it is not, state estimation can be considered to develop an output feedback MPC strategy (e.g.,[66]) but this will not be pursued here.*

3.3 Control Loop Including Valve Behavior: Process Output Responses as a Closed-Loop Effect

In this section, we analyze the class of systems from the prior section under linear control and MPC to show, at a fundamental mathematical level, that the negative responses of closed-loop systems containing sticky valves result from the coupling of the controller, process, and valve dynamics (i.e., they are closed-loop effects), and therefore also depend on the control loop architecture. We then exemplify, by demonstrating that both linear valve dynamics and the dynamics of stiction fall within the framework of Eq. 3.8, that this closed-loop perspective extends both to valve dynamics typically discussed in the literature/undergraduate process control coursework as well as to nonlinear dynamic behavior that is typically neglected at an academic level. Finally, we examine two process examples that demonstrate the complexity of the dynamics of a process-valve system and demonstrate that different effects are observed with different control designs and control loop architectures.

3.3.1 Class of Systems Analysis

Consider the system of Eq. 3.7, which represents a process-valve system subject to only a static valve nonlinearity under feedback control. The static nonlinearity impacts the dynamics of x (i.e., in the absence of the static valve nonlinearity ($u_a = u_m$), the dynamics of $\dot{x}$ would be described by $f(x(t), f_{controller}(x, \hat{\zeta}), w(t))$, which is different than the dynamics in Eq. 3.7). In addition, both $\dot{x}$ and $\dot{\hat{\zeta}}$ are functions of x, so modifying f_{static} affects the response of both x and $\hat{\zeta}$. Due to the fact that the system is nonlinear, the effect on the closed-loop response of changing f_{static} is difficult to determine without performing closed-loop simulations. This is particularly significant when there are multiple process inputs $u_{a,i}$ related to $u_{m,i}$ through different static nonlinear functions, especially assuming that the dynamics of the components of x are coupled. Then, each $u_{a,i}$ affects all components of x either directly or through coupling of those components in the vector function f, and the value of each $u_{a,i}$ is affected by all components of x due to the fact that the components of

x are coupled and at least one of those components is used to calculate $u_{m,i}$ to define $u_{a,i}$ (Eq. 3.2) due to the use of state feedback control (Eq. 3.5). Using a similar analysis, it can be deduced that changing the control law (i.e., changing $f_{controller}$ and $f_{internal}$) also impacts the closed-loop response in a manner that is difficult to determine *a priori* (without simulations).

When the valve dynamics can be described by dynamic systems of equations as in Eq. 3.8, the dynamics of the valve, controller, and process are again coupled. In this case, however, there is an additional complexity in that the valve dynamics add additional states with nonlinear dynamics (or linear in the specific case of linear valve dynamics) that are not present in the case that $u_a = u_m$. Furthermore, because $u_{m,i}$ is a function of at least one of the components of x, it is affected by the other components of x as well, assuming coupling between these components. This causes $x_{dyn,i}$ and $u_{a,i}$ to also be affected by x (Eqs. 3.3-3.4), and the components of x are affected by the values of all $u_{a,i}$ in Eq. 3.1 and thus by the valve states $x_{dyn,i}$, $i = 1, \ldots, m$, from Eq. 3.4.

The above analysis shows that from a fundamental mathematical analysis of general equations for a process-valve system, the dynamics of all valves can be seen to be coupled with the dynamics of the other valves and also with the dynamics of the process and the controller due to state feedback (this is not limited to PI control or MPC). Because the controller dynamics affect the evolution of the states and thus the process outputs, different types of controllers would be expected to result in different responses of the process outputs. Furthermore, the control loop architecture will also affect the response because it will impact the equations that describe the controller dynamics. This analysis reveals that the negative effects of valve dynamics on control loop effectiveness are related to the controller, process, and valve dynamics, in addition to the control architecture.

Remark 3.3. *In this chapter, we consider that all states of the process-valve model are coupled since this is the most general case. For specific cases when this does not hold, it may be possible to analyze the dynamics of the specific process to see if any simplifications result compared to the analysis in this chapter.*

3.3.1.1 Linear Valve Dynamics

The analysis just presented holds for linear valve dynamics which, though typically presented in transfer function form in undergraduate coursework, can be cast in state-space form in the time domain as:

$$\dot{x}_{u_{a,i}} = A_i x_{u_{a,i}} + B_i u_{m,i} \tag{3.13}$$

$$u_{a,i} = C_i x_{u_{a,i}} \tag{3.14}$$

where $x_{u_{a,i}} \in R^{p_i}$ is the vector of internal states of the linear valve dynamic model for the $i-th$ valve, and A_i, B_i, and C_i are two matrices and a vector, respectively, of appropriate dimensions. Combining the process and valve layer models gives the following process-valve model for this case (omitting the dynamics of the controller):

$$\begin{bmatrix} \dot{x} \\ \dot{x}_{u_a} \end{bmatrix} = \begin{bmatrix} f(x(t), Cx_{u_a}(t), w(t)) \\ Ax_{u_a} + Bu_m \end{bmatrix} \tag{3.15}$$

where A, B, and C are matrices and vectors of appropriate dimensions containing the elements of A_i, B_i, and C_i, $i = 1, \ldots, m$, in an appropriate order, and $x_{u_a} = [x_{u_{a,1}} \ \ldots \ x_{u_{a,m}}]^T$. Using the notation in Eqs. 3.3-3.4, $x_{dyn} = x_{u_a}$, and $\hat{x}_{dyn,i}(x_{dyn,i}, u_{m,i})$ and $f_{dynamic,i}(x_{dyn,i})$ equal the right-hand sides of Eqs. 3.13 and 3.14, respectively.

3.3.1.2 Sticky Valve Dynamics

Like linear valve dynamics, nonlinear valve dynamics also fit within the framework of Eq. 3.8. For the case that all valves are sticky (i.e., affected by friction/stiction, which prevents the valve position from appreciably changing until the force applied to the valve moving parts becomes sufficiently large) and move in a straight line (rather than rotating), the valve position $x_{v,i}$ and the valve velocity $v_{v,i}$ for the $i-th$ valve evolve in time according to the following force balance:

$$\dot{x}_{v,i} = v_{v,i} \tag{3.16}$$

$$\dot{v}_{v,i} = \frac{1}{m_{v,i}}(a_i^T F_{O,i} + c_i^T F_{A,i} - F_{fric,i}) \tag{3.17}$$

where $m_{v,i}$ is the mass of the moving parts of the $i-th$ valve, $F_{O,i}$ is a vector of non-friction forces on the valve that are not related to the controller output or friction force and which have coefficient vector a_i, $F_{A,i}$ is a vector of non-friction forces on the valve that are adjusted based on the controller output and have coefficient vector c_i, and $F_{fric,i}$ is the friction force on the $i-th$ valve. The friction force is a static function of $x_{v,i}$, $v_{v,i}$, and $z_{f,i}$ (which is a dynamic internal state of the friction model), as follows:

$$F_{fric,i} = \hat{F}_{fric,i}(x_{v,i}, v_{v,i}, z_{f,i}) \tag{3.18}$$

$$\dot{z}_{f,i} = \hat{z}_{f,i}(x_{v,i}, v_{v,i}, z_{f,i}) \tag{3.19}$$

where $\hat{z}_{f,i}$ is a nonlinear vector function describing the dynamics of the internal states of the friction model.

Assuming that $F_{A,i}$ is a static function of $u_{m,i}$ as follows:

$$F_{A,i} = f_{SO,i}(u_{m,i}) \tag{3.20}$$

where $f_{SO,i}$ is a nonlinear vector function describing the relationship between $u_{m,i}$ and $F_{A,i}$, and that $F_{O,i}$ is also a function of the valve model states, the right-hand side of Eq. 3.17 can be denoted by $\hat{v}_{v,i}(u_{m,i}, x_{v,i}, v_{v,i}, z_{f,i})$. Finally, assuming that the relationship between $u_{a,i}$ and $x_{v,i}$ can be expressed through the following static nonlinear equation describing the valve characteristic:

$$u_{a,i} = f_{flow,i}(x_{v,i}) \tag{3.21}$$

we obtain the following process-valve model (omitting the dynamics of the controller for the

process):

$$\begin{bmatrix} \dot{x} \\ \dot{x}_v \\ \dot{v}_v \\ \dot{z}_f \end{bmatrix} = \begin{bmatrix} f(x(t), f_{flow}(x_v(t)), w(t)) \\ v_v \\ \hat{v}_v(u_m, x_v, v_v, z_f) \\ \hat{z}_f(x_v, v_v, z_f) \end{bmatrix} \tag{3.22}$$

where $x_v = [x_{v,1} \cdots x_{v,m}]^T$, $v_v = [v_{v,1} \cdots v_{v,m}]^T$, $z_f = [z_{f,1} \cdots z_{f,m}]^T$, $f_{flow}(x_v(t)) = [f_{flow,1}(x_{v,1}) \cdots f_{flow,m}(x_{v,m})]^T$, $\hat{v}_v(u_m, x_v, v_v, z_f) = [\hat{v}_{v,1}(u_{m,1}, x_{v,1}, v_{v,1}, z_{f,1}) \cdots \hat{v}_{v,m}(u_{m,m}, x_{v,m}, v_{v,m}, z_{f,m})]^T$, $\hat{z}_f(x_v, v_v, z_f) = [\hat{z}_{f,1}(x_{v,1}, v_{v,1}, z_{f,1}) \cdots \hat{z}_{f,m}(x_{v,m}, v_{v,m}, z_{f,m})]^T$. In the notation of Eq. 3.8, $x_{dyn} = [x_v \; v_v \; z_f]^T$, $f_{dynamic}(x_{dyn}) = f_{flow}(x_v(t))$, and $\hat{x}_{dyn,i}(x_{dyn,i}, u_{m,i})$ is given by the right-hand sides of Eqs. 3.16-3.17 and 3.19.

For clarification on the stiction modeling concepts presented in this section, the reader may refer to Chapter 5, in which stiction is the focus of the chapter, and specifically to Figs. 5.1, 5.2, 5.4, and 5.5, which provide schematics exemplifying the concepts of forces on a valve, valve characteristics, and different amounts of flow through a valve for different valve positions.

3.3.2 Process Examples Illustrating a Closed-Loop Perspective on Effects of Valve Behavior

In this section, we provide two example process systems (a level control example and a continuous stirred tank reactor (CSTR) example) that highlight the interactions between the controller, valve, and process dynamics in a control loop where valve behavior cannot be neglected.

3.3.2.1 Single-Input/Single-Output Level Control Loop

We consider first a level control problem with a sticky valve in the control loop. The level control problem is chosen due to its simplicity, which allows us to focus on the effects of the valve dynamics in this example without the added complexity of a large-scale nonlinear process model. In the level control problem (shown in Fig. 3.1) considered, the tank inlet flow rate u_a is

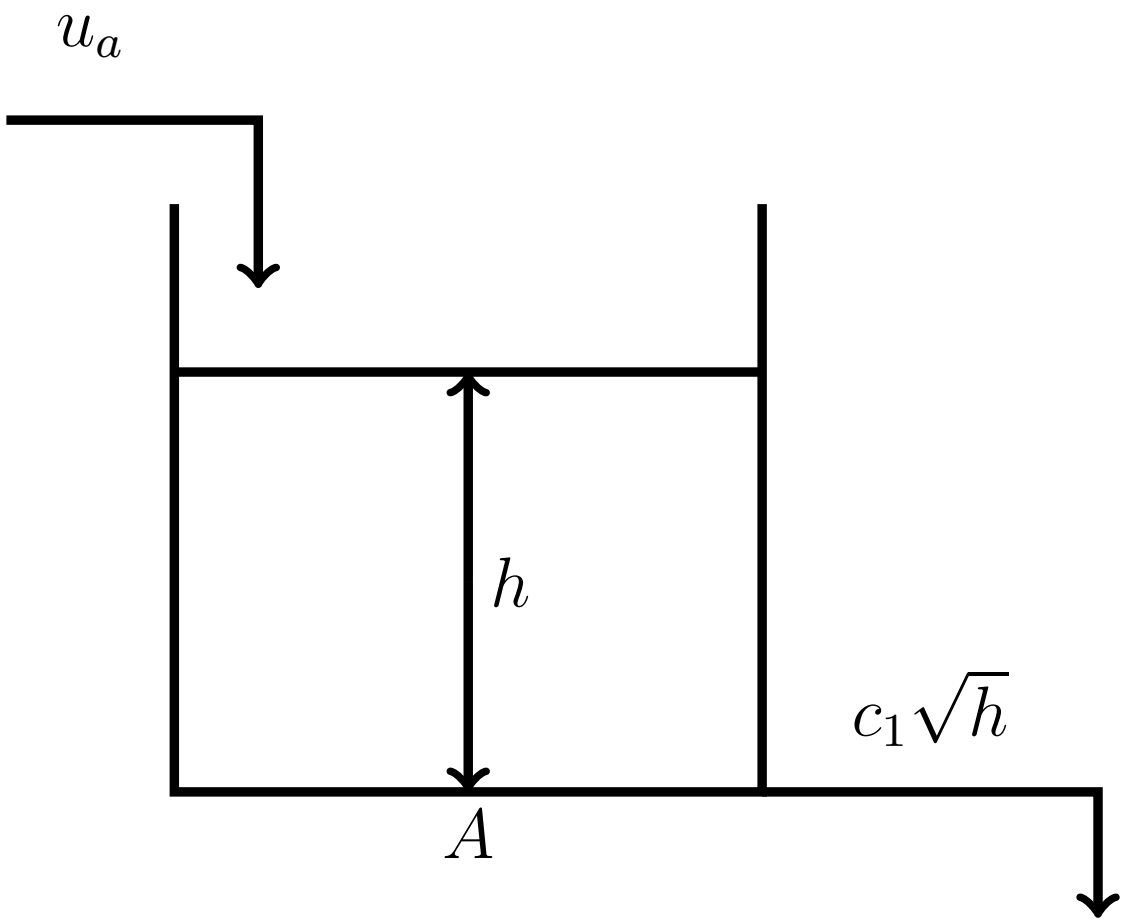

Figure 3.1: Schematic depicting the tank considered in the level control example.

the controlled variable. The dynamics of the tank level are:

$$\frac{dh}{dt} = \frac{1}{A}(u_a - c_1\sqrt{h}) \tag{3.23}$$

where $A = 0.25\ m^2$ denotes the cross-sectional area of the tank, and $c_1 = 0.008333\ m^{5/2}/s$ is the outlet resistance coefficient. On an order of magnitude consistent with an example from[118] that uses these parameter values, we define the minimum tank height as $0\ m$, the maximum tank height as $0.5184\ m$, the minimum value of u_a as $u_{a,\min} = 0\ m^3/s$ (fully closed valve), and the maximum value of u_a as $u_{a,\max} = 0.006\ m^3/s$ (fully open valve).

Without Valve Dynamics: Well-Tuned Control. We first demonstrate that when the valve dynamics can be assumed to be instantaneous (i.e., they are so fast that $u_a = u_m$ at all times is

a reasonable approximation), as is typically assumed in the chemical process control literature, a well-tuned PI controller and an MPC can be designed that effectively drive the level to its set-point.

The PI controller for the tank level is taken to have the following form:

$$\dot{\zeta} = h_{sp} - h,\ \zeta(0) = 0 \tag{3.24}$$

$$u_m = u_{as} + K_c(h_{sp} - h) + K_c\zeta/\tau_I \tag{3.25}$$

where u_m is the controller output, ζ is the dynamic (integrating) variable of the PI controller, u_{as} is the steady-state value of u_a before the set-point change, and h_{sp} is the level set-point. A tuning $K_c = 0.006$ and $\tau_I = 43.2$ was selected that prevents u_m from dipping below $u_{a,\min}$ or shooting above $u_{a,\max}$ for the set-points simulated. The response of the level of the tank of Eq. 3.23 under the PI controller of Eqs. 3.24-3.25 when $u_a = u_m$ (no valve dynamics) is shown in the top plot of Fig. 3.2, plotted every 100 integration steps, for the tank level initiated from its maximum ($u_a = 0.006\ m^3/s$, $h = 0.5184\ m$), decreased to $0.15\ m$, and then increased to $0.20\ m$ (the set-point change from $0.15\ m$ to $0.20\ m$ will be the focus in the remainder of this section to avoid the effects of possible initial transients during the first set-point change). Each set-point was held for 1040 s. The dynamic system was integrated with the Explicit Euler numerical integration method and an integration step size of $10^{-3}\ s$. At the set-point changes, the value of ζ was re-set to 0 and the value of u_{as} was set to the last applied value of u_m.

A more systematic method than tuning a PI controller for ensuring that the process meets its set-point without violating the constraints on the inputs is to use tracking MPC, which calculates control actions subject to constraints. Focusing on the second set-point change from the example above, we assume that the level has already been brought to $0.15\ m$ and that a well-tuned tracking MPC must now drive the closed-loop state h to $0.20\ m$ when there are no actuator dynamics (i.e.,

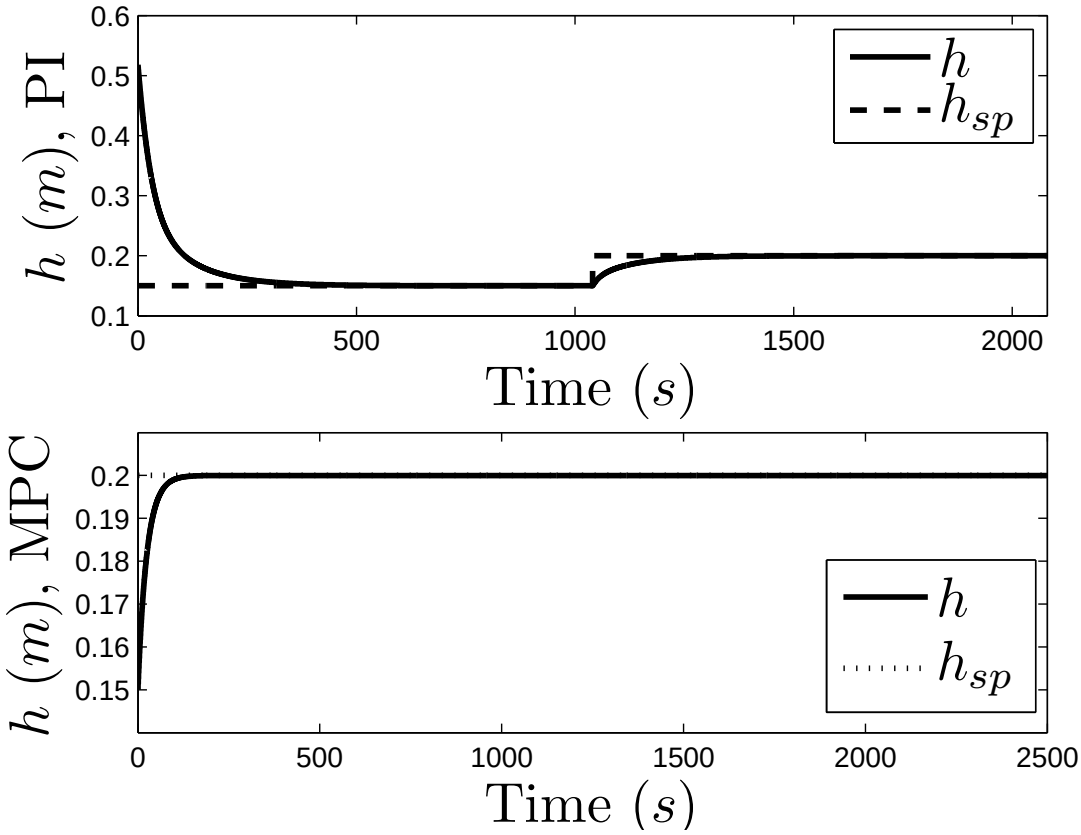

Figure 3.2: Closed-loop trajectory of level h with reference to its set-point h_{sp} for the process of Eq. 3.23 under the PI controller of Eqs. 3.24-3.25 (top plot) and under the MPC of Eq. 3.26 (bottom plot) with no actuator dynamics.

$u_a = u_m$). The MPC for this case is:

$$\min_{u_m(t)\in S(\Delta)} \quad \int_{t_k}^{t_{k+N}} Q(h_{sp}-\tilde{h})^2 + R(u_{a,sp}-u_m)^2\, d\tau \tag{3.26a}$$

$$\text{s.t.} \quad \dot{\tilde{h}} = \frac{1}{A}(u_m - c_1\sqrt{\tilde{h}}) \tag{3.26b}$$

$$\tilde{h}(t_k) = h(t_k) \tag{3.26c}$$

$$0 \le u_m(t) \le 0.006,\ \forall t \in [t_k, t_{k+N}) \tag{3.26d}$$

where $Q = 0.00001$ and $R = 1$. Using this MPC to control the process of Eq. 3.23 with an integration step size of 10^{-3} s within the MPC, an integration step size of 10^{-5} s to simulate the level, a prediction horizon of $N = 50$, a sampling period of length $\Delta = 1$ s, a final time of the simulation of 2500 s, and a set-point $h_{sp} = 0.20$ m with its corresponding steady-state flow rate $u_{a,sp} = 0.00373$ m^3/s, the state profile in the bottom plot of Fig. 3.2 is obtained (the results are plotted every 10000 integration steps). The nonlinear interior point optimization solver Ipopt[148] was used for the simulations with a tolerance of 10^{-8} on a 2.40 GHz Intel Core 2 Quad CPU Q6600 on a 64-bit Windows 7 Professional operating system with 4.00 GB of RAM.

With Stiction: Undesirable Closed-Loop Behavior. We now demonstrate that when the valve is sticky, but the PI and MPC designs shown above to be well-tuned when the valve did not have significant dynamics (i.e., before it became sticky) are applied, various set-point tracking issues can occur. This demonstrates that sustained oscillations can be set up in an originally well-tuned control loop that has become sticky (perhaps due to, for example, the valve packing being tightened to prevent chemical emissions from the plant[89]). For the sticky valve case, u_a in Eq. 3.23 is the flow rate out of a pressure-to-close spring-diaphragm sliding-stem globe valve actuated by a pressure P. If the valve is initiated from its fully open position, no pressure is initially applied and the valve stem is at its equilibrium position $x_v = 0$ m. Its fully closed position corresponds to $x_v = x_{v,\max} = 0.1016$ m. The differential equations for the valve dynamics are:[72]

$$\frac{dx_v}{dt} = v_v \tag{3.27}$$

$$\frac{dv_v}{dt} = \frac{1}{m_v}[A_v P - k_s x_v - F_f] \tag{3.28}$$

where A_v and k_s are the diaphragm area and spring constant, respectively, and the friction force F_f is determined from the LuGre friction model:[26]

$$F_f = \sigma_0 z_f + \sigma_1 \frac{dz_f}{dt} + \sigma_2 v_v \tag{3.29}$$

$$\frac{dz_f}{dt} = v_v - \frac{|v_v|\sigma_0}{F_C + (F_S - F_C)e^{-(v_v/v_s)^2}} z_f \tag{3.30}$$

The parameters of the valve dynamic model in Eqs. 3.27-3.30 are those for the "nominal valve" in[72] and are displayed in Table 3.1. In addition, we assume that the valve has a linear installed characteristic:[38]

$$u_a = \left(\frac{x_{v,\max} - x_v}{x_{v,\max}} \right) u_{a,\max} \tag{3.31}$$

The pressure to be applied to the valve for a given set-point u_m is determined from the following $u_m - P$ relationship that was developed for a low-stiction valve (its development will be described in Section 5.4.2):

$$P = \frac{(u_m/u_{a,\max}) - 0.70391/0.7042}{-\frac{0.05864}{6894.76*0.7042}} \tag{3.32}$$

Thus, we assume that the valve is operated with the pressure applied to the valve determined by a law that was developed when the valve had low friction, though this relationship does not adequately describe the valve input-output relationship for a valve with more significant stiction. Though this relationship was developed for a low-stiction valve (instead of the no-stiction valve for which the tuning of both the PI controller and MPC were determined in Fig. 3.2), the tunings developed in the no-stiction case perform well for the low-stiction valve with the $u_m - P$ relationship in Eq. 3.32 because the slope and intercept of the implicit P versus $u_m/u_{a,\max}$ relationship assumed in Fig. 3.2 (obtained from $F_f = 0\ N$ in Eq. 3.28) are only about 0.08% and 0.04% different, respectively, from the values in Eq. 3.32. The relationship of Eq. 3.32 has the form of Eq. 3.20, where P is $F_{A,i}$ and the right-hand side of Eq. 3.32 is $f_{SO,i}(u_m)$.

Table 3.1: Valve Model Parameters[72]

Parameter	Value
m_v	1.361 kg
A_v	0.06452 m^2
k_s	52538 kg/s^2
v_s	0.000254 m/s
σ_0	10^8 kg/s^2
σ_1	9000 kg/s
σ_2	612.9 kg/s
F_C	1423 $kg \cdot m/s^2$
F_S	1707.7 $kg \cdot m/s^2$

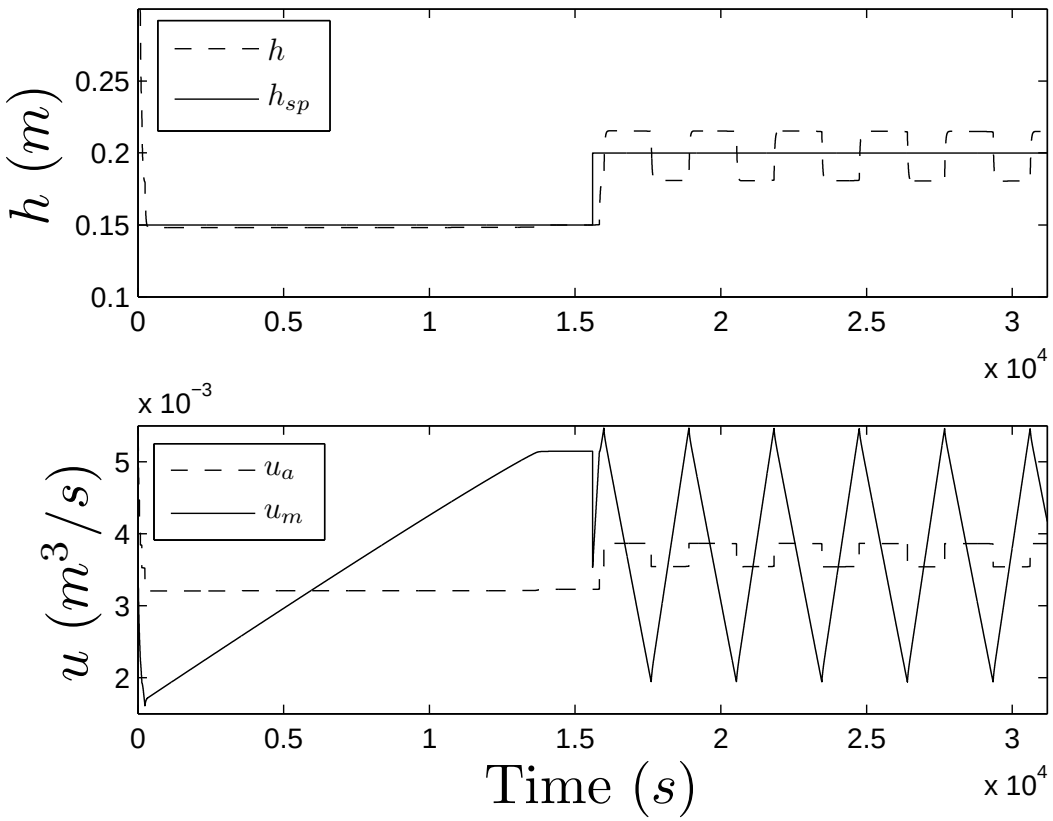

Figure 3.3: Closed-loop trajectories of h, u_a, and u_m for the process of Eq. 3.23 under the PI controller of Eqs. 3.24-3.25 with the valve dynamics in Eqs. 3.27-3.32. This data is plotted every 100000 integration steps.

Fig. 3.3 shows h, u_m, and u_a when the valve with the dynamics in Eqs. 3.27-3.32 is used to adjust the flow rate to the process of Eq. 3.23 under the PI controller of Eqs. 3.24-3.25. The valve was initiated from its fully open position (i.e., $h = 0.5184\ m$, $u_a = 0.006\ m^3/s$, $\zeta = 0\ m \cdot s$, $x_v = 0\ m$, $v_v = 0\ m/s$, $z_f = 0\ m$), and the set-point was changed to 0.15 m for 15600 s, then to 0.20 m for 15600 s. Because the second set-point change is the focus in this chapter, we will refer to the process-valve state at $t = 15600\ s$ from this simulation as q_I (the initial process-valve state for the level set-point change from 0.15 m to 0.20 m). The value of ζ was re-set to zero when the level set-point was changed, and the value of u_{as} in Eq. 3.25 was re-set to the last applied value of u_a when the set-point was changed. The trajectories were obtained using the Explicit Euler numerical integration method with an integration step size of $10^{-5}\ s$. In the simulations of the valve throughout this section, several physical considerations are taken into account: if $u_m > u_{a,\max}$ or $u_m < u_{a,\min}$, u_m is saturated at $u_{a,\max}$ or $u_{a,\min}$ respectively; if $P < 0$, P is set to 0; if $u_a > u_{a,\max}$ or $u_a < u_{a,\min}$, u_a is saturated at $u_{a,\max}$ or $u_{a,\min}$ respectively.

The cause of the oscillations that are set up at the second set-point change in Fig. 3.3 under the PI controller is related to the manner in which the forces applied to the valve change over time. The deadband/stickband causes the force applied to the valve by the pneumatic actuation to build up to a level that un-sticks the valve, allowing it to move. However, once the valve begins moving, there is a rapid drop in the friction force due to the friction dynamics for this valve (a contributor to this is that the parameter F_S, which represents the static friction coefficient, is larger than F_C, which represents the Coulomb friction coefficient). As the forces balance, the valve position changes in such a way that h_{sp} is overshot. As the valve then starts to move in the opposite direction, another series of changes in the forces on the valve causes it to move to a position that results in overshoot of h_{sp} in the opposite direction.

To clarify this point, we present some details specific to the simulation performed (the exact numbers reported are related to the integration step size utilized, but the general effects would be expected to extend qualitatively to other integration step sizes). We analyze the force balance between the times $\bar{t_1} = 17608.72441\ s$ and $\bar{t_2} = 17608.72597\ s$ in Fig. 3.3, during which P only

increases from 55942.138 to 55942.181 *Pa* due to the manner and rate at which the integral and proportional terms in the PI control law change. Within this same time period, x_v changes only slightly (from 0.036236 *m* to 0.036295 *m*). Thus, the two terms in Eq. 3.28 involving the pressure and the valve position do not change much between $\bar{t_1}$ and $\bar{t_2}$. However, in this short time, the friction force changes significantly (i.e., it is 1700.022 *N*, which is approximately the value of F_S, at $\bar{t_1}$, while it is 1501.874 *N* (closer to the value of F_C) at $\bar{t_2}$). With this rapid change of the friction force, the right-hand side of Eq. 3.28 increases from 4.1304 N/kg at $\bar{t_1}$ to 147.4380 N/kg at $\bar{t_2}$ because though the first two terms do not change much, the term for the friction force decreases significantly. When the right-hand side of Eq. 3.28 increases, the valve velocity increases, which can cause the valve to move. Though this only looks at two time instants, it shows that the rapid drop in the friction force can play an important role in changing the total force applied to the valve before it moves to a position that causes the level to overshoot its set-point (which is why slip-jump, related to this effect, is cited as one of the contributors to stiction-induced oscillations). In addition, the dynamics of the PI controller play a role in the oscillations because the dynamics do not permit the pressure on the valve stem to change at the rate necessary to keep up with the changes in the friction force (e.g., as the term related to the friction force in Eq. 3.28 decreases by close to 200 *N* between $\bar{t_1}$ and $\bar{t_2}$, the force due to the pressure only changes by 0.0027 *N*). The magnitude of the integral term is significantly larger than the magnitude of the proportional term when the level changes and overshoots its set-point, which also contributes to the length of time that the valve is stuck. However, the cause of the oscillations cannot be attributed only to the interactions of the pressure applied to the valve and the changes in the friction force; a good deal of complex behavior occurs due to the nonlinear dynamics of the valve that are coupled with those of the process and controller, including a sharp increase in the friction force after it begins decreasing followed by another decrease, the manner in which the changes in x_v affect the force balance as the valve moves, and the manner in which the dynamics of the level change the value of the pressure applied to the valve through the PI control law. Thus, closed-loop oscillations that occur when a sticky valve is within a control loop containing an integrating controller should be understood as a

closed-loop property, dependent on the interactions between all of the forces in the force balance, and the manner in which all states of the closed-loop process-valve system, including the controller states, evolve to affect the force balance through coupled dynamic equations. The root cause of stiction-induced oscillations should thus be understood as an imbalance in the forces applied to the valve that does not allow it to stabilize at values that would cause the process variable to remain at its set-point; however, there is no specific contributor in the valve dynamics, controller dynamics, or process dynamics that causes this phenomenon, but how they interact together.

The fact that the negative effects of stiction in a control loop are a closed-loop property is further emphasized by utilizing the MPC of Eq. 3.26 (i.e., an MPC that accounts only for the level dynamics and not the actuator dynamics) for the set-point change from 0.15 m to 0.20 m for the process-valve system of Eqs. 3.23 and 3.27-3.32, initiated from q_I. The process was integrated with an integration step size of 10^{-6} s using the Explicit Euler numerical integration method. The resulting trajectories of the level under the MPC are shown in Fig. 3.4, plotted every 1000 integration steps (the values of h, u_a, and u_m for this case are denoted in the legend by U, signifying that stiction is uncompensated in these results because the MPC does not account for the actuator dynamics). No oscillations are observed for this level set-point change as in Fig. 3.3, demonstrating that the stiction-induced oscillations observed under the PI controller are a closed-loop property (i.e., they depend on the controller utilized). Instead of oscillations, a persistent offset from the set-point occurs under the MPC. The reason for this is that because the MPC is unaware of the actuator dynamics, it calculates values of u_m that correspond to pressures (through Eq. 3.32) that do not allow the valve to move according to the force balance (i.e., the MPC expects that the control actions that it calculates will drive the level toward the set-point because it is anticipating that there is no friction in the valve, but due to friction the valve cannot move with the pressure applied to it). The MPC continues to compute approximately the same control action for the first sampling period of the prediction horizon at each sampling time (which is reasonable considering that the state measurement that it receives is approximately the same each time since the valve is stuck and thus the flow rate out of the valve is not appreciably changing to adjust the level). This

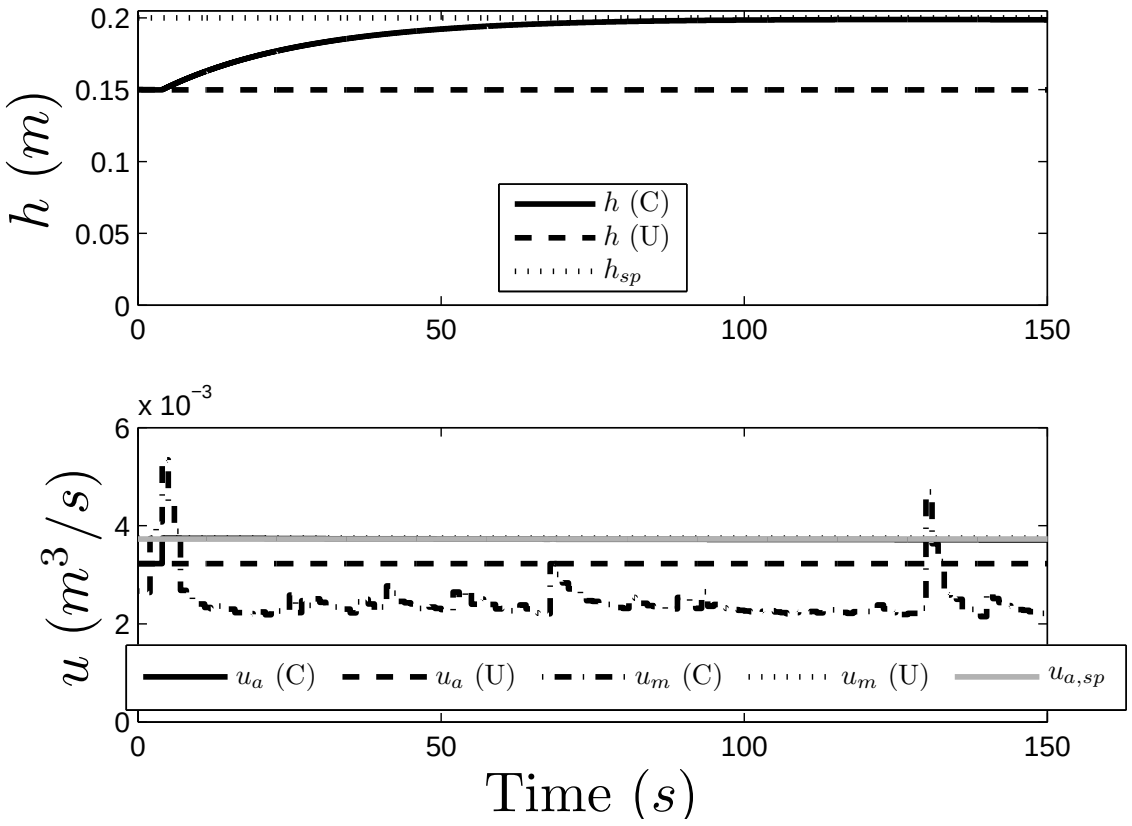

Figure 3.4: Plot of trajectories of h, u_a, u_m, and their set-points for the MPC of Eq. 3.26 (U, signifying "uncompensated") and the MPC of Eq. 4.4 (C, signifying "compensated") applied to the nonlinear process of Eqs. 3.23 and 3.27-3.32 for a level set-point change from 0.15 *m* to 0.20 *m*.

control action continues to be unable to affect the level appreciably, resulting in persistent off-set of the level from h_{sp} because the MPC has no mechanism for detecting that the set-points it has calculated are failing to make an impact on the system.

In addition to the valve behavior, controller dynamics, and process dynamics, the control loop architecture affects the response of the process outputs. This can be demonstrated by adding flow control to the valve of Eqs. 3.27-3.31. In this case, the flow rate set-point u_m is computed by the PI controller of Eqs. 3.24-3.25 for the tank level, and becomes the set-point for a minor PI control loop used to regulate u_a to u_m. This minor loop calculates the pressure P to be applied to the valve

stem based on the error $u_m - u_a$ as follows:

$$P = P_s + K_{c,p}\frac{u_m - u_a}{u_{a,\max}} + \frac{K_{c,p}}{\tau_{I,p}}\zeta_P \tag{3.33}$$

$$\dot{\zeta}_P = \frac{u_m - u_a}{u_{a,\max}},\ \zeta_P(0) = 0 \tag{3.34}$$

where P_s is the steady-state value of the pressure, and $K_{c,p} = -82737.09$, $\tau_{I,p} = 0.01$, and ζ_P are the proportional gain, integral time, and internal state, respectively, of the minor loop controller. The tuning performed successfully when u_m was constant for some time.

The valve was initially operated without flow control (i.e., Eq. 3.32 was used to relate u_m and P) for 15600 s for a level set-point change from 0.5184 m to 0.15 m to reach q_I. Subsequently, it was operated under the flow controller of Eqs. 3.33-3.34 for 15600 s for the level set-point change from 0.15 m to 0.20 m. Fig. 3.5 shows the responses of h, u_m, and u_a for the set-point change from 0.15 m to 0.20 m (the time axis is short to display the fast response of the valve under flow control). These results were obtained using an integration step size of 10^{-5} s, with the data plotted every 100000 integration steps. The integral term ζ_P of the controller for the valve was re-set to zero when the level set-point was changed, and at that point the value of P_s was also re-set to the last applied pressure. As shown in Fig. 3.5, the sustained oscillations apparent in Fig. 3.3 do not appear though the same process, sticky valve, and outer loop PI controller are used as in Fig. 3.3. Instead, when flow control is used, u_a tracks u_m well after some initial overshoot of u_m in the time period immediately after the set-point change. During these initial overshoots, the pressure applied to the valve changed rapidly according to Eqs. 3.33-3.34, causing the forces on the valve to result in the initial significant overshoots of u_a around the changing u_m set-point. However, despite these initial overshoots of u_a, the flow controller is successful at causing the forces to eventually balance on the valve in such a manner that u_a is able to track u_m and thus to drive the level to its set-point. This shows that for this example, the manner in which the forces on the valve are changed using the flow controller is able to eliminate the stiction-induced oscillations in the level. At a more fundamental level, changing the control loop architecture changed the number of coupled dynamic states in the

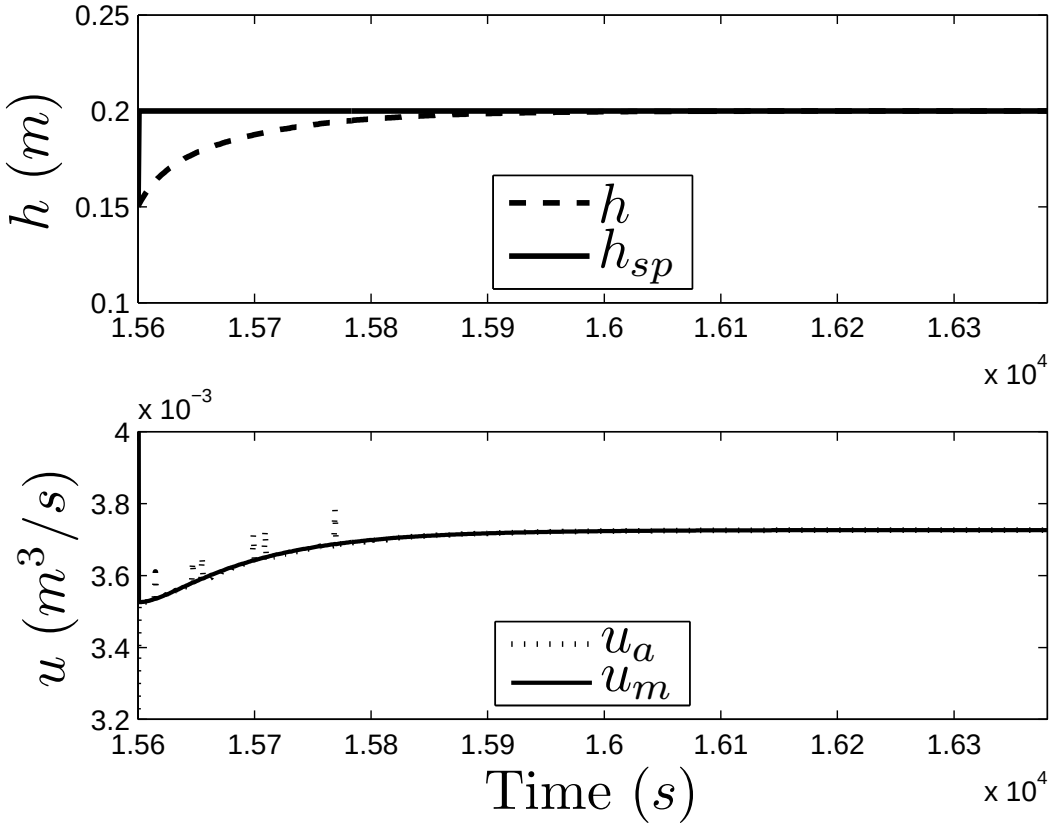

Figure 3.5: Closed-loop trajectories of h, u_a, and u_m for the process of Eq. 3.23 under the PI controller of Eqs. 3.24-3.25 with the valve in Eqs. 3.27-3.31 and the PI controller of Eqs. 3.33-3.34 used to control the valve flow rate to its set-point value for the set-point change from 0.15 *m* to 0.20 *m*.

system of nonlinear differential equations describing the process-valve system (i.e., whereas the state vector of the process-valve system without flow control included h, ζ, x_v, v_v, and z_f, it also includes ζ_P when flow control is used). Returning to the notation of Eq. 3.8, this means that x_{dyn} incorporates an extra state and its dynamics when flow control is used, which overall changes the response of the measured output (h) of the process-valve system.

Remark 3.4. *The analysis performed demonstrates that the standard valve output-controller input response for a sticky valve exhibited in Fig. 3.6 (and displayed in multiple sources in the literature such as*[33] *and*[24]*) can be understood as the response of the valve output when the force applied to the valve is ramped up and down by a controller (i.e., the closed-loop analysis above indicates*

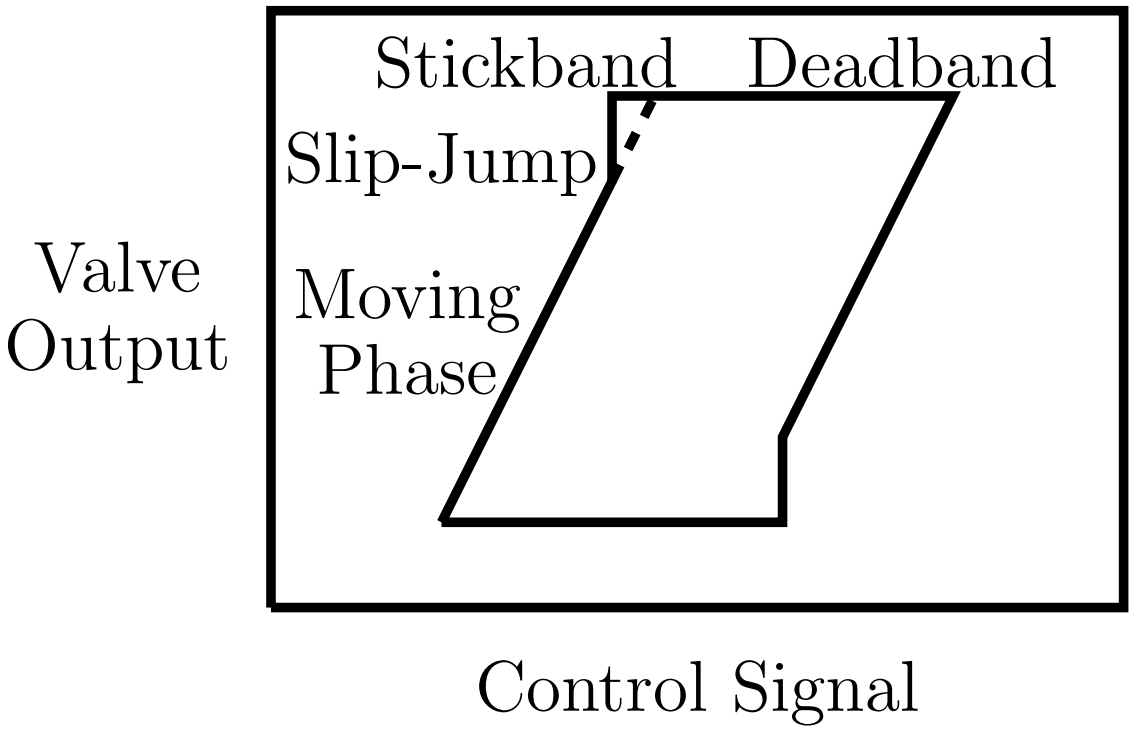

Figure 3.6: Standard controller input-valve output relationship reported for a sticky valve. The control signal to the valve changes but the valve output does not change appreciably in the regions of deadband and stickband. The valve output changes quickly in the region of slip-jump, and the valve output and control signal are linearly related in the moving phase region of the response.

that the "controller output" on the standard plots is linked to the force applied to the valve). Furthermore, Fig. 3.6 reflects the transient behavior of the valve after it begins moving (i.e., it shows the slip-jump). Because the plot can also be understood as the valve position x_v (rather than u_a) versus the controller signal as in,[86] a linear valve characteristic is assumed when the same plot is obtained for u_a versus the controller signal.

3.3.2.2 Multiple-Input/Multiple-Output Ethylene Oxidation Process

In this section, we highlight that as the complexity of the process-valve dynamics increases compared to those in the prior section (i.e., we move from a one-state, single-input process model to a four-state, three-input process model), it can be difficult to determine the effects of valve dynamics on process output responses without simulating the entire process-valve system under the proposed control design and control loop architecture. Specifically, we examine the ethylene

oxide production process from Section 2.3.1.4 with the four states x_1, x_2, x_3, and x_4, but for the case that there are three inputs to this process that are determined by valve outputs as follows:[12, 122]

$$\dot{x}_1 = u_{a,1}(1 - x_1 x_4) \tag{3.35a}$$

$$\dot{x}_2 = u_{a,1}(u_{a,2} - x_2 x_4) - A_1 exp(\gamma_1/x_4)(x_2 x_4)^{0.5} - A_2 exp(\gamma_2/x_4)(x_2 x_4)^{0.25} \tag{3.35b}$$

$$\dot{x}_3 = -u_{a,1} x_3 x_4 + A_1 exp(\gamma_1/x_4)(x_2 x_4)^{0.5} - A_3 exp(\gamma_3/x_4)(x_3 x_4)^{0.5} \tag{3.35c}$$

$$\begin{aligned}\dot{x}_4 = {} & \frac{u_{a,1}}{x_1}(1 - x_4) + \frac{B_1}{x_1} exp(\gamma_1/x_4)(x_2 x_4)^{0.5} + \frac{B_2}{x_1} exp(\gamma_2/x_4)(x_2 x_4)^{0.25} + \\ & \frac{B_3}{x_1} exp(\gamma_3/x_4)(x_3 x_4)^{0.5} - \frac{B_4}{x_1}(x_4 - u_{a,3})\end{aligned} \tag{3.35d}$$

where the process inputs $u_{a,1}$, $u_{a,2}$, and $u_{a,3}$ are dimensionless quantities corresponding to the feed volumetric flow rate, feed ethylene concentration, and coolant temperature, which are assumed to be adjusted by individual valves either directly (e.g., $u_{a,1}$) or indirectly (e.g., $u_{a,2}$ may be adjusted by opening or closing valves that allow a more concentrated ethylene stream to mix with a solvent stream, and $u_{a,3}$ may be adjusted by heating or cooling the coolant using a higher or lower flow rate of another fluid past the coolant in a heat exchanger). Due to the coupling between the states in Eq. 3.35, and the highly nonlinear dynamic equations, it is difficult to predict the evolution of x_1, x_2, x_3, and x_4, regardless of the type of controller used to calculate $u_{m,1}$, $u_{m,2}$, and $u_{m,3}$, and even if $u_{a,1} = u_{m,1}$, $u_{a,2} = u_{m,2}$, and $u_{a,3} = u_{m,3}$. Therefore, if the valves also have dynamics, linear or nonlinear, static or dynamic, or potentially different dynamics for each valve, and different controllers or control loop architectures for each valve, the number of coupled states in this system of nonlinear differential equations increases and performing simulations will be the best way to understand how each process output will respond.

3.4 Valve Behavior Compensation for Classical Control Loops

In this section, we demonstrate that the closed-loop perspective on the process output responses observed in control loops with valves for which $u_a \neq u_m$, developed in the prior sections, enables an understanding of previously proposed valve behavior compensation techniques, and the development of new compensation techniques that tackle the root cause of issues observed in many control loops (which is that they are the result of coupled, nonlinear process-valve dynamics). Due to the prevalence of compensation techniques specifically for sticky valve behavior, we will focus first on analyzing several stiction compensation methods from the literature in a closed-loop context. We will then propose a new integral term modification stiction compensation method for a control loop under PI control.

3.4.1 Stiction Compensation Methods: Flow Control

Utilizing flow control to drive u_a to u_m is a common industrial practice, and it has similarities to another common practice of adding a positioner[77,86] to a valve. Such methods can change the force applied by the actuation to the valve in an attempt to make the sum of forces balance in a manner that allows the process outputs to reach their set-points. With flow control, the force applied to the valve would be a function of u_m, u_a, and internal states of the flow controller. This method relies on the higher-level controller being well-tuned when $u_a = u_m$, so that u_a should be brought to u_m again by manipulating the forces on the valve. A PI control law for this case is:

$$\dot{\zeta}_c = (u_m - u_a),\ \zeta_c(0) = 0 \tag{3.36}$$

$$u_c = u_{cs} + K_{c,c}(u_m - u_a) + K_{c,c}\zeta_c/\tau_{I,c} \tag{3.37}$$

where ζ_c, u_c, u_{cs}, $K_{c,c}$ and $\tau_{I,c}$ are the dynamic state, control action, steady-state control action, proportional gain, and integral time of the flow controller.

3.4.2 Stiction Compensation Methods: Controller Tuning Adjustments

Re-tuning of controllers has been advocated as a method for reducing closed-loop oscillations developed in a control loop containing a sticky valve under classical PID-type control (e.g.,[111]). The re-tuning may result in an improved closed-loop response because it changes the dynamics of the PID-type controller, which, from the analysis above, alters the response of the process outputs due to the coupling of the controller, process, and valve dynamics. Reference[143] highlights the difficulty of determining an appropriate tuning for obtaining a desired response, which is consistent with the closed-loop analysis proposed above.

3.4.3 Stiction Compensation Methods: Augmented Controller Signal

The knocker[77, 134] and constant reinforcement[86] adjust the control signal received by the valve by adding either a constant or time-varying signal to the input calculated by the controller. This changes the manner in which the force applied to the valve is calculated. For example, consider the knocker applied to the level control example without flow control. The PI controller has its own dynamics that, in the absence of the knocker, dictate the pressure applied to the valve. However, with the knocker, there are times when the pressure applied to the valve is increased by an amount determined by the knocker parameters above the amount output by the PI controller, but then after a certain time period, the knocker takes away that extra amount of pressure. This allows the PI controller to retain its dynamics but permits the pressure to be adjusted using a source other than the PI controller as well, which changes the balance of forces on the valve and can result in a different closed-loop response than would be obtained without the knocker. Because the different values of the knocker parameters change the way that the forces on the valve are applied, different values of the knocker parameters cause different closed-loop responses as observed in.[134] Constant reinforcement similarly augments the output of the PI controller, adding a constant positive signal when the PI controller output is increasing and a constant negative signal when the PI controller output is decreasing, which again changes the right-hand side of the equation for the valve velocity compared to not adding such a signal. One aspect of the effect of this on the level control problem

might be, for example, that the integral term of the PI controller may not need to become as large for the pressure from the pneumatic actuation to overcome the static friction force and cause the valve to move. A method proposed by[39] for turning off the PID-type controller and the knocker is an extension of the knocker method, but as noted by[150] and clarified through the closed-loop (force balance) analysis in this section, the knocker changes the force balance but that does not guarantee that there will be no offset between the process output and its set-point so thus removing the controller and compensating pulses may not be appropriate.

3.4.4 Stiction Compensation Methods: Two Moves Method

The two moves method[135] specifies compensating signals to apply to the signal coming from a linear controller that will drive the stem position to its set-point. This method is model-based, which means that it has accounted for the coupling of the process-valve dynamics, and a number of assumptions are required to guarantee that the method can drive the valve position to its set-point, including that the plant dynamics are linear and have the origin as a stable equilibrium, that a particular data-driven stiction model is an exact representation of the stiction dynamics, and that there are no disturbances or plant-model mismatch. A method similar in concept to the two moves method (it determines how to change the set-points for a closed-loop system in a manner that brings the valve position to a desired value) is developed in[150] and is again a model-based compensator for processes that can be described with a linear model and are under linear control.

3.4.5 Stiction Compensation Methods: Integral Term Modification

A novel stiction compensation method that we describe in this chapter is intended for processes under linear control. It seeks to change the manner in which the force applied to a valve is calculated by modifying the integral term of the linear control law used to regulate the process output to its set-point. This is an alternative to the controller tuning adjustment methods discussed above, and is considered because it may be undesirable to change a controller's tuning if the tuning being utilized is known to work well for the valve when it is not sticky and thus would be the

preferred tuning after valve maintenance is performed. Furthermore, the nonlinearity of the stiction phenomenon and the complexity of the manner in which the forces on the valve balance and come out of balance makes it difficult to discern *a priori* what the best tuning to use when the valve is sticky should be. Therefore, instead of disrupting the desired tuning, in the *ad hoc* fashion that would be required, a term can be added to the integral action of the linear controller that can easily be removed or adjusted for any set-point change to attempt to alleviate stiction-induced oscillations. Given that a characteristic of the stiction-induced oscillations is that the valve output u_a does not track its set-point u_m, we propose a modification to the integral term of the controller based on the scaled difference between u_a and u_m. Specifically, for a PI controller for which ζ signifies the integral of the error between the process output set-point (assuming a single output denoted by $\hat{x}_{sp}$) and the process output ($\hat{x}$, assumed to be a component of the process state vector), the following control law defines the control action with an integral term modification:

$$u_m = u_{as} + K_c(\hat{x}_{sp} - \hat{x}) + K_c\zeta/\tau_I \tag{3.38}$$

$$\dot{\zeta} = \begin{cases} (\hat{x}_{sp} - \hat{x}) + L(u_a - u_m), \; t < t_{AW} \\ (\hat{x}_{sp} - \hat{x}) + Le^{(-\beta(t-t_{AW}))}(u_a - u_m), \; t \geq t_{AW} \end{cases} \tag{3.39}$$

$$\zeta(0) = 0$$

where L, β, and t_{AW} are tuning parameters that can be adjusted by a control engineer to attempt to mitigate stiction-induced oscillations. When $L = 0$, Eq. 3.39 reduces to the standard integral term in a PI control law, and thus has no effect. The parameters are best determined using closed-loop simulations and/or on-line adjustments of L, β, and t_{AW}; however, the general goals of adjusting the parameters provide a potential methodology for looking for an appropriate tuning. In particular, the goal of this method is to determine a tuning that can decrease $\dot{\zeta}$ in such a way that the forces on the valve equilibrate at a value that causes the controlled process output to reach its set-point. By choosing a value of L that causes the term $L(u_a - u_m)$ in Eq. 3.39 to have a sign opposite to that of the term $(\hat{x}_{sp} - \hat{x})$, it is possible to cause $\dot{\zeta}$ to decrease even before $\hat{x} = \hat{x}_{sp}$ (this would not be

possible with the standard PI control law, for which the integral term can only begin to decrease after the set-point is exceeded). Therefore, a possible strategy for tuning the term containing L in Eq. 3.39 is by first setting β and t_{AW} to zero, and then searching for a value of L that is able to cause $\dot{\zeta}$ to equal zero and stabilize the force balance by providing a constant force from the valve actuation. This may occur, however, before $\hat{x}_{sp}$ is reached, resulting in offset. Therefore, the value of t_{AW} may be set to a time at which the force balance appears to have equilibrated and that allows $\hat{x}$ to begin to approach its set-point as soon as possible after this force balancing has occurred. Then, various values of β may be tried to attempt to decrease the term containing L in $\dot{\zeta}$, which can cause this integral term to change and thus changes the force applied to the valve as a result of the control action u_m received by the valve. If a value of β can be found that changes the force applied to the valve in a manner that causes the forces to once again equilibrate, but this time at a value of the valve position that causes $\hat{x}_{sp}$ to be reached, then this control strategy is successful for the set-point change examined. However, some values of β may even cause stiction-induced oscillations to be set up once again even if the value of L examined was able to attenuate them before the time t_{AW}; this shows that the tuning problem is complex and that an appropriate tuning cannot be decided *a priori*. In addition, due to the nonlinearities in the valve and process dynamics, there is no guarantee that any appropriate tuning will be found for a given set-point change, or that the same tuning will work for a variety of set-point changes or disturbances; however, closed-loop simulations or on-line adjustment can be attempted to see if there are values of L, β, and t_{AW} that are generally appropriate for a given process.

To demonstrate this integral term modification method, we return to the level control problem. We consider that the process of Eq. 3.23 with the open-loop valve dynamics in Eqs. 3.27-3.32 was initially operated under the PI controller of Eqs. 3.24-3.25 for 15600 s for a level set-point change from 0.5184 m to 0.15 m to reach q_I. Subsequently, it was controlled using the controller of Eqs. 3.38-3.39 (with $\hat{x} = h$) for a level set-point change from 0.15 m to 0.20 m. The Explicit Euler method with a numerical integration step size of 10^{-5} s was used, and the results are shown in Fig. 3.7 (plotted every 100000 integration steps) for the case that $L = 7$, $\beta = 0.007$, and $t_{AW} =$

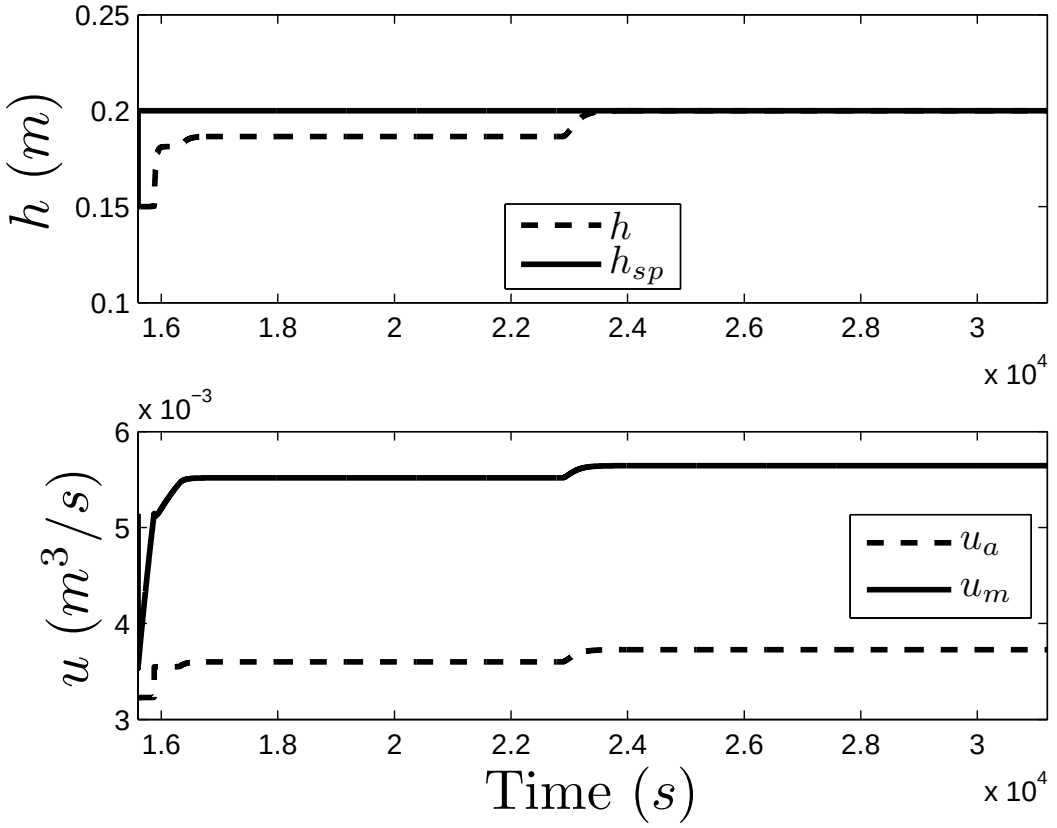

Figure 3.7: Closed-loop trajectories of h, u_a, and u_m for the process of Eq. 3.23 under the controller of Eqs. 3.39-3.38 with $L = 7$ and $\beta = 0.007$, with the open-loop valve (Eqs. 3.27-3.32), and $h_{sp} = 0.20\ m$.

22880 *s* (i.e., 7280 *s* after the set-point change from 0.15 *m* to 0.20 *m*). From comparison with Fig. 3.3, the addition of the term containing L to the integral action was able to reduce control loop oscillations (though there is some offset from the set-point for the chosen L before t_{AW} because the integrator state in Eq. 3.39 can have $\dot{\zeta} = 0$ when $h \neq h_{sp}$). After t_{AW}, the value of u_m is able to change again because $\dot{\zeta}$ becomes nonzero, and eventually the valve moves and the forces due to this strategy balance in such a way that the set-point is achieved.

3.5 Conclusions

In this chapter, we analyzed the roles of the process, valve, and controller dynamics, and also the control loop architecture, in the closed-loop response of a process-valve dynamic system. The closed-loop perspective discussed allows valve behavior typically taught in undergraduate chemical engineering coursework to be analyzed in the same framework as nonlinear dynamic valve behavior like stiction and deadband that is frequently problematic in industry. A number of stiction compensation methods from the literature were analyzed to demonstrate how they fit into this closed-loop context based on understanding the phenomena (e.g., closed-loop oscillations) that the methods seek to compensate at a fundamental mathematical level. We also described an integral term modification stiction compensation technique for control loops under PI control.

Chapter 4

Valve Nonlinearity Compensation Using Model Predictive Control

4.1 Introduction

The prior chapter elucidated the causes of the impacts of valve nonlinearities on feedback control loops and reviewed several compensation methods intended for control loops under classical linear control designs. In this chapter, we continue the discussion of valve nonlinearity compensation but for the case that the control loop is under MPC (or could be placed under MPC as a valve nonlinearity compensation strategy). The motivation for analyzing MPC-based stiction compensation methods in depth is that they provide a systematic method for handling the multivariable interactions in a process-valve system, where the models in such control designs can come from either first-principles or empirical modeling techniques. This is a continuation of the discussion from the prior chapter (i.e., the notation and equations introduced in the prior chapter continue to be used here, and the level control and ethylene oxidation examples from Chapter 3 will be utilized in this chapter to demonstrate the MPC-based valve nonlinearity compensation method).

4.2 Valve Behavior Compensation Methods: MPC for Valve Behavior Compensation

Due to the potential multivariable interactions and nonlinear process-valve dynamics that make the response of a nonlinear process-valve system difficult to predict, the stiction compensation methods in Chapter 3 that do not utilize predictions of the process-valve response in order to determine appropriate control actions to apply to the process may not provide the best control actions for compensating for stiction or may be difficult to tune to achieve a desired response. The model-based methods in[135] and[150] are more straightforward to develop once a model of the process-valve dynamics is obtained but they have not been designed for nonlinear processes. Another model-based method (an MPC method) in[153] that incorporates an inverse model of valve backlash was also designed for linear processes, as was the optimization-based method from,[135] which utilizes the Stenman model[138] of the valve dynamics in addition to a model of the linear process dynamics to make state predictions in an MPC-like framework where the objective function penalizes the error between the process variable value and its set-point, the valve stem variability, and the valve aggressiveness. Though such methods do attempt to account for the process-valve dynamics in the control design to an extent, the Stenman model may not accurately represent the valve dynamics, the process dynamics may be nonlinear, and the flexibility to adjust the objective function of an MPC-based method may be desirable. Therefore, an MPC-based stiction compensation method is proposed which is an MPC design with a general objective function, the ability to incorporate constraints that guarantee feasibility and closed-loop stability of a nonlinear process operated under the controller, and the flexibility to utilize any nonlinear process-valve dynamic model that adequately captures the dynamics for making state predictions. This is a systematic method for compensating for stiction because it accounts for multivariable interactions and nonlinear dynamics when choosing an appropriate control action to apply to the process. In addition, due to the generality of the process models that can be handled in this framework, it can predict appropriate control actions not only when multiple inputs are affected by differing

levels of stickiness of multiple control valves, but it can also account for the control valves having other behavior (e.g., pure deadband, linear dynamics, saturation, hysteresis, or an equal percentage valve characteristic). It can handle processes where a single valve exhibits multiple nonlinearities (e.g., stiction and also an equal percentage valve characteristic) or where the various inputs exhibit different dynamics (e.g., one valve is sticky but another for the same process has linear dynamics). The MPC design is able to compensate for all of these valve dynamics as long as they can be modeled and then included within the process-valve dynamic model, which allows the MPC to predict the response of the nonlinear process-valve system for various feasible control inputs and to choose those which minimize the chosen objective function.

The formulation of a tracking MPC that includes the valve and process dynamics (Eqs. 3.7-3.8) and is designed to track the states in a vector $\hat{x}$ (denoted by $\hat{q}$ for the process-valve system) to a set-point vector $\hat{q}_{sp}$ (associated with steady-state input vector $u_{a,sp}$) is as follows:

$$\min_{u_m(t)\in S(\Delta)} \quad \int_{t_k}^{t_{k+N}} (\hat{q}_{sp}-\tilde{\hat{q}})^T Q(\hat{q}_{sp}-\tilde{\hat{q}}) + (u_{a,sp}-\tilde{u}_a)^T R(u_{a,sp}-\tilde{u}_a)\, d\tau \tag{4.1a}$$

$$\text{s.t.} \quad \dot{\tilde{q}}(t) = f_q(\tilde{q}(t), u_m(t), 0) \tag{4.1b}$$

$$\tilde{q}(t_k) = q(t_k) \tag{4.1c}$$

$$\tilde{q}(t) \in Q_v, \forall t \in [t_k, t_{k+N}) \tag{4.1d}$$

$$u_m(t) \in U_m, \forall\, t \in [t_k, t_{k+N}) \tag{4.1e}$$

where the notation follows that in Eqs. 3.11-3.12. The predicted process-valve state $\tilde{q}$ follows the model of Eqs. 4.1b-4.1c and is bounded within the set Q_v (Eq. 4.1d) (the set Q_v is defined to be the bounds on the process-valve model states, which may include, for example, the state constraints restricting $x \in X$ and the state constraints corresponding to $u_a \in U$ since u_a is a function of the states from Eqs. 3.2 (since each $u_{m,i}$ is calculated by a state feedback controller) and 3.4). The notation $\tilde{u}_a$ denotes the predictions of the vector u_a. In Eq. 4.1, unlike in Eq. 3.12, the deviation of the prediction of u_a from the steady-state value of the valve output flow rate corresponding to $\hat{q}_{sp}$ is penalized instead of the deviations of the values of u_m from this steady-state valve output

flow rate since u_a is the valve output that is actually implemented on the process and therefore it is the quantity that should track the set-point. A general stage cost $L_e(\tilde{q}(\tau), u_m(\tau))$ (where L_e is a general nonlinear scalar-valued function of its arguments as in Eq. 3.11a) could be used in place of the tracking objective function in Eq. 4.1a. Additional constraints may also be added to the MPC of Eq. 4.1 to allow for closed-loop stability guarantees or to account for issues that may arise due to the properties of a specific valve nonlinearity (for example, Chapter 5 develops additional constraints required for both stability and physical reasons for an MPC used specifically for stiction compensation). A first-principles model can be used to capture the process and valve dynamics in Eq. 4.1b, or an empirical model can be used. A first-principles model may be more accurate, but an empirical model may be beneficial because it may not require detailed information on the valve layer dynamics like the details of the friction force model or valve characteristic, and it may also be less stiff than a first-principles model (an example of this is demonstrated in Section 4.3.2), resulting in a lower computation time for the MPC for valve behavior compensation. If the model utilized within the MPC can capture the dominant process-valve dynamics to provide sufficiently accurate state predictions, it would be expected to be beneficial in compensating for stiction, even if it is not an exact model, due to the incorporation of state feedback.

4.2.1 MPC for Valve Behavior Compensation with Empirical Models

Utilizing a first-principles model in Eq. 4.1b is straightforward when it is available (for example, first-principles stiction models are reviewed in[24]). With regard to empirical models, several data-driven models for stiction exist in the literature (e.g., the Choudhury model,[33] the Kano model,[90] and the He model[78]) and these generally assume that the relationship between u_a and the force applied to the valve is similar to that in Fig. 3.6, so they use an "if-then" type structure to mimic this (i.e., if the control signal has not changed enough to un-stick the valve, then the valve position does not change with a change in the control signal; if the control signal has changed enough to un-stick the valve, the valve takes a new position defined by the data-driven model). The models usually have only a few parameters that are identified through techniques that assume

a process model structure and an empirical valve model structure and then identify the parameters of both from process input/output data.[88, 137, 149]

Several potential limitations of many of the prior stiction empirical modeling methods include:

1. They relate the valve position x_v and the force on the valve determined by a controller
2. The models are specific to stiction

The first point above is a disadvantage given the complexities that may exist in the control loop architecture and the potential that the $u_a - x_v$ relationship is nonlinear. In such cases, utilizing an empirical stiction model would not eliminate the issue that some aspect of the relationship between u_m and u_a must still be modeled even when the empirical model is in place. For example, if flow control is utilized on the valve as in the example of Fig. 3.5, some knowledge of the relationship between the valve output flow rate set-point from the major loop controller and the force applied to the valve by the minor loop controller is required. If an equal percentage valve characteristic characterizes the $u_a - x_v$ relationship, the form of this model must be known. The second potential limitation of the stiction empirical modeling techniques is that they cannot capture dynamics like hysteresis or linear valve dynamics that are not observed in the response of a sticky valve to control signal changes. Therefore, for the MPC-based strategy for compensating for valve behavior in general, it is desirable to have an empirical valve layer model relating each $u_{m,i}$ and $u_{a,i}$ (rather than force to $x_{v,i}$) to avoid the need to *a priori* know/develop a first-principles model for any part of the valve behavior, and to allow the $u_{m,i} - u_{a,i}$ relationship to be general for any type of valve behavior instead of for stiction only (the valve layer for valve i is defined in this chapter to refer to all dynamics describing the relationship between $u_{m,i}$ and $u_{a,i}$). Motivated by these considerations, we propose empirical modeling of valve behavior for use in the MPC-based valve behavior compensation method using standard empirical model structures to relate each $u_{m,i}$ and $u_{a,i}$, $i = 1, \ldots, m$, but inspired by the "if-then" structure of empirical stiction models, we allow for branched ("if-then") model structures based on an understanding of the physics of the valve layer.

For example, consider that we want to develop an empirical model for the relationship between

each $u_{a,i}$ and $u_{m,i}$ when each $u_{m,i}$ is a valve output flow rate set-point from an MPC which is transmitted to a valve layer containing a sticky valve with a linear valve characteristic under flow control. We assume that $u_{m,i}$, $i = 1, \ldots, m$, is held constant for a time period Δ during which the minor loop linear controller repeatedly computes new values of the pressure applied to the valve stem to drive $u_{a,i}$ to $u_{m,i}$. To identify an empirical model between $u_{m,i}$ and $u_{a,i}$, it is necessary to first gather valve layer input-output ($u_{m,i} - u_{a,i}$) data and to have some intuition regarding how the linear controllers and sticky valves in the valve layer affect the shape of the valve layer input-output data trends so that a proper empirical model structure can be chosen. For example, if the valve output flow rate set-point change direction reverses (e.g., the set-points $u_{m,i}$ were previously increasing but the next set-point is lower than the previous one), the valve may stick throughout some or all of the time period Δ during which $u_{m,i}$ is constant, depending on whether the pressure applied to the valve changes enough throughout Δ to overcome the force required to move the valve. Not only does the direction of the set-point change affect whether the valve remains stuck throughout a sampling period, but the magnitude of the set-point change also affects the speed with which the valve overcomes deadband/stickband due to the dynamics of the minor loop controller. Because typical linear controller designs are based on the error between the set-point and the actual value of a process variable, the minor loop controller in the valve layer will calculate larger control actions when the valve output flow rate set-point changes significantly (because this creates a large error between $u_{m,i}$ and $u_{a,i}$), and such larger control actions (pressures) are more likely to overcome the deadband/stickband within the time period Δ. Therefore, it is more likely that the valve will move if the controller is aggressively tuned or if the set-point change is large and the error between $u_{m,i}$ and $u_{a,i}$ affects the controller output.

Based on the above discussion, different types of valve output responses are expected to be observed depending on the set-point change magnitude and direction. Thus, it is reasonable to postulate that an empirical valve layer model for our example sticky valve with flow control will be defined in a piecewise fashion, with the set-point changes dictating which equation is chosen to describe the valve layer input-output relationship. Also, the minor loop controller

may cause some of the parameters in the empirical model to depend on the magnitude of the set-point change (an example of this is shown in Section 4.3.2). Saturation of the valve (e.g., the pressure from the pneumatic actuation dropping to zero so that the valve can no longer move in the direction of decreasing pressure) can also define branches of the valve output response. Therefore, the procedure proposed for empirical modeling of the feedback loop for the sticky valve under consideration is as follows:

1. Collect valve layer input-output data (i.e., data relating $u_{a,i}$ and $u_{m,i}$, $i = 1, \ldots, m$), ensuring that data gathered represents all aspects of the valve layer response that should have separate equations (branches) within the piecewise model structure (e.g., sticking and slipping).

2. For each aspect of the response that requires its own model structure, select an appropriate structure based on the valve layer input-output data trends and determine what activates the different branches of the response (e.g., set-point change direction reversals).

3. Identify the parameters for the different branches of the model.

4. Develop models for any parameters that can be seen from the valve layer input-output data to be dependent on the valve layer inputs (e.g., parameters that depend on the magnitude of the valve output flow rate set-point change).

5. Validate the final piecewise-defined model.

It will be shown in Section 4.3.2 that Step 2 in the procedure above may be able to be performed with standard empirical model structures in the chemical process industries, such as second-order or first-order-plus-dead time models. Furthermore, the five steps above are general such that they are not restricted to the valve layer with a sticky valve under flow control above but can be examined for extension to other control loop architectures and valve behavior that characterize the valve layer. Furthermore, the goal of valve layer empirical modeling in this section is to develop models of valve dynamics that are flexible by not assuming *a priori* that a specific valve behavior is present in the loop, and that also are intended for use in place of a first-principles model in the

MPC-based valve behavior compensation methodology of Eq. 4.1. Because MPC is a feedback control technique, it possesses a degree of robustness to plant-model mismatch and therefore an approximate empirical model of valve behavior with a standard empirical model form may in many cases be sufficient for predicting the valve response in the MPC to compensate for valve behavior.

The following equation denotes the empirical model for use in the MPC-based valve behavior compensation method:

$$\dot{y}(t) = f_y(y, u_m) \tag{4.2}$$

where $y(t)$ is the predicted value of u_a from the empirical model at time t and has dynamics characterized by the vector function f_y. Using this notation, the MPC-based valve behavior compensation method of Eq. 4.1 (with an empirical valve layer model and general stage cost function L_e) becomes:

$$\min_{u_m(t) \in S(\Delta)} \quad \int_{t_k}^{t_{k+N}} L_e(\tilde{x}(\tau), y(\tau), u_m(\tau))\, d\tau \tag{4.3a}$$

$$\text{s.t.} \quad \dot{\tilde{x}}(t) = f(\tilde{x}(t), y(t), 0) \tag{4.3b}$$

$$\dot{y}(t) = f_y(y, u_m) \tag{4.3c}$$

$$\tilde{x}(t_k) = x(t_k) \tag{4.3d}$$

$$y(t_k) = u_a(t_k) \tag{4.3e}$$

$$\tilde{x} \in X, \; \forall\, t \in [t_k, t_{k+N}) \tag{4.3f}$$

$$y \in U, \; \forall\, t \in [t_k, t_{k+N}) \tag{4.3g}$$

$$u_m(t) \in U_m, \; \forall\, t \in [t_k, t_{k+N}) \tag{4.3h}$$

where the notation follows that in Eq. 3.11. The initial condition for the nominal first-principles model of the process states (Eq. 4.3b) is a measurement of the state x at t_k (Eq. 4.3d), while the empirical model (Eq. 4.3c) is initialized from a measurement of the valve output (Eq. 4.3e). The set-points u_m, the state predictions $\tilde{x}$, and the predictions of the valve output y are bounded (Eqs. 4.3f-4.3h).

Remark 4.1. *Prior works that have looked at MPC with a general objective function with empirical models*[3,4,6] *have focused on empirical models of the nonlinear process (rather than valves) and have indicated that significant computation time reductions may result from using empirical as opposed to first-principles models in MPC. We will demonstrate in Section 4.3.2 that empirically modeling the valve layer can result in computation time reduction even if the process is modeled with a first-principles model because it can make the process-valve combination model less stiff. Empirically modeling both the process and valve dynamics could be examined as well; however, there may arise cases in which it may not be possible to easily capture the process and valve dynamics in the same model (i.e., developing an empirical model between u_m and x only). To see why difficulty may arise, consider a process with multiple inputs, all of which are adjusted by sticky valves. Because the valves are sticky, each change in $u_{m,i}$ will either cause $u_{a,i}$ to change appreciably (which will cause x to respond to the change in $u_{m,i}$), or it will not cause $u_{a,i}$ to change appreciably (which will cause x to continue behaving after the change in $u_{m,i}$ as if $u_{m,i}$ had not changed). Due to the coupling of the dynamics of the states of a process-valve system, the combination of $u_{a,i}$'s affects the process dynamics, so a branched empirical model describing the $u_m - x$ relationship may need to include different branches for every combination of sticking and slipping for all valves, which may lead to a difficult identification task. A solution if this is found to be an issue would be to empirically model each $u_{a,i} - u_{m,i}$ relationship for each valve as well as the $u_a - x$ relationship for the process. Such a modeling strategy may also be beneficial from a valve maintenance perspective because it permits monitoring of how closely $u_{a,i}$ matches $u_{m,i}$ for each valve, allowing valve maintenance to be performed first on those valves for which $u_{a,i}$ tracks $u_{m,i}$ the least.*

Remark 4.2. *One could examine whether the MPC-based valve behavior compensation method, particularly with an empirical valve layer model, could be utilized for compensating for dynamic effects (e.g., slower movement of a valve or lack of movement) related to physical valve issues like oversizing, undersizing, corrosion, leaks through the valve packing, or diaphragm faults that can affect valve performance.*[31]

Remark 4.3. *An appropriate empirical model structure for the valve layer input-output data must be selected. Many model identification techniques for obtaining linear and nonlinear empirical models exist that can be evaluated for their suitability for modeling a given valve layer input-output trend, which fall in the categories of state-space and input-output models (see, for example,[22,102,123,145]).*

Remark 4.4. *It is possible to consider automation of the model identification procedure in this section to allow it to be carried out on-line, providing a consistently available model of the valve behavior that can be used not only to obtain reasonable state predictions of the valve layer within the MPC throughout time, but also to help detect changes in the valve behavior over time and therefore to help set valve maintenance schedules. There will need to be logic integrated within such an automated procedure that analyzes the $u_{a,i} - u_{m,i}$ data based on an understanding of the physics of the valve layer (e.g., for the valve layer comprised of a sticky valve with a linear valve characteristic under flow control used as the motivation for Steps 1-5 of the proposed empirical modeling procedure in this section, Step 1 of the empirical modeling procedure could be automated by having a computer check whether there are any regions of the $u_{a,i} - u_{m,i}$ data where $u_{m,i}$ changed but $u_{a,i}$ did not move immediately, and if so, have the computer perform step-tests including changes in $u_{m,i}$ in one direction and also in the reverse direction to ensure that data from the valve sticking and from it slipping is gathered).*

4.3 MPC-Based Valve Behavior Compensation Methods: Process Examples

This section demonstrates the MPC-based valve nonlinearity compensation method through applications to systems where a valve experiences stiction. The compensation method is demonstrated with a first-principles stiction model via the level control example described in Section 3.3.2.1 and with an empirical stiction model via the ethylene oxidation example described in Section 3.3.2.2.

4.3.1 Level Control Example with a Sticky Valve: MPC with a First-Principles Valve Layer Model

For the level control problem, we develop an MPC for stiction compensation as follows:

$$\min_{u_m(t)\in S(\Delta)} \quad \int_{t_k}^{t_{k+N}} Q(h_{sp}-\tilde{h})^2 + R(u_{a,sp}-\tilde{u}_a)^2\, d\tau \tag{4.4a}$$

$$\text{s.t.} \quad \dot{\tilde{q}}(t) = f_q(\tilde{q}(t), u_m(t), 0) \tag{4.4b}$$

$$\tilde{q}(t_k) = q(t_k) \tag{4.4c}$$

$$0 \le \tilde{u}_a(t) \le 0.006, \forall t \in [t_k, t_{k+N}) \tag{4.4d}$$

$$0 \le u_m(t) \le 0.006, \forall t \in [t_k, t_{k+N}) \tag{4.4e}$$

$$\tilde{P} \ge 0, \forall t \in [t_k, t_{k+N}) \tag{4.4f}$$

where $u_{a,sp} = 0.00373\ m^3/s$, $h_{sp} = 0.20\ m$, $Q = 0.00001$, and $R = 1$. For physical reasons (described in more detail in Chapter 5), the predicted pressure $\tilde{P}$ from the pneumatic actuation is restricted to take non-negative values in Eq. 4.4f. The process-valve state vector $q^T = [h\ x_v\ v_v\ z_f]$ is modeled for the open-loop valve using Eqs. 3.23 and 3.27-3.32. The process-valve system was initiated at q_I. The level was controlled by the MPC of Eq. 4.4 for 150 s with $\Delta = 1\ s$ and $N = 50$. An integration step of $10^{-5}\ s$ was used within the MPC to integrate Eq. 4.4b, with an integration step of $10^{-6}\ s$ used outside of the MPC to simulate the process. The constraints in Eqs. 4.4d and 4.4f were enforced once every sampling period. The objective function derivatives required by the optimization solver Ipopt were calculated using a centered finite difference, and the Ipopt limited-memory Hessian approximation option was used, so that the non-differentiability in Eq. 3.30 did not prevent a solution to the optimization problem from being obtained. The results are shown in Fig. 3.4 (designated by C because the valve dynamics are compensated) and are plotted every 1000 integration steps. They indicate that the MPC including the valve dynamics drove the level toward its set-point, in contrast to the MPC that did not include the actuator dynamics from Section 3.3.2.1 (designated by U in this figure). The reason for this is that the MPC of Eq. 4.4

incorporates the full process-valve model, and thus computes an input trajectory that accounts for the manner in which the forces on the valve will balance under the control actions calculated by the MPC.

Though the MPC was able to drive the level toward its set-point (a significant improvement with regard to set-point tracking of the level compared to the case that the valve dynamics were not accounted for within the MPC), the fact that the valve is operated without flow control reduces the flexibility of the MPC to be able to maintain the level at the set-point for all times after it first approaches the set-point in Fig. 3.4. Specifically, each time that the MPC sets u_m, the pressure applied to the valve changes according to the relationship of Eq. 3.32 since the valve is operated without flow control. However, because the MPC implements piecewise-constant control actions that are held for a sampling period, the pressure that is applied to the valve (a function of u_m calculated by the MPC) is held constant throughout a sampling period. The length of the sampling period in this example is long compared to the dynamics of the valve, such that the dynamics of the valve under a constant applied pressure dictate the final position of the valve at the end of a sampling period. The result is that the MPC is not able to find a value of u_m that will drive the valve, subject to its dynamics during the sampling period that the pressure is held constant and the MPC cannot intervene, exactly to the valve position corresponding to the steady-state flow rate through the valve at which the level set-point is achieved. Instead, the MPC must continuously calculate new values of u_m that allow the valve to stick and slip in ways that the MPC finds will minimize the tracking objective function and therefore keep the value of h in a region around the set-point over time. Based on this analysis, potential ways of improving the set-point tracking of the level include decreasing the MPC sampling period until it is on a timescale comparable to the timescale of the valve dynamics, increasing the prediction horizon to give the MPC greater foresight to potentially allow it to determine a sequence of values of u_m that can drive the value of u_a to its set-point, or adding flow control to the valve and then including the dynamics of both the valve and the flow controller in the MPC as it calculates set-points u_m for the flow controller.

Remark 4.5. *Fig. 3.4 demonstrates the effects of not accounting for the behavior of the valve*

of Eqs. 3.27-3.32 within an MPC (no significant change of the level for certain changes in the valve output flow rate set-point u_m) and the improvement that can be obtained when the dynamics are accounted for. However, other types of valve behavior that are not exhibited by the valve of Eqs. 3.27-3.32 can result in different types of negative effects when the valve behavior is not included within the MPC model for making state predictions. For example, consider a valve without stiction but with the following equal percentage valve characteristic:[38]

$$u_a = u_{a,\max} e^{\ln(0.03) x_v / x_{v,\max}} \tag{4.5}$$

developed for the case that the valve stem is fully retracted when the valve is fully open and is fully extended when the valve is fully closed. Assume that the valve can be manipulated in such a manner that the valve position is an explicit function of u_m given by Eq. 3.31 (i.e., $x_v = x_{v,\max} - \frac{u_m}{u_{a,\max}} x_{v,\max}$) though this linear relationship does not reflect the nonlinear $x_v - u_a$ relationship of Eq. 4.5. If an MPC is used to control the process but is not aware of the mismatch between the valve behavior of Eq. 4.5 and the linear $u_m - x_v$ relationship that sets the valve position (a similar concept to the mismatch between Eq. 3.32 and the actual $u_m - P$ relationship for the sticky valve of Eqs. 3.27-3.31), permanent offset of the level from its set-point can result due to the plant-model mismatch. For example, consider again the set-point change from an initial level of 0.15 m, corresponding to a steady-state flow rate of 0.00323 m^3/s, to the set-point $h_{sp} = 0.20$ m corresponding to $u_{a,sp} = 0.00373$ m^3/s. The steady-state flow rate for a level of 0.15 m corresponds to a fraction $F_{I,A} = 0.5379$ of the maximum flow rate of 0.006 m^3/s through the valve as shown in Fig. 4.1. For the equal percentage valve of Eq. 4.5, the valve position associated with the flow rate $u_{a,sp}$ is a fraction $X_{I,A} = 0.1768$ of its maximum. When the set-point of the level is changed to 0.2 m, the flow rate out of the valve should increase to achieve this (ideally it should reach the fraction of the maximum flow rate $F_D = 0.62113$ shown Fig. 4.1). For the equal percentage valve of Eq. 4.5, this flow rate is achieved at a fraction of 0.1358 of the maximum stem position. The $u_m - x_v$ relationship used to set the stem position based on x_v, however, is linear, so when the

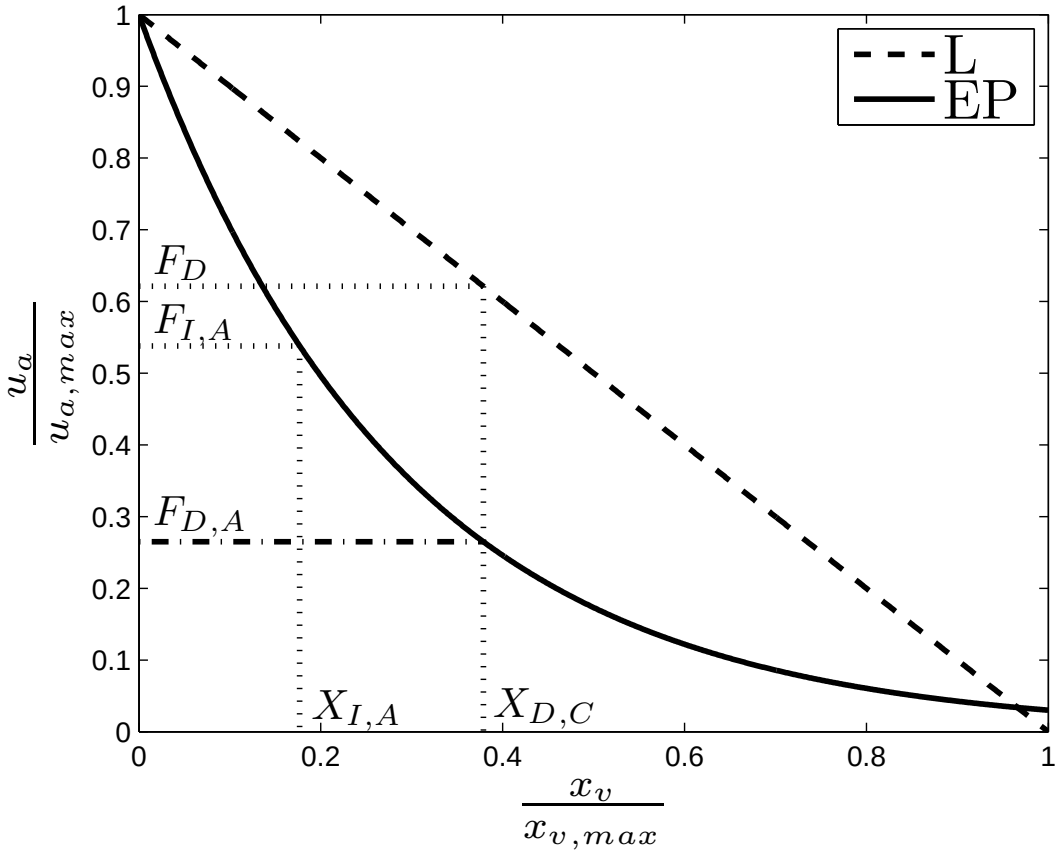

Figure 4.1: Figure depicting linear (L) and equal percentage (EP) valve characteristics of Eqs. 3.31 and 4.5, respectively, along with several fractions of the maximum flow rate ($F_{I,A} = 0.5379$, $F_D = 0.62113$, and $F_{D,A} = 0.2649$) and of the maximum stem position ($X_{I,A} = 0.1768$ and $X_{D,C} = 0.37887$) for the level control example.

MPC requests that $u_m = u_{a,sp}$, the linear $u_m - x_v$ relationship moves the valve stem to a position corresponding to a fraction $X_{D,C} = 0.37887$ of the maximum stem position. However, when the fraction of the stem position for an equal percentage valve is 0.37887, the fraction of the maximum flow through the valve is $F_{D,A} = 0.2649$ (corresponding to a flow rate lower than the initial value instead of above it as desired). This example highlights that including valve behavior in MPC can be beneficial for many types of valve behavior. Also, the example valve in this section has a $u_m - u_a$ relationship of the form in Eq. 3.2 since x_v in the linear $u_m - x_v$ relationship can be substituted in terms of u_m in the $u_a - x_v$ relationship of Eq. 4.5.

4.3.2 Ethylene Oxidation Example with a Sticky Valve: MPC with an Empirical Valve Layer Model

In this section, we return to the ethylene oxidation example of Section 3.3.2.2 (with the parameters listed in Table 2.1) for the case that $u_{a,2} = 0.5$ and $u_{a,3} = 1.0$. We consider that the value of $u_{a,1}$ is adjusted by a pneumatic spring-diaphragm sliding-stem globe valve (because it is the only manipulated input considered for this process in the following example, we will drop the "1" in the subscript for this section and refer to the process input as "u_a"). This valve is under flow control and has the same design as the valve described in Section 3.3.2.1 (i.e., it is pneumatically actuated and pressure-to-close, with no pressure applied to the valve initially when it is in its fully open position, it has $x_v = 0\ m$ when the valve is fully open and $x_v = x_{v,\max} = 0.1016\ m$ when the valve is fully closed with $u_a = 0$, and the valve layer dynamics are described by Eqs. 3.27-3.31 and 3.33-3.34) except that the time unit for all parameters and variables is denoted by a dimensionless unit t_d instead of s for consistency with the dimensionless units in Eq. 3.35 (i.e., all valve model parameter values in Table 3.1 apply for this valve except that each instance of the unit s in that table is replaced with t_d in this example) and the fully open valve position corresponds to $u_a = u_{a,\max} = 0.7042$. The values of ζ_P and of the steady-state value of the pressure P_s are re-set each time that u_m changes (ζ_P is re-set to zero, and P_s is set to the last applied pressure). The value of u_m is changed by an EMPC every sampling period of length $\Delta = 0.2\ t_d$.

The control objective is to maximize the yield of ethylene oxide utilizing an EMPC that accounts for the valve dynamics, where the yield is given by the following ratio of the amount of ethylene oxide produced from the reactor in a time period of length $t_f - t_0$ to the amount of ethylene fed to the reactor in that time:

$$Y(t_f) = \frac{\int_{t_0}^{t_f} u_a(\tau) x_3(\tau) x_4(\tau) d\tau}{\int_{t_0}^{t_f} 0.5 u_a(\tau) d\tau} \tag{4.6}$$

We also consider that the valve output flow rate is constrained between the minimum flow through the valve (0) and the maximum flow (0.7042), and is also required to satisfy the following

restriction on the amount of ethylene that can be fed in a time period of length $t_f - t_0$:

$$\frac{1}{t_f - t_0} \int_{t_0}^{t_f} 0.5 u_a(\tau) d\tau = 0.175 \tag{4.7}$$

This constraint requires that the amount of ethylene fed to the process in a time period of length $t_f - t_0$ must equal the amount that would be fed in that time period under steady-state operation. We seek to avoid fully closing the valve by requiring the MPC to keep the value of u_m between 0.0704 and 0.7042.

To achieve the control objectives, we will utilize an MPC with an empirical model of the valve dynamics, and we will compare the computation time of that controller with the computation time of an MPC that includes a first-principles model of the valve dynamics. We develop the empirical model for the valve layer described in Eqs. 3.27-3.31 and 3.33-3.34 according to the steps outlined in Section 4.2.1. According to Step 1, we first gather $u_m - u_a$ data, and notice that when the set-points repeatedly change in the same direction, the valve responds rapidly to the set-point change, but when the set-point change direction reverses, there is a delay before the valve responds. Also, there is a greater delay for small set-point changes than for large set-point changes when the deadband is encountered due to the use of the PI controller in the valve layer. In addition, the valve layer input-output data indicates that when the valve output set-point is kept constant for multiple sampling periods, the valve output will not exhibit deadband if the next change in the set-point is in the same direction as the changes prior to the valve set-point remaining constant, but will exhibit deadband if the next change in the set-point is in the opposite direction to the last changes. The valve layer data also suggests that valve output flow rates above about 0.5164 are not achievable with the pressure available from the pneumatic actuation after the valve first begins to close because stiction alters the $u_a - P$ relationship (as will be discussed in Chapter 5) such that these flow rates would require negative pressures to be reached (i.e., since the valve is initialized with $u_a = 0.7042$, it can only close (it cannot reverse direction to open more) until $u_a \sim 0.5164$, and subsequently cannot reach flow rates above that value).

The above observations are used in Step 2 of the model identification procedure to postulate that the dynamics between u_a and u_m can be captured in a piecewise-defined model with two branches, one corresponding to the response of u_a when the set-point changes in u_m are repeatedly in the same direction (no deadband), and another corresponding to the response when the set-point changes switch direction (deadband), with a special consideration for the case that the set-point does not change between two sampling periods. The part of the model corresponding to the case when there is deadband before the valve moves should have different speeds of response of the valve for different set-point change magnitudes. The valve layer input-output data should be gathered while avoiding increasing the set-point u_m above 0.5164 to avoid gathering data for flow rates where the pressure is saturated (the decision was made not to add branches to the empirical model to account for saturation of the actuation pressure due to the complexity that this adds to the empirical model, but to instead seek to avoid saturating the pressure during process operation by utilizing input rate of change constraints as in Chapter 2 in the MPC used to control the process).

Step 3 of the model identification procedure will now be carried out to identify the equations for the two branches of the proposed model. We first verify that such a piecewise-defined valve layer model is necessary by showing the results of attempting to identify a single model for the valve layer based on the valve layer input-output data. The valve layer input-output data was gathered by initializing the valve at its fully open position ($u_a = 0.7042$, $P_s = 0\ kg/m \cdot t_d^2$, $\zeta_P = 0$, $z_f = 0\ m$, $x_v = 0\ m$, $v_v = 0\ m/t_d$) and integrating the first-principles valve layer model in Eqs. 3.27-3.31 and 3.33-3.34 with the Explicit Euler numerical integration method and an integration step of $h_I = 10^{-6}\ t_d$ for 19 step changes in the set-point (the set-point was first decreased from $u_m = 0.7042$ to 0.7, and was subsequently decreased to 0.15 in increments of 0.05, and then increased to 0.5 in increments of 0.05, with each set-point held for a sampling period). A subset of the $u_m - u_a$ data generated is shown in Fig. 4.2. Based on the data generated, the valve output response to a set-point change was postulated to be able to be described by a second-order linear dynamic model. The values of u_m and u_a were measured every 10^{-4} time units (every 100 integration steps; i.e., $\Delta_e = 10^{-4}\ t_d$ according to the notation in Section 3.2.1), and the following ARX model was fit to

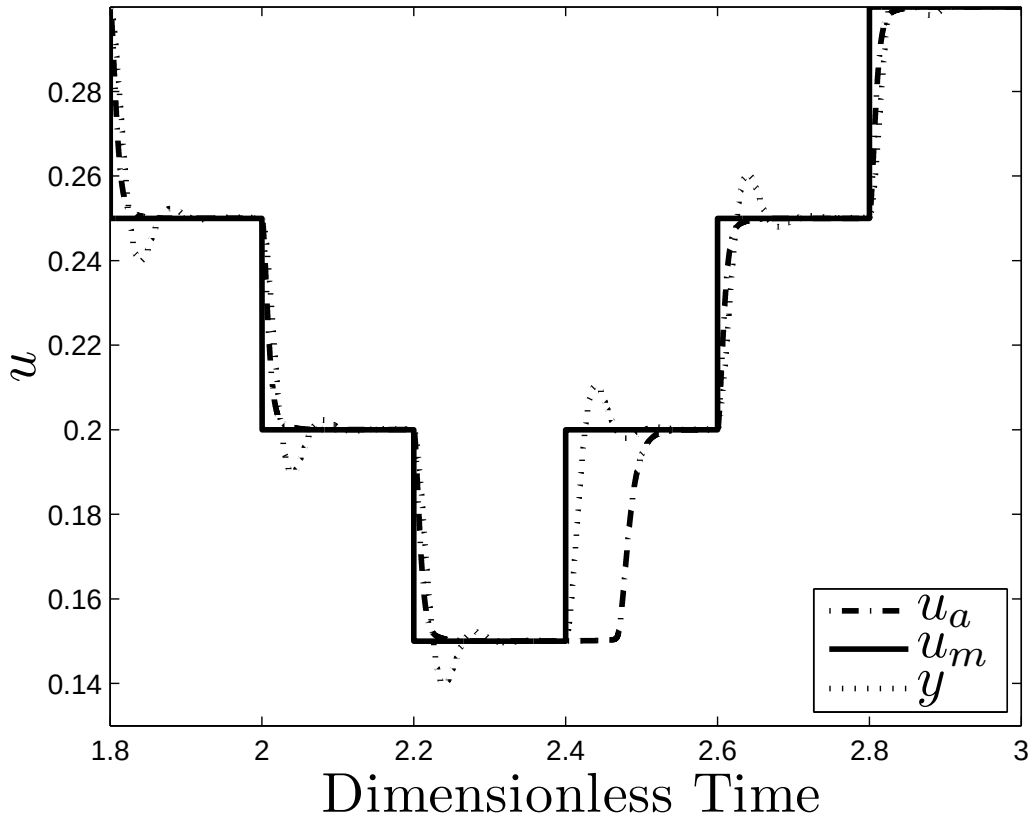

Figure 4.2: Comparison of valve layer set-point (u_m), valve layer output (u_a), and prediction of the valve layer output (y) from Eq. 4.8 when 19 set-point changes are applied (a subset of the data is shown).

the data by using a least-squares regression:

$$y(\tilde{t}_j) = 1.99212y(\tilde{t}_{j-1}) - 0.99219y(\tilde{t}_{j-2}) + 0.00035u_m(\tilde{t}_{j-1}) - 0.00027u_m(\tilde{t}_{j-2}) \tag{4.8}$$

where $y(\tilde{t}_j)$ refers to the predicted value of u_a for the $j-th$ measurement of the valve layer output data (i.e., at time $\tilde{t}_j$, where the notation follows that in Section 3.2.1). When the predictions y are generated from this model and the input data, they overshoot the values of u_a, and there is poor agreement with u_a when the valve velocity changes sign (deadband is reached), as shown in Fig. 4.2.

Though it was not possible to identify an adequate second-order model using the input-output data for the entire set of 19 set-point changes, it is possible to successfully identify a second-order

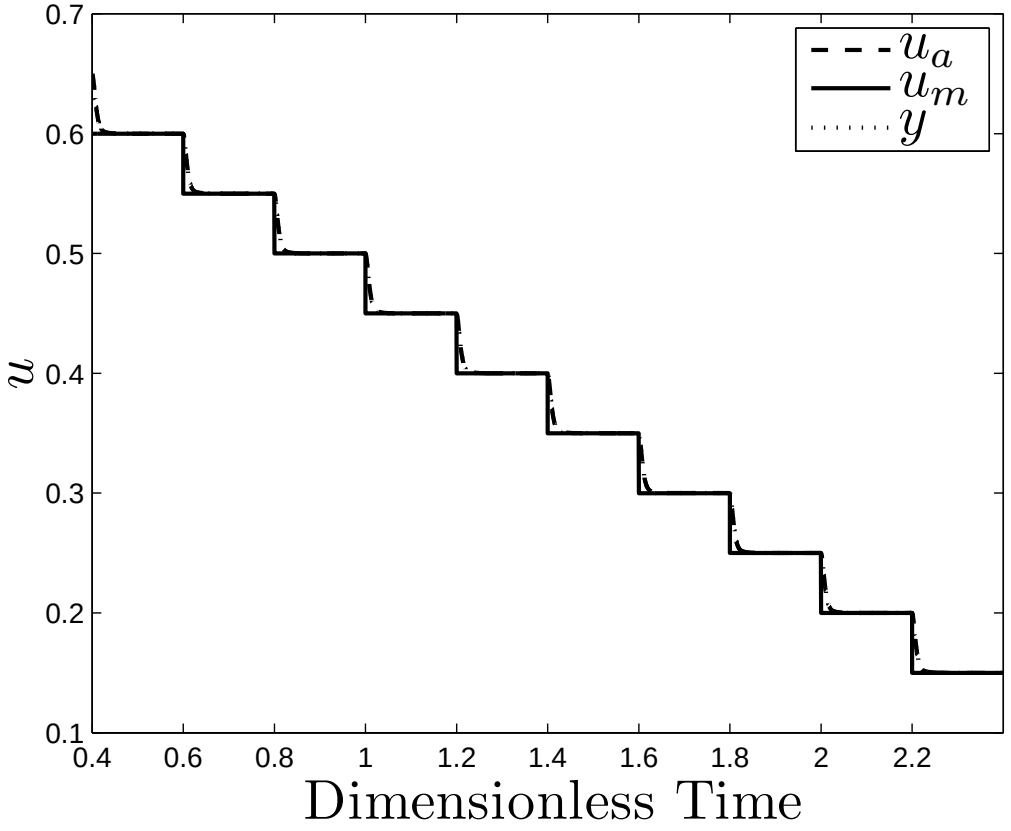

Figure 4.3: Comparison of valve layer set-point (u_m), valve layer output (u_a), and prediction of the valve layer output (y) using the set-points decreasing between 0.6 and 0.15 and Eq. 4.9 (y overlays u_a).

model if only the data corresponding to the set-point decreases between 0.6 and 0.15, for which no deadband occurs, are used to identify the model. In this case, the following model is obtained:

$$y(\tilde{t}_j) = 1.96209y(\tilde{t}_{j-1}) - 0.96249y(\tilde{t}_{j-2}) + 0.00038u_m(\tilde{t}_{j-1}) + 0.00002u_m(\tilde{t}_{j-2}) \tag{4.9}$$

When the decreasing set-points between 0.6 and 0.15 are used as inputs in Eq. 4.9, the predictions y of the valve output closely match the actual values, as shown in Fig. 4.3.

To complete Step 3 of the empirical modeling procedure, it is necessary to complement Eq. 4.9 with a model for the case that deadband is observed. Based on the valve layer input-output data in Fig. 4.2 corresponding to the deadband when u_m changes from 0.15 to 0.2, it is postulated that the response of the valve output to set-point change direction reversals can be modeled as a first-order

process with time delay. However, the values of the time constant τ and of the delay α in such a model are dependent on the magnitude of the set-point changes because the speed of the response of the valve layer to a set-point change in u_m depends on the magnitude of the set-point change. Closed-loop simulations indicate that for a set-point change direction reversal, set-point changes less than approximately 0.02 are unable to cause the PI controller to overcome the deadband within a sampling period. To determine the dependence of the delay on the magnitude of the set-point change, in accordance with Step 4 of the model identification procedure, u_m was decreased from 0.7042 to 0.15, and subsequently u_m was increased by set-point changes of different magnitudes. The regression method in[118] for the determination of the parameters of a first-order-plus-dead-time model was applied to the data generated for each set-point change. A plot of the resulting delays against the set-point changes with which they were associated was fit to the function a/x using the MATLAB function lsqcurvefit, with $a = 0.0037$ providing the best fit. The values of τ associated with each delay were averaged to give $\tau = 0.0123$ for the first-order-plus-dead-time model. Thus, the first-order-plus-dead-time model is written in discrete-time form as:

$$y(\tilde{t}_j) = \begin{cases} y(\tilde{t}_{j-1}),\ \tilde{t}_j - t_k < \alpha \\ y(t_k) + exp(-\Delta_e/\tau)(y(\tilde{t}_{j-1}) - y(t_k)) + K(1 - exp(-\Delta_e/\tau)) \times \\ \qquad (u_m(t_k) - u_m(t_{k-1})),\ \tilde{t}_j - t_k \geq \alpha \end{cases} \tag{4.10}$$

where

$$\alpha = \begin{cases} \Delta,\ |u_m(t_k) - u_m(t_{k-1})| < 0.02 \\ a/(|u_m(t_k) - u_m(t_{k-1})|),\ |u_m(t_k) - u_m(t_{k-1})| \geq 0.02 \end{cases} \tag{4.11}$$

In Eqs. 4.10-4.11, k is the value of k that brings t_k closest to $\tilde{t}_j$ ($t_k \leq \tilde{t}_j$), and $K = 1$.

Incorporating the above considerations, the following discrete-time empirical valve layer model was devised and validated to perform well for a number of valve layer input-output data points, completing Step 5 of the model identification procedure:

1. If the set-point has not changed between t_k and t_{k-1} and also did not change between t_{k-1} and t_{k-2}, set $y(\tilde{t}_j) = y(t_k)$ for all $\tilde{t}_j \in [t_k, t_{k+1})$.

2. If two set-point changes are changing in the same direction, or if the set-point has been constant for some time but has now changed in the same direction that it was changing prior to becoming constant, use the model of Eq. 4.9.

3. If two set-point changes are in opposite directions, or if the set-point has been constant for some time but has now changed in the opposite direction to that in which it was changing prior to becoming constant, use the model of Eqs. 4.10-4.11.

The MPC-based stiction compensation strategy incorporating the empirical model described above is as follows:

$$\min_{u_m(t)\in S(\Delta)} \quad \int_{t_k}^{t_{k+N_k}} -y(\tau)\tilde{x}_3(\tau)\tilde{x}_4(\tau)\,d\tau \tag{4.12a}$$

$$\text{s.t.} \quad \dot{\tilde{x}}(t) = f(\tilde{x}(t), y(t), 0) \tag{4.12b}$$

$$\dot{y}(t) = f_y(y, u_m) \tag{4.12c}$$

$$\tilde{x}(t_k) = x(t_k) \tag{4.12d}$$

$$y(\tilde{t}_0) = u_a(t_0) \tag{4.12e}$$

$$0.0704 \leq u_m(t) \leq 0.7042, \forall\, t \in [t_k, t_{k+N}) \tag{4.12f}$$

$$0 \leq y(t) \leq 0.7042, \forall t \in [t_k, t_{k+N}) \tag{4.12g}$$

$$|u_m(t_k) - u_m^*(t_{k-1}|t_{k-1})| \leq 0.1 \tag{4.12h}$$

$$|u_m(t_j) - u_m(t_{j-1})| \leq 0.1,\ j = k+1, ..., k+N-1 \tag{4.12i}$$

$$\int_{t_k}^{t_{k+N_k}} y(\tau)d\tau + \int_{(p-1)t_p}^{t_k} u_a^*(\tau)d\tau = 0.175 t_p/C_e \tag{4.12j}$$

where the notation follows that in Eqs. 3.11 and 4.3. The notation $u_m^*(t_{k-1}|t_{k-1})$ signifies the value of u_m that was determined to be optimal at the prior sampling time and was applied to the process for the sampling period between t_{k-1} and t_k. Minimization of the objective function in Eq. 4.12a maximizes the yield of ethylene oxide when the amount of reactant fed to the process over the $p-th$ operating period of length $t_p = 1\ t_d$ meets the constraint in Eq. 4.12j (the notation $u_a^*(t)$ signifies a value of u_a that was applied to the process at a past time t). Enforcing the constraint

of Eq. 4.12j ensures that Eq. 4.7 is satisfied by the final time t_f of operation. Two operating periods were simulated under this EMPC; though a longer simulation may reduce the effects from the transient on the results, the two operating periods simulated are sufficient for demonstrating that an empirical model of the valve dynamics can readily be used in place of a first-principles model in the MPC for valve behavior compensation. A shrinking prediction horizon N_k was used in each operating period with an initial length of 5 at the beginning of each operating period. At each subsequent sampling time, the prediction horizon was decreased by 1. The process model of Eq. 4.12b (the ethylene oxide process model from Section 3.3.2.2 with a single input as noted above) is integrated using the Explicit Euler numerical integration method with an integration step size of $h_{emp} = 10^{-4}\ t_d$ for making state predictions. Eq. 4.12c signifies that the predictions y of u_a in the EMPC come from the empirical model developed in this section, which evolves in time every $\Delta_e = h_{emp}$. Though the empirical model developed in this section is a discrete-time model as opposed to a continuous-time model, both the discretized (with Explicit Euler) process dynamic model and the empirical valve dynamics model evolve every $10^{-4}\ t_d$ when state predictions are made within the EMPC, and therefore, the discrete-time nature of the empirical model poses no issues for combining it with the continuous-time process model for making state predictions. In the simulations, the value of y was not updated with a state measurement of u_a at each sampling time but instead evolved in an open-loop fashion (the notation in Eq. 4.12e signifies that the initial data required for simulating the valve layer based on the empirical model (i.e., $y(\tilde{t}_0)$ and $y(\tilde{t}_{-1})$) are known and used to integrate the empirical model for all times without feedback of u_a). The state constraint in Eq. 4.12g was enforced every integration step. The input rate of change constraints in Eqs. 4.12h-4.12i are added to reduce the likelihood that the EMPC will request (unreachable) flow rates that would cause the pressure from the pneumatic actuation to become saturated at zero. The optimization problems were solved using the open-source interior-point optimization solver Ipopt[148] with a tolerance of 10^{-10}.

Fig. 4.4 shows the trajectories of u_a, u_m, and y initiated from $[x_1\ x_2\ x_3\ x_4\ x_v\ v_v\ z_f\ \zeta_P] = [0.997\ 1.264\ 0.209\ 1.004\ 0.051\ m\ 2.000 \times 10^{-6}\ m/t_d\ 1.426 \times 10^{-5}\ m\ 0]$ resulting from the use

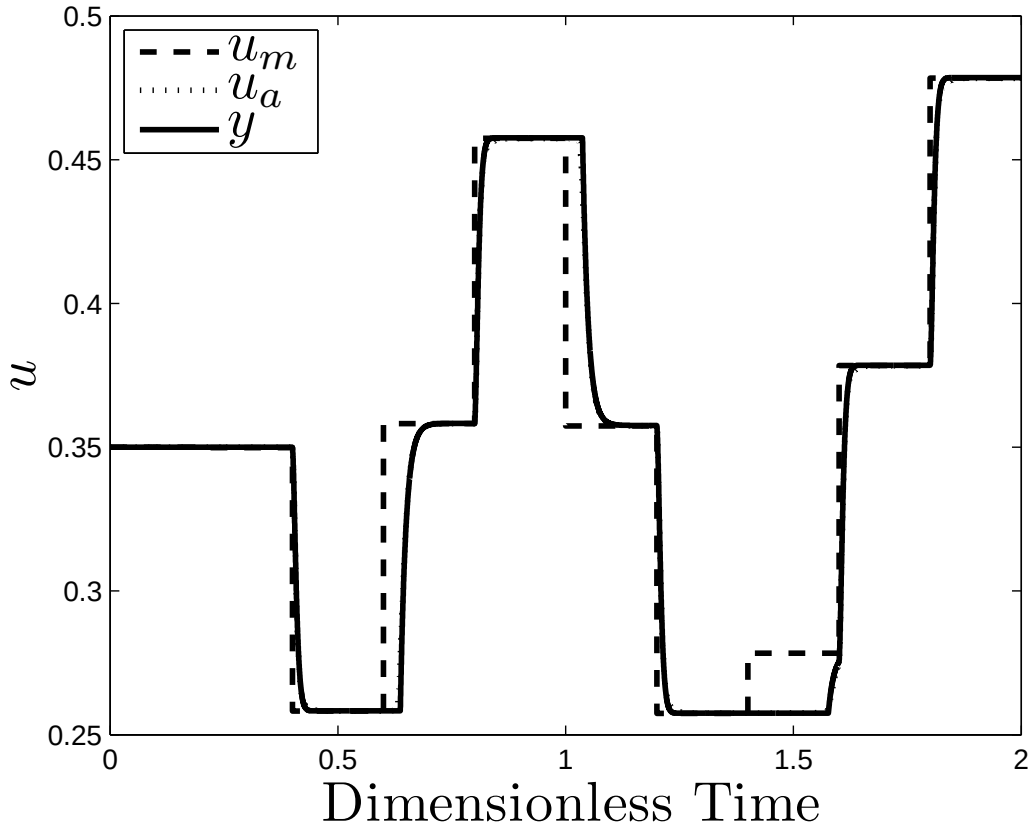

Figure 4.4: Comparison of valve layer set-point (u_m), valve layer output (u_a), and prediction of the valve layer output (y) under the EMPC using an empirical valve layer model (y almost overlays u_a).

of the empirical EMPC. The empirical model was successfully able to capture the behavior of u_a, and the EMPC calculated set-points that the valve layer could track. Fig. 4.5 shows the pressure applied to the valve throughout this closed-loop simulation, which never saturated at zero with the help of the input rate of change constraints. Fig. 4.6 shows the closed-loop process states under the empirical EMPC.

In addition to calculating reachable set-points and preventing pressure saturation in the two operating periods simulated, the MPC-based valve behavior compensation strategy with an empirical model was also able to ensure that the integral material constraint was not significantly violated. In the first operating period, the empirical EMPC used only 0.02% less material than required by the material constraint, and in the second operating period only 0.05% less.

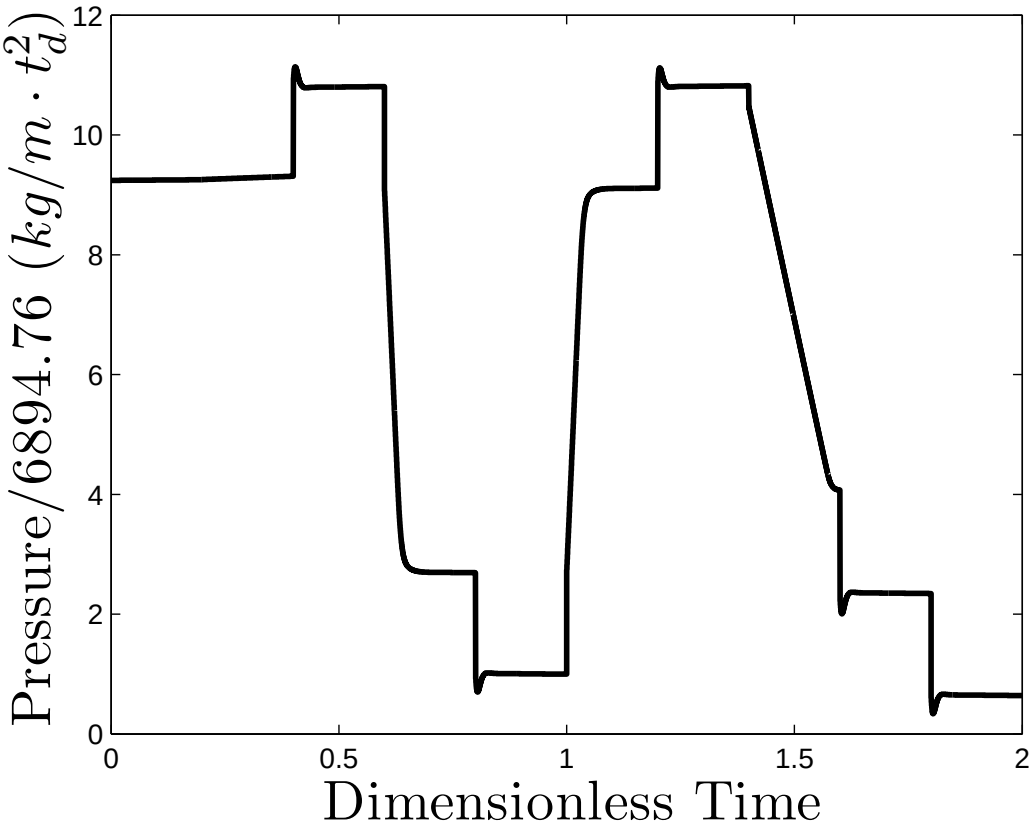

Figure 4.5: Pressure applied to the valve when the EMPC using an empirical valve layer model is used.

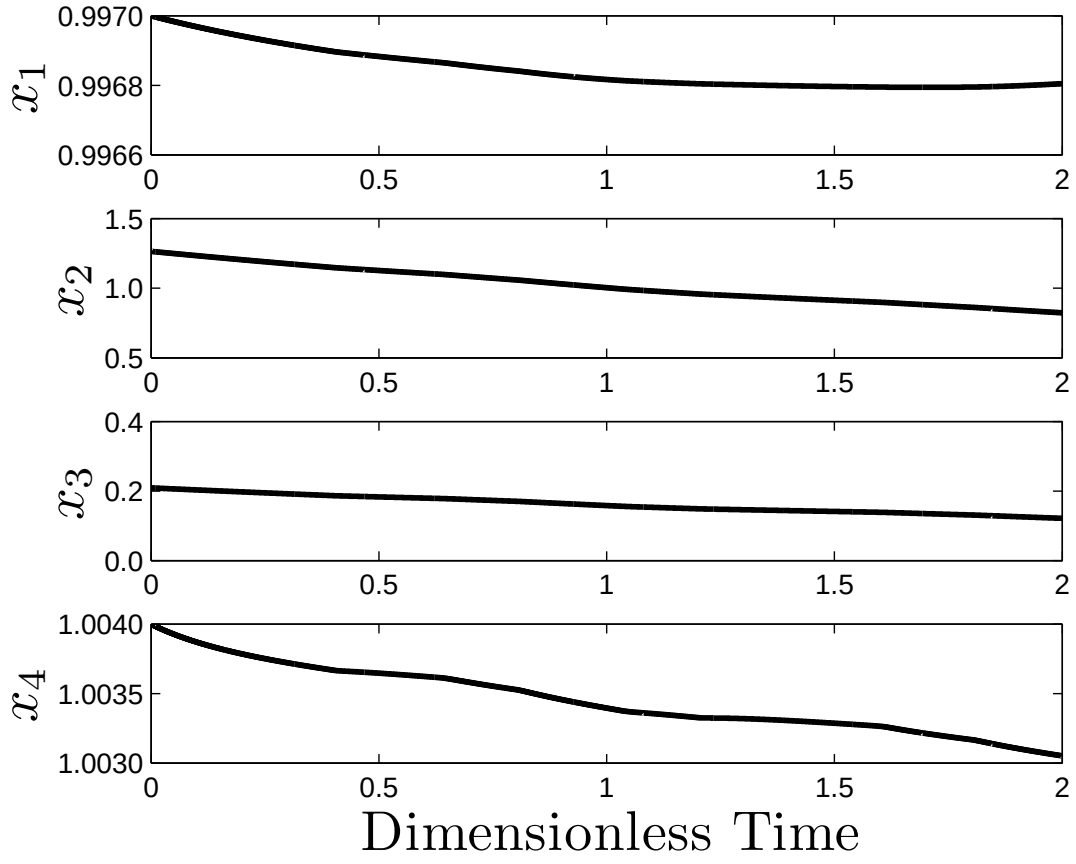

Figure 4.6: Closed-loop process states under the EMPC using an empirical valve layer model.

A comparison of a simulation of the form of Eq. 4.12 but with the first-principles valve layer model of Eqs. 3.27-3.31 and 3.33-3.34 in place of the empirical model of Eqs. 4.9-4.11 was formulated, in which the first-principles model for both the valve and process was simulated with an integration step of $10^{-5}\ t_d$ within the MPC, and state feedback of the process-valve states was obtained at each sampling time. The integration step size is smaller than for the simulation with the empirical EMPC because the first-principles model of Eqs. 3.27-3.31 and 3.33-3.34 cannot be integrated with a step size of $10^{-4}\ t_d$ using Explicit Euler due to numerical stability issues. The constraint of Eq. 4.12g was enforced on u_a every 10 integration steps so that it was enforced every $10^{-4}\ t_d$ as for the empirical EMPC. The finite difference approximation used for the gradients of the objective function and constraints used a perturbation one order of magnitude smaller than in the empirical EMPC. The resulting simulation of two operating periods took approximately three times longer to solve than the EMPC of Eq. 4.12 with the empirical valve layer model where the integration step within the MPC was $10^{-4}\ t_d$. Though the difference in computation time depends on a large number of factors such as the code used and the integration step size, it is significant that the empirical model is less stiff than the first-principles model.

4.4 Perspectives on Valve Nonlinearity Compensation

A conclusion of the results in this chapter and Chapter 3 is that an MPC design that utilizes models of both the process and valve behavior for making state predictions provides a systematic method for driving an output to its set-point that can account for multivariable interactions in a process-valve dynamic system and constraints such as valve output and actuation magnitude (e.g., actuator pressure) saturation that can lead to undesirable closed-loop behavior. This method is not restricted to linear plant dynamics, and it does not require tuning of compensator-specific parameters that are not clearly tied to the process output responses as do some of the stiction compensation methods discussed in Chapter 3 such as flow control, the integral term modification method, and knocker-type methods. The significant benefits of an MPC including valve dynamics

for improving the issues commonly observed due to valve behavior indicate that it may be beneficial for industry to consider wider use of MPC due to analysis not only of whether the chemical process itself would benefit from being controlled by an MPC (which is the typical analysis performed), but also of whether it might provide better valve behavior compensation in the long run (undesirable behavior like valve stiction can develop over time) that may reduce efficiency and profit in the long-term and therefore may make MPC a more attractive option than classical regulatory control designs. Thus, more analysis of the impact of actuator dynamics at the initial design phase may allow for better controller designs to be chosen that can handle changes in the actuator dynamics that often plague processes at a later phase and are much more difficult to handle when non-model-based control strategies are attempted to be used to handle nonlinear valve behavior.

Though the MPC-based valve nonlinearity compensation method was shown in the process examples in this chapter to be beneficial at compensating for the valve behavior, it was also shown that it has limitations in handling valve nonlinearities. For example, in Section 4.3.1, it was noted that a valve without flow control under MPC accounting for valve stiction may not be able to keep a process output at its set-point for all times when the MPC sampling period is long compared to the timescale of the valve dynamics such that the MPC is not able to regularly adjust the force applied by the valve actuation throughout a sampling period. An alternative to this is to use a flow controller for the valve or a small sampling period for the MPC to allow the force from the valve actuation to be adjusted frequently as the valve position changes according to its dynamics to try to drive it to the position corresponding to the valve output set-point. However, this may cause significant variations in the valve actuation during the time that the valve position is being adjusted, which may increase actuator wear.[86] This indicates that an MPC-based valve behavior compensation method must seek to balance actuator wear and set-point offset for certain control architectures and valve nonlinearities through appropriate constraints and design of parameters such as the sampling period. Another conclusion of this chapter and Chapter 3 is that because the effects observed in control loops due to valve behavior are closed-loop effects, changing the

control design of a system may result in different process output responses in a control loop in which valve dynamics cannot be neglected. This is important to consider as controllers at a plant are re-tuned or as upgrades are made to the control design.

Finally, the closed-loop perspective on valve behavior developed in this chapter and Chapter 3 can impact the stiction detection and quantification literature. It gives greater insight into the benefits and limitations of the detection/quantification methods for stiction in the literature, which are reviewed in[24] and include shape-based methods and model identification-based methods. Many of the shape-based methods (e.g.,[32, 82, 132, 136]) assume that a specific pattern exists in the data from the measured outputs of the system (process outputs or valve outputs), often in relation to the controller outputs. It has been highlighted that the process and controller dynamics will affect the patterns and thus may reduce the effectiveness of shape-based methods (e.g.,[78] notes that the stiction detection method in[82] may give different results depending on the controller tuning, and[32] and[89] also note that the pattern-based methods are not always effective because patterns depend on the controller, process, and valve dynamics). Chapter 3 gives a general mathematical framework for analyzing the difficulties noted with pattern-based methods through a process-valve dynamic model. It also gives greater insight into the conditions under which the assumption that oscillations are occurring in a process output due to stiction, made in multiple pattern-based stiction detection/quantification works, may not hold (e.g., when the controller, process, and valve dynamics produce the uncompensated case in Fig. 3.4). Multiple model identification-based stiction detection/quantification methods (see, for example,[89, 137]) assume that the process can be described by a linear model, which may be a limiting assumption especially as the requirement of steady-state operation is being challenged by the recent developments in EMPC. The primary goal of stiction detection methods is to identify problematic valve behavior so that maintenance can be performed on a valve, and quantification methods are intended to be used to prioritize valve maintenance based on which valves are most sticky. The empirical modeling strategy in this chapter could be considered as a valve behavior detection/quantification strategy that is not limited to stiction. The $u_{m,i} - u_{a,i}$ relationship could be developed for every valve if $u_{m,i} - u_{a,i}$,

$i = 1, \ldots, m$, data is available. The difference between $u_{m,i}$ and $u_{a,i}$ could then be tracked over time, and when it becomes significant, the valve could be flagged for maintenance. The valves for which $u_{a,i}$ deviates most significantly from $u_{m,i}$ could be given priority in the maintenance schedule. Though measurements of flow through a valve ($u_{a,i}$) are not always available in industrial applications when the control loop is not a flow control loop,[143] this analysis indicates that new instrumentation to provide measurements of process variables such as flow (when it is not already measured) may be beneficial long-term for detecting and compensating for valve behavior by allowing empirical models to be developed for a process-valve system when it may be difficult to obtain a process-valve model without the flow measurement (Remark 4.1).

A final observation is that many contributions to the stiction literature have focused on stiction as the nonlinearity in the process-valve system (i.e., many works examine linear processes and linear controllers); the results of this chapter and Chapter 3 indicate that nonlinear processes, especially with multiple inputs all affected by nonlinear valve behavior, may be particularly interesting to consider in future works on stiction detection, quantification, and compensation, due to the multivariable interactions of the process-valve states, which may, as noted above, best be handled with multiple-input/multiple-output nonlinear control designs.

4.5 Conclusions

This chapter demonstrated that an MPC design incorporating a dynamic model (first-principles or empirical) of the full process-valve system is able to systematically address the root cause of negative effects (nonlinear, multivariable interactions between the states of a process-valve dynamic model) in control loops with valve behavior that cannot be neglected (both for sticky valves and for valves exhibiting other behavior). This analysis indicates that consideration of valve behavior at the control design phase may warrant greater use of MPC in industry. A level control example and a continuous stirred tank reactor were used to demonstrate the MPC-based valve nonlinearity compensation strategy.

Chapter 5

Valve Nonlinearity Compensation via Model Predictive Control for Nonlinear Processes: Theoretical Considerations and Actuation Magnitude Constraints for Compensating for Valve Stiction

5.1 Introduction

Chapter 4 developed an MPC framework for compensating for valve nonlinearities and demonstrated its applicability through two chemical process examples focused on stiction. The discussion of the examples in Sections 4.3.1-4.3.2 indicated that stiction may change the u_a-P relationship for a sticky valve and could cause the values of u_a requested to not be physically realizable with the given actuation energy (e.g., no non-negative values of the pressure may be capable of driving u_a to its set-point value from the MPC in certain circumstances). This issue deserves further discussion, which will be a goal of this chapter. Furthermore, this chapter

proposes systematic methods for accounting for such issues. Building from the developments in Chapter 2, this chapter examines the conditions under which feasibility and closed-loop stability of a nonlinear process under the MPC for valve nonlinearity compensation are guaranteed when the MPC is augmented with constraints designed for the specific case of stiction compensation (e.g., actuator magnitude and input rate of change constraints with a process-valve dynamic model for a sticky valve). This chapter concludes with a chemical process example that motivates the need for actuation magnitude constraints, particularly in EMPC in which extreme values of the valve output flow rate may be requested by the MPC since the process is not necessarily operated at steady-state. The example demonstrates the benefits of including the actuation magnitude constraints in EMPC when a sticky valve is in the control loop. This chapter thus provides an indication of how the MPC-based valve nonlinearity compensation method of the prior chapter can be modified through changes in the constraints as desired to handle issues arising in the control loop specific to a certain valve nonlinearity, indicating the flexibility of the overall approach in Chapter 4. Because this chapter focuses on stiction compensation, the remainder of this introduction provides background on the stiction valve nonlinearity.

Valve stiction is a phenomenon caused by friction between valve components and refers to the tendency of a valve not to move upon the change of the control signal sent to the valve until the control signal exceeds a certain threshold, at which time there may be a sudden movement of the valve components causing the valve output (i.e., process manipulated input) to change quickly. The percentage of the available range of valve outputs traversed when the valve output changes quickly quantifies the phenomenon of slip-jump. When the valve is moving (in the moving phase), the valve output typically is linearly related to the valve input until the changes in the valve input change sign (i.e., the valve input begins to decrease when it was previously increasing, or vice versa), at which point the valve begins to stick again. Because stiction has been characterized in various ways by different authors, the authors of[33] compile some of the stiction definitions, ending with the definition determined by the authors based on observations of plant data, which classifies stiction as a friction effect that manifests itself through a sudden change in the valve output in

response to a changing input signal. Specifically, the authors of [33] define four major regimes in the dynamic response of the control valve output to changes in the input to the valve determined by the controller: deadband, stickband, slip-jump, and the moving phase. In the absence of slip-jump, only deadband (the percentage of the available range of the input signals to the valve throughout which the valve output does not change in the absence of slip-jump) and the moving phase exist. When a valve experiences slip-jump, the valve remains stuck throughout the deadband and also throughout a percentage of the available range of inputs beyond the deadband (called the stickband) until it slips from the value at which it was stuck to a value in the moving phase.

Stiction has posed a significant issue in chemical process control throughout the last several decades. Reports from the 1990s indicated that stiction negatively affected control loop performance at the time,[72,91] and a report from Honeywell indicated that when studying 26,000 proportional-integral-derivative (PID) controllers, the performance of about one third was classified in the lowest of the classification categories ("poor" and "fair"), with valve issues, including stiction, causing about one third of these low classifications.[46] More recently,[29] cited stiction as a contributor to plantwide oscillations and included plant data from the Mitsubishi Chemical Corporation for a plant where stiction contributed to plantwide oscillations. In addition, in,[30] the proposed stiction detection and quantification method is performed on industrial data for plants with sticky valves, demonstrating that the problem of valve stiction remains a challenging one. As a result, a significant level of research has been performed throughout the years in an attempt to more accurately model, detect, quantify, and combat stiction (see the review paper[24] for a general overview of stiction modeling, detection, quantification, and compensation).

The physical cause of stiction in control valves is best explained using a specific valve type for clarity of presentation, but the same basic principles will hold for other valve types as well. For example, a pneumatic spring-diaphragm sliding-stem globe valve has a valve stem that, in response to a pressure applied to a diaphragm, moves to adjust the valve output. In a valve with stiction, the valve output may not approach the value requested due to friction forces between the valve stem and the packing that can prevent the valve stem from moving to the required position

until the pressure applied to the valve diaphragm is large enough to overcome the breakaway force for the packing-stem contact. The cause of friction between the valve stem and the packing is that the materials from which the stem and packing are made are rough at a microscopic level, with protrusions called asperities. The interactions of the asperities on the two surfaces result in friction forces.[18] The friction phenomenon is often described using static, Coulomb, and viscous friction, as well as the Stribeck effect. However, there are a number of other phenomena that result from friction, including rising static friction, presliding displacement (micro-slip), frictional memory in sliding, stick-slip,[18] hysteresis with nonlocal memory during presliding,[140] velocity weakening, the lift-up effect,[1] and asymmetric stiction.[151]

Friction models have been developed throughout the years that model these friction effects to varying degrees. For example, the Classical[72, 120] model only accounts for the Coulomb and viscous forces and the Stribeck effect in the sliding regime, representing any presliding dynamics with a static friction force. As models were developed throughout time, such as the Dahl,[41, 119] LuGre,[26] Leuven,[95, 140] Elasto-Plastic,[48] and generalized Maxwell-Slip[94] models, they began to incorporate some of the more subtle friction effects in both the presliding and sliding regimes. A generic model that attempted to represent the known friction dynamics by modeling various interactions between asperities was also developed.[1] A number of researchers have also developed algorithm-based empirical friction models, known as data-driven models, that attempt to represent friction dynamics using decision tree structures. This class of models includes the Stenman,[138] Choudhury,[33] Kano,[90] and He[78] models.

A number of works utilizing friction models in control strategies to counter friction have examined adapting friction model parameters.[70, 71, 85] In addition, the parameters of the friction model change with time for a valve as stiction worsens over time, which may occur for reasons such as tightening of the valve packing or degradation or depletion of materials that comprise or lubricate the valve.[77, 133] For example, in[72] and,[91] it is seen that as stiction worsens in a pneumatic sliding-stem globe valve, the range of stem positions that can be reached with a given range of pressures applied to the valve is reduced. This is significant because the pressure available to be

applied to a valve is limited,[38] with the result that as stiction worsens, the given range of pressures cannot move the valve stem as significantly as when stiction was minimal. This shows that a negative effect of stiction is that it changes the valve dynamics and in effect constrains the range of valve outputs available for a given range of actuation magnitudes.

Other negative effects of stiction include set-point tracking issues and oscillations in control loops that result from deadband/stickband and slip-jump. For example, when a valve has deadband/stickband, the valve output does not change in response to changes in the control signal to the valve until the control signal overcomes the deadband/stickband, which prevents the valve output from tracking its set-point. Oscillations can occur in a control loop with integral action as demonstrated in Chapter 3.

A good deal of work has been performed to reduce the negative effects of stiction on engineering processes. As mentioned above with respect to adapting friction model parameters, a number of methods have been developed to reduce the tracking offset that can result from friction (many appear in the literature for high-precision mechanical applications such as machining) using control laws based on a friction model (see, for example,[87, 91]). Much of the stiction compensation literature for sticky valves in chemical plant control loops has focused on reducing oscillations. Methods for oscillation reduction include those reviewed in Section 3.4 such as the knocker and variations upon it,[39, 77, 133, 134] the constant reinforcement method of,[86] the two moves method and its extensions,[40, 135, 150] the optimization method of,[135] and retuning methods.[73, 99, 111]

In addition to the stiction compensation methods mentioned above, predictive control methods have also been looked at for compensating for friction. In,[27] a predictive controller for applications requiring high precision of mechanical movement was augmented by time delay control and zero phase error tracking control to improve its tracking performance in the presence of nonlinear friction effects. In,[152] an inverse backlash model and valve saturation are incorporated in an MPC for linear systems to overcome the deadband associated with backlash, and this controller is applied to a system with stiction in.[153] In,[45] the bounds on the optimization variables computed by an MPC are adjusted based on the knowledge that the MPC is in series with a unit that applies the inverse

model for deadzone, stiction, or backlash to the output from the MPC and sends this signal to a valve with nonlinear dynamics that can saturate. The prior chapter developed an MPC-based valve nonlinearity compensation framework, which will now be investigated to develop constraints that should be developed to handle issues that may arise due to stiction and to guarantee feasibility and closed-loop stability of a process operated under the control design. The results of this chapter originally appeared in.[49,52]

5.2 Preliminaries

5.2.1 Notation

In this chapter, $t_k = k\Delta$, $k = 0,1,2,\ldots$ refers to synchronous time instants separated by a sampling period Δ. The Euclidean norm of a vector is denoted by $|\cdot|$. A function $\alpha : [0,a) \to [0,\infty)$ with $\alpha(0) = 0$ belongs to class $\mathscr{K}$ if it is continuous and strictly increasing. A level set of a scalar-valued positive definite function $V(x)$ is defined to be the set $\Omega_\rho := \{x \in R^n \mid V(x) \leq \rho\}$. Set subtraction is denoted using '/' (i.e., $x \in A/B := \{x \in R^n \mid x \in A,\ x \notin B\}$).

5.2.2 Class of Systems

In this chapter, we consider a process-valve model for use in MPC that incorporates the dynamics of the process as well as the dynamics of the valves. This model includes dynamic equations for the process, the valve position, the valve output, and a linear controller for the valve. We introduce these equations separately, and then present the integrated model that combines them.

5.2.2.1 Class of Nonlinear Processes

As in Chapters 3-4, we consider nonlinear processes of the form in Eq. 3.1. We assume that each input $u_{a,i}$, $i = 1,\ldots,m$, to the process is bounded within a set U_i ($U_i := \{u_{a,i} \ : \ u_{a,i,\min} \leq u_{a,i} \leq u_{a,i,\max}\}$). We also assume that the disturbance is bounded ($w \in W := \{w \ : \ |w| \leq \theta, \theta > 0\}$).

We note that the model of Eq. 3.1 can be constructed either through first-principles or system identification techniques.

5.2.2.2 Nonlinear Valve Dynamics

The dynamics of the position $x_{v,i}$ and velocity $v_{v,i}$ of the moving parts of the $i-th$ valve relative to the valve surfaces causing friction are given by Eqs. 3.16-3.17. The friction force experienced by the valve moving parts for the $i-th$ valve ($F_{fric,i}$) and the dynamics of the internal friction model states $z_{f,i} \in R^{z_i}$ are given by Eqs. 3.18-3.19, respectively. Assuming that each valve controls one process input, we define $a = [a_1, \ldots, a_m]^T$, $c = [c_1, \ldots, c_m]^T$, $F_O = [F_{O,1}^T \ ... \ F_{O,m}^T]^T$, and $F_A = [F_{A,1}^T \ ... \ F_{A,m}^T]^T$. Here, $F_{O,i} \in R^{\tilde{p}_i}$ and $F_{A,i} \in R^{\tilde{s}_i}$, so $a_i \in R^{\tilde{p}_i}$ and $c_i \in R^{\tilde{s}_i}$ as well. The notation $\hat{v}_v(a(t), F_O(t), c(t), F_A(t), x_v(t), v_v(t), z_f(t)) = [\hat{v}_{v,1}(a_1(t), F_{O,1}(t), c_1(t), F_{A,1}(t), x_{v,1}(t), v_{v,1}(t), z_{f,1}(t)) \ \ldots$
$\hat{v}_{v,m}(a_m(t), F_{O,m}(t), c_m(t), F_{A,m}(t), x_{v,m}(t), v_{v,m}(t), z_{f,m}(t))]^T$ signifies the vector containing the right-hand side of Eq. 3.17 for all valves $i = 1, \ldots, m$. In addition, we define:

$$z = \sum_{i=1}^{m} z_i \tag{5.1}$$

To clarify the valve model dynamics presented in this section, Fig. 5.1 depicts a sliding-stem globe valve with a friction force and a force from the actuator acting upon it. This valve figure does not provide a detailed schematic of the inside of the valve, but helps to clarify how some of the forces described above may act on an example valve. It should also be noted that the discussion above is not limited to this sliding-stem globe valve type.

Remark 5.1. *We note that the form of Eqs. 3.16-3.17, which define the position and velocity of the valve using a force balance, implies that the moving parts of the valve under consideration move linearly, as would be the case with, for example, a sliding-stem globe valve. A variety of other valve types exist, however, and the moving parts of many of these do not move linearly, but rather rotate (this is the case with, for example, a ball or butterfly valve).*[21,23,101] *Appropriate equations*

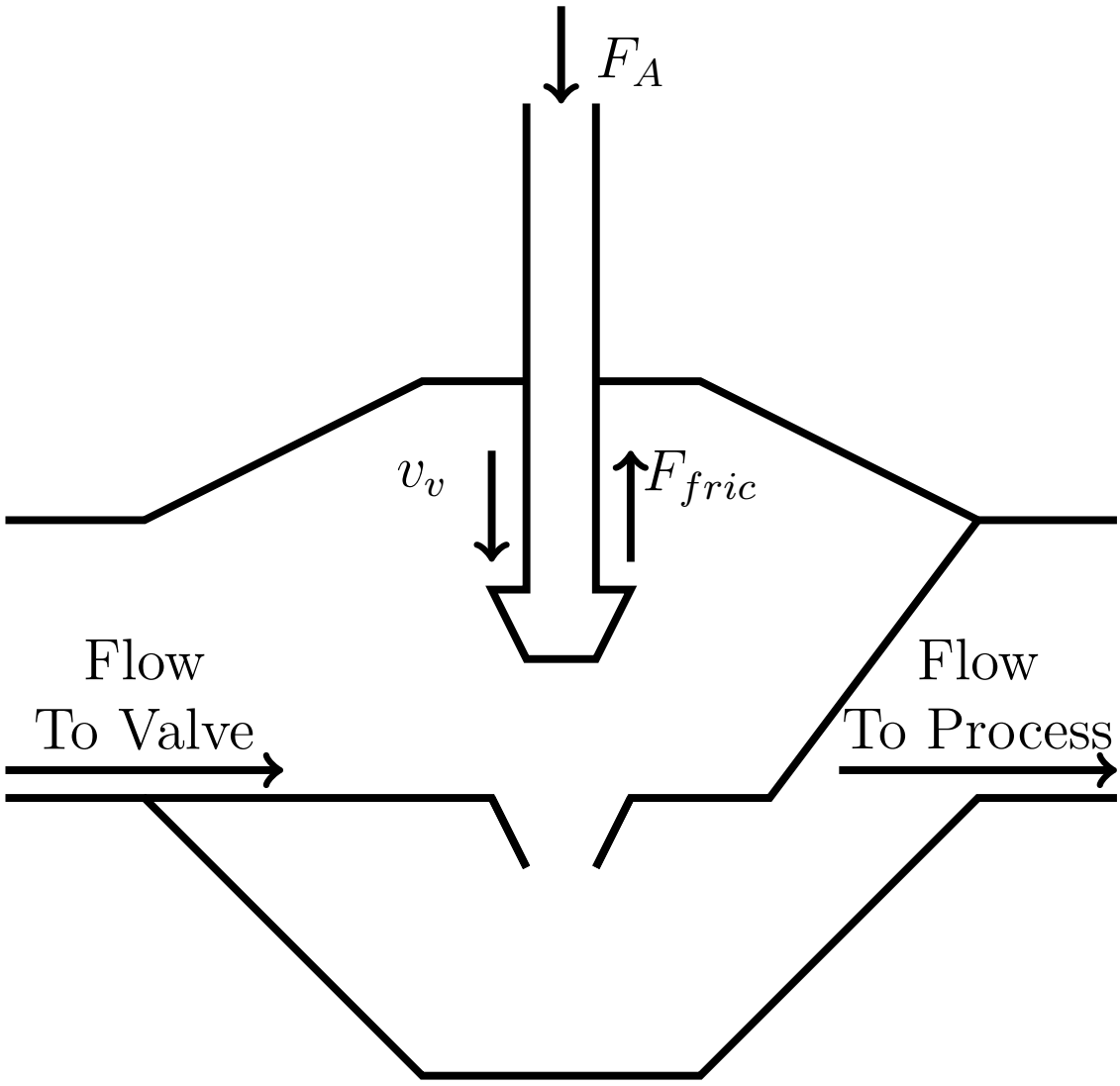

Figure 5.1: Schematic of forces on an example valve (v_v, F_{fric}, and F_A denote the valve velocity, friction force, and force from the actuation, respectively).

for the dynamics and friction for a valve that does not have linear movement could be substituted for Eqs. 3.16-3.17.

Remark 5.2. *The data-driven friction models use decision-tree structures traversed based on the evaluation of Boolean expressions, and thus are not immediately in the first-order ordinary differential equation form of Eqs. 3.16-3.19. However, such models can be used to simulate a system, and then model identification utilizing the simulation data could be investigated for developing continuous-time state-space models describing the valve dynamics.*

5.2.2.3 Relating Valve Position and Valve Output

We relate $u_{a,i}$ to $x_{v,i}$ through the nonlinear relationship in Eq. 3.21, where $f_{flow,i}$ is a one-to-one continuous nonlinear function. As an example of possible relationships between $u_{a,i}$ and $x_{v,i}$, Fig. 5.2 presents a plot of two types of relationships (linear and equal percentage) between $u_{a,i}$ and $x_{v,i}$ that are described in the literature for sliding-stem globe valves, and depicts the case that the zero of the valve position corresponds to zero flow.[21,38]

Remark 5.3. *As noted in,[38] $u_{a,i}$ depends not only on $x_{v,i}$, but also on the fluid pressures upstream and downstream of the valve. In Eq. 3.21, we assume that the upstream and downstream pressures are fixed for a given value of $x_{v,i}$ such that we are able to write $u_{a,i}$ as a function of $x_{v,i}$ only by writing the pressure differential as a function of $x_{v,i}$ as well. However, for the case that this is not possible and the pressures are varying, it is possible to instead write Eq. 3.21 as a function of $x_{v,i}$ as well as of the upstream and downstream pressures and to still apply the method proposed in this chapter to the resulting system if the dynamics of the pressure variations are added to the process-valve model.*

5.2.2.4 Linear Controller Dynamics

It is customary in industry to implement a regulatory layer where classical linear controllers are used to influence the valve dynamics and force the valve output to be closer to the valve

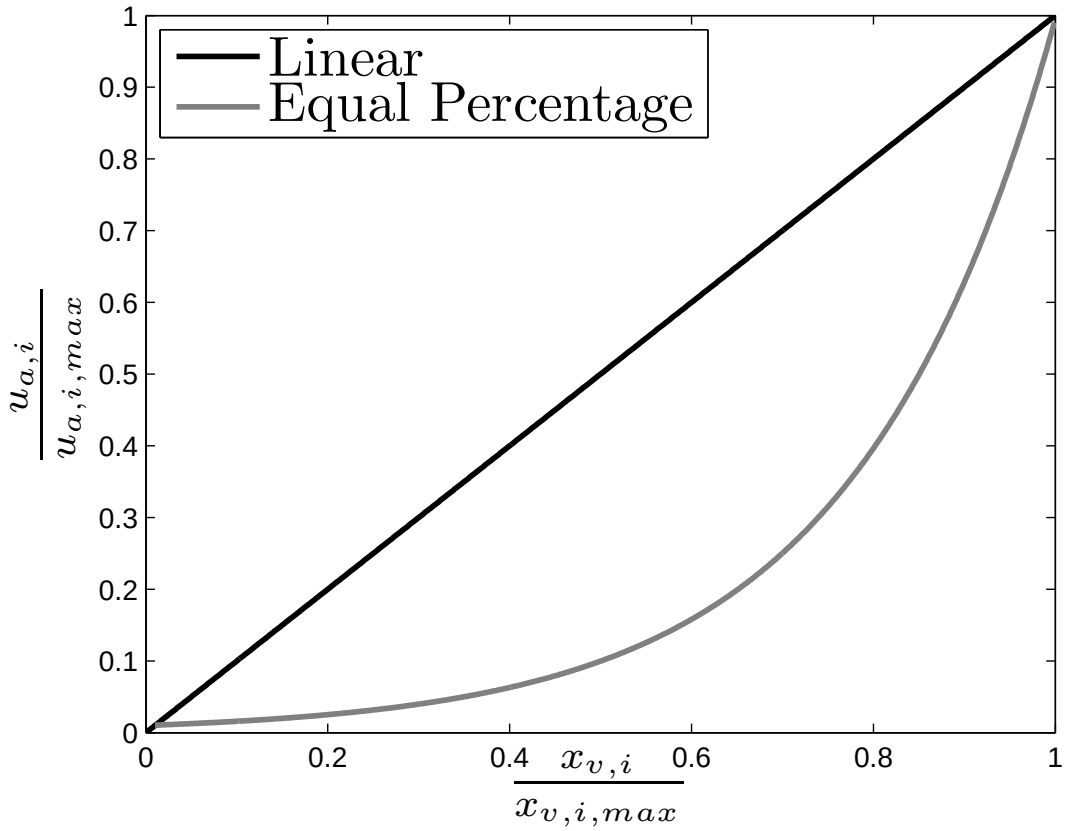

Figure 5.2: Examples of relationships between $u_{a,i}$ and $x_{v,i}$ for a valve. $x_{v,i,\max}$ is the maximum stem position of the valve. In this figure, $x_{v,i,\max}$ corresponds to the stem position when the valve is fully open.

output set-point computed by the model predictive controller.[42] Thus, for consistency with industrial practice, we assume that a linear controller (for example, a proportional (P) controller, a proportional-integral (PI), or a proportional-integral-derivative (PID) controller) is used, as opposed to a nonlinear controller, to regulate the flow rate from the valve to its set-point. Because $x_{v,i}$ and $u_{a,i}$ are related through a one-to-one nonlinear algebraic equation, this is equivalent to assuming that the linear controller regulates the stem position of the valve to its set-point (though the dynamics of the controller in terms of $x_{v,i}$ are not necessarily linear if the dynamics in terms of $u_{a,i}$ were linear since $f_{flow,i}$ in Eq. 3.21 may be a nonlinear function). The dynamics of this controller are described (in terms of the valve layer states instead of the valve output flow rate) by:

$$\dot{\zeta}_i = f_{LC,i}(\zeta_i, x_{v,i}, v_{v,i}, u_{m,i}) \tag{5.2}$$

where $\zeta_i \in R^{r_i}$ is the vector of controller states for the linear controller of the $i-th$ valve output (this is the zero vector if a static controller is used), $u_{m,i}$ is the set-point for the valve output of the $i-th$ valve, which is set by the MPC, and $f_{LC,i}$ is a nonlinear vector function associated with the dynamics of the linear controller for the $i-th$ valve. In addition, we define $f_{LC}(\zeta, x_v, v_v, u_m) = [f_{LC,1}(\zeta_1, x_{v,1}, v_{v,1}, u_{m,1}) \ \ldots \ f_{LC,m}(\zeta_m, x_{v,m}, v_{v,m}, u_{m,m})]^T$ and:

$$r = \sum_{i=1}^{m} r_i \tag{5.3}$$

5.2.2.5 Combined Process-Valve Model

Given the differential and algebraic equations describing the dynamics of the process-valve system in Eqs. 3.1, 3.16-3.19, 3.21, and 5.1-5.3 to be controlled by MPC, we now combine these equations

into one process-valve dynamic model with state vector $q = [x^T\ x_v^T\ v_v^T\ z_f^T\ \zeta^T]^T$:

$$\dot{q} = \begin{bmatrix} \dot{x} \\ \dot{x}_v \\ \dot{v}_v \\ \dot{z_f} \\ \dot{\zeta} \end{bmatrix} = f_q(q(t), a(t), F_O(t), c(t), F_A(t), u_m(t), w(t)) = f_q(q(t), u_m(t), w(t)) = \tag{5.4}$$

$$\begin{bmatrix} f(x(t), f_{flow}(x_v(t)), w(t)) \\ v_v(t) \\ \hat{v}_v(a(t), F_O(t), c(t), F_A(t), x_v(t), v_v(t), z_f(t)) \\ \hat{z}_f(x_v(t), v_v(t), z_f(t)) \\ f_{LC}(\zeta, x_v, v_v, u_m) \end{bmatrix}$$

where A and B are matrices containing the entries of every A_i and B_i, respectively, in appropriate orders. The statement that $f_q(q(t), a(t), F_O(t), c(t), F_A(t), u_m(t), w(t)) = f_q(q(t), u_m(t), w(t))$ follows because the vectors a, F_O, c, and F_A will be functions of the states q and/or the inputs u_m when they are defined for a system.

Defining $q_v = n + 2m + z + r$, we assume that $f_q : R^{q_v} \times R^m \times R^w \to R^{q_v}$ is a locally Lipschitz function of its arguments with the origin of the unforced nominal system (the system of Eq. 5.4 with $u_m(t) \equiv 0$ and $w(t) \equiv 0$) at the origin (i.e., $f_q(0,0,0) = 0$). We further assume that the inputs $u_{m,i}$, $i = 1, ..., m$ are restricted as follows: $u_{m,i} \in U_{m,i} := \{u_{m,i} \ : \ u_{m,i,\min} \leq u_{m,i} \leq u_{m,i,\max}\}$. It is noted that a valve set-point $u_{m,i}$ from the MPC need not be restricted to the same set U_i that the actual valve output is restricted within (for example, it may be restricted to a smaller set $U_{m,i}$ if it is known that the linear controller controlling the valve output overshoots the set-point). In addition to the restriction that each $u_{m,i} \in U_{m,i}$, we consider that there may be additional input constraints that depend on the current states, inputs, or both (as opposed to constraints that may depend on past and future values of the inputs or states). Thus, we consider that each $u_{m,i} \in U_{T,i}(q)$, where $U_{T,i}(q)$ represents the set of allowable values of the input $u_{m,i}$ given all constraints involving this

input, and it is defined separately at each state-space point q since the input constraints may depend on the current state.

We further assume that a Lyapunov-based controller $h_v(q) = [h_{v,1}(q) \ \ldots \ h_{v,m}(q)]^T$ with $h_v(0) = 0$ exists for the nominal system of Eq. 5.4 that can render the origin locally asymptotically stable while meeting the input constraints in the sense that[35,92] a sufficiently smooth, positive definite Lyapunov function $V(q)$ and class $\mathscr{K}$ functions $\alpha_1(\cdot)$, $\alpha_2(\cdot)$, $\alpha_3(\cdot)$, and $\alpha_4(\cdot)$ exist that satisfy the following inequalities:

$$\alpha_1(|q|) \leq V(q) \leq \alpha_2(|q|) \tag{5.5a}$$

$$\frac{\partial V(q)}{\partial q} f_q(q, h_v(q), 0) \leq -\alpha_3(|q|) \tag{5.5b}$$

$$\left| \frac{\partial V(q)}{\partial q} \right| \leq \alpha_4(|q|) \tag{5.5c}$$

$$h_{v,i}(q) \in U_{T,i}(q), \ i = 1, \ldots, m \tag{5.5d}$$

for all $q \in D \subseteq R^{q_v}$, where D is an open neighborhood of the origin.

There may be constraints on the states of the system of Eq. 5.4 (for example, the constraint that each $u_{a,i} \in U_i$), which will restrict the allowable states within the set Q_v. The stability region of the process-valve system of Eq. 5.4 under the controller $h_v(q)$ is defined as the level set $\Omega_\rho \subseteq Q_v \subseteq D$ of the Lyapunov function. In addition to the requirements on $h_{v,i}$ in Eq. 5.5d, we require that each $h_{v,i}$, $i = 1, \ldots, m$ be locally Lipschitz as follows:

$$|h_{v,i}(q_1) - h_{v,i}(q_2)| \leq L_v |q_1 - q_2|, \ i = 1, \ldots, m \tag{5.6}$$

for all $q_1, q_2 \in \Omega_\rho$ where $L_v > 0$ can satisfy the Lipschitz condition for every $h_{v,i}$ (i.e., L_v is greater than or equal to the minimum Lipschitz constant that can satisfy the Lipschitz condition for the control law $h_{v,i}$ that has the largest minimum Lipschitz constant from all $i = 1, \ldots, m$). We note that when $h_v(q)$ is applied to the system of Eq. 5.4 in sample-and-hold, it can render the origin practically stable for sufficiently small sampling periods (Proposition 2.3).

From Lipschitz continuity of f_q, from the bounds on $u_{m,i}$ and w, and from the fact that $V(q)$ is sufficiently smooth, there exist positive constants $\bar{M}$, $\bar{L}_q$, $\bar{L}_w$, $\bar{L}'_q$, and $\bar{L}'_w$ such that:

$$|f_q(q,u_{m,1},...,u_{m,m},w)| \leq \bar{M} \tag{5.7}$$

$$|f_q(q_1,u_{m,1},...,u_{m,m},w) - f_q(q_2,u_{m,1},...,u_{m,m},0)| \leq \bar{L}_q|q_1-q_2| + \bar{L}_w|w| \tag{5.8}$$

$$\left|\frac{\partial V(q_1)}{\partial q} f_q(q_1,u_{m,1},...,u_{m,m},w) - \frac{\partial V(q_2)}{\partial q} f_q(q_2,u_{m,1},...,u_{m,m},0)\right| \leq \bar{L}'_q|q_1-q_2| + \bar{L}'_w|w| \tag{5.9}$$

for all $q,q_1,q_2 \in \Omega_\rho$, $u_{m,i} \in U_{T,i}(q)$, $i = 1,...,m$, and $|w| \leq \theta$. A consequence of Eq. 5.7 and the continuity of q is that the following inequality holds:

$$|q(t) - q(t_{k-1})| \leq \bar{M}\Delta \tag{5.10}$$

for all $q(t), q(t_{k-1}) \in \Omega_\rho$ when $t \in [t_{k-1}, t_k]$, and a Δ sufficiently small.

Remark 5.4. *In Eq. 5.4, disturbances are only considered in the process states. It is noted that disturbances could also be added to the states x_v, v_v, and z_f if desired, and all results in this chapter would continue to hold if the resulting noise vector was bounded as w is assumed to be.*

5.3 MPC for Stiction Compensation

A stiction compensation strategy should address the negative effects of stiction on control loop performance, including that it can prevent a valve from effectively tracking the set-points it receives. Another negative effect of stiction can be changes in the valve dynamics as stiction worsens that affect the range of values that the valve output can take with the available actuation energy. The MPC proposed in this section can help to alleviate these negative impacts of valve stiction. We first discuss the proposed control loop architecture, and then proceed to develop the model predictive controller formulation incorporating the process and valve dynamics, actuation magnitude constraints, and input rate of change constraints. We also include Lyapunov-based

stability constraints that will be used to prove feasibility of the proposed MPC optimization problem and stability of the closed-loop system under the MPC. We discuss how the proposed formulation addresses the various issues associated with stiction and provide the proofs of feasibility and closed-loop stability for a sufficiently small sampling period.

5.3.1 MPC Architecture and Formulation for Stiction Compensation

The proposed control architecture, shown in Figure 5.3, incorporates an MPC controlling a process by providing set-points for the valve outputs (process manipulated inputs) to a linear controller that drives the valve output quickly to its set-point. It is noted that the control of the valve output set-point, rather than the stem position itself, is chosen for consistency with the control architectures incorporating MPC and a lower layer with linear controllers in industry. The proposed

MPC computes control actions by solving the following optimization problem:

$$\min_{u_{m,1}(t),\ldots,u_{m,m}(t)\in S(\Delta)} \quad \int_{t_k}^{t_{k+N}} L_{MPC}(\tilde{q}(\tau), u_{m,1}(\tau), \ldots, u_{m,m}(\tau))\, d\tau \tag{5.11a}$$

$$\text{s.t.} \quad \dot{\tilde{q}}(t) = f_q(\tilde{q}(t), u_{m,1}(t), \ldots, u_{m,m}(t), 0) \tag{5.11b}$$

$$\tilde{q}(t_k) = q(t_k) \tag{5.11c}$$

$$\tilde{q}(t) \in Q_v, \forall t \in [t_k, t_{k+N}) \tag{5.11d}$$

$$u_{m,i}(t) \in U_{m,i}, \forall i = 1, \ldots, m,\ t \in [t_k, t_{k+N}) \tag{5.11e}$$

$$g_{act,1}(\tilde{q}(t), u_{m,1}(t), \ldots, u_{m,m}(t)) = 0,\ \forall t \in [t_k, t_{k+N}) \tag{5.11f}$$

$$g_{act,2}(\tilde{q}(t), u_{m,1}(t), \ldots, u_{m,m}(t)) \leq 0, \forall t \in [t_k, t_{k+N}) \tag{5.11g}$$

$$|u_{m,i}(t_k) - h_{v,i}(q(t_k))| \leq \varepsilon,\ i = 1, \ldots, m \tag{5.11h}$$

$$|u_{m,i}(t_j) - h_{v,i}(\tilde{q}(t_j))| \leq \varepsilon,\ i = 1, \ldots, m,\ j = k+1, \ldots, k+N-1 \tag{5.11i}$$

$$\tilde{g}_{MPC,1}(\tilde{q}(t), u_{m,1}(t), \ldots, u_{m,m}(t)) = 0, \forall t \in [t_k, t_{k+N}) \tag{5.11j}$$

$$\tilde{g}_{MPC,2}(\tilde{q}(t), u_{m,1}(t), \ldots, u_{m,m}(t)) \leq 0, \forall t \in [t_k, t_{k+N}) \tag{5.11k}$$

$$V(\tilde{q}(t)) \leq \rho_e,\ \forall\, t \in [t_k, t_{k+N}) \text{ if } t_k < t' \text{ and } V(q(t_k)) \leq \rho_e \tag{5.11l}$$

$$\begin{aligned} &\frac{\partial V(q(t_k))}{\partial q} f_q(q(t_k), u_{m,1}(t_k), \ldots, u_{m,m}(t_k), 0) \leq \\ &\qquad \frac{\partial V(q(t_k))}{\partial q} f_q(q(t_k), h_{v,1}(q(t_k)), \ldots, h_{v,m}(q(t_k)), 0) \\ &\qquad \text{if } t_k \geq t' \text{ or } V(q(t_k)) > \rho_e \end{aligned} \tag{5.11m}$$

where the notation follows that in Eq. 4.1. The general stage cost L_{MPC} (Eq. 5.11a) is a function of the predicted state $\tilde{q}$ from the full process-valve model (Eq. 5.11b, with initial condition in Eq. 5.11c) and the vector of valve set-points u_m, which is the decision variable of the optimization problem (this is in contrast to, for example, Eq. 3.11, where the objective function depends only on $\tilde{x}$ and u_m; an example of an objective function that fits within the framework of Eq. 5.11a is Eq. 4.1a where $\tilde{\tilde{q}}$ is considered to include predictions of the process state but $\tilde{u}_{a,i}$ can be written as a function of the valve layer state $x_{v,i}$ through Eq. 3.21 and thus the objective function includes

both process and valve model states). The solution to the optimization problem of Eq. 5.11 at time t_k is denoted as $u^*_{m,i}(t|t_k)$, $i = 1,...,m$, $t = t_k, t_{k+1},...,t_{k+N-1}$.

In Eq. 5.11, the predicted state $\tilde{q}$ is restricted to the set Q_v (Eq. 5.11d; Q_v bounds the process-valve state vector as noted in Section 4.2), and each manipulated input $u_{m,i}$ is restricted to the set $U_{m,i}$, $i = 1,...,m$ (Eq. 5.11e) (note that the predicted values of $u_{a,i}$ are restricted by Eq. 5.11d and Eq. 3.21). In addition to such constraints on the actuation of each valve, the use of the detailed stiction model within the MPC allows additional restrictions to be placed on the actuation magnitude, including the equality and inequality constraints in Eqs. 5.11f-5.11g, to prevent the MPC from calculating undesirable or non-physical set-points $u_{m,i}$ (these constraints were written with the states and inputs as arguments, though they are functions of $a(t)$, $F_O(t)$, $c(t)$, and $F_A(t)$, using the simplification noted in Section 5.2.2.5 that $a(t)$, $F_O(t)$, $c(t)$, and $F_A(t)$ will be functions of the states and inputs when they are explicitly defined for the given valve). Input rate of change constraints can also be added, as in Eqs. 5.11h-5.11i, to reduce actuator wear as described in Chapter 2. The input rate of change constraints are written with respect to the controller $h_{v,i}$ but for a given $\varepsilon_{desired}$, these constraints constrain the rates of change $|u_{m,i}(t_k) - u^*_{m,i}(t_{k-1}|t_{k-1})| \leq \varepsilon_{desired}$ and $|u_{m,i}(t_j) - u_{m,i}(t_{j-1})| \leq \varepsilon_{desired}$, $j = k+1,...,k+N-1$, when a sufficiently small sampling period Δ and an appropriate value of ε are chosen (from Theorem 2.1, which is placed within the notation of the process-valve system through Proposition 5.3 below). Eqs. 5.11j and 5.11k represent general equality and inequality constraints, respectively, for the process-valve states and valve output flow rate set-points described by functions $\tilde{g}_{MPC,1}$ and $\tilde{g}_{MPC,2}$ that can be added to the optimization problem to achieve desired performance goals. As stated in Section 5.2.2.5, we require that the constraints in Eqs. 5.11f-5.11g and 5.11j-5.11k be constraints defined point-wise in space (they only depend on the current states and inputs, and not on past values of these variables).

In addition to the constraints designed to improve process performance in the presence of stiction, the Lyapunov-based constraints in Eqs. 5.11l-5.11m have been added to prove feasibility and closed-loop stability of the proposed MPC formulation. These constraints define two modes of operation of the MPC. When the constraint of Eq. 5.11l is active, Mode 1 of the MPC is active

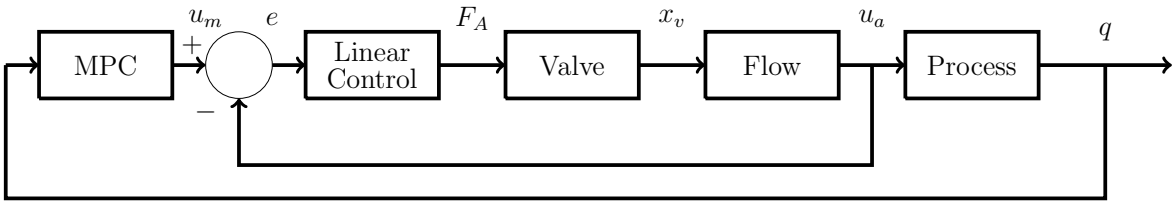

Figure 5.3: Proposed architecture for MPC incorporating valve dynamics and actuation magnitude constraints for stiction compensation. For simplicity of presentation, the only force on the valve presented is one which is calculated by the linear controller.

and the process performance is optimized to the maximum extent possible within a subset of the stability region, $\Omega_{\rho_e} \subset \Omega_\rho$, which is defined such that if the MPC is initialized at time t_k from any state within Ω_{ρ_e}, the state at time t_{k+1} is still within Ω_ρ. This Mode 1 constraint is specific to Lyapunov-based economic model predictive control,[79] the goal of which is to maximize the process profit to the maximum extent possible using dynamic operation in Mode 1. In Mode 2, the contractive constraint in Eq. 5.11m drives the state to a neighborhood of the origin. Mode 1 and Mode 2 are activated by either the location of the measured state in state-space, or by the current time (t' denotes the time at which process operation switches from Mode 1 to Mode 2). For tracking MPC, the Mode 2 constraint would be active for all times (i.e., $t' = 0$ and the MPC formulation in Eq. 5.11 is like that proposed as Lyapunov-based model predictive control (LMPC) in[36]).

Remark 5.5. *Due to the generality of the proposed MPC formulation, it is possible for a different stabilizing formulation, such as a terminal cost with a terminal region constraint,[13,105] a terminal state constraint,[47,67] or an infinite horizon,[84] to be used in place of Eqs. 5.11l-5.11m (see also[63,106] and the references therein for more information on various types of constraints that can be used in MPC and EMPC). However, due to the ease of establishing the state-space points from which feasibility and closed-loop stability are guaranteed using Eqs. 5.11l-5.11m and the fact that these properties can be proven for the process under the MPC with those constraints without any assumptions on the cost function structure, we choose to establish feasibility and stability of the proposed method in this chapter by using the stability constraints in Eqs. 5.11l-5.11m.*

Remark 5.6. *In a practical setting, the parameters of the stiction model may change with time as stiction worsens. Thus, it may be desirable to re-identify the parameters of the stiction model at various points in time. In addition, it may be necessary to re-tune[14,98,146] the linear controller of the valve as the valve dynamics change due to stiction. Therefore, an assumption of the proposed design is that one can successfully detect and identify stiction and re-tune the controller as desired.*

Remark 5.7. *As commonly noted in the literature, the negative impact of valve stiction cannot be fully remedied unless valve maintenance is performed.[73] However, there are circumstances in which maintenance is not performed on sticky valves until a planned process shutdown, which is often infrequent (every 6 months to 3 years).[135] If MPC is used to control a process-valve system for stiction compensation purposes, it may also aid in allowing valve maintenance to be performed before a planned shutdown through an actuator preventive maintenance strategy using MPC like that developed in.[96]*

5.3.2 Analysis of MPC Formulation

The power of the proposed stiction compensation strategy lies in its flexibility. Because of the incorporation of the stiction dynamics in the MPC, a control engineer can adjust the cost function and the constraints to minimize the negative impacts of stiction. To clarify this point, we present a number of remarks that exemplify how the proposed MPC could be modified to counter various control loop issues due to stiction. Though the control architecture considered in this chapter is that from Fig. 5.3, we will address the case that the flow controller is not present in Remarks 5.9-5.10 below for completeness.

Remark 5.8. *The linear controller for the valve can be used to speed the response of the valve to a valve output flow rate set-point change, even a valve output flow rate set-point change in the direction opposite to previous set-point changes (i.e., a set-point change that causes the valve to stick). If the controller is aggressive, it can cause the control input to the valve to quickly overcome the deadband, reducing set-point tracking issues arising from stiction (if the aggressiveness does not cause oscillations).*

Remark 5.9. *The MPC cost function could include a penalty on deviations of the valve output from a target value throughout time (e.g., a quadratic objective function). Because the MPC incorporates a model of the stiction dynamics and thus is aware that the valve will slip and by how much, this penalty would encourage the MPC to choose valve output flow rate set-points that bring the valve output to or close to the target (this was shown to be beneficial, for example, in the compensated case of Fig. 3.4).*

Remark 5.10. *If the proposed method is implemented with an economics-based objective function, the proposed method could be used to choose valve output flow rate set-points that are more economically optimal than if the MPC was unaware of the process dynamics. Even if the response is not that of the ideal case with no valve dynamics, the sequence of valve output flow rate set-points would still be the most economically optimal method for operating the system (given limitations such as the sampling period and prediction horizon length in addition to the valve dynamics) because the MPC included the effect of the valve dynamics in its determination of the optimal valve output flow rate set-points.*

Remark 5.11. *Some stiction compensation methods such as constant reinforcement and the knocker that add signals to the output of the controller being sent to the valve are cited as sources of valve wear and tear, which makes these methods short-term solutions.*[39,86] *Several stiction compensation strategies have been developed to address this, including an optimization-based stiction compensation method that minimizes a cost function including a term representing the degree of movement of the valve to seek compensating signals to add to the valve controller output that will minimize the valve movement.*[135] *The MPC stiction compensation method proposed in this chapter is flexible and could include similar penalties in the objective function (in addition to input rate of change constraints) if valve wear and tear is a concern. This flexibility to add penalties on valve variability to the objective function may be particularly beneficial in cases where it may not be obvious what value of ε in Eq. 5.11 provides an acceptable level of variability of the valve.*

Remark 5.12. *A major contribution of the proposed method is that it accounts for changes in the range of valve outputs that can be achieved with the given actuation energy as stiction worsens.*

MPC strategies previously developed for stiction compensation have not explicitly addressed the change in constraints that results as the valve output-actuation magnitude dynamics change, though[45,152,153] address valve output saturation. The proposed method of this chapter, however, introduces actuation magnitude constraints in Eqs. 5.11f-5.11g to constrain the valve actuation magnitude and prevent the process-valve model from predicting non-physical values for such forces. A benefit of these constraints is that if they are based on hard limitations of the valve actuators, they may not need to be updated over time even if the valve model parameters are updated due to changes, for example, in the friction force characteristics. This will be further clarified in Section 5.4.

5.3.3 Feasibility and Stability

In this section, we prove that the optimization problem of Eq. 5.11 is feasible for all times and that the closed-loop system of Eq. 5.4 is stable under the MPC of Eq. 5.11 when a sufficiently small sampling period is used. We first re-state two propositions from Chapter 2 in terms of the process-valve states and the notation of this chapter (e.g., Eqs. 5.7-5.9) to define parameters and equations that will be used in the feasibility and stability proof. We then state the results of Theorem 2.1 as a proposition in terms of the notation of this chapter to motivate the introduction of a constraint that we will impose on Δ in the feasibility and stability proof. Finally, we combine the results of the propositions to prove feasibility and stability of the proposed MPC.

Proposition 5.1. *(c.f.[79,110]) Consider the systems*

$$\dot{q}_a(t) = f_q(q_a(t), u_{m,1}(t), ..., u_{m,m}(t), w(t)) \tag{5.12a}$$

$$\dot{q}_b(t) = f_q(q_b(t), u_{m,1}(t), ..., u_{m,m}(t), 0) \tag{5.12b}$$

with initial states $q_a(t_0) = q_b(t_0) \in \Omega_\rho$. There exists a $\mathcal{K}$ function $\bar{f}_W(\cdot)$ such that

$$|q_a(t) - q_b(t)| \leq \bar{f}_W(t - t_0) \tag{5.13}$$

for all $q_a(t), q_b(t) \in \Omega_\rho$ and all $w(t) \in W$ with

$$\bar{f}_W(\tau) = \frac{\bar{L}_w \theta}{\bar{L}_q}(e^{\bar{L}_q \tau} - 1) \tag{5.14}$$

Proposition 5.2. *(c.f.[79,110]) Consider the Lyapunov function $V(\cdot)$ of the nominal system of Eq. 5.4 under the controller $h_v(q)$. There exists a quadratic function $\bar{f}_V(\cdot)$ such that*

$$V(q) \leq V(q') + \bar{f}_V(|q - q'|) \tag{5.15}$$

for all $q, q' \in \Omega_\rho$ with

$$\bar{f}_V(s) = \alpha_4(\alpha_1^{-1}(\rho))s + \bar{M}_v s^2 \tag{5.16}$$

where $\bar{M}_v$ is a positive constant.

Proposition 5.3. *Consider the system of Eq. 5.4 in closed-loop with the MPC of Eq. 5.11. If a Lyapunov-based controller $h_v(q)$ that meets the assumptions of Eqs. 5.5 and 5.6 exists, then the constraints of Eqs. 5.11h-5.11i ensure that for a given $\varepsilon_{desired}$,*

$$|u_{m,i}(t_k) - u^*_{m,i}(t_{k-1}|t_{k-1})| \leq \varepsilon_{desired} \tag{5.17}$$

and

$$|u_{m,i}(t_j) - u_{m,i}(t_{j-1})| \leq \varepsilon_{desired},\ j = k+1, \ldots, k+N-1 \tag{5.18}$$

when $\Delta < \Delta_1$ and ε in Eqs. 5.11h-5.11i are chosen such that

$$2\varepsilon + L_v \bar{M} \Delta \leq \varepsilon_{desired} \tag{5.19}$$

Proof. The proof follows that of Theorem 2.1. Specifically, from the bound in Eq. 5.10 and the Lipschitz continuity of $h_{v,i}(q)$ in Eq. 5.6,

$$|h_{v,i}(q(t_k)) - h_{v,i}(q(t_{k-1}))| \leq L_v |q(t_k) - q(t_{k-1})| \leq L_v \bar{M} \Delta \tag{5.20}$$

and

$$|h_{v,i}(\tilde{q}(t_j)) - h_{v,i}(\tilde{q}(t_{j-1}))| \leq L_v|\tilde{q}(t_j) - \tilde{q}(t_{j-1})| \leq L_v\bar{M}\Delta \tag{5.21}$$

for $q(t_k), \tilde{q}(t_j), \tilde{q}(t_{j-1}) \in \Omega_\rho$ for $j = k+1, ..., k+N-1$ and a sufficiently small $\Delta < \Delta_1$ that maintains $q(t)$ within Ω_ρ at all times for the MPC of Eq. 5.11 (the conditions under which Δ_1 exists such that $\Delta < \Delta_1$ maintains $q(t) \in \Omega_\rho$ when $q(t_0) \in \Omega_\rho$ for the system of Eq. 5.4 under the MPC of Eq. 5.11 are given in the theorem below). Combining this with Eqs. 5.11h-5.11i and following steps similar to those in Eqs. 2.27-2.28, it is shown that

$$|u_{m,i}(t_k) - u^*_{m,i}(t_{k-1}|t_{k-1})| \leq 2\varepsilon + L_v\bar{M}\Delta \tag{5.22}$$

and

$$|u_{m,i}(t_j) - u_{m,i}(t_{j-1})| \leq 2\varepsilon + L_v\bar{M}\Delta \tag{5.23}$$

for $j = k+1, ..., k+N-1$, and $i = 1, \ldots, m$. Thus, the desired constraints in Eqs. 5.17 and 5.18 are satisfied when $2\varepsilon + L_v\bar{M}\Delta \leq \varepsilon_{desired}$. □

Theorem 5.1. *Consider the system of Eq. 5.4 in closed-loop under the MPC design of Eq. 5.11 based on a controller $h_v(q)$ that satisfies the conditions of Eqs. 5.5-5.6 and assume that $u^*_i(t_0|t_0) = h_i(x(t_0))$, $i = 1, ..., m$. Let $\tilde{\varepsilon}_w > 0$, $\Delta > 0$, $\theta > 0$, $\rho > \rho_e \geq \tilde{\rho}_s > 0$ satisfy*

$$\rho_e \leq \rho - \bar{f}_V(\bar{f}_W(\Delta)) \tag{5.24}$$

$$-\alpha_3(\alpha_2^{-1}(\tilde{\rho}_s)) + \bar{L}'_q\bar{M}\Delta + \bar{L}'_w\theta \leq \frac{-\tilde{\varepsilon}_w}{\Delta} \tag{5.25}$$

and

$$2\varepsilon + L_v\bar{M}\Delta \leq \varepsilon_{desired} \tag{5.26}$$

If $q(t_0) \in \Omega_\rho$, $\tilde{\rho}_s \leq \tilde{\rho}_{\min}$, and $N \geq 1$ where

$$\tilde{\rho}_{\min} = \max\{V(\bar{q}(t+\Delta)) \ : \ V(\bar{q}(t)) \leq \tilde{\rho}_s\} \tag{5.27}$$

then the state $q(t)$ of the closed-loop system is always bounded in Ω_ρ and is ultimately bounded in $\Omega_{\tilde{\rho}_{\min}}$.

Proof. Feasibility of the proposed formulation will be proven by showing that when the Lyapunov-based controller $h_v(q)$ exists that satisfies the constraints in Eqs. 5.5-5.6, it is a feasible solution for the MPC optimization problem at all times if $q(t) \in \Omega_\rho$ for all times. The proof of closed-loop stability of the proposed method follows that in[79] and will not be repeated here, but it shows that the proposed MPC of Eq. 5.11 can maintain the states within the region Ω_ρ for all times if a sampling period $\Delta < \Delta_1$ is used, where Δ_1 is the largest value of Δ that causes Eqs. 5.24-5.25 and 5.27 to be satisfied. The proof in[79] also shows that if $t_k \geq t'$, the state is driven into $\Omega_{\tilde{\rho}_{\min}}$ (defined by Eq. 5.27 where $\bar{q}(t)$ represents the state of Eq. 5.4 under any sample-and-hold control actions $u_{m,i} \in U_{m,i}$, $i = 1,\ldots,m$, which is similar to the definition used for $\bar{x}$ in Section 2.2.4). Closed-loop stability of a process under the proposed MPC follows from[79] with the only bounds on Δ being those coming from Eqs. 5.24-5.25 and 5.27. In this theorem, in order to obtain the desired rates of change in Eqs. 5.17-5.18, we also add the requirement from Proposition 5.3 that Eq. 5.26 must be satisfied as well; however, this is not required for closed-loop stability to be proven.

The feasibility of the state, input, Lyapunov-based, and input rate of change constraints will be addressed when $u_{m,i}(t_k) = h_{v,i}(q(t_k))$ and $u_{m,i}(t_j) = h_{v,i}(\tilde{q}(t_j))$, $j = k+1,...,k+N-1$, $i = 1,\ldots,m$, and $q(t_k), \tilde{q}(t) \in \Omega_\rho$. Due to the definition of the stability region Ω_ρ, which included the requirement that it be a region within which all state constraints are satisfied, the state constraint in Eq. 5.11d is satisfied for all states within Ω_ρ. Also, by Eq. 5.5d, $u_{m,i}(t_k) = h_{v,i}(q(t_k))$ and $u_{m,i}(t_j) = h_{v,i}(\tilde{q}(t_j))$, $j = k+1,...,k+N-1$, $i = 1,\ldots,m$, satisfy the input constraints in Eqs. 5.11e-5.11g and 5.11j-5.11k. Furthermore, by design of the Lyapunov-based constraints and when $\Delta < \Delta_1$, $u_{m,i}(t_k) = h_{v,i}(q(t_k))$ and $u_{m,i}(t_j) = h_{v,i}(\tilde{q}(t_j))$, $j = k+1,...,k+N-1$, $i = 1,\ldots,m$, satisfy the Lyapunov-based constraints in Eqs. 5.11l-5.11m. This is because Eq. 5.11m is trivially satisfied by $u_{m,i}(t_k) = h_{v,i}(q(t_k))$ and $u_{m,i}(t_j) = h_{v,i}(\tilde{q}(t_j))$, $j = k+1,...,k+N-1$, $i = 1,\ldots,m$, and when Eqs. 5.25 and 5.27 are met, it can be shown[79,112] that $u_{m,i}(t_k) = h_{v,i}(q(t_k))$ and

$u_{m,i}(t_j) = h_{v,i}(\tilde{q}(t_j))$, $j = k+1,...,k+N-1$, $i = 1,\ldots,m$, will cause $V(\tilde{q}(t)) \leq V(q(t_k))$ for $t \in [t_k, t_{k+1})$ such that Eq. 5.11l is therefore satisfied by those control actions. Finally, by design of the input rate of change constraints in Eqs. 5.11h-5.11i with respect to the Lyapunov-based control law, $u_{m,i}(t_k) = h_{v,i}(q(t_k))$ and $u_{m,i}(t_j) = h_{v,i}(\tilde{q}(t_j))$, $j = k+1,...,k+N-1$, $i = 1,\ldots,m$, also satisfy those equations. Thus, feasibility of the proposed MPC at each sampling time is ensured. □

5.4 Application to a Chemical Process Example

In this section, we present a case study that shows how an MPC incorporating stiction dynamics and actuation magnitue constraints may be designed for a specific chemical process example. For this study, we focus on EMPC because EMPC can dictate a dynamic operating policy, which has interesting implications for the constraints that need to be added to the EMPC for effective stiction compensation in this example, and thus helps to illustrate the considerations that may go into the design of the MPC in Eq. 5.11 to ensure that it adequately prevents the negative effects of stiction.

5.4.1 Dynamic Model Development

We first define the valve and process models that will be used in this example.

5.4.1.1 Nonlinear Process Model

We consider control of the catalytic oxidation of ethylene in a continuous stirred tank reactor (CSTR) for which the reactions in Eqs. 2.39-2.41 occur. The dimensionless material and energy balances for this process from,[122] which use reaction rate equations from,[12] form the following nonlinear process model of the system, which has the form of Eq. 3.35 but with a single input u_a as follows:

$$\frac{dx_1}{dt} = u_a(1 - x_1x_4) \tag{5.28a}$$

$$\frac{dx_2}{dt} = u_a(C_e - x_2x_4) - A_1 exp(\frac{\gamma_1}{x_4})(x_2x_4)^{0.5} - A_2 exp(\frac{\gamma_2}{x_4})(x_2x_4)^{0.25} \tag{5.28b}$$

$$\frac{dx_3}{dt} = -u_a x_3 x_4 + A_1 exp(\frac{\gamma_1}{x_4})(x_2 x_4)^{0.5} - A_3 exp(\frac{\gamma_3}{x_4})(x_3 x_4)^{0.5} \tag{5.28c}$$

$$\begin{aligned}\frac{dx_4}{dt} = \frac{1}{x_1}(u_a(1-x_4) + B_1 exp(\frac{\gamma_1}{x_4})(x_2 x_4)^{0.5} + B_2 exp(\frac{\gamma_2}{x_4})(x_2 x_4)^{0.25} + \\ B_3 exp(\frac{\gamma_3}{x_4})(x_3 x_4)^{0.5} - B_4(x_4 - T_c))\end{aligned} \tag{5.28d}$$

where x_1, x_2, x_3, and x_4 are the dimensionless quantities from Section 2.3.1.4 (the gas density in the reactor, the reactor ethylene and ethylene oxide concentrations, and the reactor temperature). The process input (valve output) u_a is the dimensionless volumetric flow rate of the feed. The dimensionless concentration of ethylene in the feed (C_e) and the dimensionless coolant temperature T_c are set to their values corresponding to an open-loop asymptotically stable steady-state of the reactor at $[x_{1s}\ x_{2s}\ x_{3s}\ x_{4s}] = [0.998\ 0.424\ 0.032\ 1.002]$ when $u_{as} = 0.35$, $C_e = 0.5$, and $T_c = 1.0$). The other parameters in Eq. 5.28 are taken from[122] and are noted in Table 2.1.

5.4.1.2 Nonlinear Valve Model

In this section, we describe the model of the valve dynamics for the valve that adjusts u_a. Due to their prevalence in industry, we model a pneumatic spring-diaphragm sliding-stem globe valve using the values for the valve parameters from,[72] with the exception that the time units of all parameters are changed to the dimensionless time unit t_d for consistency with the time units in the process model of Eq. 5.28, and are given in Table 3.1 (but with s replaced by t_d). The valve is modeled as a pressure-to-close valve with no pressure initially applied by the pneumatic actuation at the fully open valve position. The valve stem can travel a maximum of 0.1016 m from the fully open valve position (which corresponds to the flow rate $u_a = 0.7042$) to the fully closed position (with corresponding flow rate $u_a = 0$). Figures 5.4-5.5 depict the fully open and fully closed valve positions; however, these are not detailed drawings of the valve interior and are meant only for clarification of how the stem's location is related to the valve opening. In accordance with,[33,72,91] we assume that the differential equations in Eqs. 3.27-3.28 are sufficient for describing the stem position and velocity for the valve adjusting u_a (i.e., as in,[33,72,91] we neglect additional forces known to be present in sliding-stem globe valves, such as the additional force required to

move the valve plug into the seat and the force due to the pressure drop of the fluid as it moves through the valve). The actuator applies a pressure P determined from the linear controller for the valve to the valve diaphragm, and a spring opposes the movement of the diaphragm when pressure is applied. We associate the fully open position of the valve with the equilibrium spring position $x_v = 0\ m$, and we associate the fully closed valve position with the maximum stem position $x_v = x_{v,\max} = 0.1016\ m$.

To determine the value of the friction force F_f in Eq. 3.28 at each time instant, we use the LuGre[26] friction model due to its relative simplicity (it is a dynamic model with only one differential equation) and ability to qualitatively describe many of the effects of friction (e.g., presliding displacement, hysteresis in the friction force with velocity changes in the sliding regime, and a lowering of the force required for breakaway as the applied force increases more quickly;[26] also see[72] for information on the ability of a valve simulated using the LuGre model and the valve parameters in this paper to qualitatively exhibit the behavior expected when subjected to valve tests developed by the Instrumentation, Systems, and Automation (ISA) Society). The LuGre model describes friction using the differential and algebraic equations in Eq. 3.29 and:[26]

$$\frac{dz_f}{dt} = v_v - \frac{|v_v|}{g(v_v)} z_f \tag{5.29}$$

where σ_0, σ_1, and σ_2 are model parameters, z_f is an internal state variable of the friction model, and $g(v_v)$ is a nonlinear function of the valve stem velocity. Though the LuGre model is fundamentally a set of equations that can dynamically capture the effects of friction through the introduction of an appropriately formulated state variable z_f, a somewhat physical interpretation of z_f arises if one imagines asperity junctions to behave like contacting bristles that bend against one another until they slip, with stiffness σ_0 and damping coefficient σ_1, and z_f representing the average deflection of the bristles. The last term of the friction force is for the viscous friction, with viscous friction coefficient σ_2. The function $g(v_v)$ aids in defining the Stribeck effect and the friction-velocity

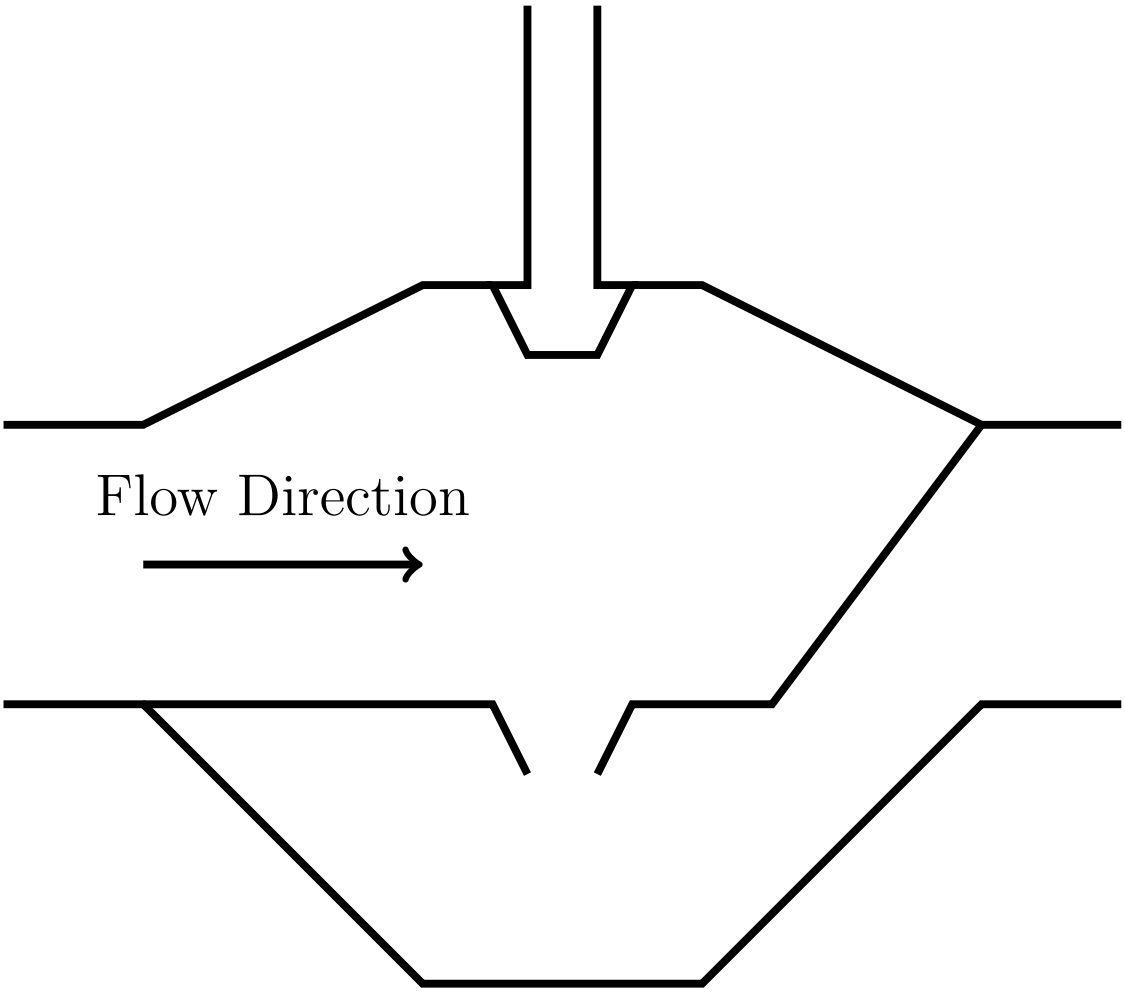

Figure 5.4: Schematic depicting a pressure-to-close pneumatic sliding-stem globe valve in the open position. In this chapter, it is considered that no pressure is being applied to the valve initially when it is in this position, and the stem position is considered to be at $x_v = 0$ m from the valve's equilibrium, fully open position.

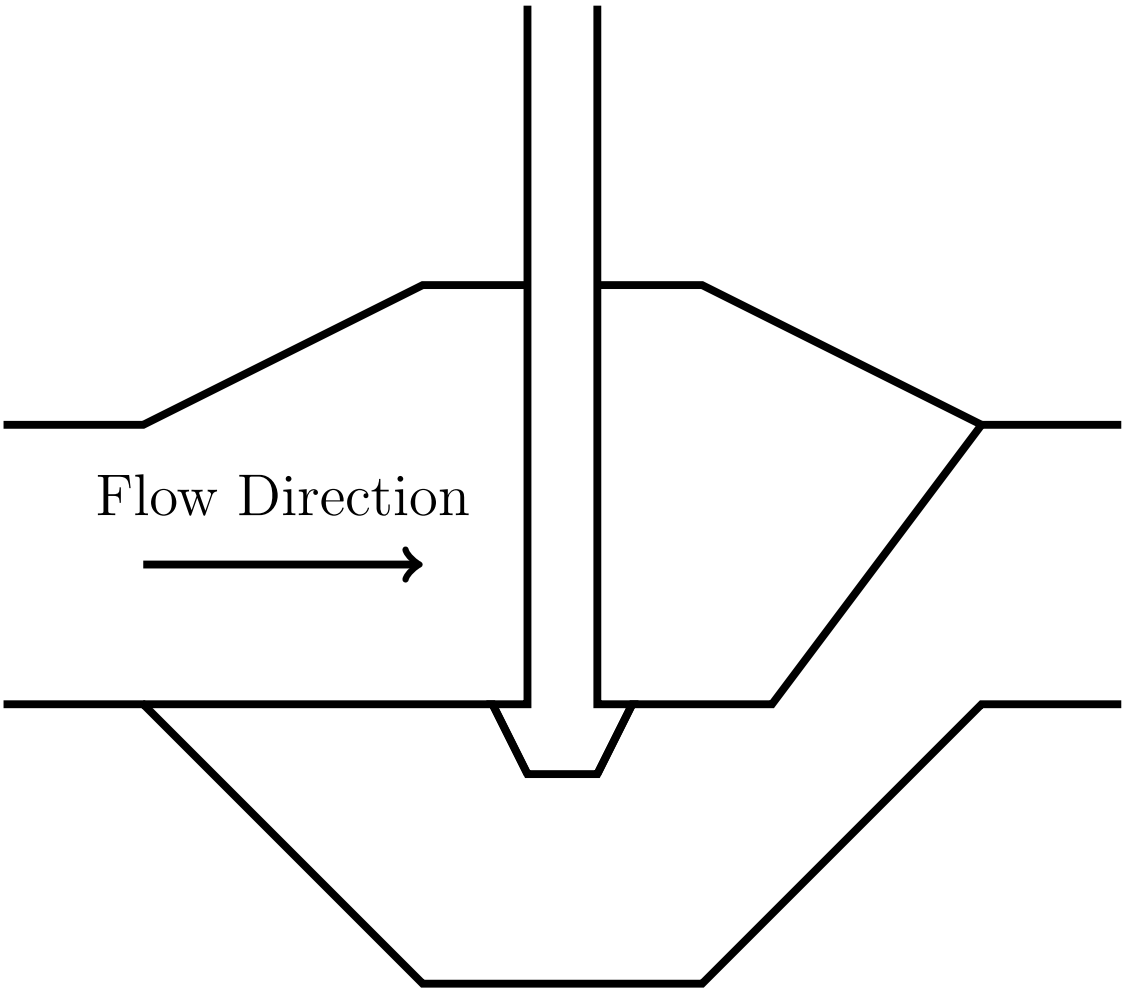

Figure 5.5: Schematic depicting a pressure-to-close pneumatic sliding-stem globe valve in the closed position. In this chapter, the stem position for the closed valve is $x_{v,\max} = 0.1016\ m$ from the valve's equilibrium, fully open position, and is maintained in this position by the application of pressure to the valve diaphragm.

characteristics at constant velocity, and for consistency with [26,72] will be taken to be:

$$g(v_v) = \frac{1}{\sigma_0}\left[F_C + (F_S - F_C)e^{-(v_v/v_s)^2}\right] \tag{5.30}$$

where F_C is the Coulomb friction coefficient, F_S is the static friction coefficient, and v_s is the Stribeck velocity. The parameters of the friction model in Eqs. 3.29 and 5.29-5.30 are defined in Table 3.1. The notation in these equations follows that in Eqs. 3.18-3.19.

Remark 5.13. *The LuGre model is used in this example because its simplicity makes it more suitable for use in MPC than some of the more complex stiction models. Despite its relative simplicity and ability to qualitatively represent a number of friction effects, the LuGre model is neither the most accurate nor the most current friction model available (see, for example,[48] for a criticism of its ability to model stiction when an oscillating force with magnitude less than the Coulomb friction level is applied after breakaway, and[140] for a criticism of some of its hysteresis features in presliding, as well as [1,94,95] for more detailed friction models). For the purposes of the example in this chapter, which demonstrates the general effects that stiction may have on a chemical process and how the incorporation of the dynamics in a model predictive controller can reduce the undesirable effects of stiction, a stiction model that shows qualitatively correct behavior for many scenarios is sufficient.*

5.4.1.3 Relating Valve Position and Valve Output

We assume that the valve has a linear installed characteristic[38] so that the valve output is linearly related to the stem position in the sense that Eq. 3.31 holds.

Remark 5.14. *The assumption of a linear installed characteristic was made for simplicity of presentation for this example. A variety of other valve characteristics are possible (for example, an equal percentage or quick opening inherent valve characteristic, or an installed valve characteristic affected by the pressure drop across the valve);[21,38,101,130] however, the focus of this example is the valve behavior in the presence of stiction, rather than the relationship between the*

flow and the stem position, so the assumption of a linear installed valve characteristic is considered sufficient. For more information on inherent valve characteristics and how valve installation may affect these characteristics, see.[21,38,130]

5.4.1.4 Linear Controller Model

In this example, we use a PI controller to regulate the valve output u_a to the set-point u_m set by the EMPC. The PI controller determines the pressure that the valve pneumatic actuation element should apply according to the following equations, which have the form given in Eq. 5.2:

$$P = P_s + 6894.76\left(K_c\left(\frac{u_m - u_a}{u_{a,\max}}\right) + \frac{K_c}{\tau_I}\zeta\right) \tag{5.31}$$

$$\frac{d\zeta}{dt} = \left(\frac{u_m - u_a}{u_{a,\max}}\right) \tag{5.32}$$

where $K_c = -12$ and $\tau_I = 0.01$ are the controller gain and integral time, chosen for a fast valve response to a set-point change even with the deadband of the stiction model used in this example. P_s is the steady-state value of the control signal. To ensure that P changes in the correct direction and to prevent the integral error from the previous set-point from impacting the approach to a new set-point once the set-point is changed, we set P_s to the last applied value of P and the value of ζ (where ζ denotes the internal state of the PI controller in this example) to 0 at a set-point change. Combining Eqs. 3.27-3.29, 3.31, and 5.28-5.32, we obtain a combined process-valve dynamic model as in Eq. 5.4, with state $q = [x_1\ x_2\ x_3\ x_4\ x_v\ v_v\ z_f\ \zeta]^T$ and input u_m, which we define as $\dot{q} = f_q(x_1, x_2, x_3, x_4, x_v, v_v, z_f, \zeta, u_m)$.

5.4.2 Motivation for Actuation Magnitude Constraints

When the process of Eqs. 3.27-3.29, 3.31, and 5.28-5.32 is controlled using EMPC, the EMPC will output a set-point u_m for the valve that controls u_a for each sampling period. The set-point u_m will be used in Eqs. 5.31-5.32 to determine the pressure that should be applied to the valve

to bring it to the requested set-point. Because the dynamics between u_a, u_m, and P are critical to the EMPC's choice of the value of its optimization variable u_m, it is necessary that the dynamics be understood and appropriately constrained to avoid non-physical situations. This concept will be made clear in this section, which will show that the effect of stiction on the valve dynamics requires the introduction of additional constraints to the EMPC with the form of Eqs. 5.11f-5.11g.

To demonstrate the manner in which stiction changes the dynamics, we first examine the relationship between u_m and P for the open-loop valve in the presence of low stiction and in the presence of significant stiction (the open-loop valve is considered because the parameters K_c and τ_I in Eqs. 5.31-5.32 for the closed-loop valve can be adjusted for both the low stiction and significant stiction cases to cause the closed-loop response of the valve output to a set-point change to be rapid). A valve with low stiction can be modeled using the parameters listed in Table 3.1, with the exception that the values of F_C and F_S in the table are both replaced by 44.48 $kg \cdot m/t_d^2$. This low stiction valve will be referred to as having "vendor" parameters, in keeping with the terminology used in.[72] The valve parameters listed in Table 3.1 are referred to as "nominal" valve parameters.[72]

To determine a relationship between u_m and P that can be used to determine the pressure to apply to the open-loop valve to bring u_a to u_m, we start by determining the steady-state relationship between the valve output and the applied pressure for the vendor valve. This relationship is determined by ramping the pressure applied to the valve up and down between 0 $kg/m \cdot t_d^2$ and 82737 $kg/m \cdot t_d^2$ in increments of 69 $kg/m \cdot t_d^2$ every 0.5 t_d and recording the value of u_a at the end of every 0.5 t_d, using the Explicit Euler numerical integration method with an integration time step of 10^{-6} t_d. The resulting plot of the steady-state value of u_a versus input pressure is almost linear, as shown in Fig. 5.6. If we assume that $u_m \approx u_a$ for the valve because stiction is low so the valve output should track its set-point well, we obtain the following relationship between u_m and P for the vendor valve using a least-squares optimization on the vendor valve data (neglecting the initial transient) shown in Fig. 5.6:

$$u_m = -\frac{0.05864}{6894.76} * P + 0.70391 \tag{5.33}$$

We now assume that we have a series of desired set-points u_m that we would like to achieve for

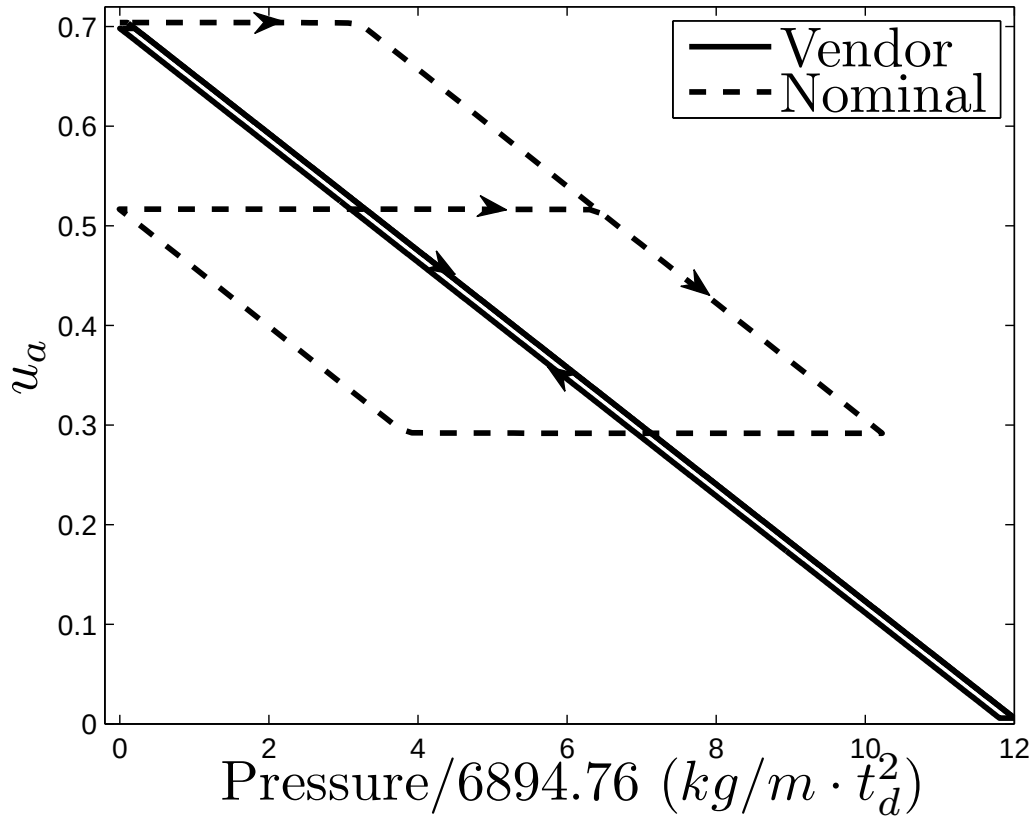

Figure 5.6: Comparison of steady-state relationship between u_a and P for the vendor and nominal valve parameters.

the open-loop valve with significant stiction (nominal valve). We investigate whether the $u_m - P$ relationship developed for the vendor valve is applicable for the nominal valve by developing the $u_a - P$ relationship when the pressure value calculated from Eq. 5.33 is applied to the nominal valve to attempt to achieve the desired value of u_m. Accordingly, we ramp the set-point u_m up and down between 0.1042 and 0.7042 in increments of 0.01 every 0.5 t_d and record the value of u_a at the end of every 0.5 t_d, again using the Explicit Euler numerical integration method with an integration time step of 10^{-6} t_d (the Explicit Euler numerical integration method with an integration time step of 10^{-6} t_d was used for all simulations of the nominal valve in Section 5.4.2). The resulting $u_a - P$ relationship can no longer be described as one linear relation, but two that depend on whether the pressure is being increased or decreased, and the deadband at a velocity change is visible in Fig. 5.6. In addition, it can be observed from the figure that because of the effect of stiction on the $u_a - P$ relationship, there are certain flow rates that can be achieved with a positive pressure for the vendor valve that would require a negative pressure for the nominal valve, which is physically not possible to achieve. This is the first hint that to compensate for stiction, additional constraints of the form of Eqs. 5.11f-5.11g will need to be added to the EMPC to prevent physically unrealizable set-points from being requested.

As shown in Fig. 5.6, the linear relationship between u_m and P developed in Eq. 5.33 is not sufficient to control a valve subject to stiction. Further evidence of this comes from ramping the set-point u_m of the nominal open-loop valve up and down between 0.1042 and 0.7042 in increments of 0.01 every sampling period of length $\Delta = 0.2$ t_d and determining the pressure to apply to the valve from Eq. 5.33. The dynamic response (i.e., not steady-state; this is the reason for the step-like quality of the trajectories) of the valve output to these set-point changes is shown in Figs. 5.7-5.8. Fig. 5.7 shows the insufficiency of Eq. 5.33 to determine the pressure value that should be applied to the valve for a desired u_m because it shows that for this sticky valve, u_a does not effectively track u_m (the $u_a - u_m$ plot in Fig. 5.7 is not linear). This is further emphasized in Fig. 5.8, which also shows the deadband when u_m begins to change in the opposite direction to that in which it was changing previously. This demonstrates that a different relationship between u_m and P is needed

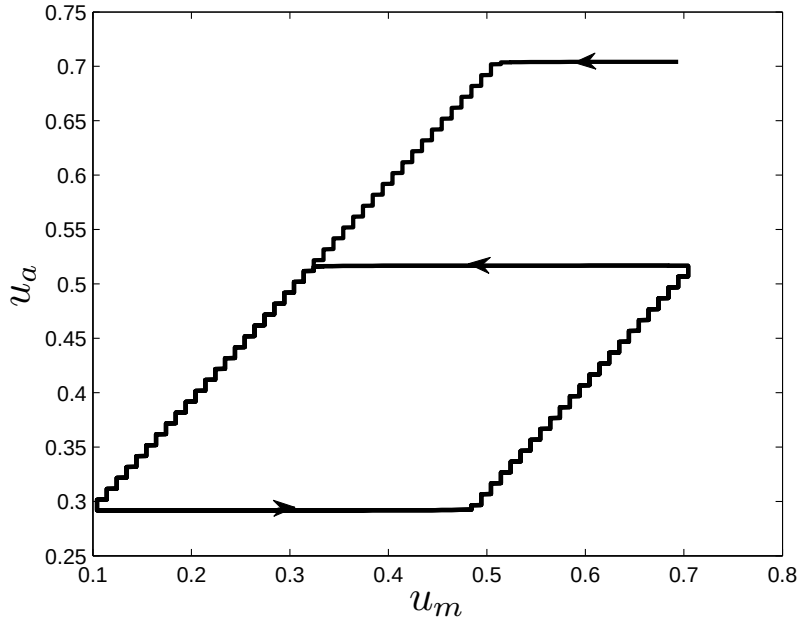

Figure 5.7: Open-loop values of u_a and u_m for the nominal valve.

to control the nominal valve than that provided by Eq. 5.33 to ensure good set-point tracking.

In the proposed method, the linear controller of Eqs. 5.31-5.32 is used to improve the set-point tracking performance of u_a. To demonstrate that this does indeed improve the set-point tracking, we ramp the set-point u_m to the nominal valve in closed-loop with the linear controller in Eqs. 5.31-5.32, again ramping it up and down between 0.1042 and 0.7042 in increments of 0.01 every $\Delta = 0.2\ t_d$. The dynamic response of the valve is shown in Figs. 5.9-5.10 which show that the $u_a - u_m$ relationship is close to linear under the linear controller, and that u_a is able to closely track u_m in time and is quickly able to overcome the deadband caused by stiction. However, despite its benefit in providing good set-point tracking performance, the use of Eqs. 5.31-5.32 does not ensure that the value of P requested will not become negative. This is demonstrated in Figs. 5.11-5.12, which plot the dynamic response of the closed-loop valve to eight set-point changes (u_m = 0.35, 0.2, 0.35, 0.2, 0.3, 0.4, 0.5, and 0.6) each held for $\Delta = 0.2\ t_d$ when initialized from the fully open position (i.e., $u_a = 0.7042$, $P_s = 0\ kg/m \cdot t_d^2$, $x_v = 0\ m$, $v_v = 0\ m/t_d$, $z_f = 0\ m$ initially). The results in Fig. 5.11 again show that the PI control law developed in Eqs. 5.31-5.32 helps the valve to effectively track its set-points even when there is deadband because the direction of the valve stem

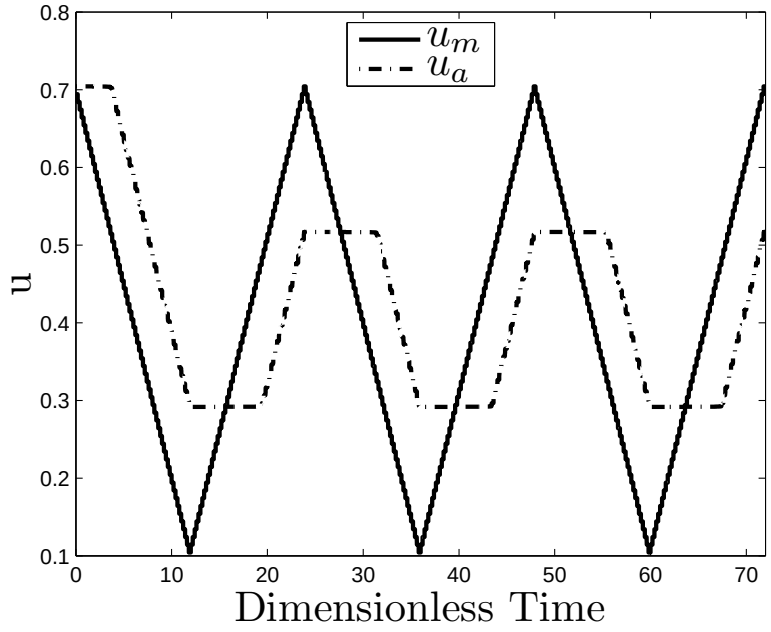

Figure 5.8: Open-loop values of u_a and u_m with time for the nominal valve.

movement changes. However, the results of Fig. 5.12 show that the good set-point tracking can only be achieved when the pressure is able to adjust as necessary, including becoming negative, which is physically impossible. From Figs. 5.11-5.12 it can be deduced that if the pressure is saturated at 0 $kg/m \cdot t_d^2$ when a lower pressure is requested, the valve output would not be able to reach all of the set-points in this simulation. This indicates that when the control law of Eqs. 5.31-5.32 is used, the constraints of the EMPC need to ensure that the pressure does not become negative at the set-points it requests, because the control law itself does not ensure this.

Remark 5.15. *The constraint $\tilde{P} \geq 0$ $kg/m \cdot t_d^2$ (where $\tilde{P}$ signifies the prediction of the pressure from the pneumatic actuation based on the process-valve model) was developed for the EMPC in this section to ensure that the set-points calculated by the EMPC are physically realizable (i.e., that they do not require the pressure to become negative for u_a to meet u_m). Based on the plots presented in this section, other methods for handling this scenario could be considered as well. For example, based on Fig. 5.6, another method for preventing negative pressures for this example may be to decrease the range of allowable values of u_m as stiction worsens such that the allowable values of u_m always correspond to positive pressures. However, it may be difficult to determine*

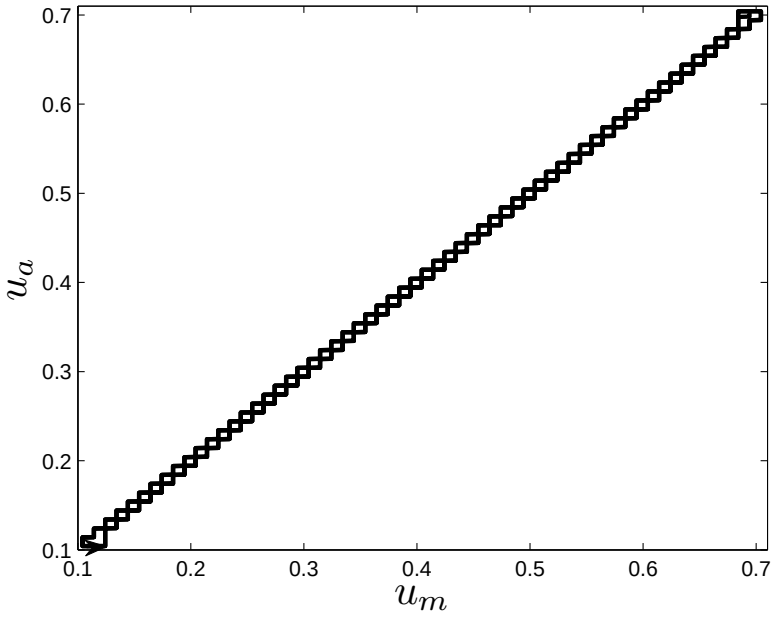

Figure 5.9: Closed-loop values of u_a and u_m for the nominal valve under PI control. The plot depicts that u_a increases with increasing u_m and decreases with decreasing u_m when the value of u_m is changed by 0.01 every Δ. The arrow in the lower left corner of the plot shows the direction in which the increasing and decreasing steps in the plot are traversed.

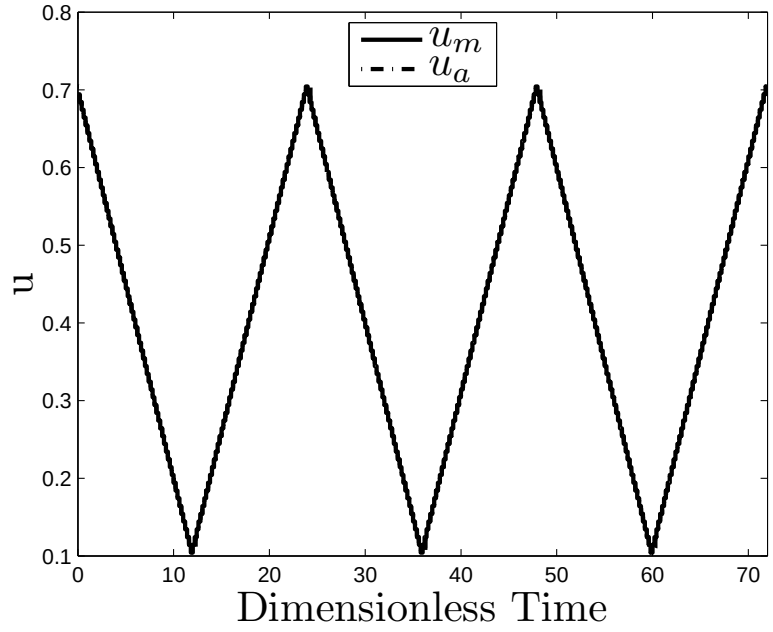

Figure 5.10: Closed-loop values of u_a and u_m with time for the nominal valve under PI control.

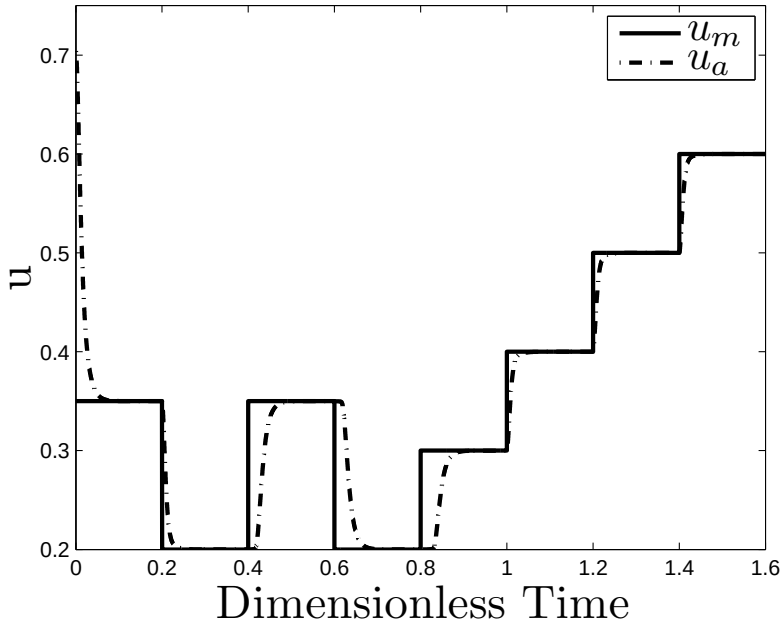

Figure 5.11: Closed-loop values of u_a and u_m with time for the nominal valve under PI control for several set-point changes.

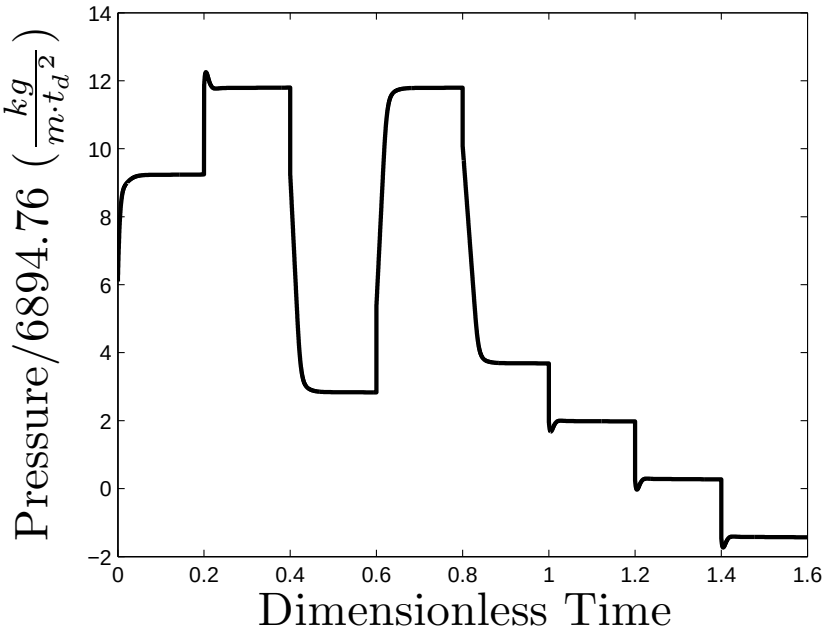

Figure 5.12: Closed-loop values of the pressure with time for the nominal valve under PI control for several set-point changes.

what the new bound on u_m should be without doing an off-line test to generate data like that in Fig. 5.6, and the valve stiction may continue to worsen with time, meaning that new ranges for u_m may need to be determined throughout time. In addition, because the profit from EMPC may be improved by allowing operation over a larger region of state-space, it is not desirable to choose extremely conservative bounds on u_m to avoid the calculation of set-points that would require negative pressures because that may lower profit below that which could be realized. Finally, the steady-state $u_a - P$ data in Fig. 5.6 may not be sufficient for determining an appropriate bound on u_m because it does not show the transient behavior (e.g., under the linear controller, u_a may overshoot u_m before settling to u_m). Motivated by these considerations, for the EMPC in this example, we set the constraint of Eq. 5.11g in our proposed MPC compensation strategy to be a constraint that the actuator pressure must never become negative.

Remark 5.16. *We note that the basic relationships between u_m, u_a, and P presented in this section are well-known; for example, one can find plots similar to those in Figs. 5.6-5.8 in.*[33,72,91] *In addition, it is well-known that control of the valve position may help to improve the response of a valve in the presence of valve nonlinearities (for example,*[91] *suggests a control law to bring the valve position to its set-point in the presence of stiction, and*[135] *states that valve positioners are often able to improve a valve's response if it exhibits deadband). The results in this section are novel, however, because they present the dynamic plots of the open and closed-loop valve responses as an analysis tool useful for the design of an MPC with appropriate constraints for stiction compensation and show how this analysis can be carried out using plots of this type. Furthermore, this discussion is not meant to be applicable only to this example, but to suggest the type of thinking and analysis that may need to go into the design of the proposed MPC for other processes.*

Remark 5.17. *Fig. 5.6 and Fig. 3.6 can be compared. Fig. 5.6 relates u_a and P for a low-stiction valve and a valve experiencing more significant stiction upon increasing and decreasing the pressure applied to the valve stem and holding it for some time upon each increase or decrease; however, only the final values of u_a and P at the end of each hold time are plotted, such that the*

transient response of u_a to the P changes is not shown. Furthermore, the ramping of the pressure in Fig. 5.6 is performed for the valve in open-loop in the sense that no controller is computing the values of the pressure to be applied to the stem, but the pressure is being independently increased and decreased. These features of the plot in Fig. 5.6 contrast with the features of the plot in Fig. 3.6, for which a controller is assumed to be an important part of the dynamic plot (it is the label on the x-axis); therefore, coupling between the controller, process, and valve dynamics for a system for which such a plot is obtained may play a role in the response observed and there is a potential that the plots may look different for the same valve when a different controller or process is present in the loop. For example, a plot of u_a versus P for the level control problem without flow control in Fig. 3.3 would not have a significant moving phase because the controller begins to seek to move the valve stem back in the direction from which it just moved soon after the valve slips.

5.4.3 Proposed MPC Formulation

In this section, we describe the performance of an EMPC formulation meeting the form of our proposed MPC stiction compensation strategy in Eq. 5.11 with the process-valve model of Eqs. 3.27-3.29, 3.31, and 5.28-5.32 and the constraint that $\tilde{P} \geq 0\ kg/m \cdot t_d^2$ at all times.

The control objective is to maximize the yield of the product ethylene oxide. The yield of ethylene oxide between the initial and final times of the plant operation (t_0 and t_f) is defined by Eq. 4.6. However, we assume that the volumetric flow rate of the inlet stream is bounded such that between t_0 and t_f, the integral in Eq. 4.7 holds. Combining Eqs. 4.6-4.7, the objective of the EMPC becomes the maximization of the time integral of the stage cost L_{MPC}, where L_{MPC} is defined as follows:

$$L_{MPC} = u_a(\tau)x_3(\tau)x_4(\tau) \tag{5.34}$$

The input u_a is physically bounded between the flow rates at the maximum and minimum valve openings as follows:

$$u_{a,\min} \leq u_a \leq u_{a,\max} \tag{5.35}$$

with $u_{a,\min} = 0$ (valve fully closed) and $u_{a,\max} = 0.7042$ (valve fully open). The value of u_a is computed using the actuator layer equations in Eqs. 3.27-3.29, 3.31, and 5.29-5.32.

We assume that the only data available to aid in choosing the allowable range of valve set-points u_m that the EMPC calculates is the vendor data in Fig. 5.6. Thus, we assume that the bounds developed for the EMPC include set-points that can only be met with negative pressures by the nominal valve, though they can be met with positive pressures by the vendor valve. The set-points u_m are thus restricted as follows:

$$u_{m,\min} \leq u_m \leq u_{m,\max} \tag{5.36}$$

with $u_{m,\min} = 0.0704$ and $u_{m,\max} = 0.7042$ (the minimum value of u_m is greater than 0 because we assume that we want to avoid fully closing the valve for this process). Physically, the pressure applied to the valve diaphragm cannot drop below 0 $kg/m \cdot t_d^2$.

For this example, the optimization variable u_a does not have a large effect on the process economics. Thus, we emphasize that the choice to use EMPC for this example is primarily driven, as previously noted, by the ability of EMPC to promote time-varying operation such that it computes set-points at the bounds of what is physically possible to maximize the process profit and thus effectively illustrates the advantages of including the constraint on the actuation magnitude (pressure). Furthermore, the profitability of EMPC over steady-state operation for a variety of processes has been well-documented in the literature (see, for example,[79] and[60]), including for the present example when two actuators are used as in,[54] and is not the focus of this chapter. However, it is noted that the process in the absence of stiction or valve dynamics has a steady-state yield of 6.63% over 468 t_d and a yield of 32.22% over 2 t_d when initiated from $[x_{1I}\ x_{2I}\ x_{3I}\ x_{4I}]^T = [0.997\ 1.264\ 0.209\ 1.004]^T$. This shows that for the two operating periods considered in this study, the effect of the transient is very strong because the average steady-state yield is much larger over the 2 t_d considered in this study than it is after a longer time period.

To achieve the above objectives while countering stiction, we develop an EMPC, termed $EMPC-A$, that incorporates actuator dynamics to aid in stiction compensation and maximizes the yield of ethylene oxide subject to the integral material constraint and constraints on the allowable

values of the valve output, valve set-point, and actuator output to prevent non-physical situations. This EMPC solves the following optimization problem:

$$\min_{u_m(t)\in S(\Delta)} \quad -\int_{t_k}^{t_{k+N_k}} \tilde{u}_a(\tau)\tilde{x}_3(\tau)\tilde{x}_4(\tau)\,d\tau \tag{5.37a}$$

$$\text{s.t.} \quad \dot{\tilde{q}}(t) = f_q(\tilde{q}(t), u_m(t)) \tag{5.37b}$$

$$\tilde{q}(t_k) = q(t_k) \tag{5.37c}$$

$$0 \leq \tilde{u}_a(t) \leq 0.7042, \forall t \in [t_k, t_{k+N}] \tag{5.37d}$$

$$0.0704 \leq u_m(t) \leq 0.7042, \forall t \in [t_k, t_{k+N}) \tag{5.37e}$$

$$\tilde{P}(t) \geq 0, \forall t \in [t_k, t_{k+N}] \tag{5.37f}$$

$$\int_{t_k}^{t_{k+N_k}} \tilde{u}_a(\tau)d\tau + \int_{(j-1)t_p}^{t_k} u_a^*(\tau)d\tau = \frac{0.175 t_p}{C_e} \tag{5.37g}$$

where the cost function in Eq. 5.37a represents the total yield of ethylene oxide throughout the prediction horizon when the material constraint is met, and Eq. 5.37g is the method for implementing the integral material constraint by constraining the value of u_a to meet the material constraint in each operating period. Eq. 5.37g states that the time-average value of the sum of the predicted valve output $\tilde{u}_a$ plus the previously applied valve outputs u_a^* must be no greater than $\frac{0.175}{C_e}$ over the $j-th$ operating period ($j = 1, 2, ...$). A shrinking prediction horizon is used, such that the prediction horizon $N_k = 5$ at the beginning of an operating period of length $t_p = 1\ t_d$ ($\Delta = 0.2\ t_d$) but is decremented by 1 at each subsequent sampling time in the operating period. The use of this shrinking horizon allows the integral material constraint of Eq. 4.7 to be implemented in Eq. 5.37g. The state constraints in Eqs. 5.37d and 5.37f were enforced every two integration steps. Because this process has an asymptotically stable steady-state and no closed-loop stability issues were encountered during the simulations, the Lyapunov-based constraints of Eqs. 5.11l-5.11m were not considered. The dynamic equation in Eq. 5.37b was integrated within the EMPC using the Explicit Euler numerical integration method with an integration step of $h_A = 10^{-6}\ t_d$. Centered finite difference approximations of derivatives required for the solution of the optimization problem

were obtained by perturbing the optimization variables by 10^{-6}.

For comparison with $EMPC-A$, we also introduce an EMPC that does not include the valve dynamics, which will be referred to as $EMPC-B$, formulated as follows:

$$\min_{u_m(t)\in S(\Delta)} \quad -\int_{t_k}^{t_{k+N_k}} u_m(\tau)\tilde{x}_3(\tau)\tilde{x}_4(\tau)\,d\tau \tag{5.38a}$$

$$\text{s.t.} \quad \dot{\tilde{x}}(t) = f(\tilde{x}(t), u_m(t)) \tag{5.38b}$$

$$\tilde{x}(t_k) = x(t_k) \tag{5.38c}$$

$$0.0704 \le u_m(t) \le 0.7042, \forall t \in [t_k, t_{k+N}) \tag{5.38d}$$

$$\int_{t_k}^{t_{k+N_k}} u_m(\tau)d\tau + \int_{(j-1)t_p}^{t_k} u_m^*(\tau)d\tau = \frac{0.175t_p}{C_e} \tag{5.38e}$$

where the notation in Eq. 5.38b signifies that u_a in Eqs. 5.28a-5.28d is replaced by u_m in the model used to predict the process states within $EMPC-B$. Numerical integration of the dynamic equations in Eq. 5.38b was performed using the Explicit Euler method with an integration time step of $h_B = 10^{-4}\,t_d$. Centered finite difference approximations of derivatives required for the solution of the optimization problem were obtained by perturbing the optimization variables by 10^{-4}.

A third EMPC, $EMPC-C$, was also developed with the form of $EMPC-B$ but with rate of change constraints added, for reasons that will be clarified below. $EMPC-C$ solves the following

optimization problem:

$$\min_{u_m(t)\in S(\Delta)} \quad -\int_{t_k}^{t_{k+N_k}} u_m(\tau)\tilde{x}_3(\tau)\tilde{x}_4(\tau)\,d\tau \tag{5.39a}$$

$$\text{s.t.} \quad \dot{\tilde{x}}(t) = f(\tilde{x}(t), u_m(t)) \tag{5.39b}$$

$$\tilde{x}(t_k) = x(t_k) \tag{5.39c}$$

$$0.0704 \leq u_m(t) \leq 0.7042, \forall t \in [t_k, t_{k+N}) \tag{5.39d}$$

$$\int_{t_k}^{t_{k+N_k}} u_m(\tau)d\tau + \int_{(j-1)t_p}^{t_k} u_m^*(\tau)d\tau = \frac{0.175t_p}{C_e} \tag{5.39e}$$

$$|u_m(t_k) - u_m^*(t_{k-1}|t_{k-1})| \leq \gamma \tag{5.39f}$$

$$|u_m(t_j) - u_m(t_{j-1})| \leq \gamma,\ j = k+1, ..., k+N_k-1 \tag{5.39g}$$

where γ in Eqs. 5.39f-5.39g is a constant that defines the change in u_m that will be accepted between sampling periods. In the following simulations, $\gamma = 0.1$. Eq. 5.39b was numerically integrated using the Explicit Euler numerical integration method with an integration step size of $h_C = 10^{-4}\ t_d$. Centered finite difference approximations of derivatives required for the solution of the optimization problem were obtained by perturbing the optimization variables by 10^{-4}.

Outside of $EMPC-A$, $EMPC-B$, and $EMPC-C$, the actual process was simulated using Eqs. 3.27-3.29, 3.31, and 5.28-5.32 with an Explicit Euler integration step size of $h = 10^{-6}\ t_d$, with the pressure saturated at $0\ kg/m\cdot t_d^2$ if a lower pressure was requested (u_a would have been saturated at $u_{a,\min}$ or $u_{a,\max}$ if those values were exceeded, but neither of these extremes were violated in these simulations). All three EMPC's used $t_p = 1\ t_d$, $\Delta = 0.2\ t_d$, and simulated the results for two operating periods. They were initiated from the point $q_I = [0.997\ 1.264\ 0.209\ 1.004\ 0.051\ 2.000 \times 10^{-6}\ 1.426 \times 10^{-5}\ 0]^T$, where the process states are dimensionless and the states of the actuator layer have SI units except for a dimensionless time unit, and the initial value of the steady-state pressure is $P_s = 63713\ kg/m\cdot t_d^2$. All optimizations were performed using the open-source nonlinear interior point optimization solver Ipopt[148] and were coded in the C++ programming language. The Ipopt convergence tolerance for optimization termination was set to 10^{-10} for $EMPC-A$, and to

10^{-8} for $EMPC-B$ and $EMPC-C$. Simulations were carried out on a 2.40 GHz Intel Core 2 Quad CPU Q6600 on a 64-bit Windows 7 Professional operating system with 4.00 GB of RAM.

Figs. 5.13-5.14 show the values of u_a, u_m, and P for the valve with time when the system of Eqs. 3.27-3.29, 3.31, and 5.28-5.32 is controlled by $EMPC-A$ and $EMPC-B$. These figures show that the inclusion of valve dynamics and actuation magnitude constraints in EMPC causes $EMPC-A$ to calculate lower set-points than $EMPC-B$, which allows the valve output to track the EMPC-requested set-points throughout the two operating periods, even when the pressure drops, because $EMPC-A$ is aware of the limitations of the pneumatic actuation and thus calculates set-points that the valve output can reach (it is noted that there are two small set-point changes in Fig. 5.13 that u_a for $EMPC-A$ does not track; the reason for this will be explained further below, but the overall trend that u_a tracks u_m well under $EMPC-A$ can be deduced from Fig. 5.13). Figs. 5.13-5.14 show that when the actuator dynamics are not included in EMPC and stiction develops with time such that the pressure-flow rate relationship is altered, the valve output is not able to track the $EMPC-B$ set-points because $EMPC-B$ calculates set-points for which the pressure would need to drop to negative values to allow the valve to move enough to reach them (because this is physically impossible, the pressure under $EMPC-B$ saturates at its minimum value of 0 $kg/m\cdot t_d^2$ for four sampling periods, though the pressure under $EMPC-A$ does not because the set-points calculated by $EMPC-A$ are reachable). The inability of the valve to reach the set-points calculated by $EMPC-B$ causes the $EMPC-B$ optimization problem to become infeasible in the last two sampling periods of each operating period and causes $EMPC-B$ to be unable to meet the integral constraint (it cannot use all available material; the value of the integral constraint in Eq. 4.7 calculated for each operating period (i.e., between $(j-1)t_p$ and jt_p, $j=1,2$, instead of between t_0 and t_f) is approximately 0.133, which is 24% less than the required value of 0.175). The yield of $EMPC-A$ throughout two operating periods according to Eq. 4.6 is 32.4%, while that of $EMPC-B$ according to Eq. 4.6 is 35.1%. This at first appears to suggest that $EMPC-B$ out-performs $EMPC-A$ economically; however, because $EMPC-B$ did not meet a hard constraint of the process, the yield that it achieved without meeting this constraint cannot

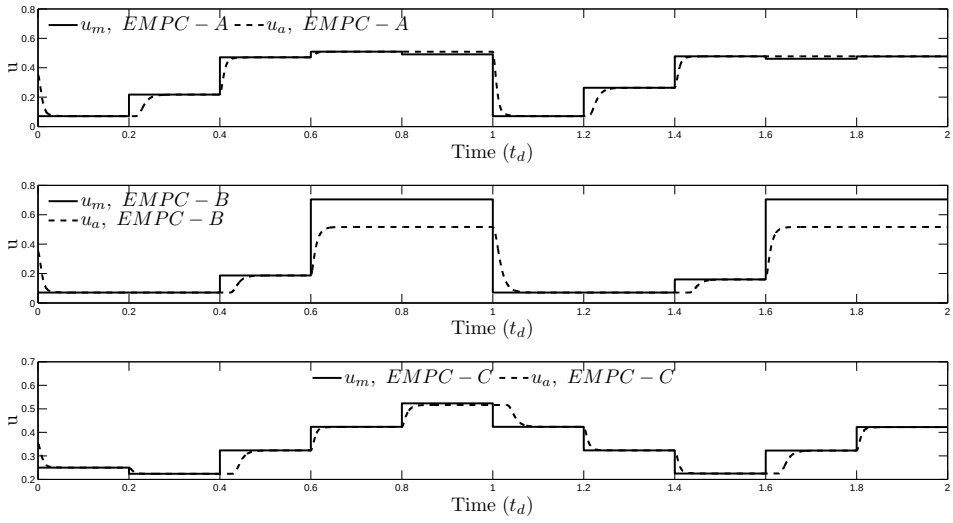

Figure 5.13: Valve output set-points u_m (solid trajectories) and actual valve outputs u_a (dashed trajectories) throughout two operating periods for $EMPC-A$, $EMPC-B$, and $EMPC-C$.

be compared with the yield of a process that did meet the constraint. Thus, no further discussion of yields under the various EMPC's will be pursued, and the discussion will focus on the degree to which the various formulations ensure that the process constraints are satisfied. In contrast to $EMPC-B$, $EMPC-A$ is feasible in both operating periods.

Despite the advantages of using $EMPC-A$ rather than $EMPC-B$ to ensure that all process constraints are met, the computational burden of $EMPC-A$ due to the enforcement of the constraints on the pressure and on u_a at every other integration step $h_A = 10^{-6}\ t_d$ within the EMPC is much larger than that for $EMPC-B$. In an actual plant, this computation time increase could prohibit the use of $EMPC-A$ if the process has fast dynamics such that a short sampling period is required for effective control. However, the input rate of change constraints discussed in this chapter for the design of an MPC incorporating nonlinear valve dynamics may be considered for use in $EMPC-B$ to minimize the large jumps in u_m that cause $EMPC-B$ to be unable to meet the material constraint at the end of the operating periods but without adding much computation time. Thus, we demonstrate the use of input rate of change constraints and how they affect the trajectories of u_m, u_a, and P using $EMPC-C$. Figs. 5.13-5.14 show these trajectories and show that

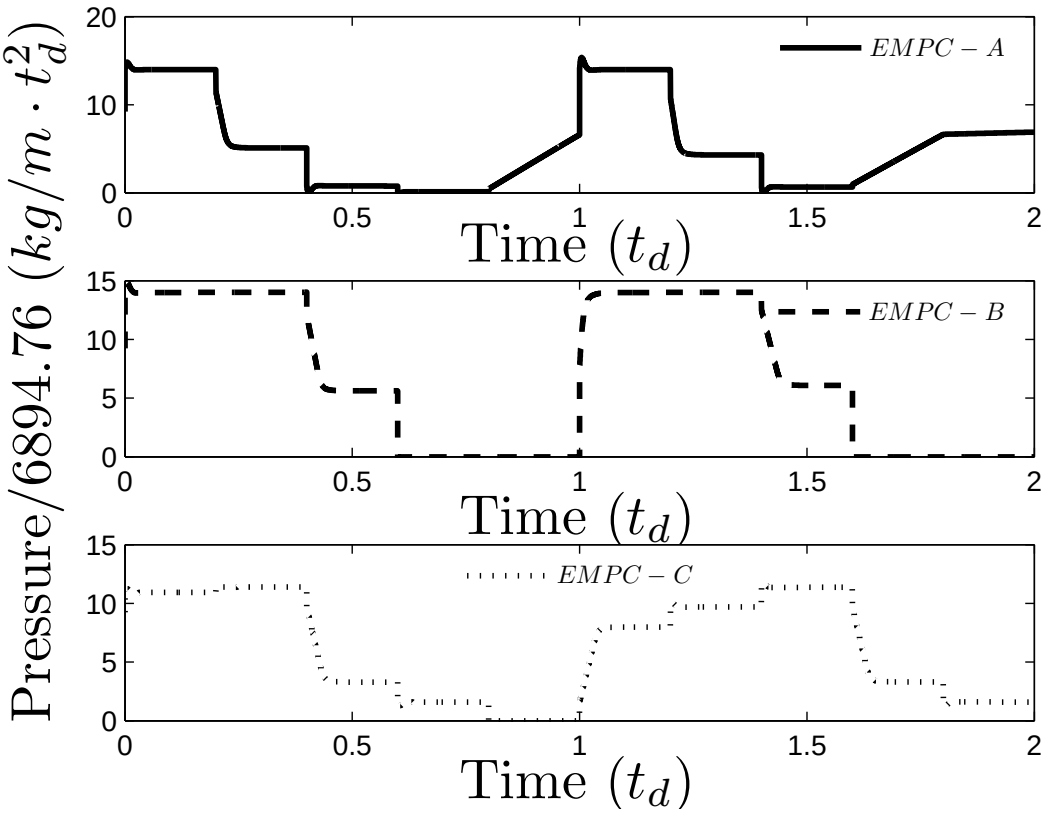

Figure 5.14: Actuator pressure applied to valve stem throughout two operating periods for $EMPC - A$ (solid trajectory), $EMPC - B$ (dashed trajectory), and $EMPC - C$ (dotted trajectory).

the addition of the input rate of change constraints to $EMPC-B$ to form $EMPC-C$ significantly improves the set-point tracking performance compared to $EMPC-B$. In contrast to $EMPC-B$, for which four of the set-points were not reachable and caused significant offset, there is only one set-point calculated by $EMPC-C$ in Fig. 5.13 for which offset is observed, and the offset is much smaller than those for $EMPC-B$. In addition, the pressure in Fig. 5.14 only saturates at its minimum value for one sampling period under $EMPC-C$, instead of the four during which it saturates under $EMPC-B$. Though $EMPC-C$ is infeasible for three sampling periods (the last two sampling periods of the first operating period and the last sampling period of the second operating period) and the integral constraint is not met at the end of either operating period, the degree to which the integral constraint is violated is significantly less than under $EMPC-B$ (the integral constraint is 0.171 at the end of the first operating period and 0.172 at the end of the second under $EMPC-C$, such that in each operating period, it is only about 2% less than the required value of 0.175). In addition, the computation time of $EMPC-C$ is, as for $EMPC-B$, much lower than that for $EMPC-A$ owing to the use of a lower-order model than $EMPC-A$. The rate of change constraints were added to $EMPC-C$ in an *ad hoc* fashion and are not guaranteed to reduce the negative effects of stiction on the controller performance, but the positive impact that they had on the process performance does indicate the breadth of constraints that could be considered to combat the effects of stiction with both the proposed MPC and also with MPC's for processes that cannot fully incorporate the proposed method due to computation time constraints.

Figs. 5.15-5.16 show the closed-loop process and actuator layer states under $EMPC-A$, $EMPC-B$, and $EMPC-C$. Fig. 5.15 shows that the process state trajectories are not drastically affected by the differences between the trajectories of u_a under the three EMPC's, which contributes to the fact that the focus of this example is not on the profitability of the proposed EMPC compared to the other methods, but rather on its ability to meet the constraints of the process when the valve is affected by stiction. The plot of the controller state ζ in Fig. 5.16 shows the manner in which the integral term of the controller is affected by the different EMPC formulations. In $EMPC-B$, the integral term becomes large in the sampling periods in which

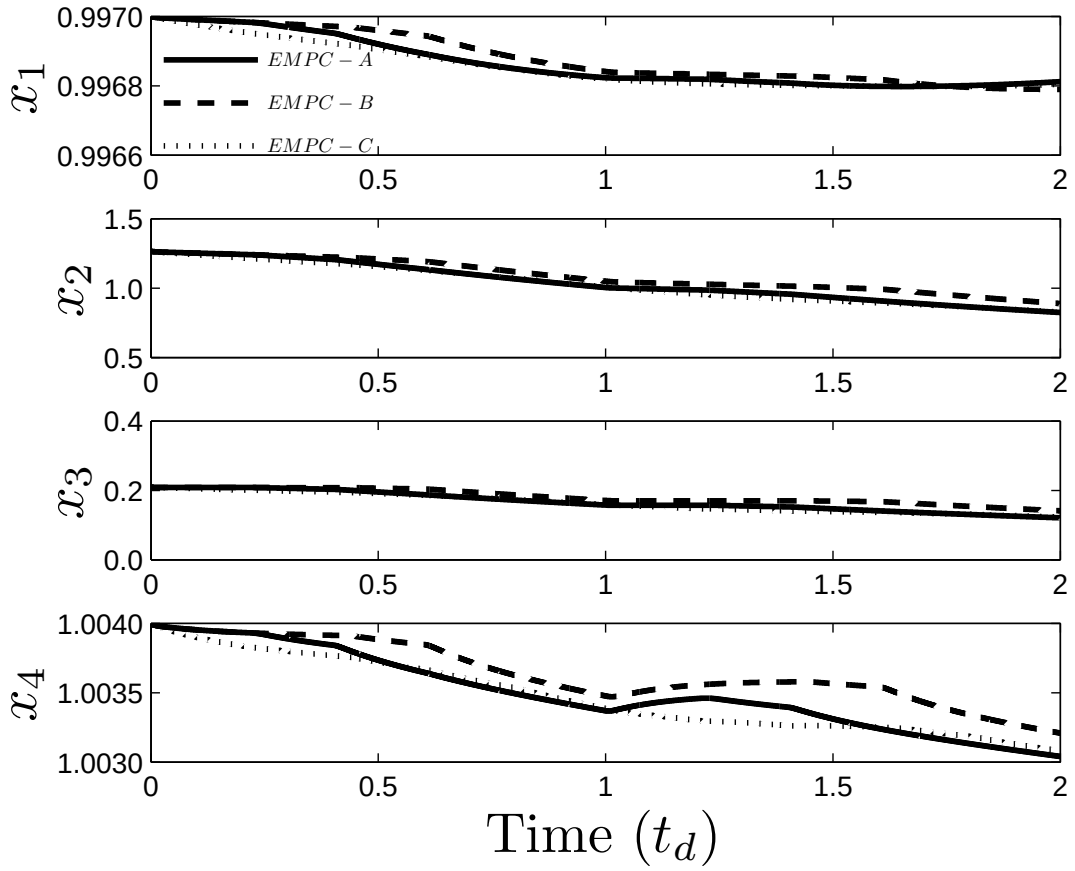

Figure 5.15: Closed-loop process states x_1, x_2, x_3, and x_4 throughout two operating periods under $EMPC-A$ (solid trajectories), $EMPC-B$ (dashed trajectories), and $EMPC-C$ (dotted trajectories).

the EMPC cannot reach its set-points. This plot also shows the benefits of re-setting the value of ζ to zero at each set-point change so that, for example, the value of ζ for $EMPC-B$ at the beginning of the second operating period is not large from the integration of this state at the end of the first operating period. In addition, the plot shows that the inclusion of the actuator dynamics and constraints on the pressure in $EMPC-A$ and rate of change constraints in $EMPC-C$ prevent the integral term from becoming large because they ensure that the set-points can be met or (in the case of $EMPC-C$) reached closely enough so that the integral term does not reach large values. In addition, the increase in ζ at a direction change of the velocity to allow the pressure to overcome the deadband is visible in this plot as well.

The trajectories in Figs. 5.13-5.14 and 5.16 show the relationships between the physical states

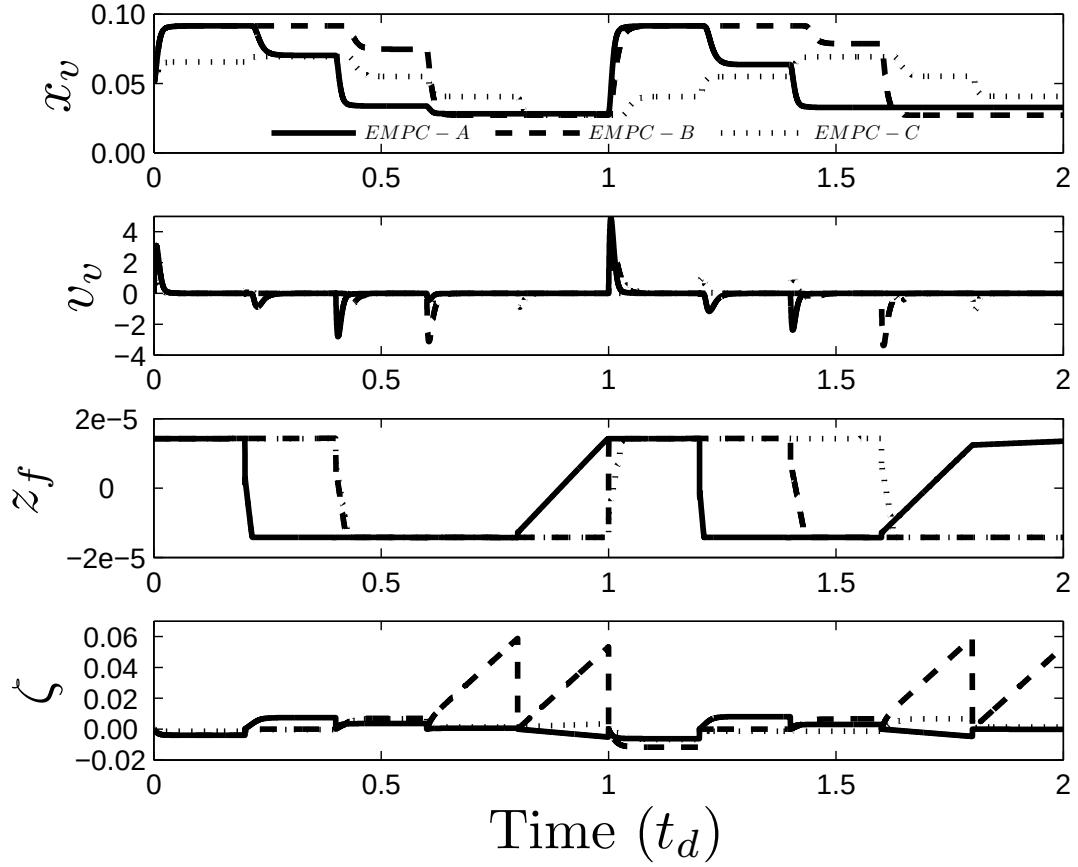

Figure 5.16: Closed-loop actuator layer states x_v, v_v, z, and ζ throughout two operating periods under $EMPC-A$ (solid trajectories), $EMPC-B$ (dashed trajectories), and $EMPC-C$ (dotted trajectories).

x_v and v_v of the valve and the valve output and pressure applied to the valve for the process under $EMPC-A$, $EMPC-B$, and $EMPC-C$. Because the value of u_a is an explicit function of x_v, changes in u_a occur when x_v changes. A comparison of the trajectories of x_v and u_a with the values of P for $EMPC-A$ shows the deadband where the pressure is increasing but the values of x_v and u_a do not change much because the error (and thus ζ) is not large enough to cause much stem movement for the small set-point changes toward the end of the first and second operating periods of the EMPC. The set-point changes in $EMPC-B$ and $EMPC-C$ are all significant enough that the deadband is overcome within a sampling period. The velocity v_v for all three EMPC's is non-zero when x_v and thus u_a are changing, but is zero when u_a reaches u_m and the friction force balances the pressure and spring forces on the valve.

The trajectories of z_f in Fig. 5.16 show that when deadband is encountered, the state z_f is driven through zero. This is consistent with the physical visualization of z_f suggested by the authors of the LuGre model,[26] which related it to the average deflection of theoretical bristles on two contacting surfaces, whose bending caused friction. It would be expected that bristles would be deflected from an equilibrium (zero) location corresponding to the starting position of the valve when the stem position first begins to move in a given direction. In addition, it is necessary for continuity of the friction force in Eq. 3.29 that the value of z_f approach this zero value in a dynamic fashion, rather than abruptly. The passing of z_f through zero at a change in the direction of set-point changes allows the friction force of Eq. 3.29 to change direction so that it continues to be in the direction opposite the applied force.

We now address the fact that $EMPC-A$ calculated set-points that are not reachable (see Fig. 5.13) though it could predict the dynamics of the valve with respect to the set-point changes. Stiction is often noticeable when pressure is applied to a valve, but the valve stem does not move because the opposing friction force is significant. This phenomenon is exhibited during the two set-point changes for $EMPC-A$ that the valve output does not track. Due to the small set-point reversals in u_m requested by $EMPC-A$ at the end of the first and second operating periods, the value of the pressure applied to the valve according to Eqs. 5.31-5.32 does not change quickly

since the error between u_m and u_a (and thus ζ) is low. However, though the valve is considered to be stuck at this time, as the pressure changes, the dynamics in Eqs. 3.27-3.29, 3.31, and 5.28-5.32 cause the stem position and velocity (in addition to z_f) to continue to change, though slowly. It is because of this effect that $EMPC-A$ calculates set-points that it cannot reach; it does so to manipulate the numerical results such that the valve stem and thus output would move just enough in the sampling periods in which unreachable set-points are calculated to allow all constraints to be met, including the integral constraint. While this suggests that the results are dependent on the friction model used, it also shows that including the friction model within the EMPC allows the EMPC to make smart set-point choices that are not necessarily intuitive.

To demonstrate the robustness of the proposed approach to disturbances and plant-model mismatch, the process of Eqs. 3.27-3.29, 3.31, and 5.28-5.32 was controlled by $EMPC-A$ and was simulated with different levels of bounded Gaussian white noise in the process and actuator states, and the closed-loop stability of the process under $EMPC-A$ was found to be robust with respect to the different noise levels. In addition, when the process was simulated with noise in the process states with standard deviation $\sigma_w = [0.1\ 300\ 60\ 0.4\ 0\ 0\ 0\ 0]^T$ and bound $\theta = [0.3\ 900\ 180\ 1.2\ 0\ 0\ 0\ 0]^T$ (this standard deviation and bound on the noise were chosen because they provided a meaningful perturbation to the process states when added to the right-hand side of Eqs. 5.28a-5.28d), the integral material constraint was met in both operating periods.

Remark 5.18. *In the example of this section, the addition of input rate of change constraints to an MPC was shown to be beneficial for valve behavior compensation, and in Chapter 2, such constraints were suggested to help prevent actuator wear. It should be noted, however, that input rate of change constraints may cause issues for effective process control if stiction is present in the control loop and the constraints are not carefully designed. For example, returning to the results in Fig. 3.4 for the sticky valve without flow control of Eqs. 3.27-3.32, we see that the valve does not move due to friction if the changes in the valve output flow rate set-point u_m are not significant enough to increase the pressure to a level that overcomes the static friction force. If input rate of change constraints are included in an MPC that accounts for the stiction dynamics in this case,*

they may prevent u_m from changing enough to cause the level to move in some sampling periods. However, for the example in this chapter, because the valve is under flow control, the pressure applied to the valve can change throughout a sampling period (i.e., it is not fixed by u_m but can be adjusted even for a fixed u_m by the flow controller). Therefore, when the magnitude of $u_m - u_a$ is large in Eqs. 3.24-3.25, the magnitude of P may become large, resulting in the actuation magnitude saturation seen in this example. The input rate of change constraints can thus be beneficial in this case because they are not bounding P directly (i.e., P can still adjust as required to cause u_a to reach u_m if the pressure does not saturate), but they are instead reducing the flexibility that the controller has to change the valve output flow rate set-point to values that would cause the value of P to saturate. This emphasizes the need to carefully design an MPC for stiction compensation with the understanding developed in Chapter 3 that the effects of stiction are closed-loop effects and therefore different MPC constraint designs may be needed for different control loop architectures, for example.

5.5 Conclusions

In this chapter, we showed that MPC can be used to compensate for the effects of stiction by including detailed valve dynamics for sticky valves in addition to constraints on the rate of change of inputs and the actuation magnitude. The flexibility of the MPC-based stiction compensation strategy, which allows it to incorporate a variety of cost functions or constraints to reduce tracking offset in control loops, was discussed. In addition, closed-loop stability and feasibility of the MPC optimization problem including Lyapunov-based stability constraints were proven for a sufficiently small sampling period. Using a chemical process example, we showed how constraints can be developed for the MPC for stiction compensation and demonstrated that this MPC can result in better valve layer set-point tracking and constraint satisfaction than an MPC that does not account for stiction.

Chapter 6

Conclusion

This dissertation developed a framework for accounting for actuator constraints and nonlinearities for control loops with various control designs, ranging from state-of-the-art control methods such as EMPC to classical control designs like PI control.

Chapter 2 discussed methods of accounting for actuator wear through input rate of change constraints in EMPC. It was demonstrated that the constraints can be developed within the context of an EMPC design with Lyapunov-based stability constraints in a manner that not only ensures that the value of each implemented input differs from the value of the last implemented value of that input by no more than a desired value $\varepsilon_{desired}$ between two sampling periods, but also guarantees feasibility of the EMPC design and closed-loop stability in the sense of boundedness of the closed-loop state within a pre-defined region of state-space for all times and uniform ultimate boundedness of the closed-loop state within a neighborhood of the origin when a contractive constraint in the EMPC formulation is activated for all times. It was also demonstrated that the EMPC design could be formulated with a terminal constraint such that even with input rate of change constraints, a nonlinear process operated under the EMPC is guaranteed to have an economic performance at least as good as that of a Lyapunov-based controller implemented in sample-and-hold on both the finite-time and infinite-time intervals. The EMPC with input rate of change constraints was demonstrated through an ethylene oxidation example, and the terminal

constraint was demonstrated utilizing a CSTR.

Chapter 3 analyzed valve nonlinearities from a fundamental mathematical perspective and also through simulation. It was shown that the interactions among the states describing the process model and the valve model are nonlinear and coupled, and as a result, the negative impacts of valve nonlinearities such as stiction on control loop performance should be analyzed in a closed-loop context. A level control example was used to illustrate this by demonstrating the set-point tracking issues occurring in the control loop containing a sticky valve when the tank level is controlled by either a PI controller or an MPC. The closed-loop insights obtained were then utilized to place some of the stiction compensation literature for systems under classical linear control designs in a closed-loop context, and to demonstrate via the level control example how a flow control compensation method and an integral term modification method improve the closed-loop response when the sticky valve is in the loop.

In Chapter 4, the closed-loop perspective on valve nonlinearity compensation was utilized to propose model predictive control methodologies with empirical and first-principles process-valve models for making state predictions as valve nonlinearity compensation methodologies. A level control example and an ethylene oxidation example demonstrated the effectiveness of making the MPC aware of the valve dynamics through the process model and constraints. Finally, Chapter 5 extended the developments of Chapter 4 to focus specifically on MPC for stiction compensation. It demonstrated that special considerations (e.g., actuation magnitude or input rate of change constraints) may be beneficial for preventing the MPC from calculating unreachable set-points for the valve output flow rates due to changes in the valve dynamics that arise due to stiction. An ethylene oxidation example motivated the use of the actuation magnitude constraints and showed that an EMPC that does not account for the valve dynamics in the process model and pneumatic actuation in the constraints may cause the input trajectories computed by the EMPC to violate hard process constraints, whereas accounting for the valve layer dynamics in the EMPC can allow the resulting input trajectories to cause the constraints to be met.

In conclusion, this dissertation has provided a framework for accounting for actuator

dynamics/constraints in classical control designs, MPC, and EMPC by adjusting the process model and constraints to improve set-point tracking and reduce actuator wear.

Bibliography

[1] F. Al-Bender, V. Lampaert, and J. Swevers. A novel generic model at asperity level for dry friction force dynamics. *Tribology Letters*, 16:81–93, 2004.

[2] A. Alanqar, H. Durand, F. Albalawi, and P. D. Christofides. An economic model predictive control approach to integrated production management and process operation. *AIChE Journal*, 63:1892–1906, 2017.

[3] A. Alanqar, H. Durand, and P. D. Christofides. On identification of well-conditioned nonlinear systems: Application to economic model predictive control of nonlinear processes. *AIChE Journal*, 61:3353–3373, 2015.

[4] A. Alanqar, H. Durand, and P. D. Christofides. Error-triggered on-line model identification for model-based feedback control. *AIChE Journal*, 63:949–966, 2017.

[5] A. Alanqar, H. Durand, and P. D. Christofides. Fault-tolerant economic model predictive control using error-triggered on-line model identification. *Industrial & Engineering Chemistry Research*, 56:5652–5667, 2017.

[6] A. Alanqar, M. Ellis, and P. D. Christofides. Economic model predictive control of nonlinear process systems using empirical models. *AIChE Journal*, 61:816–830, 2015.

[7] F. Albalawi, A. Alanqar, H. Durand, and P. D. Christofides. A feedback control framework for safe and economically-optimal operation of nonlinear processes. *AIChE Journal*, 62:2391–2409, 2016.

[8] F. Albalawi, H. Durand, and P. D. Christofides. Distributed economic model predictive control for operational safety of nonlinear processes. *AIChE Journal*, in press.

[9] F. Albalawi, H. Durand, and P. D. Christofides. Distributed economic model predictive control with Safeness-Index based constraints for nonlinear systems. *Systems & Control Letters*, submitted.

[10] F. Albalawi, H. Durand, and P. D. Christofides. Process operational safety using model predictive control based on a process Safeness Index. *Computers & Chemical Engineering*, 104:76–88, 2017.

[11] A. Alessandretti, A. P. Aguiar, and C. N. Jones. On convergence and performance certification of a continuous-time economic model predictive control scheme with time-varying performance index. *Automatica*, 68:305–313, 2016.

[12] F. Alfani and J. J. Carberry. An exploratory kinetic study of ethylene oxidation over an unmoderated supported silver catalyst. *La Chimica e L'Industria*, 52:1192–1196, 1970.

[13] R. Amrit, J. B. Rawlings, and D. Angeli. Economic optimization using model predictive control with a terminal cost. *Annual Reviews in Control*, 35:178–186, 2011.

[14] K. L. Anderson, G. L. Blankenship, and L. G. Lebow. A rule-based adaptive PID controller. In *Proceedings of the IEEE Conference on Decision and Control*, pages 564–569, Austin, Texas, 1988.

[15] J. Andersson, J. Åkesson, and M. Diehl. CasADi: A symbolic package for automatic differentiation and optimal control. In S. Forth, P. Hovland, E. Phipps, J. Utke, and A. Walther, editors, *Recent Advances in Algorithmic Differentiation*, volume 87 of *Lecture Notes in Computational Science and Engineering*, pages 297–307. Springer, Heidelberg, Germany, 2012.

[16] D. Angeli, R. Amrit, and J. B. Rawlings. On average performance and stability of economic model predictive control. *IEEE Transactions on Automatic Control*, 57:1615–1626, 2012.

[17] D. Angeli, A. Casavola, and F. Tedesco. On average performance of economic model predictive control with time-varying cost and terminal constraints. In *Proceedings of the American Control Conference*, pages 2974–2979, Chicago, Illinois, 2015.

[18] B. Armstrong-Hélouvry, P. Dupont, and C. Canudas De Wit. A survey of models, analysis tools and compensation methods for the control of machines with friction. *Automatica*, 30:1083–1138, 1994.

[19] R. Bacci di Capaci, M. Vaccari, and G. Pannocchia. A valve stiction tolerant formulation of MPC for industrial processes. In *Proceedings of the 20th IFAC World Congress*, in press, Toulouse, France, 2017.

[20] J. E. Bailey, F. J. M. Horn, and R. C. Lin. Cyclic operation of reaction systems: Effects of heat and mass transfer resistance. *AIChE Journal*, 17:818–825, 1971.

[21] Belimo AirControls (USA), Inc. Electronic Valve Applications Guide. DOC.V4.2-03.99-7.5M. Available at: http://www.belimo.us/americas/resources.html. Accessed on October 20, 2015.

[22] S. A. Billings. *Nonlinear System Identification: NARMAX Methods in the Time, Frequency, and Spatio-Temporal Domains*. John Wiley & Sons, Chichester, West Sussex, 2013.

[23] T. Bishop, M. Chapeaux, L. Jaffer, K. Nair, and S. Patel. Ease control valve selection. *Chemical Engineeering Progress*, pages 52–56, 2002.

[24] A. S. R. Brásio, A. Romanenko, and N. C. P. Fernandes. Modeling, detection and quantification, and compensation of stiction in control loops: The state of the art. *Industrial & Engineering Chemistry Research*, 53:15020–15040, 2014.

[25] E. F. Camacho and C. Bordons. *Model Predictive Control*. Springer-Verlag, London, England, second edition, 2007.

[26] C. Canudas de Wit, H. Olsson, K. J. Åström, and P. Lischinsky. A new model for control of systems with friction. *IEEE Transactions on Automatic Control*, 40:419–425, 1995.

[27] C.-C. Cheng, C.-Y. Chen, and G. T.-C. Chiu. Predictive control with enhanced robustness for precision positioning in frictional environment. *IEEE/ASME Transactions on Mechatronics*, 7:385–392, 2002.

[28] D. Chmielewski and V. Manousiouthakis. On constrained infinite-time linear quadratic optimal control. *Systems & Control Letters*, 29:121–129, 1996.

[29] M. A. A. S. Choudhury. Plantwide oscillations diagnosis - current state and future directions. *Asia-Pacific Journal of Chemical Engineering*, 6:484–496, 2011.

[30] M. A. A. S. Choudhury, M. Jain, and S. L. Shah. Stiction - definition, modelling, detection and quantification. *Journal of Process Control*, 18:232–243, 2008.

[31] M. A. A. S. Choudhury, S. L. Shah, and N. F. Thornhill. *Diagnosis of Process Nonlinearities and Valve Stiction: Data Driven Approaches*. Springer-Verlag, Berlin, Germany, 2008.

[32] M. A. A. S. Choudhury, S. L. Shah, N. F. Thornhill, and D. S. Shook. Automatic detection and quantification of stiction in control valves. *Control Engineering Practice*, 14:1395–1412, 2006.

[33] M. A. A. S. Choudhury, N. F. Thornhill, and S. L. Shah. Modelling valve stiction. *Control Engineering Practice*, 13:641–658, 2005.

[34] P. D. Christofides, J. F. Davis, N. H. El-Farra, D. Clark, K. R. D. Harris, and J. N. Gipson. Smart plant operations: Vision, progress and challenges. *AIChE Journal*, 53:2734–2741, 2007.

[35] P. D. Christofides and N. H. El-Farra. *Control of Nonlinear and Hybrid Process Systems: Designs for Uncertainty, Constraints and Time-Delays*. Springer-Verlag, Berlin, Germany, 2005.

[36] P. D. Christofides, J. Liu, and D. Muñoz de la Peña. *Networked and Distributed Predictive Control: Methods and Nonlinear Process Network Applications*. Advances in Industrial Control Series. Springer-Verlag, London, England, 2011.

[37] P. D. Christofides, R. Scattolini, D. Muñoz de la Peña, and J. Liu. Distributed model predictive control: A tutorial review and future research directions. *Computers & Chemical Engineering*, 51:21–41, 2013.

[38] D. R. Coughanowr and S. E. LeBlanc. *Process Systems Analysis and Control*. McGraw-Hill, Boston, Massachusetts, 3rd edition, 2009.

[39] M. A. d. S. L. Cuadros, C. J. Munaro, and S. Munareto. Novel model-free approach for stiction compensation in control valves. *Industrial & Engineering Chemistry Research*, 51:8465–8476, 2012.

[40] M. A. d. S. L. Cuadros, C. J. Munaro, and S. Munareto. Improved stiction compensation in pneumatic control valves. *Computers & Chemical Engineering*, 38:106–114, 2012.

[41] P. R. Dahl. A solid friction model. TOR-0158(3107-18)-1. Technical report, El Segundo, California: Aerospace Corporation, 1968.

[42] M. L. Darby, M. Nikolaou, J. Jones, and D. Nicholson. RTO: An overview and assessment of current practice. *Journal of Process Control*, 21:874–884, 2011.

[43] J. Davis, T. Edgar, J. Porter, J. Bernaden, and M. Sarli. Smart manufacturing, manufacturing intelligence and demand-dynamic performance. *Computers & Chemical Engineering*, 47:145–156, 2012.

[44] G. De Souza, D. Odloak, and A. C. Zanin. Real time optimization (RTO) with model predictive control (MPC). *Computers & Chemical Engineering*, 34:1999–2006, 2010.

[45] M. del Carmen Rodríguez Liñán and W. P. Heath. MPC for plants subject to saturation and deadzone, backlash or stiction. In *Proceedings of the 4th IFAC Nonlinear Model Predictive Control Conference*, pages 418–423, Noordwijkerhout, Netherlands, 2012.

[46] L. Desborough and R. Miller. Increasing customer value of industrial control performance monitoring-Honeywell's experience. In *AIChE Symposium Series*, pages 172–192. American Institute of Chemical Engineers, New York, 2002.

[47] M. Diehl, R. Amrit, and J. B. Rawlings. A Lyapunov function for economic optimizing model predictive control. *IEEE Transactions on Automatic Control*, 56:703–707, 2011.

[48] P. Dupont, B. Armstrong, and V. Hayward. Elasto-plastic friction model: Contact compliance and stiction. In *Proceedings of the American Control Conference*, pages 1072–1077, Chicago, IL, 2000.

[49] H. Durand and P. D. Christofides. Actuator stiction compensation via model predictive control for nonlinear processes. *AIChE Journal*, 62:2004–2023, 2016.

[50] H. Durand and P. D. Christofides. Economic model predictive control for nonlinear processes incorporating actuator magnitude and rate of change constraints. In *Proceedings of the American Control Conference*, pages 5068–5074, Boston, Massachusetts, 2016.

[51] H. Durand and P. D. Christofides. Empirical modeling of control valve layer with application to model predictive control-based stiction compensation. In *Proceedings of the IFAC Symposium on Nonlinear Control Systems*, pages 41–46, Monterey, California, 2016.

[52] H. Durand and P. D. Christofides. Stiction compensation via model predictive control. In *Proceedings of the American Control Conference*, pages 4488–4493, Boston, Massachusetts, 2016.

[53] H. Durand and P. D. Christofides. Elucidation and compensation of valve stiction-induced oscillations in closed-loop systems. In *Proceedings of the American Control Conference*, in press, Seattle, Washington, 2017.

[54] H. Durand, M. Ellis, and P. D. Christofides. Integrated design of control actuator layer and economic model predictive control for nonlinear processes. *Industrial & Engineering Chemistry Research*, 53:20000–20012, 2014.

[55] H. Durand, M. Ellis, and P. D. Christofides. Economic model predictive control designs for input rate-of-change constraint handling and guaranteed economic performance. *Computers & Chemical Engineering*, 92:18–36, 2016.

[56] H. Durand, R. Parker, A. Alanqar, and P. D. Christofides. Elucidating and handling effects of valve-induced nonlinearities in industrial feedback control loops. *Computers & Chemical Engineering*, submitted.

[57] N. H. El-Farra and P. D. Christofides. Bounded robust control of constrained multivariable nonlinear processes. *Chemical Engineering Science*, 58:3025–3047, 2003.

[58] M. Ellis and P. D. Christofides. On finite-time and infinite-time cost improvement of economic model predictive control for nonlinear systems. *Automatica*, 50:2561–2569, 2014.

[59] M. Ellis and P. D. Christofides. Optimal time-varying operation of nonlinear process systems with economic model predictive control. *Industrial & Engineering Chemistry Research*, 53:4991–5001, 2014.

[60] M. Ellis and P. D. Christofides. Real-time economic model predictive control of nonlinear process systems. *AIChE Journal*, 61:555–571, 2015.

[61] M. Ellis and P. D. Christofides. On closed-loop economic performance under Lyapunov-based economic model predictive control. In *Proceedings of the American Control Conference*, pages 1778–1783, Boston, Massachusetts, 2016.

[62] M. Ellis, H. Durand, and P. D. Christofides. A tutorial review of economic model predictive control methods. *Journal of Process Control*, 24:1156–1178, 2014.

[63] M. Ellis, H. Durand, and P. D. Christofides. Elucidation of the role of constraints in economic model predictive control. *Annual Reviews in Control*, 41:208–217, 2016.

[64] M. Ellis, I. Karafyllis, and P. D. Christofides. Stabilization of nonlinear sampled-data systems and economic model predictive control application. In *Proceedings of the American Control Conference*, pages 5594–5601, Portland, Oregon, 2014.

[65] M. Ellis, J. Liu, and P. D. Christofides. *Economic Model Predictive Control: Theory, Formulations and Chemical Process Applications*. Springer International Publishing, Switzerland, 2017.

[66] M. Ellis, J. Zhang, J. Liu, and P. D. Christofides. Robust moving horizon estimation based output feedback economic model predictive control. *Systems & Control Letters*, 68:101–109, 2014.

[67] L. Fagiano and A. R. Teel. Generalized terminal state constraint for model predictive control. *Automatica*, 49:2622–2631, 2013.

[68] Y. Fang and A. Armaou. Carleman approximation based quasi-analytic model predictive control for nonlinear systems. *AIChE Journal*, 62:3915–3929, 2016.

[69] T. Faulwasser and D. Bonvin. On the design of economic NMPC based on an exact turnpike property. In *Proceedings of the 9th International Symposium on Advanced Control of Chemical Processes*, Whistler, British Columbia, 2015.

[70] M. Feemster, P. Vedagarbha, D. M. Dawson, and D. Haste. Adaptive control techniques for friction compensation. In *Proceedings of the American Control Conference*, pages 1488–1492, Philadelphia, Pennsylvania, 1998.

[71] B. Friedland and Y.-J. Park. On adaptive friction compensation. *IEEE Transactions on Automatic Control*, 37:1609–1612, 1992.

[72] C. Garcia. Comparison of friction models applied to a control valve. *Control Engineering Practice*, 16:1231–1243, 2008.

[73] J. Gerry and M. Ruel. How to measure and combat valve stiction online. In *Proceedings of the ISA International Fall Conference*, Houston, Texas, 2001.

[74] P. Grieder, F. Borrelli, F. Torrisi, and M. Morari. Computation of the constrained infinite time linear quadratic regulator. *Automatica*, 40:701–708, 2004.

[75] L. Grüne. Economic receding horizon control without terminal constraints. *Automatica*, 49:725–734, 2013.

[76] L. Grüne and M. Stieler. Asymptotic stability and transient optimality of economic MPC without terminal conditions. *Journal of Process Control*, 24:1187–1196, 2014.

[77] T. Hägglund. A friction compensator for pneumatic control valves. *Journal of Process Control*, 12:897–904, 2002.

[78] Q. P. He, J. Wang, M. Pottmann, and S. J. Qin. A curve fitting method for detecting valve stiction in oscillating control loops. *Industrial & Engineering Chemistry Research*, 46:4549–4560, 2007.

[79] M. Heidarinejad, J. Liu, and P. D. Christofides. Economic model predictive control of nonlinear process systems using Lyapunov techniques. *AIChE Journal*, 58:855–870, 2012.

[80] M. Heidarinejad, J. Liu, and P. D. Christofides. Algorithms for improved fixed-time performance of Lyapunov-based economic model predictive control of nonlinear systems. *Journal of Process Control*, 23:404–414, 2013.

[81] A. C. Hindmarsh, P. N. Brown, K. E. Grant, S. L. Lee, R. Serban, D. E. Shumaker, and C. S. Woodward. SUNDIALS: Suite of nonlinear and differential/algebraic equation solvers. *ACM Transactions on Mathematical Software*, 31:363–396, 2005.

[82] A. Horch. A simple method for detection of stiction in control valves. *Control Engineering Practice*, 7:1221–1231, 1999.

[83] T. G. Hovgaard, K. Edlund, and J. B. Jørgensen. The potential of economic MPC for power management. In *Proceedings of the IEEE Conference on Decision and Control*, pages 7533–7538, Atlanta, Georgia, 2010.

[84] R. Huang, L. T. Biegler, and E. Harinath. Robust stability of economically oriented infinite horizon NMPC that include cyclic processes. *Journal of Process Control*, 22:51–59, 2012.

[85] S. N. Huang, K. K. Tan, and T. H. Lee. Adaptive friction compensation using neural network approximations. *IEEE Transactions on Systems, Man, and Cybernetics, Part C: Applications and Reviews*, 30:551–557, 2000.

[86] L. Z. X. Ivan and S. Lakshminarayanan. A new unified approach to valve stiction quantification and compensation. *Industrial & Engineering Chemistry Research*, 48:3474–3483, 2009.

[87] Z. Jamaludin, H. Van Brussel, and J. Swevers. Design of a disturbance observer and model-based friction feedforward to compensate quadrant glitches. In H. Ulbrich and L. Ginzinger, editors, *Motion and Vibration Control*, pages 143–154. Springer, The Netherlands, 2009.

[88] M. Jelali. Estimation of valve stiction in control loops using separable least-squares and global search algorithms. *Journal of Process Control*, 18:632–642, 2008.

[89] M. Jelali and B. Huang, editors. *Detection and Diagnosis of Stiction in Control Loops: State of the Art and Advanced Methods*. Springer-Verlag, London, England, 2010.

[90] M. Kano, H. Maruta, H. Kugemoto, and K. Shimizu. Practical model and detection algorithm for valve stiction. In *Proceedings of the IFAC Symposium on Dynamics and Control of Process Systems*, pages 859–864, Cambridge, Massachusetts, 2004.

[91] A. Kayihan and F. J. Doyle III. Friction compensation for a process control valve. *Control Engineering Practice*, 8:799–812, 2000.

[92] H. K. Khalil. *Nonlinear Systems*. Prentice Hall, Upper Saddle River, New Jersey, third edition, 2002.

[93] D. S. Laila, D. Nešić, and A. Astolfi. Sampled-data control of nonlinear systems. In A. Loría, F. Lamnabhi-Lagarrigue, and E. Panteley, editors, *Advanced Topics in Control Systems Theory*, volume 328 of *Lecture Notes in Control and Information Science*, pages 91–137. Springer, London, 2006.

[94] V. Lampaert, F. Al-Bender, and J. Swevers. A generalized Maxwell-Slip friction model appropriate for control purposes. In *Proceedings of the International Conference on Physics and Control*, pages 1170–1177, St. Petersburg, Russia, 2003.

[95] V. Lampaert, J. Swevers, and F. Al-Bender. Modification of the Leuven integrated friction model structure. *IEEE Transactions on Automatic Control*, 47:683–687, 2002.

[96] L. Lao, M. Ellis, and P. D. Christofides. Smart manufacturing: Handling preventive actuator maintenance and economics using model predictive control. *AIChE Journal*, 60:2179–2196, 2014.

[97] L. Lao, M. Ellis, H. Durand, and P. D. Christofides. Real-time preventive sensor maintenance using robust moving horizon estimation and economic model predictive control. *AIChE Journal*, 61:3374–3389, 2015.

[98] A. Leosirikul, D. Chilin, J. Liu, J. F. Davis, and P. D. Christofides. Monitoring and retuning of low-level PID control loops. *Chemical Engineering Science*, 69:287–295, 2012.

[99] C. Li, M. A. A. S. Choudhury, B. Huang, and F. Qian. Frequency analysis and compensation of valve stiction in cascade control loops. *Journal of Process Control*, 24:1747–1760, 2014.

[100] Y. Lin and E. D. Sontag. A universal formula for stabilization with bounded controls. *Systems & Control Letters*, 16:393–397, 1991.

[101] B. G. Liptak and W. H. Boyes. Applying control valves. In W. Boyes, editor, *Instrumentation Reference Book*, pages 631–636. Butterworth-Heinemann, Boston, Massachusetts, fourth edition, 2010.

[102] L. Ljung. *System Identification: Theory for the User*. Prentice Hall PTR, Upper Saddle River, New Jersey, 1999.

[103] T. E. Marlin and A. N. Hrymak. Real-time operations optimization of continuous processes. In *Proceedings of the 5th International Conference on Chemical Process Control*, pages 156–164, Tahoe City, California, 1996.

[104] J. L. Massera. Contributions to stability theory. *Annals of Mathematics*, 64:182–206, 1956.

[105] D. Q. Mayne. Control of constrained dynamic systems. *European Journal of Control*, 7:87–99, 2001.

[106] D. Q. Mayne, J. B. Rawlings, C. V. Rao, and P. O. M. Scokaert. Constrained model predictive control: Stability and optimality. *Automatica*, 36:789–814, 2000.

[107] D. I. Mendoza-Serrano and D. J. Chmielewski. HVAC control using infinite-horizon economic MPC. In *Proceedings of the IEEE Conference on Decision and Control*, pages 6963–6968, Maui, Hawaii, 2012.

[108] P. Mhaskar, N. H. El-Farra, and P. D. Christofides. Stabilization of nonlinear systems with state and control constraints using Lyapunov-based predictive control. *Systems & Control Letters*, 55:650–659, 2006.

[109] P. Mhaskar and A. B. Kennedy. Robust model predictive control of nonlinear process systems: Handling rate constraints. *Chemical Engineering Science*, 63:366–375, 2008.

[110] P. Mhaskar, J. Liu, and P. D. Christofides. *Fault-Tolerant Process Control: Methods and Applications*. Springer-Verlag, London, England, 2013.

[111] M. Ale Mohammad and B. Huang. Compensation of control valve stiction through controller tuning. *Journal of Process Control*, 22:1800–1819, 2012.

[112] D. Muñoz de la Peña and P. D. Christofides. Lyapunov-based model predictive control of nonlinear systems subject to data losses. *IEEE Transactions on Automatic Control*, 53:2076–2089, 2008.

[113] M. A. Müller, D. Angeli, and F. Allgöwer. On the performance of economic model predictive control with self-tuning terminal cost. *Journal of Process Control*, 24:1179–1186, 2014.

[114] M. A. Müller and L. Grüne. Economic model predictive control without terminal constraints: Optimal periodic operation. In *Proceedings of the IEEE Conference on Decision and Control*, pages 4946–4951, Osaka, Japan, 2015.

[115] C. J. Munaro, G. B. de Castro, F. A. da Silva, O. F. B. Angarita, and M. V. G. Cypriano. Reducing wear of sticky pneumatic control valves using compensation pulses with variable amplitude. In *Proceedings of the 11th IFAC Symposium on Dynamics and Control of Process Systems, including Biosystems*, pages 389–393, Trondheim, Norway, 2016.

[116] K. R. Muske and J. B. Rawlings. Linear model predictive control of unstable processes. *Journal of Process Control*, 3:85–96, 1993.

[117] U. Nallasivam, S. Babji, and R. Rengaswamy. Stiction identification in nonlinear process control loops. *Computers & Chemical Engineering*, 34:1890–1898, 2010.

[118] B. A. Ogunnaike and W. H. Ray. *Process Dynamics, Modeling, and Control*. Oxford University Press, New York, New York, 1994.

[119] H. Olsson. *Control Systems with Friction*. PhD thesis, Lund Institute of Technology, 1996.

[120] H. Olsson, K. J. Åström, C. Canudas de Wit, M. Gäfvert, and P. Lischinsky. Friction models and friction compensation. *European Journal of Control*, 4:176–195, 1998.

[121] B. P. Omell and D. J. Chmielewski. IGCC power plant dispatch using infinite-horizon economic model predictive control. *Industrial & Engineering Chemistry Research*, 52:3151–3164, 2013.

[122] F. Özgülşen, R. A. Adomaitis, and A. Çinar. A numerical method for determining optimal parameter values in forced periodic operation. *Chemical Engineering Science*, 47:605–613, 1992.

[123] J. Paduart, L. Lauwers, J. Swevers, K. Smolders, J. Schoukens, and R. Pintelon. Identification of nonlinear systems using polynomial nonlinear state space models. *Automatica*, 46:647–656, 2010.

[124] N. R. Patel, M. J. Risbeck, J. B. Rawlings, M. J. Wenzel, and R. D. Turney. Distributed economic model predictive control for large-scale building temperature regulation. In *Proceedings of the American Control Conference*, pages 895–900, Boston, Massachusetts, 2016.

[125] S. J. Qin and T. A. Badgwell. An overview of nonlinear model predictive control applications. In F. Allgöwer and A. Zheng, editors, *Nonlinear Model Predictive Control*, pages 369–392. Birkhäuser, Basel, Switzerland, 2000.

[126] S. J. Qin and T. A. Badgwell. A survey of industrial model predictive control technology. *Control Engineering Practice*, 11:733–764, 2003.

[127] J. B. Rawlings. Tutorial: Model predictive control technology. In *Proceedings of the American Control Conference*, pages 662–676, San Diego, California, 1999.

[128] J. B. Rawlings, D. Angeli, and C. N. Bates. Fundamentals of economic model predictive control. In *Proceedings of the 51st IEEE Conference on Decision and Control*, pages 3851–3861, Maui, Hawaii, 2012.

[129] J. B. Riggs. *Chemical Process Control*. Ferret Publishing, Lubbock, Texas, 1999.

[130] A. Romanenko, L. O. Santos, and P. A. F. N. A. Afonso. Application of agent technology concepts to the design of a fault-tolerant control system. *Control Engineering Practice*, 15:459–469, 2007.

[131] P. L. Silveston. Periodic operation of chemical reactors - a review of the experimental literature. *Sadhana*, 10:217–246, 1987.

[132] A. Singhal and T. I. Salsbury. A simple method for detecting valve stiction in oscillating control loops. *Journal of Process Control*, 15:371–382, 2005.

[133] S. Sivagamasundari and D. Sivakumar. A new methodology to compensate stiction in pneumatic control valves. *International Journal of Soft Computing and Engineering*, 2:480–484, 2013.

[134] R. Srinivasan and R. Rengaswamy. Stiction compensation in process control loops: A framework for integrating stiction measure and compensation. *Industrial & Engineering Chemistry Research*, 44:9164–9174, 2005.

[135] R. Srinivasan and R. Rengaswamy. Approaches for efficient stiction compensation in process control valves. *Computers & Chemical Engineering*, 32:218–229, 2008.

[136] R. Srinivasan, R. Rengaswamy, and R. Miller. Control loop performance assessment. 1. A qualitative approach for stiction diagnosis. *Industrial & Engineering Chemistry Research*, 44:6708–6718, 2005.

[137] R. Srinivasan, R. Rengaswamy, S. Narasimhan, and R. Miller. Control loop performance assessment. 2. Hammerstein model approach for stiction diagnosis. *Industrial & Engineering Chemistry Research*, 44:6719–6728, 2005.

[138] A. Stenman, F. Gustafsson, and K. Forsman. A segmentation-based method for detection of stiction in control valves. *International Journal of Adaptive Control and Signal Processing*, 17:625–634, 2003.

[139] L. E. Sterman and B. E. Ydstie. Periodic forcing of the CSTR: An application of the generalized Π-criterion. *AIChE Journal*, 37:986–996, 1991.

[140] J. Swevers, F. Al-Bender, C. G. Ganseman, and T. Prajogo. An integrated friction model structure with improved presliding behavior for accurate friction compensation. *IEEE Transactions on Automatic Control*, 45:675–686, 2000.

[141] F. Tahersima, J. Stoustrup, H. Rasmussen, and S. A. Meybodi. Economic COP optimization of a heat pump with hierarchical model predictive control. In *Proceedings of the IEEE Conference on Decision and Control*, pages 7583–7588, Maui, Hawaii, 2012.

[142] A. R. Teel, D. Nešić, and P. V. Kokotović. A note on input-to-state stability of sampled-data nonlinear systems. In *Proceedings of the IEEE Conference on Decision and Control*, pages 2473–2478, Tampa, Florida, 1998.

[143] N. F. Thornhill and A. Horch. Advances and new directions in plant-wide disturbance detection and diagnosis. *Control Engineering Practice*, 15:1196–1206, 2007.

[144] C. R. Touretzky and M. Baldea. Integrating scheduling and control for economic MPC of buildings with energy storage. *Journal of Process Control*, 24:1292–1300, 2014.

[145] P. Van Overschee and B. L. De Moor. *Subspace Identification for Linear Systems: Theory-Implementation-Applications*. Kluwer Academic Publishers, Norwell, Massachusetts, 1996.

[146] M. Veronesi and A. Visioli. Performance assessment and retuning of PID controllers for integral processes. *Journal of Process Control*, 20:261–269, 2010.

[147] A. Wächter. Short tutorial: Getting started with Ipopt in 90 minutes. In *Combinatorial Scientific Computing*, Dagstuhl, Germany, 2009.

[148] A. Wächter and L. T. Biegler. On the implementation of an interior-point filter line-search algorithm for large-scale nonlinear programming. *Mathematical Programming*, 106:25–57, 2006.

[149] G. Wang and J. Wang. Quantification of valve stiction for control loop performance assessment. In *IEEE 16th International Conference on Industrial Engineering and Engineering Management*, pages 1189–1194, Beijing, China, 2009.

[150] J. Wang. Closed-loop compensation method for oscillations caused by control valve stiction. *Industrial & Engineering Chemistry Research*, 52:13006–13019, 2013.

[151] J. Wang and Q. Zhang. Detection of asymmetric control valve stiction from oscillatory data using an extended Hammerstein system identification method. *Journal of Process Control*, 24:1–12, 2014.

[152] H. Zabiri and Y. Samyudia. A hybrid formulation and design of model predictive control for systems under actuator saturation and backlash. *Journal of Process Control*, 16:693–709, 2006.

[153] H. Zabiri and Y. Samyudia. MIQP-based MPC in the presence of control valve stiction. *Chemical Product and Process Modeling*, 4:85–97, 2009.

[154] M. Zachar and P. Daoutidis. Nonlinear economic model predictive control for microgrid dispatch. *IFAC-PapersOnLine*, 49:778–783, 2016.

[155] J. Zeng and J. Liu. Economic model predictive control of wastewater treatment processes. *Industrial & Engineering Chemistry Research*, 54:5710–5721, 2015.

[156] J. Zhang, S. Liu, and J. Liu. Economic model predictive control with triggered evaluations: State and output feedback. *Journal of Process Control*, 24:1197–1206, 2014.